Systematic improvement of parton showers with effective theory

Matthew Baumgart, Claudio Marcantonini, and Iain W. Stewart

Phys. Rev. D **83**, 034011 — Published 10 February 2011

DOI: 10.1103/PhysRevD.83.034011

Systematic Improvement of Parton Showers with Effective Theory

Matthew Baumgart,[1,2,3,*] Claudio Marcantonini,[4,†] and Iain W. Stewart[4,‡]

[1] *Jefferson Physical Laboratory, Harvard University, Cambridge, MA 02138, USA*

[2] *School of Natural Sciences, Institute for Advanced Study, Princeton, NJ 08540, USA*

[3] *Department of Physics and Astronomy, Johns Hopkins University, Baltimore, MD 21218, USA*

[4] *Center for Theoretical Physics, Massachusetts Institute of Technology, Cambridge, MA 02139, USA*

We carry out a systematic classification and computation of next-to-leading order kinematic power corrections to the fully differential cross section in the parton shower. To do this we devise a map between ingredients in a parton shower and operators in a traditional effective field theory framework using a chain of soft-collinear effective theories. Our approach overcomes several difficulties including avoiding double counting and distinguishing approximations that are coordinate choices from true power corrections. Branching corrections can be classified as hard-scattering, that occur near the top of the shower, and jet-structure, that can occur at any point inside it. Hard-scattering corrections include matrix elements with additional hard partons, as well as power suppressed contributions to the branching for the leading jet. Jet-structure corrections require simultaneous consideration of potential $1 \to 2$ and $1 \to 3$ branchings. The interference structure induced by collinear terms with subleading powers remains localized in the shower.

*Electronic address: baumgart@pha.jhu.edu
†Electronic address: cmarcant@mit.edu
‡Electronic address: iains@mit.edu

I. INTRODUCTION

For scattering problems involving strongly-interacting particles, we are often interested in final states with large multiplicities, sometimes including thousands of hadrons. To get to this level, we cannot rely solely on full fixed-order calculations. Tree-level event generators [1–4] only go up to 8-10 external particles as Monte Carlo for higher multiplicity phase space is increasingly intractable. At one-loop, the frontier is $2 \to 4$ processes, which have been done at the level of differential cross sections for $W+$ 3 jets [5, 6] and $t\bar{t}b\bar{b}$ [7]. At two-loops, there are $2 \to 1$ exclusive calculations for weak boson production by hadrons followed by decay (W and Z [8] and W [9] to leptons, and H decaying to photons [10, 11].). Additionally, $e^+e^- \to 3$ jets to NNLO is known [12–15]. In any case, a strict fixed order counting is not suitable for exclusive observables with large multiplicities, nor for many inclusive observables where certain regions of phase space receive kinematic enhancement by large logarithms. If Q is a hard scale in the process, then a subset of the amplitude gets enhanced so that its coefficient is $(\alpha_s \ln^2(Q/p))^m$, where $p \ll Q$ refers to a small scale that is induced by the choice of observable or cuts. Since we can resum these large logs by systematically treating real radiation, we can give a leading log (LL) description of these observables without performing multiloop computations. The soft and collinear limits that yield these large logs also allow us to simplify the amplitude. Therefore, capturing the dominant contributions to these observables and simulating processes with a large number of particles becomes feasible. This is a main goal of parton Shower Monte Carlo (SMC).

A final state SMC is based on the "strongly-ordered limit," which describes the leading log contribution (accounting for soft emission by angular ordering or other approximations). In this kinematic configuration, each radiated particle comes off much more collinear to its parent than the previous one, a situation that can be formulated in terms of perpendicular momenta or virtualities, *i.e.*

$$q_{0\perp} \gg q_{1\perp} \gg q_{2\perp} \gg \dots, \qquad \text{or} \qquad q_0^2 \gg q_1^2 \gg q_2^2 \gg \dots . \tag{1}$$

Furthermore, and important for practical computation, in this limit each collinear emission is independent of the previous one. Thus, if we have calculated the differential cross section for i-parton emission, $d\sigma_i$, then we can obtain the $(i+1)$-parton case as

$$d\sigma_{i+1} \propto \frac{P^{(0)}_{j\to kl}}{q_i^2}\, d\sigma_i, \tag{2}$$

where $P^{(0)}$ is the leading order (LO) "splitting function" that captures the probability for the i^{th} emitted parton, of type j, to split into two others, kl, and q_i^2 is its virtuality. Thus, we can formulate the process in terms of a probabilistic Markov chain of i $1 \to 2$ particle splittings. The probabilities are determined by the functions $P^{(0)}_{j\to kl}$, which are the LO Altarelli-Parisi kernels. As an example, for $q \to qg$, after averaging and summing over spins,

$$P^{(0)}_{q\to qg} = \frac{\alpha_s}{2\pi} C_F \frac{1+z^2}{1-z}, \tag{3}$$

where z is the longitudinal momentum fraction of the daughter with respect to the parent. This classical, probabilistic process gives rise to the SMC algorithms used by event generators such as Pythia [16, 17] and Herwig [18, 19] to model radiation. For a virtuality-ordered shower, such as the original version of Pythia, given some initial offshellness, q_0^2, and an initial momentum fraction, x_0, SMCs generate the virtuality and the momentum fraction of the daughter particle after the spitting. The former is determined by a Sudakov factor, $\Delta(q^2, q_0^2)$, which gives the probability of a parton to evolve from q_0^2 to q^2 without branching,

$$\Delta(q^2, q_0^2) = \exp\left[-\int_{q_0^2}^{q^2} \frac{dq'^2}{q'^2} \int dz\, \frac{\alpha_s}{2\pi} P^{(0)}_{jk}(z) \right]. \tag{4}$$

The traditional LL parton shower makes the multiplicity problem tractable, but it has shortcomings related to the leading log approximation. Even though Eq. (2) is only correct in the collinear limit, the shower is used everywhere in order to generate events that cover the full phase space. In addition, since each collinear emission is independent from the previous one in the shower, the LL approximation does not include their spin or color correlations, nor any of their interference. The situation is different for soft gluons where the inclusion of color effects allows one to work in the simplifying limit of angular ordering.

The hierarchy of scales in the parton shower makes it amenable to an effective field theory treatment. Since the shower regime occurs for particles in the soft and collinear regions, we can describe it with Soft-Collinear Effective Theory (SCET) [20–23]. Like any EFT, SCET comes with an expansion that allows, in principle, for systematic

improvement. The first work on parton showers using SCET came in [24, 25], which we review in Sec. II B, where the authors showed how the splitting functions and corresponding Sudakov factors, along with the factorization of emissions emerge naturally. Furthermore, they could include virtual corrections by matching to QCD at higher order in α_s. Unfortunately, in reproducing the LL shower in SCET, they introduced many conventions whose extension to higher orders in the kinematic expansion is unclear. We therefore develop a modified approach to alleviate these difficulties.

Before discussing our setup, we give an overview of advances in the parton shower literature beyond the basic LL picture. The structure of these advances depends on what aspect of the shower one aims to improve. Possible motivations include accuracy at higher orders in α_s, higher order in logs, and higher order in powers of the kinematic expansions. We first introduce some terminology for higher order log resummation. If the resummation of large logs, L, is at the cross section level

$$d\sigma \sim \Big[\sum_k (\alpha_s L^2)^k\Big]_{\rm LL} + \Big[\sum_k \alpha_s L(\alpha_s L^2)^k\Big]_{\rm NLL} + \dots \tag{5}$$

then we will refer to it as LL, NLL, etc, as indicated. If the cross section transformed to an appropriate set of variables has a resummation of logs in the exponent

$$\ln d\sigma \sim L\Big[\sum_k (\alpha_s L)^k\Big]_{\rm LL_{exp}} + \Big[\sum_k (\alpha_s L)^k\Big]_{\rm NLL_{exp}} + \dots \tag{6}$$

then we will attach a subscript "exp" to the orders to indicate this.

A major concern with parton showers is how one handles the merging with matrix element (ME) calculations that describe the initial underlying hard process. One can consider a simple setup where one declares that a scale, μ_0, divides collinear from hard radiation. Here, emissions above μ_0 are described through tree-level ME calculations, and those beneath by running SMC. Each regime would get a reasonable treatment, but naively interfacing the two leaves leading-log sensitivity to μ_0. This is because the LO (in α_s) result contains no Sudakov log resummation. Methods for carrying out matrix element and parton shower merging including this information have been considered in Refs. [26–28] and are referred to as CKKW-L and MLM. In CKKW-L, one distributes the particles in an event according to the probabilities given by the exact tree-level matrix element, with μ_0^2 as a lower cutoff related to the perpendicular momentum between any two particles. One then clusters the event using the k_T algorithm [29] to determine the splitting scales, $q_{i\,T}^2$. With these in hand, one reweights the event by multiplication by appropriate Sudakov factors, as well as factors of $\alpha_s(q_{i\,T})/\alpha_s(Q)$, where Q is some hard scale. We can then run a parton shower algorithm on these squared amplitudes, vetoing any splitting $q_{i\,T}$ harder than μ_0^2 to avoid double counting. It was demonstrated that the n-jet rate depends on μ_0 only beyond NLL order, with the first missing term being $\alpha_s^2 \ln^2(Q/\mu_0)$. CKKW-L has been built into Sherpa [30].

Another important effect concerns soft gluons, which are also kinematically enhanced. Collinear emissions reinforce the picture of partonic radiation as an isolated jet since they get distributed within some narrow cone about the original hard parton. *A priori*, soft gluons have no preferred direction and can communicate between elements of the shower. Fortunately, wide-angle radiation only observes the net color charge contained in the cone of emission. Therefore, the pattern of soft radiation far from the collinear jet is not sensitive to splittings that have taken place within it. This coherent branching and angular ordering can be accommodated by methods such as evolving the shower by decreasing angle monotonically, as is done in Herwig [31], or by enforcing it with a veto in a virtuality-ordered shower (the rightmost expression in Eq. (1)), which is an option in Pythia [16]. Accounting for coherence properties leads to LL resummation for the soft emissions [32–36]. Additional considerations treated in shower programs include putting α_s at the k_T scale of each splitting, and encoding momentum conservation at each vertex, which give the parton shower information beyond an analytic LO/LL calculation. These along with the overall choice in evolution variable (mass, $k_\perp$, angle, *etc.*) are treated in different fashions by different SMC codes.

There are of course further corrections to include to go to NLO in α_s, denoted NLO(α_s), NLL in kinematic logs, and/or NLO in power corrections to the strong ordering, denoted NLO(λ). The most effort to date has gone to working out the NLO(α_s)/LL contribution to incorporate one-loop corrected amplitudes at the top of the shower. Adding α_s corrections involves the numerical challenge of combining real and virtual results which separately have IR divergences. The basic resolution is to extract the pole-portion of the real emission of i-partons and include it along with the virtual contributions to the $i-1$ case. Unfortunately, this does not sum leading logs. One cannot blindly extend the CKKW procedure to NLO(α_s)/LL, as it leads to double-counting problems; the Sudakov factors in the reweighting contain a portion of the one-loop contributions. Separately adding the full one-loop result would clearly overcount.

There are two main solutions to the NLO(α_s)/LL merging problem in the context of standard $1 \to 2$ splittings. MC@NLO [37] works by means of subtraction, finding the places where the Sudakovs will contribute at NLO(α_s),

and removing the splitting function contribution. This approach is conceptually clear. Since the full amplitude and splitting function portions are calculated separately before subtraction, the latter for each SMC program, this is time-consuming. Furthermore, since the subtractions occur for the amplitude squared, one cannot guarantee positivity of the result and must deal with negatively weighted events. To avoid the computational difficulties of process-by-process subtraction and negative weights, an alternative is the POWHEG algorithm [38]. It keeps the IR-safe NLO(α_s) cross section manifest, and defines a Sudakov factor based on a modified splitting function to handle $\mathrm{LL}_{\mathrm{exp}}$ and a subset of $\mathrm{NLL}_{\mathrm{exp}}$ resummation for the hardest emission. In this way, it makes use of quantities already obtained in the fixed order NLO(α_s) calculation, requiring fewer additional steps for its implementation for each known process. The conservation of probability obeyed by the splittings and related Sudakov factors avoid double countings and give back σ_{NLO} upon integration.

A separate set of approaches goes beyond the $1 \to 2$ formalism to consider the radiation's effects on one or more "spectators." The consideration of an additional parton in the pre-emission configuration has led to work known as dipole subtraction and dipole antennas. The former was initially developed in [39, 40]. It explicitly subtracts the IR divergence from real emission via a simplified "dipole" term. Refs. [41, 42] have proposed algorithms based on these techniques. There has also been development on the theoretical side of subtractions by Nagy and Soper [43–46], with the aim of including spin and color effects, while improving the efficiency of implementation [47]. The original use of antennas came in the ARIADNE program, which treats the $2 \to 3$ splitting as its basic unit [48–51] and allows for exact momentum conservation. There have since been more systematic attempts to extract the $2 \to 3$ "antenna" functions from QCD and implement them in a shower, *e.g.* VINCIA [52]. Ref. [53] even derives spin-dependent antenna functions, though its SMC implementation is yet to appear.

A different approach is the GenEvA framework [54, 55] which allows the issues of phase space double counting and combining matrix elements and log resummation to be treated independently. This is done using effective theory ideas for how to separate scales. In this setup, one manifestly avoids negative weights and double counting by using multiplicative merging. For example, GenEvA yields a calculation that is equivalent to POWHEG for the NLO(α_s)/LL matching and at the same time a CKKW-L type matching onto LO(α_s)/LL type matching for additional emissions. In a similar fashion, the power suppressed matrix element computations and subleading no-branching probabilities derived here could be implemented in GenEvA, and work in this direction is commencing.

Another approach to go beyond LL is to incorporate the contribution of the $\mathcal{O}(\alpha_s^2)$ corrections to the Altarelli-Parisi splitting kernels, $P_{qq}^{(1)}$. This was done to resum soft logs to NLL for semi-inclusive variables in DIS and Drell-Yan [56]. In order to conserve probability, these corrections must be correctly accounted for in both the probability for real emission in Eq. (3), as well as no-branching branching probabilities. This is related to why POWHEG only implements them for the hardest splitting, where they have information from the full fixed-order computation. The KRKMC group incorporates the subleading real emission contributions into fully exclusive partonic configurations in SMC [57–59]. Some of the subleading contributions take the form of $1 \to 3$ splittings, requiring a modification of the usual $1 \to 2$ algorithm. Similar to CKKW, the KRKMC groups corrections take the form of a multiplicative reweighting. For a particular configuration of partons in phase space, they reweight by a factor that includes the insertion of $1 \to 3$ "defects" and loop-corrected $1 \to 2$ splittings that account for the effects of $P_{qq}^{(1)}$. If ρ is the fully differential cross section, they define a corrected weight for n partons, w_n as:

$$w_n = \frac{\rho_{\mathrm{LO}}(k_1, \ldots, k_n) + \sum_{r=1}^{n/2} \rho_{\mathrm{N^rLO}}(k_1, \ldots, k_n)}{\rho_{\mathrm{LO}}(k_1, \ldots, k_n)}, \tag{7}$$

where r determines the number of defect insertions in any configuration. Since this reweighting involves splitting probabilities and not subleading no-branching probabilities, it does not clearly improve the level of log resummation.

In this work we set up an EFT framework to classify and study perturbative α_s corrections, higher order log resummation and/or kinematic power corrections to parton showers. While the ultimate goal is to facilitate the implementation of a NLL/NLO(α_s) parton shower algorithm accounting for the leading deviations from strong ordering, our task here is much more modest.[1] We focus primarily on kinematic power corrections in the fully differential cross section for an arbitrary number of final state emissions. That is, our main goal is to compute

$$\frac{d\sigma^{\mathrm{LO}}}{d\vec{p}_1^{\,3} \cdots d\vec{p}_n^{\,3}} + \frac{d\sigma^{\mathrm{NLO}(\lambda)}}{d\vec{p}_1^{\,3} \cdots d\vec{p}_n^{\,3}}\,. \tag{8}$$

Here NLO(λ) is the next-to-leading order power correction in the cross section, which involves terms that are NLO(λ) and NNLO(λ) in the amplitude. Similarly to [24, 25], we use an operator approach based on SCET. A main issue

[1] In particular we note that soft NLL resummation may only be feasible at leading orders in $1/N_c$ [60, 61].

to resolve is taking into account different possibilities for the kinematic configurations of subsequent emissions, to go beyond the strong ordering described in Eq (1). The hierarchy between regions is expressed by the power counting parameter $\lambda \ll 1$. We overcome this issue by setting up a tower of related soft collinear effective theories, called SCET_i, which also helps us deal with several technical obstacles. We formulate the shower description as a standard matching procedure between operators in different SCET_i. Power corrections are encoded by performing matching computations at subleading order in the kinematic expansion. These corrections modify the processes that initiate the shower, modify certain early branching probabilities, and open up the $1 \to 3$ splitting channel. Virtual perturbative α_s corrections are included by performing matching calculations beyond tree level between SCET_i theories. Finally, corrections to the Sudakov no-branching probabilities are encoded through anomalous dimensions of leading and subleading operators at the appropriate order within different SCET_i's. When we refer to a parton shower in the context of our calculations, we mean an explicit amplitude formula that would agree numerically with a corresponding shower algorithm. We will carry out the necessary computations for the power corrected matching equations, and a subset of the required calculations for anomalous dimensions occurring for operators beyond the LL shower. This analysis includes the leading corrections to the shower from interference and from spin correlations. As much as possible, we attempt to give pointers for additional computations that are needed in places where our analysis is incomplete. For example, to simplify things we have not treated color correlations since doing so increases the basis of operators and the number of computations, but does not change the conceptual setup.

The outline of our paper is as follows. We present a brief overview of SCET in Section II A. We review the Bauer-Schwartz SCET shower method in Section II B and discuss the technical obstructions to extending it to include power corrections. In Section II C, we present our SCET_i framework to resolve these issues. In Section III, we analyze the LL shower in the SCET_i framework, and show that the transition between SCETs, $\mathrm{SCET}_i \to \mathrm{SCET}_{i+1}$, can be encoded by operator replacement rules on single parton collinear fields. Soft emissions in SCET_i are discussed, and we summarize the correspondence between SCET_i objects and LL shower ingredients. In Section IV, we use the SCET_i formulation to classify and compute various corrections to the shower to $\mathcal{O}(\lambda^2)$ in the cross section. Two main categories of branching corrections emerge, which we refer to as "hard-scattering" and "jet-structure." We also discuss ingredients needed for renormalization group evolution corresponding to no-branching probabilities, derive all the LL anomalous dimensions for our subleading operators. Additionally, we mention the issues involved in obtaining $\mathrm{NLL}_{\mathrm{exp}}$ resummation from our results. A summary of corrections in the SCET_i framework is presented as a table in section IV E, including the type of corresponding ingredients needed in a subleading shower. We present in Eqs. (104)-(106) a parton shower reweighting factor that should allow one to implement our corrections. We also discuss the correspondence of these corrections with those currently included in other Monte Carlos. Conclusions are given in Section V. At the present time, we do not have an algorithmic implementation of our power suppressed shower results, but work in this direction is in progress.

Many details are relegated to the Appendices. Further details about SCET can be found in Appendix A. We describe finite reparametrization transformations in Appendix B, which is an important symmetry that we use in our matching computations to disentangle kinematic coordinate conventions from kinematic power corrections. Details on the matching of QCD $\to \mathrm{SCET}_1$, $\mathrm{SCET}_1 \to \mathrm{SCET}_2$, and $\mathrm{SCET}_2 \to \mathrm{SCET}_3$ can be found in Appendices C, D, and E, respectively. A complete list of the operators needed to compute Eq. (8) in SCET_N is given in App. E. Appendix F contains a cross-check on our results, where we integrate a subset of our power suppressed terms to rederive the abelian terms in $P^{(1)}_{q\to qg}$, namely the $\mathcal{O}(\alpha_s)$ correction to the $q \to qg$ splitting function [62].

Those readers looking to find a quick summary of our results should look in Secs. III C and IV E.

II. OBTAINING THE PARTON SHOWER WITH SCET

A. SCET Basics

Soft-Collinear Effective Theory is an effective field theory of QCD that describes the interactions of collinear and soft particles [20–23]. We present here the basic ideas needed for our analysis of the parton shower, including how collinear sectors are organized into equivalence classes by the power counting parameters. Further SCET concepts are reviewed in Appendix A.

The momentum, p, of any particle can be decomposed along two light-cone vectors, n and $\bar{n}$, with $n^2 = 0$, $\bar{n}^2 = 0$ and $n \cdot \bar{n} = 2$, as

$$p^\mu = \bar{p}\,\frac{n^\mu}{2} + p_\perp^\mu + n{\cdot}p\frac{\bar{n}^\mu}{2}\,, \tag{9}$$

where $\bar{p} = \bar{n} \cdot p$ and the particle's invariant mass is $p^2 = n \cdot p\, \bar{p} + p_\perp^2$. We use a Minkowskian notation for $p_\perp^2 = -\vec{p}_\perp^{\,2}$, where $\vec{p}_\perp$ is Euclidean. SCET's degrees of freedom include n_i-collinear fields for a set of distinct directions $\{n_i\}$, and

soft fields.[2] A particle is collinear to a direction n if its momentum scales as:

$$(n\cdot p,\,\bar{p},\,p_\perp)\sim(\lambda^2,\,1,\,\lambda)\,\bar{p}\,, \tag{10}$$

where $\bar{p}\sim Q$ is some hard scale in the process, and $\lambda\ll 1$ is the SCET power counting parameter. A particle is soft if

$$(n\cdot p,\,\bar{p},\,p_\perp)\sim(\lambda^2,\,\lambda^2,\,\lambda^2)\,Q\,. \tag{11}$$

Collinear and soft fields have virtuality $\sim Q^2\lambda^2$ and $Q^2\lambda^4$, respectively. We obtain SCET from QCD by expanding in powers of λ, integrating out hard modes, and dividing the remaining ones into collinear and soft fields. Our collinear and soft degrees of freedom also contain all the IR regions that can be obtained by a rescaling of $\lambda\to\lambda^i$, for $i>1$. The leading order SCET Lagrangian is

$$\mathcal{L}^{(0)}_{\rm SCET}=\mathcal{L}^{(0)}_s+\sum_{n\in\{n_i\}}\mathcal{L}^{(0)}_n\,, \tag{12}$$

where $\mathcal{L}^{(0)}_n$ is defined in Eq. (A9) and has only interactions among particles collinear to the same n. $\mathcal{L}^{(0)}_s$ is the Lagrangian for soft interactions discussed further in App. A. Particles collinear to different directions can interact either by the exchange of soft modes, or from their coupling to other sectors in external operators. Two collinear sectors in SCET, n_1 and n_2, are distinct if [63]:

$$n_1\cdot n_2\gg\lambda^2\,, \tag{13}$$

so any particle is collinear in at most one direction within a given SCET. The collinear sectors $\{n_i\}$ in SCET are really sets of equivalence classes of null vectors, $\{[n_i]\}$, where the equivalence class is $[n_j]=\{n\in[n_j]|\,n\cdot n_j\lesssim\lambda^2\}$. A class $[n_j]$ consists of all light-like vectors connected to n_j^μ by a type-I reparametrization invariance (RPI) transformation, $n_j^\mu\to n_j^\mu+\Delta^\mu_{n_j\perp}$, where the scaling of the transformation parameter is $\Delta^\mu_{n_j\perp}\sim\lambda$ (see App. B for a detailed discussion of RPI). Physically, the class $[n_j]$ corresponds to light-like vectors for particles whose momenta is in a cone centered on $\vec{n}_j$ with an opening angle $\sim\lambda$ (*cf.* Fig. 15).

Thus, the defining concepts of a SCET-theory are its hard-scale Q, its collinear sectors $\{[n_i]\}$, and its power counting parameter λ which governs the importance of operators and the size of the collinear sectors in phase space.

Most of our discussion will involve interactions with collinear fields, and we use the notation χ_n for quarks and $\mathcal{B}^\mu_{n\perp}$ for gluons (definitions of these fields can be found in Eq. (A13), and they incorporate collinear Wilson lines built out of $\bar{n}\cdot A_n$ fields). We can match QCD onto a series of SCET operators organized by powers of λ. The key building blocks are: χ_n, $\mathcal{B}^\mu_{n\perp}$, and $\mathcal{P}^\mu_{n\perp}$ (a type of derivative operator that yields the perpendicular momentum of an n-collinear field), each of which scale as λ in the kinematic power counting. A general notation for the i-parton operators we will consider is:

$$\mathcal{O}^{(j,k,\ell)}\big(n_1^{[\ell_1]},\ldots,n_{j+k}^{[\ell_{j+k}]}\big)=\Big[\prod_{a=1}^{j/2}(\mathcal{P}_{n_a\perp})^{\ell_a}\chi_{n_a}\Big]\Big[\prod_{b=j/2+1}^{j}(\mathcal{P}_{n_b\perp})^{\ell_b}\bar{\chi}_{n_b}\Big]\Big[\prod_{c=1}^{k}(\mathcal{P}_{n_c\perp})^{\ell_c}g\mathcal{B}_{n_c\perp}\Big], \tag{14}$$

where the number of partons is the sum of quarks and gluons, $j+k=i$, and the total number of $\perp$ derivatives is $\ell=\sum_{m=1}^{j+k}\ell_m$. In the operator argument, we list the index labels, n_d, of the parton fields on the RHS. The superscripts in the argument on the LHS denote the number of derivatives acting on the field with the corresponding direction. There may be a degeneracy among the index labels, n_d, and so the operator has at most i distinct collinear directions. The scaling of these operators is $\mathcal{O}^{(j,k,\ell)}\sim\lambda^{j+k+\ell}$. They are tensors in the space of spinors and Lorentz vectors, and the indices get contracted with structures contained in the Wilson coefficient C for the operator. If $C\mathcal{O}$ is a Lorentz scalar, then j is even. Since the collinear fields carry a label referring to a specific light-cone vector, these operators describe particles in a specific region of phase space. SCET therefore distinguishes situations with the same particle content, but different kinematics, in a straightforward way.

For example, one can take an amplitude for three external particles: a quark, gluon, and antiquark. We can consider two different configurations, $|q_{n_0}g_{n_0}\bar{q}_{\bar{n}}\rangle$ and $|q_{n_1}g_{n_1'}\bar{q}_{\bar{n}}\rangle$. In the first, shown in Fig. 1(I), the quark and the gluon are

[2] Our primary interest here is the perturbative structure of jets, so we use SCET$_{\rm I}$ theories with collinear and ultrasoft modes. For simplicity we will always use the phrase soft in place of ultrasoft.

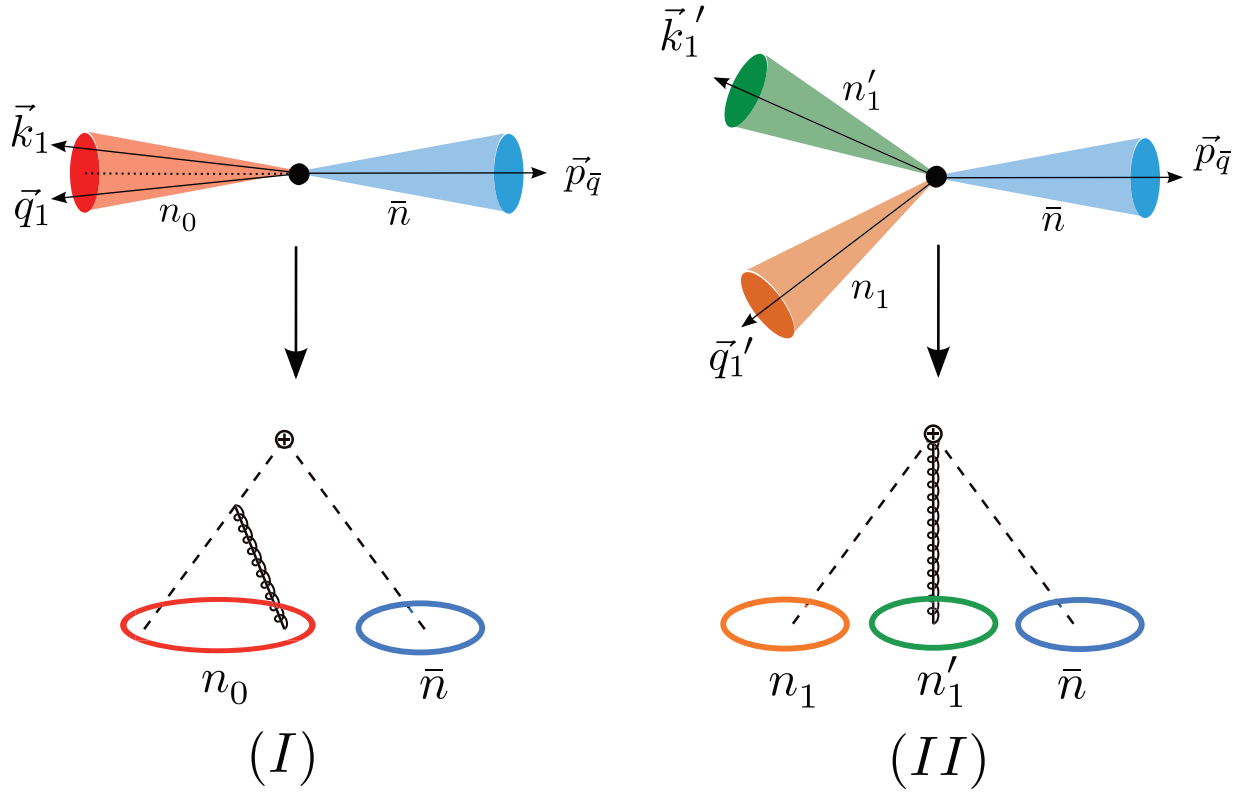

FIG. 1: Different kinematic configurations of a final state with a quark, antiquark, and gluon are described by different SCET operators. In (I), the quark and the gluon are collinear to the direction n_0, represented by their sharing a common cone. In (II), the vectors q_1' and k_1' are too far apart to be collinear. The Feynman diagrams show that collinear particles can come from Lagrangian insertions, whereas non-collinear ones arise exclusively from higher-multiplicity operators. The Feynman diagram in (I) only depicts the first term on the RHS of Eq. (16).

n_0-collinear, and the antiquark is collinear to a different direction, $\bar{n}$. Here the amplitude is described by operators with two distinct directions, say

$$\mathcal{O}^{(2,0,0)}(n_0,\bar{n}) = \bar{\chi}_{n_0}\Gamma\chi_{\bar{n}} \sim \lambda^2\,, \qquad \mathcal{O}^{(2,1,0)}(n_0,n_0,\bar{n}) = \bar{\chi}_{n_0} g\mathcal{B}^{\mu}_{n_0\perp}\Gamma'\chi_{\bar{n}} \sim \lambda^3\,, \tag{15}$$

where the form of the Dirac structures Γ and Γ' are not central to our discussion here. $\mathcal{O}^{(2,0,0)}$ can emit $\bar{n}\cdot A_{n_0}$ gluons from the Wilson line in χ_{n_0}, but requires a Lagrangian insertion to emit an $A^{\perp}_{n_0}$ gluon. Schematically, the amplitude for a transverse gluon has contributions:

$$A^I = \int dx\, \langle 0|T\left\{\mathcal{L}^{(0)}_{n_0}(x)\,\bar{\chi}_{n_0}\Gamma\chi_{\bar{n}}(0)\right\}|q_{n_0}g_{n_0}\bar{q}_{\bar{n}}\rangle + \langle 0|\bar{\chi}_{n_0}g\mathcal{B}^{\mu}_{n_0\perp}\Gamma'\chi_{\bar{n}}(0)|q_{n_0}g_{n_0}\bar{q}_{\bar{n}}\rangle\,. \tag{16}$$

In Fig. 1(II), each of the particles is collinear to a distinct direction, so no cone of size $\sim\lambda$ fits two of the momenta. In this case, the amplitude can only come from an operator with three distinct labels, such as $\bar{\chi}_{n_1}\mathcal{B}^{\mu}_{n_1'\perp}\Gamma''\chi_{\bar{n}}$:

$$A^{II} = \langle 0|\bar{\chi}_{n_1}g\mathcal{B}^{\mu}_{n_1'\perp}\Gamma''\chi_{\bar{n}}|q_{n_1}g_{n_1'}\bar{q}_{\bar{n}}\rangle\,. \tag{17}$$

The ability of SCET to cleanly separate contributions such as those in Eqs. (16) and (17) will be useful for formulating a complete set of power suppressed corrections to the parton shower.

B. Bauer-Schwartz Method

The original application of SCET to study and improve the parton shower was carried out in [24, 25] by Bauer & Schwartz. The main reasons why SCET is useful for this are:

- The SCET fields, soft and collinear quarks and gluons, have support in the infrared exactly where the parton shower amplitudes have their dominant contributions in phase space.

- Since SCET is improvable order-by-order in the kinematic expansion parameter, λ, one has the potential to systematically correct the shower.

We will give a short overview of the Bauer-Schwartz approach, and then discuss the complications that arise when trying to extend the analysis to NLO in the λ expansion, namely NLO(λ). In this section we will use notation that is not found elsewhere in the paper to retain consistency with [24, 25].

The procedure of [24, 25] starts by constructing i-parton operators, $\mathcal{O}_i$, through matching SCET to QCD at a hard scale. For example, their $\mathcal{O}_2$ will equal $\mathcal{O}^{(2,0,0)}(n_1,\, n_2)$ in the notation of Eq. (14), and $\mathcal{O}_3$ will be $\mathcal{O}^{(2,1,0)}(n_1,\, n_2,\, n_3)$. As we run $\mathcal{O}_i(\mu)$ down, the leading log renormalization group evolution (LL RGE) does not mix operators and the exponential evolution kernel encodes the no-branching probability. The evolution continues until another parton becomes apparent at a scale $\mu = p_T$.

If we have an i-parton operator, $\mathcal{O}_i = \mathcal{O}^{(j,i-j,0)}(n_1, \ldots, n_i)$ with all n's distinct, then it has the RG solution $\mathcal{O}_i(\mu) = U^{(j,i-j,0)}(Q,\mu)\mathcal{O}_i(Q)$ with

$$U^{(j,i-j,0)}(Q,\, \mu) \,=\, \exp\left[-\int_\mu^Q \frac{d\mu'}{\mu'}\gamma^{(j,i-j,0)}(\mu')\right], \tag{18}$$

where $\gamma^{(j,i-j,0)}$ is the operator's anomalous dimension. The leading-log resummation effects of the Sudakov factor in the PS enter through one-loop operator running in SCET, as dictated by the cusp anomalous dimension. The one-loop cusp portion is especially easy to calculate in SCET as it depends solely on the number of collinear fields, even though the calculations have loops involving soft ones as well [24, 25],

$$\gamma_{\rm LL}^{(n_q,n_g,0)}(\mu) \,=\, -\frac{\alpha_s}{\pi}\left[\frac{n_q}{2}C_F + \frac{n_g}{2}C_A\right]\log\frac{\mu^2}{Q^2}\,. \tag{19}$$

This form of the kernel gives a product of Sudakov factors which are the no-branching probabilities for each parton in the operator:

$$U_{\rm LL}^{(j,i-j,0)}(Q,\, \mu) \,=\, \Delta_q^{\frac{j}{2}}(Q,\, \mu)\Delta_g^{\frac{i-j}{2}}(Q,\, \mu). \tag{20}$$

Here, as in [27], one accounts for leading-log effects for any particle multiplicity by simply multiplying matrix elements by appropriate Sudakov factors.

As we run $\mathcal{O}_i(\mu)$ down, another parton becomes apparent at a scale $\mu = p_T$. To account for this, Bauer-Schwartz devised a "threshold matching" of $\mathcal{O}_i$ to a new, higher multiplicity operator, $\mathcal{O}_{i+1}^{(i)}$, where the subscript still denotes the number of partons in the operator and the superscript tracks the parent operator. The general threshold matching equation is

$$\left[C_n^{(j)}\langle\mathcal{O}_n^{(j)}\rangle\right]_{\mu=p_T+\epsilon} = \left[C_{n+1}^{(j)}\langle\mathcal{O}_{n+1}^{(j)}\rangle\right]_{\mu=p_T-\epsilon}. \tag{21}$$

After further running and threshold matching, we eventually have $\mathcal{O}_n^{(i)}$ for various $n > i$. The $n-i$ particles emitted at increasingly lower scales by this process correspond to the parton showering of the original fields created at the hard scale by $\mathcal{O}_i$. Additionally, they also showed that an appropriate list of SCET operators ($\mathcal{O}_i$'s and $\mathcal{O}_i^{(n)}$'s) can interpolate between fixed-order QCD and parton shower (PS) calculations of IR-safe observables. Furthermore, they derived the $\mathcal{O}(\alpha_s)$ effects from matching QCD to SCET at one-loop for $\mathcal{O}_3$.

That subsequent emissions reproduce the usual parton shower splitting function emerges easily from SCET. Consider an operator $\mathcal{O}_i = \bar\chi_{n_0}\Omega$, where Ω is arbitrary and we have made explicit a single collinear quark field, $\bar\chi_{n_0}$. If we emit a collinear gluon from this quark, $q(q_0^\mu) \to q(q_1^\mu)g(k_1^\nu)$, the amplitude for the process is

$$A_{LO}^{X+qg} \,=\, \bar u_{n_0}(q_1)\rho^\alpha\frac{\bar q_0}{q_0^2}\Omega, \tag{22}$$

where u_{n_0} is the collinear quark spinor, and ρ^α is the combination of the SCET single gluon emission Feynman rule plus the $\bar\chi_{n_0}$ Wilson line emission (the quark $\mathcal{L}_n^{(0)}$ can be found in Eq. A9),

$$\rho^\alpha = n_0^\alpha + \frac{(\not q_1)_{n_0\perp}\gamma^\alpha_{n_0\perp}}{\bar q_1} + \frac{\gamma^\alpha_{n_0\perp}(\not q_0)_{n_0\perp}}{\bar q_1} - \frac{\bar n^\alpha}{\bar q_0}\left[\frac{q_0^2}{\bar k_1} + \frac{(\not q_1)_{n_0\perp}(\not q_0)_{n_0\perp}}{\bar q_1}\right]. \tag{23}$$

Note that ρ^α in SCET comes entirely from $\bar\chi_{n_0}$ without reference to anything residing in Ω. The subscript $(n_0\,\perp)$ refers to components perpendicular to n_0^μ and $\bar n^\mu$, which we denote by $\perp$ for the remainder of this computation.

The amplitude in Eq. (22) is gauge invariant and $k_1^\alpha \rho_\alpha = 0$. Squaring A_{LO}^{X+qg} and summing over spins we have $\sum_{spin} \bar{u}_{n_0}(q_1) u_{n_0}(q_1) = \bar{q}_1 \not{n}_0/2$, and the gluon polarization sum denoted $\sum_{spin} \epsilon_\alpha \epsilon^*_\beta = d_{\alpha\beta}$. Since ρ^α commutes with $\not{n}_0$, we get an answer proportional to $\rho^\alpha \rho^{\dagger\beta} d_{\alpha\beta}$, where without loss of generality we can use a light-cone gauge, $d_{\alpha\beta} = -g_{\alpha\beta} + (\bar{n}_\alpha k_{1\beta} + k_{1\alpha}\bar{n}_\beta)/\bar{k}_1$. Crucially, this is a Dirac scalar:

$$\rho^\alpha \rho^{\dagger\beta} d_{\alpha\beta} \;\equiv\; |\rho|^2 \;=\; 2\Big(\frac{2\,q_0^2}{\bar{k}_1\bar{q}_0} - \frac{q_{1\perp}^2}{\bar{q}_1^2} + \frac{2q_{0\perp}\cdot q_{1\perp}}{\bar{q}_0\bar{q}_1} - \frac{q_{0\perp}^2}{\bar{q}_0^2}\Big) \times \mathbb{I}_4, \tag{24}$$

where we have used the on-shell conditions $q_1^2 = 0$ and $k_1^2 = 0$.

In a frame where $q_0^\perp = 0$ we have $q_{1\perp} = -k_{1\perp}$ and $\bar{q}_0/q_0^2 = 1/(n_0\cdot q_0)$. Here $n_0\cdot q_0 = n_0\cdot k_1 + n_0\cdot q_1 = -k_{1\perp}^2/[\bar{q}_0\, z(1-z)]$, where $z \equiv \bar{q}_1/\bar{q}_0$. Thus we have the simpler expression

$$\rho^\alpha = n_0^\alpha + \frac{(\not{q}_1)_{n_0\perp}\gamma^\alpha_{n_0\perp}}{\bar{q}_1}, \tag{25}$$

which we have written in light-cone gauge without the Wilson line contribution ($\propto \bar{n}^\alpha q_0^2$), and

$$\rho^\alpha \rho^{\dagger\beta} d_{\alpha\beta} \;=\; 2\Big(\frac{2\,n\cdot k_1}{\bar{k}_1} - \frac{2q_{1\perp}^2}{\bar{q}_1\bar{k}_1} - \frac{q_{1\perp}^2}{\bar{q}_1^2}\Big) \times \mathbb{I}_4 = -\frac{2\,k_{1\perp}^2}{\bar{q}_0^2}\,\frac{(1+z^2)}{z^2(1-z)^2}\,. \tag{26}$$

Putting these properties together in the full amplitude squared we get

$$\begin{aligned} |A_{LO}^{X+qg}|^2 &= \frac{g^2 C_F}{(n_0\cdot q_0)^2}\frac{\bar{q}_1}{2}\,\mathrm{Tr}\left[\not{n}_0 \rho^\alpha \Omega\Omega^\dagger \rho^{\dagger\beta}\right] d_{\alpha\beta} = \frac{g^2 C_F\,\bar{q}_1}{(n_0\cdot q_0)^2}|\rho|^2\,\mathrm{Tr}\left[\frac{\not{n}_0}{2}\Omega\Omega^\dagger\right] \\ &= g^2 C_F\, 2z\,\frac{(1+z^2)}{|k_{1\perp}|^2}\,\mathrm{Tr}\left[\bar{q}_0\frac{\not{n}_0}{2}\Omega\Omega^\dagger\right]. \end{aligned} \tag{27}$$

Thus, all information about the emission factors out to the front and is independent of the rest of the process encoded by Ω. Since the power expansion is built into SCET, there was no need to expand terms in the amplitude to obtain this result (unlike the analogous computation in full QCD). In order to recover Eq. (3), we still need to include the z-dependence from phase space, since $P_{jk}^{(0)}(z)$ operates at the level of the cross section. Using $d^3k/(2E_k) = d\bar{k}d^2k_\perp/(2\bar{k})$, for q_1 and k_1 we have

$$\frac{d\bar{q}_1 d^2q_{1\perp}}{2\bar{q}_1}\frac{d\bar{k}_1 d^2k_{1\perp}}{2\bar{k}_1} \to \frac{d\bar{q}_0 d^2q_{0\perp}}{2\bar{q}_0}\frac{dz\,d^2k_{1\perp}}{2z(1-z)}, \tag{28}$$

where the arrow means that we insert $d^4q_0\,\delta^{(4)}(q_0 - q_1 - k_1)$ and integrate d^3q_1 along with $d(n_0\cdot q_0)$. Thus, we recover the expected $1/(1-z)$ dependence from the measure. Combining pieces and performing the trivial azimuthal integral $d\phi_{k_1}$, we get the expected expression:

$$d\sigma_{X+qg} \;=\; dz\,\frac{dk_{1\perp}^2}{k_{1\perp}^2} P_{q\to qg}^{(0)}(z)\, d\sigma_{X+q}, \tag{29}$$

where $P_{q\to qg}^{(0)}(z)$ is the quark splitting function in Eq. (3). Here $d\sigma_{X+q}$ is the cross section for the rest of the process with emission of a momentum q_0 quark, and the corresponding amplitude squared is $\mathrm{Tr}\left[\frac{\bar{q}_0}{2}\not{n}_0\Omega\Omega^\dagger\right]$. Whether Ω represents a simple hard current or an entire chain of collinear splittings, we see that the $q \to qg$ emission factors out with the expected soft-collinear double pole, as in Eq. (2).

In order to obtain their results, Bauer-Schwartz introduced choices and approximations at several points which obscure the path toward systematically computing NLO(λ) corrections. Indeed, they concluded that obtaining these corrections may be prohibitively difficult [25]. Some of the issues one encounters trying to work at higher orders are:

1. At NLO(λ), it becomes crucial to distinguish which simplifications correspond to approximations with power corrections, and which involve a choice of coordinates where a symmetry makes the final answer coordinate independent. For example, a collinear state typically has nonzero momentum components perpendicular to the index n of the field that annihilates it. Refs. [24, 25], however, dictated that collinear SCET fields in their operators only create particles whose momenta perfectly align with their index direction, n:

$$\chi_n|q\rangle \;=\; \delta_{n,n_q}, \quad \text{where } n_q^\mu = q^\mu/E_q, \tag{30}$$

leaving it ambiguous what amount of symmetry protects this choice. Eq. (30) enforces certain kinematical restrictions on final state particles, and requires that fermion fields be rotated to an appropriate n_q^μ via $\xi_n \to (\not{n}\not{\bar{n}}/4)\xi_{n_q}$.

2. At LO, it was possible to avoid a potential double counting between collinear and soft fields by dropping soft emission and Wilson line emission, and taking only collinear emissions with transverse polarization. The threshold matching procedure is designed to avoid double counting of collinear operators, such as a Lagrangian emission from $\mathcal{O}_2$ and direct emission from $\mathcal{O}_3^{(2)}$, since only one of these is allowed to operate at a time. However, the threshold matching in Eq. (21) makes the technical procedure for incorporating power corrections unclear.

3. Threshold matching contains another impediment to systematic improvement. Through this procedure, the initial operator $\mathcal{O}_2$ has nonzero projection onto Fock states of any multiplicity, but the number of particles created by an operator is a scale-dependent question. The matching scales are determined by the strong ordering kinematics, $p_{1\perp} \gg \ldots \gg p_{m\perp}$. At the scale of an emission, say $p_{1\perp}$, one threshold matches to the operator $\mathcal{O}_3^{(2)}$, which only adds one parton at a time. However, going to higher orders in the shower necessitates more general configurations.

In carrying out their method, Bauer-Schwartz carefully enumerated the above approximations. They affect the ability to include corrections in λ, but do not impact the terms necessary for a LL shower.

Building on the work of Refs. [24, 25], the main goal of the framework we develop in the next section is to overcome this list of issues so that we can determine power corrections to the shower using SCET.

C. Using SCET$_i$

The main feature of the parton shower is the ability to capture the dominant physics of particles emitted in kinematically hierarchical regions of phase space. Our goal is to formulate the SCET interface with the shower using a standard sequence of matching and running steps in different versions of SCET,

$$\text{QCD} \to \text{SCET}_1 \to \text{SCET}_2 \to \cdots \to \text{SCET}_N \,. \tag{31}$$

We refer to this as the SCET$_i$ procedure. The key distinction between a SCET at one stage and the next is the definition of the corresponding resolution parameters $1 \gg \lambda_1 \gg \lambda_2 \gg \cdots \gg \lambda_N$, where λ_i sets the power counting for SCET$_i$. As we move down the chain, the corresponding SCET resolves smaller $\sim (Q\lambda_j)^2$ invariant masses and relative squared perpendicular momenta, and has a different meaning for its collinear sectors $\{[n_i]\}_{\text{SCET}_j}$. To keep track of this, we will attach a subscript to the operators to denote the SCET$_i$ in which its fields live,

$$\mathcal{O}_i^{(j,k,\ell)}(n_1, \ldots, n_{j+k}) \,. \tag{32}$$

Effectively with Eq. (31), we partition the momenta of partons in the shower history into classes,

$$\Omega_0 \supset \Omega_1 \supset \ldots \supset \Omega_N \,, \tag{33}$$

where Ω_j contains the momenta of all propagators having $p^2 \sim (Q\lambda_j)^2$ or smaller, or an equivalent condition on relative perpendicular momenta. The allowed momenta in Ω_i correspond to the collinear modes of SCET$_i$. The sequence of SCET$_i$'s is truncated when we resolve a scale of order the parton shower cutoff, $Q\lambda^N = p_T^{\text{cut}} \simeq 1\,\text{GeV}$, that is in SCET$_N$.

Note that we do not associate a large hierarchy to the hard scales $\bar{p}_i$ between SCET$_j$ and SCET$_{j+1}$. That is to say we do not associate the energy loss due to splitting with a power of λ_j. Instead if Q is the scale of the primary hard interaction then we consider $\bar{p}_i \sim \eta^j\, Q$ in SCET$_j$, where $\eta \gg \lambda_j$ and for numerical estimates we can take $\eta \sim \frac{1}{2}$. (For each branching the geometric mean of the two daughters' $\bar{p}$ fraction averages to 0.4 which is roughly one half.) Parametrically, the decrease in the parton energy is not as rapid as that for the perpendicular momenta encoded in the power counting parameter λ_j. In principle, we can account for η as a separate factor. In practice, we will be most interested in tracking powers of λ_j and will only include η factors in places where the corresponding powers of two have a numerical impact on the implementation, or if we wish to disentangle the changes in offshellness due to strong-ordering effects and those coming from the more modest decrease in $\bar{p}_i$.

The strongly ordered configuration of partons in Eq. (1) corresponds with removing a single q_j^2 in Ω_j as we pass from $\Omega_j \to \Omega_{j+1}$. However, with Eq. (33), nothing stops us from having multiple emissions at a single scale. If two mother particles, with q_j^2 and q_{j+1}^2, are associated to the same Ω_k, then when we integrate out that scale in SCET$_{k+1}$ this configuration just contributes to an operator with a different parton multiplicity from the strongly ordered one. Thus, with Eq. (31) there is no obstacle to considering corrections from an arbitrary assignment of q_j^2's to Ω_k's. This resolves issue 3. of Sec. II B since we can treat emissions where the shower tree has momenta with the same parametric scaling in λ.

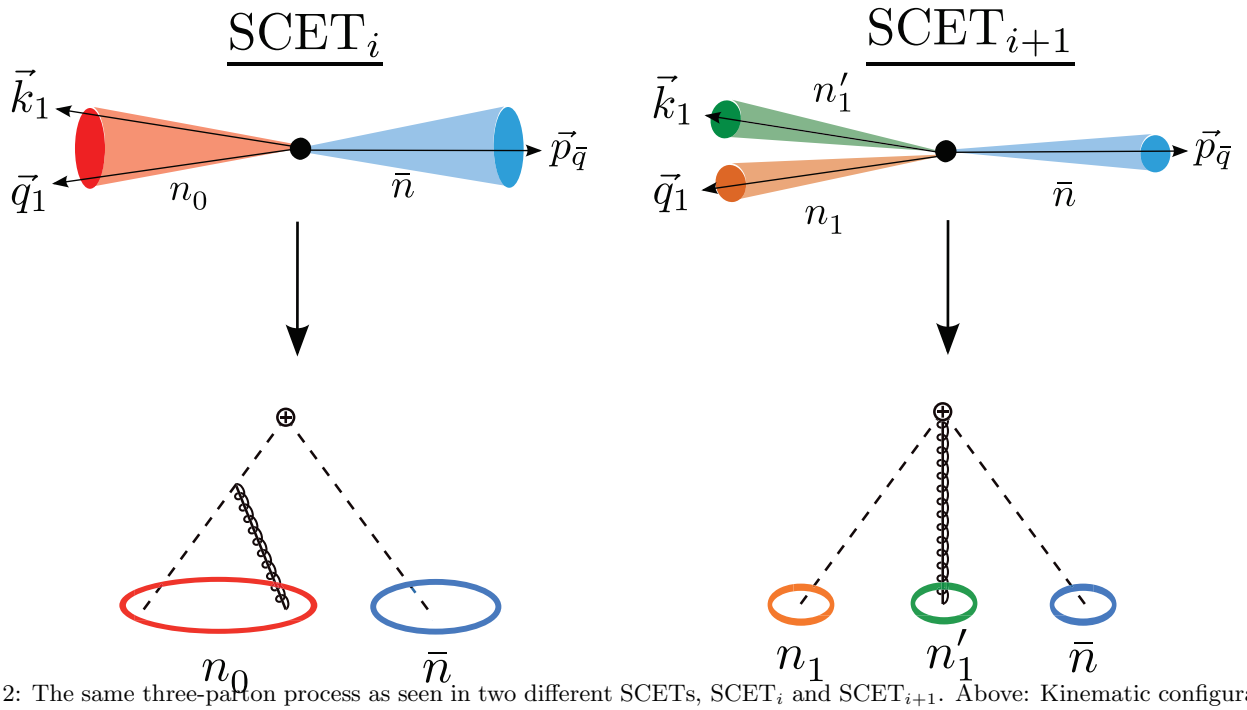

FIG. 2: The same three-parton process as seen in two different SCETs, SCET$_i$ and SCET$_{i+1}$. Above: Kinematic configuration of the quarks and gluon. The solid cones represent the regions considered collinear to the vectors drawn. Below: Feynman diagrams for the corresponding amplitude. Note that in SCET$_{i+1}$ we have removed a degree of freedom that propagates in SCET$_i$. The amplitude thus comes from a higher dimension operator $\mathcal{O}_{i+1}^{(1)}$, rather than from a time-ordered product of $\mathcal{L}_{\text{SCET}_i}$ with $\mathcal{O}_i^{(0)}$, as it did in SCET$_i$.

.

To carry out calculations in the SCET$_i$ framework, it is convenient and sufficient to take a specific definition of the power counting parameters, $\lambda_i = (\lambda)^i$. We want the hierarchy between neighboring splittings to stay the same throughout the shower so as not to privilege any portion of it. We will see in Sec. IV D that this democratic setup allows us to interpret part of our $\mathcal{O}(\lambda)$ corrections to i-parton amplitudes as universal corrections to the splitting probability, given at LO by Eq. (3). As we go to lower scales, our definition of collinearity also changes, and by analogy to Eq. (10), fields collinear to n within Ω_i have:

$$(n\cdot q_i,\, \bar{q}_i,\, q_{i\perp}) \sim (\lambda^{2i},\, 1,\, \lambda^i)\, \bar{q}_i, \tag{34}$$

and virtuality $\sim (\bar{q}_i)^2\lambda^{2i}$. In SCET$_i$, $\mathcal{L}_n^{(0)}$ again only couples collinear fields in the same direction n. Since different SCET$_i$'s have different definitions of collinearity, our description of identical physical processes changes when we switch to a theory with a lower scale. For convenience, we will use the same auxiliary vector $\bar{n}^\mu$ for any n_j-collinear field in any SCET$_i$. If $\bar{n}$ is a valid auxiliary vector for n-collinear fields in SCET$_1$, then it is readily apparent that it will be a valid choice for all subsequent collinear fields in SCET$_i$'s that descend from an n-collinear mother in SCET$_1$. Our default choice is stronger: given a set of light-like vectors in $\{n_j\}$ in SCET$_1$ we take a light-like $\bar{n}$ that is parametrically close or aligned with the antiquark direction. We then adjust the magnitude of n_j^0 and of $\vec{n}_j$ so that $n_j^2 = 0$ and $\bar{n}\cdot n_j = 2$ (for a related discussion based on RPI see Appendix C).

We depict the different descriptions of the same physical configuration in Fig. 2, where the left panel is in SCET$_i$ and the right panel is in SCET$_{i+1}$. In SCET$_i$, the quark ($\vec{q}_1$) and gluon ($\vec{k}_1$) are n_0-collinear. This means that at LO they are emitted from a qqg vertex in the LO SCET$_i$ Lagrangian (or a Wilson line interaction). Schematically, the amplitude for a $\perp$-polarized gluon looks like[3]

$$A^{q\bar{q}g} \;=\; C^{(2,0,0)} \int dx \langle 0|T\{\mathcal{L}_{\text{SCET}_i}(x)\mathcal{O}^{(2,0,0)}\}|q\bar{q}g\rangle, \tag{35}$$

[3] From here on, we will drop the superscript (0) and the subscript n from the collinear Lagrangian.

namely like the first term in Eq. (16). The right-hand panel of Fig. 2 denotes the same configuration as seen by SCET_{i+1}. The scale of this theory is lower and the definition of collinearity stricter, so the quark and gluon are not collinear here. Therefore, the amplitude now comes from a three-parton operator,

$$A^{q\bar{q}g} \,=\, C^{(2,1,0)}\langle 0|\mathcal{O}^{(2,1,0)}|q\bar{q}g\rangle, \tag{36}$$

as in Eq. (17). We match $\mathrm{SCET}_i \,\to\, \mathrm{SCET}_{i+1}$ to calculate $C^{(2,1,0)}$.

Given the above conventions and with the notation in Fig. 2 at hand, it is worth stating some simple kinematic relations that we will use later on. Take an n_0-collinear mother particle of momentum $q_0^\mu = q_0^+(\bar{n}^\mu/2) + \bar{q}_0(n_0^\mu/2)$. Let q_0 decay to two onshell massless daughters, k_1 and q_1, with momentum fractions x and $(1-x)$, back-to-back $\perp$-momenta $\vec{k}_\perp$, and light-like directions n_1 and n_1', then

$$k_1^\mu = k_1^+\frac{\bar{n}^\mu}{2} + \bar{k}_1\frac{n_0^\mu}{2} + k_\perp^\mu = \bar{k}_1\frac{n_1'^\mu}{2}\,, \qquad\qquad q_1^\mu = q_1^+\frac{\bar{n}^\mu}{2} + \bar{q}_1\frac{n_0^\mu}{2} - k_\perp^\mu = \bar{q}_1\frac{n_1^\mu}{2}\,. \tag{37}$$

Note that our convention of using the same $\bar{n}^\mu$ auxillary vector ensures that in these decompositions the momentum multiplying n_0^μ is the same as the momentum multiplying $n_1^{(\prime)\mu}$. The collinearity of k_1 and q_1 can be determined by the size of $k_\perp^2$, q_0^2, or $n_1\cdot n_1'$, and the relation between these three choices is

$$n_1\cdot n_1' = \frac{2\,\vec{k}_\perp^2}{(\bar{q}_0)^2\,x^2(1-x)^2} = \frac{2\,q_0^2}{(\bar{q}_0)^2\,x(1-x)}\,. \tag{38}$$

Since we take $\vec{k}_\perp^2/(\bar{q}_0)^2 \sim \lambda_i^2$ in SCET_i, we have $q_0^2/(\bar{q}_0)^2 \sim \lambda_i^2/\eta^2$ and $n_1\cdot n_1' \sim \lambda_i^2/\eta^4$. Thus, all three choices are equivalent for counting powers of λ_i, but differ with respect to how powers of the energy loss parameter $\eta \sim 1/2$ appears.

After this introduction to SCET_i, we now list some technical advantages of this framework for our analysis:

1. Collinear fields in SCET with different n-labels, as well as soft fields, do not overlap in Hilbert space. This allows us to separate an i-jet process with i distinguished partons, from an $(i-1)$-jet process with i partons, where two are collinear and unresolved. Lower-scale SCET_i's distinguish configurations more finely based on their stricter definition of collinearity. This resolves issue 2, avoiding the double-counting of similar configurations, from Sec. II B. This SCET property also illuminates simplified structures in the power corrections, such as the form of the amplitude interference (cf. section IV D).

2. Soft modes communicate between collinear sectors and threaten the factorization of different jets. Fortunately, SCET constrains the interactions they have with collinear fields. In fact, one can decouple them using soft Wilson lines in the LO SCET Lagrangian. At LO, using the SCET_i soft Wilson lines, we maintain factorization, obtain angular ordering, and rederive the coherent branching of soft emissions (cf. section III B). Soft interactions which are power suppressed can also be systematically studied in SCET with Lagrangians available in the literature [64–66], which we give in Eq. (108).

3. In SCET_i, we have a symmetry group RPI_i which corresponds to coordinate choices. In SCET_{i+1}, only a subset of this, $\mathrm{RPI}_{i+1} \,\subset\, \mathrm{RPI}_i$, remains a symmetry of the new theory. The kinematics in the coset portion $\mathrm{RPI}_i/\mathrm{RPI}_{i+1}$ within SCET_i give a set of higher-dimension operators in SCET_{i+1}, and describe configurations which would not otherwise be contained in the SCET_{i+1} Lagrangian (cf. section III and Appendix B). This resolves issue 1. from Sec. II B making the difference clear between approximations and conventions chosen for simplicity.

4. In matching between SCET_i and SCET_{i+1}, suppressed operators in the lower-scale theory are needed to reproduce the physics of the higher one. It can be proven that all higher order purely collinear operators can be built from quark fields (χ_n), perpendicular gluon fields ($\mathcal{B}_{\perp n}$), and the perpendicular momentum operators ($\mathcal{P}_{\perp n}$) [67]. Thus the symmetries and equations of motion of SCET greatly simplify the operator basis one needs to consider at each order in λ (cf. section IV and Appendices C, D, and E).

The final SCET_N corresponds to the scale where the shower stops, *i.e.* where $Q\eta^N\lambda^N \sim p_T^{\mathrm{cut}}$. In SCET_N, we only need the coefficients of the operators where all collinear partons have distinct n-labels, and which have no $\mathcal{P}_{n\perp}$'s, $C_N^{(j,k,0)}\mathcal{O}_N^{(j,k,0)}$. Once we reach the physical resolution scale, it is only meaningful to have one collinear parton in each distinguished block of phase space. Using RPI_N, we can set $n_j^\mu = p_j^\mu/p_j^0$. This is as in Eq. (30), but we only do this when we run up against the physical limit that requires just one parton per equivalence class. At intermediate stages, we allow different fields to share n-labels, which also results in operators containing $\mathcal{P}_{n\perp}$. The coefficients

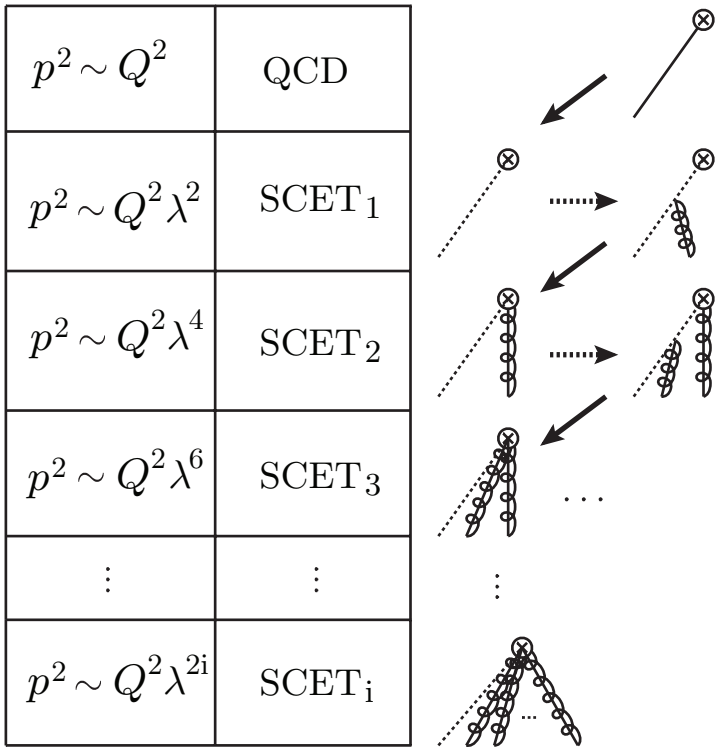

FIG. 3: Operators that reproduce strongly-ordered gluons are constructed through a series of matching computations with emissions in different SCET_j. The horizontal dashed arrows refer to the radiation of a gluon from a time-ordered product of the SCET_j Lagrangian with the operator creating fields at the point marked by $\otimes$. The diagonal solid arrows denote the matching onto a higher multiplicity operator in SCET_{j+1}.

$C_N^{(j,k,0)}$ encode the history of the shower. They can be written entirely in terms of: dot products $n_i \cdot n_{i'}$, equivalent to products of final parton momenta, which carry the scaling in λ; hard momenta $\bar{p}_i$, the renormalization scale μ, and collinear cutoff parameters encoded in Θ-functions.

As far as the shower is concerned, λ is merely a bookkeeping device which determines what pieces are needed beyond LO. One could try defining $\lambda_1 = k_{1\perp}/Q$, $\lambda_2 = k_{2\perp}/Q$, etc., but this is not ideal since there is a chance for events where $k_{1\perp} \sim Q$ or $k_{1\perp} \sim p_T^{\mathrm{cut}}$. The organization in Eq. (33) instead exploits the fact that *on average* showers are strongly-ordered. Our expansion in λ will then *on average* give a description of the most likely deviations from strong-ordering. Our goal in using the SCET_i framework is to extract an amplitude suitable for reweighing the parton shower to this level of accuracy.[4] From the SCET side, we pass to the shower weights built from SCET_N squared amplitudes (*cf.* Eqs. 104-107). They contain the information needed to describe a strongly-ordered shower and its leading kinematic corrections.

Before proceeding to our computations, it is worth commenting explicitly on which shower ingredients we do not compute. We only treat the case of a showering quark $q \to qg$ and in general take the abelian limit of QCD ($C_A = 0$). We have left out gluon splittings, $g \to q\bar{q}$ and $g \to gg$, from this analysis, though we expect that the extension to these cases should be straightforward. We have also not determined the effect of NLO(λ) power corrections from subleading soft interactions, although we briefly examine the factorized structure of LO softs in section (III B). These items are all left to future investigations.

III. PARTON SHOWER IN SCET VIA OPERATOR REPLACEMENT

In the previous section, we presented our approach of using a series of EFTs, the SCET_i, to handle processes with a hierarchy of many scales. We will now use this technique to calculate the leading contribution to a series of collinear

[4] As a well-defined EFT, one certainly could also do standard factorized cross section computations in any SCET_i if one wanted.

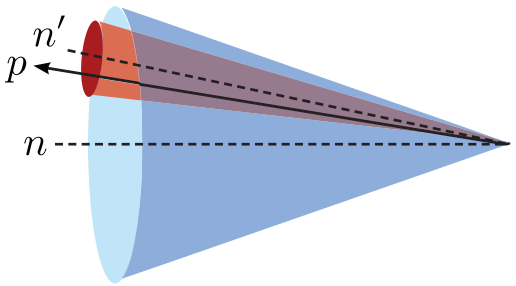

FIG. 4: The opening angle of the light grey (blue) cone is $\sim \lambda^{2i}$, and the opening angle of the dark grey (red) one is $\sim \lambda^{2(i+1)}$. The particle with momentum p is collinear to both n and n' in SCET$_i$, but only to n' in SCET$_{i+1}$. RPI$_i$ allows us to move the field label, n, to any location inside the appropriate cone for SCET$_i$ while keeping the theory invariant.

emissions, as occurs in the parton shower. Our ultimate goal is to incorporate corrections, but as a starting point we want to easily reproduce the strongly-ordered configuration of Eq. (1). We can do this if we declare that in a shower, the i^{th} particle decomposes as:

$$(n \cdot q_i,\, \bar{q}_i,\, q_{i\perp}) \sim (\lambda^{2i},\, 1,\, \lambda^i)\, \bar{q}_i, \tag{39}$$

and therefore has virtuality $q_i^2 \sim (\bar{q}_i)^2 \lambda^{2i}$ (*cf.* Fig. 8). This is exactly the same condition as Eq. (34), which we used to define the EFT, SCET$_i$.

To calculate the operators that describe i emissions in the strongly-ordered limit, we will perform a series of matchings SCET$_i \to$ SCET$_{i+1}$. We will find that the most efficient way to describe the process at LO in λ is to be in SCET$_{i+1}$ for i-parton radiation. Thus, we emit and match i-times in series, as shown by Fig. 3. At LO, we will show that one can implement this using an operator replacement rule. In the case of $q \to qg$ emission, it takes the form:

$$\chi_{n_1} \to c\, g \mathcal{B}^{\alpha}_{n_3\perp}\, \chi_{n_2}\,, \tag{40}$$

where χ_n and $\mathcal{B}^{\alpha}_{n\perp}$ are the SCET fields associated with collinear quarks and gluons, respectively, and c is the Wilson coefficient whose spin and color indices are suppressed. Though we do not compute them, there are similar $\mathcal{B}^{\alpha}_{n_1\perp} \to c'\, \bar{\chi}_{n_2} \chi_{n_3} + c''\, \mathcal{B}^{\beta}_{n_2\perp} \mathcal{B}^{\gamma}_{n_3\perp}$ rules as well. In SCET, each collinear field carries the label n, which gives its direction of collinearity. Note that the quark field on the LHS of (40) has a different one from those on the RHS. This relates to the stricter definition of collinearity in SCET$_{i+1}$ shown in Fig. 4. In order to perform the matching, we will make use of the reparametrization invariance (RPI) discussed in point 3. of Sec. II C to change fields' n-labels.

A. Leading Shower Revisited

We first want to reproduce the strongly-ordered contribution to i-gluon radiation from the quark in an initial $\gamma^* \to q\overline{q}$ pair production. Our iterative matching procedure for multiple EFTs takes a particularly simple form at LO in λ. For our standard example, we take the process $e^+e^- \to$ jets. Starting in QCD, we couple the quarks to another sector via the operator, $J^{\mu}_{\rm QCD} = \bar{q}\,\Gamma^{\mu} q$. This allows us to avoid complications that come from the initial state such as backward evolution. In SCET$_1$ (which is equivalent to the usual SCET), matching to QCD at tree-level converts the quark coupling to the following operator at LO: $\bar{\chi}_{n_0}\Gamma^{\mu}\chi_{\bar{n}}$, which produces q and $\bar{q}$ in different collinear directions. Details on the matching of QCD to SCET$_1$ are given in App. C. Using the notation in Eq. (14), we write the SCET$_1$ operator in the following way:

$$\bar{\chi}_{n_0}\Gamma^{\mu}\chi_{\bar{n}} = \left(C^{(2,0,0)}_{1,\,\rm LO}\right)_{ij} \left(\mathcal{O}^{(2,0,0)}_1(n_0,\bar{n})\right)_{ij}\,, \tag{41}$$

where

$$\begin{aligned} \left(\mathcal{O}^{(2,0,0)}_1(n_0,\bar{n})\right)_{ij} &= (\bar{\chi}_{n_0})_i (\chi_{\bar{n}})_j\,, \\ \left(C^{(2,0,0)}_{1,\,\rm LO}\right)_{ij} &= (\Gamma^{\mu})_{ij}\,, \end{aligned} \tag{42}$$

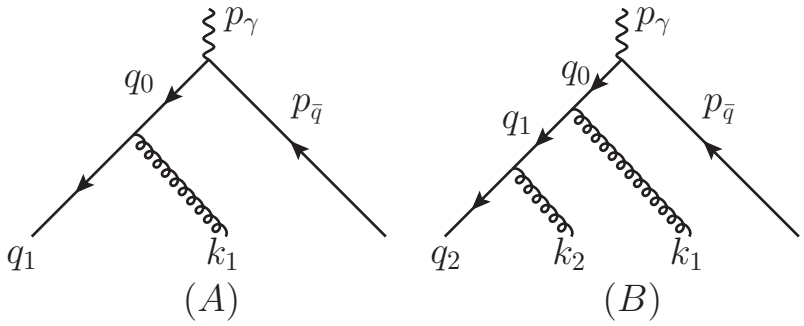

FIG. 5: Momentum labels for single (A) and double (B) gluon emission.

and i and j are spinor indices. The subscripts 1 in Eq. (42) indicate that the fields are defined in SCET_1. Our focus is on gluon emissions from the quark, and we always take the antiquark in the same direction, $\bar{n}$, therefore we drop it from the list of n-labels. Also, we will use the following shorthand notation for the most common operator,

$$\mathcal{O}_i^{(2,k,0)}(n_1, n_1', \ldots, n_k', \bar{n}) \equiv \mathcal{O}_i^{(k)}(n_1, n_1', \ldots, n_k')\,, \tag{43}$$

where the subscript marks these as being in SCET_i. In the rest of the paper, we will often drop the spinor indices. Using the above convention, we write the operator in Eq. (41) as:

$$\bar{\chi}_{n_0}\Gamma^\mu\chi_{\bar{n}} = C_{1,\,\mathrm{LO}}^{(0)}\mathcal{O}_1^{(0)}(n_0)\,. \tag{44}$$

The LO derivations are independent of the exact structure of Γ^μ. In fact, even the antiquark is a spectator, and we could just as easily use $\mathcal{O}^{(q)} = \bar{\chi}_{n_0}\Omega$, where Ω is arbitrary. However, as we will discuss in Sec. IV, matching QCD to SCET_1 at higher orders requires us to specify Ω.

To calculate operators in SCET_2, we start with single gluon radiation. In this case, shown in Fig. 5, the emission amplitude is:[5]

$$\begin{aligned} A_{\mathrm{LO}}^{q\bar{q}g} &= C_{1,\,\mathrm{LO}}^{(0)}\langle 0|\int dx\, T\{\mathcal{L}^{\mathrm{SCET}_1}(x)\mathcal{O}_1^{(0)}(n_0)\}|q_{n_0}g_{n_0}\bar{q}_{\bar{n}}\rangle & (45)\\ &= g\,\bar{u}_{n_0}(q_1)\left(n_0^\alpha + \frac{(\not{q}_1)_{n_0\perp}\gamma_{n_0\perp}^\alpha}{\bar{q}_1}\right)\frac{\bar{q}_0}{q_0^2}\Gamma^\mu v_{\bar{n}}(p_{\bar{q}}), & (46)\end{aligned}$$

where we have labeled the collinear directions of the particles in the state $|q_{n_0}g_{n_0}\bar{q}_{\bar{n}}\rangle$ for later convenience. The SCET_1 Lagrangian is given in Eq. (A9). Here we study the process in the center of mass frame with $p_\gamma = (Q, 0, 0, 0)$ and the quark (q_0) and antiquark ($p_{\bar{q}}$) along the directions $n_0 = (1, 0, 0, 1)$ and $\bar{n} = (1, 0, 0, -1)$, respectively:

$$\begin{aligned} p_\gamma^\mu &= \frac{Q}{2}n_0^\mu + \frac{Q}{2}\bar{n}^\mu\\ p_{\bar{q}}^\mu &= \frac{n_0\cdot p_{\bar{q}}}{2}\bar{n}^\mu,\\ q_0^\mu &= \frac{\bar{q}_0}{2}n_0^\mu + \frac{n_0\cdot q_0}{2}\bar{n}^\mu\,. \end{aligned} \tag{47}$$

We decompose the emitted quark (q_1) and gluon (k_1) along the directions $(n_0, \bar{n})$,

$$\begin{aligned} q_1^\mu &= \frac{\bar{q}_1}{2}n_0^\mu + (q_1)_{n_0\perp}^\mu + \frac{n_0\cdot q_1}{2}\bar{n}^\mu\,, & (48)\\ k_1^\mu &= \frac{\bar{k}_1}{2}n_0^\mu + (k_1)_{n_0\perp}^\mu + \frac{n_0\cdot k_1}{2}\bar{n}^\mu\,. \end{aligned}$$

The variables are illustrated in Fig. 5. By momentum conservation we have $(k_1)_{n_0\perp} = -(q_1)_{n_0\perp}$, $Q = \bar{q}_0 = \bar{k}_1 + \bar{q}_1$ and $n_0\cdot p_{\bar{q}} = Q - n_0\cdot q_1 - n_0\cdot k_1$. We take all the external particles on-shell, thus $n_0\cdot q_1 = -(q_1)_{n_0\perp}^2/\bar{q}_1$ and similarly for

[5] All the amplitudes we write in this work refer only to the hadronic part of $e^+e^- \to$ jets, thus $A_{\mathrm{LO}}^{q\bar{q}g}$ is the amplitude of $\gamma^* \to q\bar{q}g$.

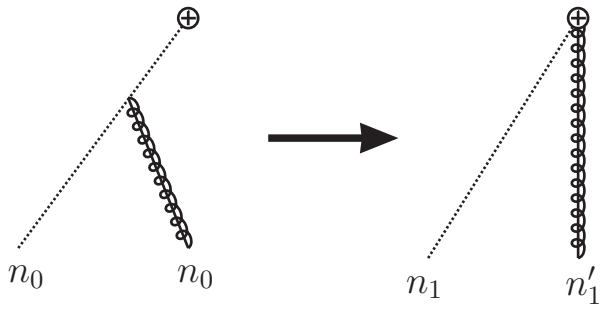

FIG. 6: (Left panel) Single gluon emission in SCET_1 comes from the time-ordered product of the Lagrangian with a quark-creating operator, $A = \langle 0|T\{\mathcal{L}_{\mathrm{SCET}_1}\mathcal{O}_1^{(0)}\}|qgX\rangle$. (Right panel) For parent quarks with virtuality $\gg Q^2\lambda^4$, the gluon comes from the central vertex in SCET_2 via a higher-dimensional operator, $A = \langle 0|\mathcal{O}_2^{(1)}|qgX\rangle$.

$n_0 \cdot k_1$. As we discussed in Section II B, [24, 25] showed that single gluon emission in SCET reproduces the splitting function, Eq. (3), and factorization behavior, Eq. (27), of the standard parton shower. This simple behavior for a single radiation will reproduce the shower for an arbitrary number of gluons.

We now want to match the single emission to SCET_2 (*cf.* Fig. 6). There is a slight technical complication due to the different definitions of collinearity in the two theories, as illustrated by Fig. 4. In SCET_i, a collinear field with label n can annihilate a state containing a particle whose momentum vector lies anywhere in a cone with angle $\sim \lambda^i$ about n. When we change to a lower-scale theory in a matching equation, we have to take care that the operators' n-labels are appropriate for the desired amplitude. Using the terminology of Fig. 4, while any label vector in the light (blue) cone is sufficient for a particle with momentum p in SCET_i, for SCET_{i+1} we need one in the dark (red) cone. This is where RPI_i comes in, as mentioned in Sec. II C. We use it in SCET_i to transform all quantities in the amplitude (spinors and vectors) that depend on the label vectors, such that the label after rotation lies within a collinear cone with angle $\sim \lambda^{i+1}$ about the particle momentum.

The simplest convention is to choose the n-label to align perfectly with the particle. If desired, we could make any choice consistent with RPI_{i+1} transformations. For the process under consideration, we define labels, n_1, n_1' such that,

$$\begin{aligned} q_1 &= \bar{q}_1 \frac{n_1}{2}\,, \\ k_1 &= \bar{k}_1 \frac{n_1'}{2}\,. \end{aligned} \tag{49}$$

In SCET_1, we are free to use n_0 or n_1 to describe the q_1 quark and k_1 gluon because of the RPI_1 symmetry. Since n_1 is a valid index for the quark field in SCET_2, we do the matching computation using the same spinor, $u_{n_1}(q_1)$, in both theories. In App. B, we derive the RPI transformations we use here and other rotation formulas. For now, we quote the results we need:

$$\begin{aligned} u_{n_0} &= \frac{\not{n}_0 \not{\bar{n}}}{4} u_{n_1}, \\ n_1^\alpha &= n_0^\alpha + \frac{2(q_1)_{n_0\perp}}{\overline{q}_1} - \frac{(q_1)_{n_0\perp}^2}{\bar{q}_1^2}\bar{n}^\alpha\,, \\ n_1'^\alpha &= n_0^\alpha + \frac{2(k_1)_{n_0\perp}}{\overline{k}_1} - \frac{(k_1)_{n_0\perp}^2}{\bar{k}_1^2}\bar{n}^\alpha. \end{aligned} \tag{50}$$

As required, the two different n_i-vectors' directions lie within cones of size λ about n_0. It is simple to check that in the new basis, $(q_1)_{n_1\perp} = q_1 - (n_1\cdot p)\bar{n}/2 - \bar{q}_1\, n_1/2 = 0$ and similarly for $(k_1)_{n_1'\perp}$. Acting on Eq. (46), we get:

$$A_{\mathrm{LO}}^{q\bar{q}g} = g\frac{\bar{q}_0}{q_0^2}\bar{u}_{n_1}\left(n_0^\alpha + \frac{(\not{q}_1)_{n_0\perp}\gamma^\alpha_{n_1'\perp}}{\bar{q}_1}\right)\frac{\not{\bar{n}}\not{n}_0}{4}\Gamma^\mu v_{\bar{n}}\,, \tag{51}$$

where $q_0 = q_1 + k_1$. Having changed bases, we can easily write the SCET_2 operator that reproduces Eq. (51),

$C^{(1)}_{2,\mathrm{LO}}\,\mathcal{O}^{(1)}_2(n_1,n_1')$, where:[6]

$$\begin{aligned}\mathcal{O}^{(1)}_2(n_1,n_1') &= (\bar\chi_{n_1})_j\, g\mathcal{B}^{\alpha}_{n_1'\perp}\,(\chi_{\bar n})_k\ ,\\ C^{(1)}_{2,\mathrm{LO}}(n_1,n_1') &= U^{(2,0,0)}_{\mathrm{LL}}(n_0;\,Q,\mu_1)\left[\frac{\bar q_0}{q_0^2}\left(n_0^\alpha+\frac{(\not q_1)_{n_0\perp}\gamma^\alpha_{n_1'\perp}}{\bar q_1}\right)\frac{\not n\not n_0}{4}\Gamma^\mu\right]_{jk}\Theta_{\delta_2}[n_1\cdot n_1']\,.\end{aligned}\tag{52}$$

We note that we have also given the Wilson coefficient the n-labels of the operator it multiplies. In cases where it is clear, we will only explictly label one of C or $\mathcal{O}$. In addition to the expected tree-level amplitude term in brackets, we also give the RG kernel, $U^{(2,0,0)}_{LL}$, and an angular phase-space cutoff, Θ_{δ_2}. We discuss each of them in turn.

The former comes from running the SCET$_1$ operator $\mathcal{O}^{(0)}_1$ from Q to the scale $\mu_1\sim\lambda Q$. When U_{LL} refers to an operator where all collinear directions are distinct, we will drop n's from the notation. From Eq. (20), we have

$$U^{(2,0,0)}_{\mathrm{LL}}(n_0;\,Q,\mu_1)=\Delta_q(Q,\mu_1)\,,\tag{53}$$

where LL refers to the fact that we take the one-loop cusp anomalous dimension, which resums the leading logs of this running. As mentioned in Sec. II B, [24, 25] showed this resummation to be equivalent to that of no-branching Sudakov factors of CKKW-L. We discuss the running of our operators in more detail in Sec. IV C.

The phase-space cutoff $\Theta_{\delta_2}[n_1\cdot n_1']$ encodes that $n_1\cdot n_1'\lesssim\lambda^2/\eta^4$ (the power of η^{-4} was discussed in Sec. II C). The SCET$_2$ operator, $\mathcal{O}^{(1)}_2(n_1,n_1')$, can only distinguish that the quark and gluon are not collinear in SCET$_2$, but does not know that they *were* collinear in SCET$_1$. Thus, we put a cutoff on how far apart they are using $n_1\cdot n_1'$ to ensure that this SCET$_2$ operator cannot create them in a region of phase-space where they would have been non-collinear, even in SCET$_1$. As an example, we could choose Θ to be the usual step-function

$$\begin{aligned}\Theta_{\delta_k}[n_i\cdot n_j] &= \begin{cases}1 & n_i\cdot n_j\ \le\ \delta_k\\ 0 & n_i\cdot n_j\ >\ \delta_k\end{cases}\ ,\\ \tilde\Theta_{\delta k} &= 1-\Theta_{\delta_k}\,.\end{aligned}\tag{54}$$

For later convenience, we defined the complement, $\tilde\Theta_{\delta_k}$. In working with SCET$_i$ operators, we relate δ_k to λ. In general, the Wilson coefficient in SCET$_i$ has to encode whether $n_i\cdot n_j\ \le\ \lambda^{2(i-1)}/\eta^4$ or $n_i\cdot n_j\ >\ \lambda^{2(i-1)}/\eta^4$, in order to do it we will set $\delta_i=\lambda^{2i-3}/\eta^4$. This satisfies the necessary criteria since $\lambda^{2i-2}\ll\lambda^{2i-3}\ll 1$ (and recall that η is the parameter that accounts for the decrease in $\bar p$ of a daughter relative to its mother). For $C^{(1)}_{2,\mathrm{LO}}$ above, this means $\delta_2=\lambda/\eta^4$. At the end of Sec. II C, we discussed how λ gives us a way to parametrize strong-ordering and deviations from it. To this end, we did not need to assign it a numerical value beyond $\lambda\ll 1$. Here for the implementation, we do have to make an explicit choice as to where our Θ functions turn over, and for this purpose we will use fixed values such as $\lambda=0.1$ and $\eta=1/2$. This means $\delta_2=1.6$ and since the η^{-4} is a common overall factor that all $\delta_{k\ge 3}\le 0.16$. The smoothness of both Θ and our physical processes gives us great leeway in the choice for λ, and we expect that any $\lambda\simeq 0.1$ will suffice (*cf.* Fig. 10).

Once we square and integrate our operators, we have certain practical considerations to take into account. For example, it is better to use a smoothed step. We give an example of such a function in Eq. (D21), and plot it in Fig. 7. where we choose an appropriate numerical value for δ_k. If one only wishes to recover the LL shower, then one should use $\Theta=1$, as the errors induced by this do not affect the leading resummation. Furthermore, taking $\Theta=1$ ensures that the LL shower can cover all of phase space. Once we include corrections, though, then it is important to keep different types of collinearity distinct and include non-trivial Θ's. In the presence of corrections, there will always be amplitudes with a Θ and others with a $\tilde\Theta$, which together cover all of phase space (see also Fig. 10).

Unlike standard SCET, where all the coefficients are of order λ^0, $C^{(1)}_{2,\mathrm{LO}}$ has an overall weight of λ^{-1}. We get λ^{-2} from the SCET$_1$ propagator, $1/q_0^2$. The numerator is proportional to λ and comes from the vertex: $\left(n_0^\alpha+(\not q_1)_{n_0\perp}\gamma^\alpha_{n_1'\perp}/\bar q_1\right)$. The second term is straightforwardly $\mathcal{O}(\lambda)$ from $(\not q_1)_{n_0\perp}$. Since n_0^α gets contracted with $\mathcal{B}^\alpha_{n_1'\perp}$, it only contributes its perpendicular component in the n_1' frame. From Eq. (50), we see that $(n_0)_{n_1'\perp}\sim n_0-n_1'\sim(k_1)_{n_0\perp}/\bar k_1\sim\lambda$.

---

[6] See Appendix D for more detail on this matching. Though we have written Eq. (52) to look as much like the SCET$_1$ amplitude as possible, we can rewrite it purely in terms of external momenta, as in Eq. (D13).

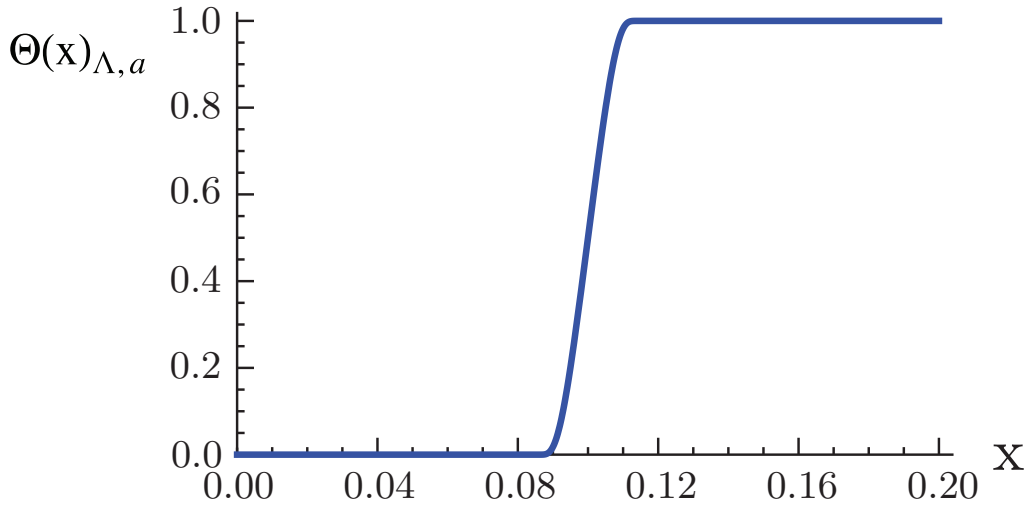

FIG. 7: Plot of the smoothed Θ-function, $\Theta(x)_{\Lambda,a}$, defined in Eq. (D21), taking $\Lambda = 0.1$ and $a = 0.016$. The parameter Λ determines the value of x where the function switches from 0 to 1, and $2a$ is the range in x over which the transition is made. Comparing this smoothed Θ-function to Θ_δ in Eq. (54), we have parametrically $\Lambda \simeq \delta_k$ and $a \ll \delta_k$. This plot is for the case $\delta_3 = 0.1$.

$C^{(1)}_{2,\mathrm{LO}}$ is gauge invariant despite the presence of the Θ_{δ_k} function. This follows from writing Eq. (52) only in terms of scalar products of n vectors, (*cf.* Eq. D13), since collinear directions are invariant under collinear gauge transformations [23].

We note that we can obtain $C^{(1)}_{2,\mathrm{LO}}\mathcal{O}^{(1)}_2(n_1, n_1')$ from the original two-parton operator, $C^{(0)}_{1,\mathrm{LO}}\mathcal{O}^{(0)}_1(n_0)$, in two steps: first we multiply it by the running factor

$$U^{(2,0,0)}_{\mathrm{LL}}(n_0; Q, \mu_1) = \Delta_q(Q, \mu_1)\,, \tag{55}$$

where the formulas for $U^{(0)}_{\mathrm{LL}}$ are given in Eqs. (18-19). Secondly, we apply the replacement rule

$$(\bar\chi_{n_0})_i \to (c^\alpha_{\mathrm{LO}}(n_0))_{ji}\,(\bar\chi_{n_1})_j g\mathcal{B}^\alpha_{n_1'\perp}, \tag{56}$$

where c^α_{LO} is:

$$c^\alpha_{\mathrm{LO}}(n_0) = \frac{\bar q_0}{q_0^2}\left(n_0^\alpha + \frac{(q_1)^\mu_{n_0\perp}\gamma^\alpha_{n_1'\perp}}{\bar q_1}\right)\frac{\not{n}\not{n}_0}{4}\,\Theta_{\delta_2}[n_1\cdot n_1']\,. \tag{57}$$

The relation (56) is the operator statement of splitting in the parton shower. The scale μ_1 defines the endpoint of running in the UV theory. As we evolve down, more partons become apparent. We can see this here by the presence of two fields where there had been one. It makes the basic aspects of the shower manifest. The replacement rule affects the quark alone, and so we see that the amplitude for splitting factorizes off from the rest of the process. The RG kernel reflects the no-branching probability. Lastly, we can interpret the vertex portion of c^α_{LO} as the "square root" of the splitting function. The spinor projector $(\not{n}\not{n}_0/4)$ in Eq. (57) rotates the spin-sum from $\not{n}_1$ to $\not{n}_0$ in accordance with Eq. (2). The remaining part of c^α_{LO} after stripping off the Θ_{δ_2} is:

$$P_\alpha \equiv \frac{\bar q_0}{q_0^2}\left(n_0^\alpha + \frac{(\not{q}_1)_{n_0\perp}\gamma^\alpha_{n_1'\perp}}{\bar q_1}\right), \tag{58}$$

which squares to a trivial Dirac structure. Furthermore, even though $\rho_\alpha(\bar q/q_0^2) \neq P_\alpha$ because of the RPI rotations we performed (where ρ is defined in Eq. 25), we have $|\rho|^2(\bar q_0/q_0^2)^2 = |P|^2$ with respect to the gauge polarization sum, $d_{\alpha\beta}$, so

$$|P|^2 = \frac{1+z^2}{k_{1\perp}^2}. \tag{59}$$

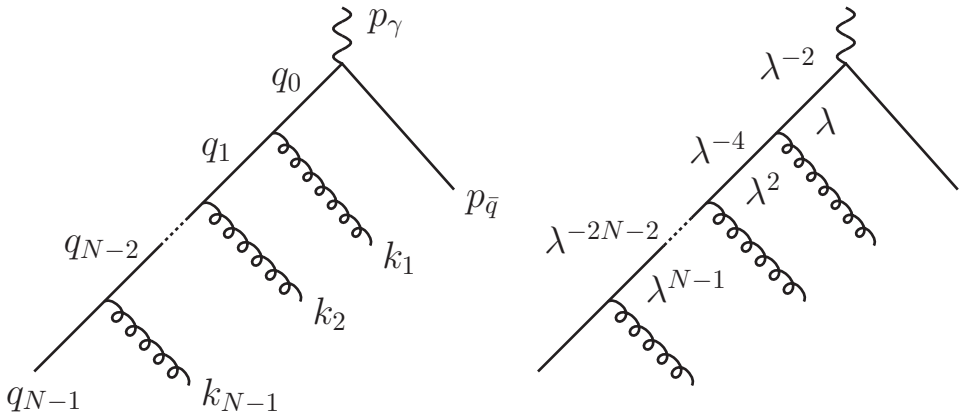

FIG. 8: (Left panel) Our kinematic convention for a strongly ordered process. Quark momenta are denoted by q_i and gluon momenta by k_i. (Right panel) Power counting of the LO coefficient in SCET_N. The powers of λ with negative exponents refer to the propagator contribution to the amplitude. Those with positive exponents refer to the perpendicular momentum of the gluon with respect to its parent, which appears in the SCET vertex Feynman rule.

Just as before, including the z-dependence from the measure and spin-sum, we recover the the standard splitting function $\propto (1+z^2)/(1-z)$. Thus, c^α_{LO} weights the probability assigned to the expectation value of $C^{(1)}_{2,\mathrm{LO}}\mathcal{O}^{(1)}_2(n_1,n_1')$ appropriately.

Having computed the LO result for a single gluon, it is straightforward to proceed to an arbitrary number of emissions. In SCET_2, we know that a two-gluon process comes from the T-product of the Lagrangian with $C^{(1)}_{2,\mathrm{LO}}\mathcal{O}^{(1)}_2(n_1,n_1')$. Similarly to before, the amplitude has the contribution,

$$A^{q\bar{q}gg}_{\mathrm{LO}} = C^{(1)}_{2,\mathrm{LO}}\langle 0|\int dx\, T\{\mathcal{L}_{\mathrm{SCET}_2}(x)\mathcal{O}^{(1)}_2(n_1,n_1')\}|q_{n_1}g_{n_1}g_{n_1'}\bar{q}_{\bar{n}}\rangle\,. \tag{60}$$

The vertex for gluon emission in the SCET_2 Lagrangian is identical to that in SCET_1. Thus, integrating out the parent of the Lagrangian-emitted gluon, we obtain a two-gluon SCET_3 operator, $C^{(2)}_{3,\mathrm{LO}}\mathcal{O}^{(2)}_3(n_2,n_1',n_2')$, similarly to before. Also like in the matching $\mathrm{SCET}_1\to\mathrm{SCET}_2$, we can obtain $C^{(2)}_{3,\mathrm{LO}}\mathcal{O}^{(2)}_3(n_2,n_1',n_2')$ from the SCET_2, $C^{(1)}_{2,\mathrm{LO}}\mathcal{O}^{(1)}_2(n_1,n_1')$, by multiplying it by the running factor for $\mathcal{O}^{(1)}_2$,

$$U^{(1)}_{\mathrm{LL}} = \Delta_q(\mu_0,\mu_2)\,\Delta_g(\mu_1,\mu_2)^{1/2}, \tag{61}$$

with $\mu_0\sim Q$ and applying the replacement rule:

$$\begin{aligned}(\bar{\chi}_{n_2})_i &\to (c^\alpha_{\mathrm{LO}}(n_1))_{ji}\,(\bar{\chi}_{n_3})_j\, g\mathcal{B}^\alpha_{n_2'\perp}, \\ c^\alpha_{\mathrm{LO}}(n_1) &= \frac{\overline{q}_1}{q_1^2}\left(n_1^\alpha + \frac{(\not{q}_2)_{n_1\perp}\gamma^\alpha_{n_2'\perp}}{\overline{q}_2}\right)\frac{\not{\bar{n}}\not{n}_1}{4}\,\Theta_{\delta_3}[n_2\cdot n_2']\,,\end{aligned} \tag{62}$$

where n_2 and n_2' are directions proportional to the quark and second gluon momenta, defined in Eq. (B15), and $\delta_3=\lambda^3/\eta^4$. One can iterate this procedure to obtain the LO result for $(N-1)$-gluon emission. If we use the replacement rule $N-1$ times we go down to the SCET_N operator $C^{(N-1)}_{N,\mathrm{LO}}\mathcal{O}^{(N-1)}_N(n_{N-1},n_1',\ldots,n_{N-1}')$, after which Lagrangian emissions are no longer distinguished as separate particles. We have:

$$\begin{aligned}\mathcal{O}^{(N-1)}_N(n_{N-1},n_1',\ldots,n_{N-1}') &= \bar{\chi}_{n_N}\left(\prod_{k=1}^{N-1} g\mathcal{B}^{n_k'\perp}_{\alpha_k}\right)\chi_{\bar{n}}\,, \\ C^{(N-1)}_{N,\mathrm{LO}}(n_{N-1},n_1',\ldots,n_{N-1}') &= \left(\prod_{k=1}^{N-1} U^{(k-1)}_{\mathrm{LL}}(\mu_{k-1},\mu_k)\,c^{\alpha_k}_{\mathrm{LO}}(n_{k-1})\right)\Gamma^\mu, \\ c^{\alpha_k}_{\mathrm{LO}}(n_{k-1}) &= \frac{\overline{q}_{k-1}}{q^2_{k-1}}\left(n^{\alpha_k}_{k-1}+\frac{(\not{q}_k)_{n_{k-1}\perp}\gamma^{\alpha_k}_{n_k'\perp}}{\overline{q}_k}\right)\frac{\not{\bar{n}}\not{n}_{k-1}}{4}\,\Theta_{\delta_k}[(n_k\cdot n_k')]\,,\end{aligned} \tag{63}$$

$$U_{\rm LL}^{(k-1)}(\mu_{k-1},\mu_k) = \Delta_q(\mu_{k-1},\mu_k)(\Delta_g(\mu_{k-1},\mu_k))^{(k-1)/2}\,.$$

The variables for $N-1$ emissions are illustrated in Fig. 8, where $q_{k-1} = \left(q_{N-1} + \sum_{j=k}^{N-1} k_j\right)^2$ and $\delta_k = \lambda^{2k-3}/\eta^4$. From the power counting one knows that $\mu_0 = Q$, and $\mu_k \sim Q\lambda^k$, where the latter scaling determines how μ_k depends on $p_\perp^j$ momenta, but not how it depends on ratios of the large $\bar{q}_j$ momenta. To sum $\mathrm{LL}_{\rm exp}$ the approach taken by CKKW and elsewhere is to use $\mu_k^2 = k_\perp^2$, namely the transverse momentum squared of the emission [29, 68–71]. This accounts for soft interference effects and coherent branching, see Ref. [69] for a review. To investigate this scale choice in the SCET_i framework requires an examination of the logs in the one-loop matching computation for $c_{\rm LO}$, and consideration of soft gluons in SCET_i and SCET_{i+1}. Having not carried out this computation ourselves, we rely on the previous literature. For our variables using Eq. (38) this implies

$$\mu_k^2 = \left(\frac{\bar{q}_k\bar{k}_k}{\bar{q}_{k-1}}\right)^2 \frac{|n_k\cdot n_k'|}{2}\,. \tag{64}$$

(In contrast, the choice of invariant mass q_{k-1}^2 would have yielded $\mu_k^2 = (\bar{q}_k\bar{k}_k)|n_k\cdot n_k'|/2$, but this leads to incomplete cancellations of soft divergences, and therefore problems with the resummation of soft logs [68].) The directions n_k and n_k' are aligned with the external quark, q_k, and the gluon momenta, k_k. They are related to n_{k-1} through an RPI_k transformation. We can extend the argument to calculate the scaling of $C_{2,\rm LO}^{(1)}$ to the SCET_N coefficient in Eq. (63). Counting the contributions from the tree-level terms, $c_{\rm LO}^{\alpha_k}$, $C_{N,\rm LO}^{(N-1)} \sim \prod_i^{N-1} 1/\lambda^{-i} = \lambda^{-N(N-1)/2}$, *cf.* Fig. 8.

Similarly to the discussion above Eq. (59), we can extract the vertex part of $c_{\rm LO}^{\alpha_k}$ to define P^{α_k}. We get that:

$$|P^{\alpha_k}|^2 \;=\; \frac{1+z_k^2}{(q_k^2)_{n_{k-1}\perp}}, \tag{65}$$

where $z_k \equiv \bar{q}_k/\bar{q}_{k-1}$. Thus, the amplitude squared goes like the factorized product of the appropriate $1\to 2$ splitting functions. Since $\mathcal{O}_N^{(N-1)}(n_{N-1}, n_1', \ldots, n_{N-1}')$ is just built up from the repeated use of Eq. (56), we see that it requires no added information after we compute the first $q\to qg$ splitting. Thus, what we need to pass to a shower algorithm comes just from single real and single virtual gluon computations, as we list below in Sec. III C in Table I. The collinear splitting needed for a LL shower is entirely handled by the replacement rule in Eq. (56).[7]

Lastly, we note that at higher orders in SCET_N, we will only ever need to compute the Wilson coefficient, $C_N^{(N-1)}$, of $\mathcal{O}_N^{(N-1)}$. Since each field in this theory has its own direction by the physical resolution constraint, we can use RPI_N to make all operators with $\mathcal{P}_{n\perp}$ equal to zero.

B. Soft Emissions

SCET describes soft degrees of freedom using soft quark and gluon fields: $q_s(x)$ and $A_s(x)$. In this work, we focus on fully differential cross sections where we can always distinguish collinear and soft modes. In an integrated cross section in SCET, we have to implement soft emissions with some form of zero-bin subtractions [72] to avoid double counting between soft and collinear radiation. (In the shower literature a proper treatment of softs is also often implemented by subtraction methods [39, 40, 43–46, 73].) The collinear sector and the soft sector couple through the covariant derivative,

$$iD_s^\mu = i\partial^\mu + gA_s^\mu\,, \tag{66}$$

acting on the collinear fields. At LO in λ, the collinear particles only couple to the $n\cdot A_s$ component of the soft gluons and the soft-collinear factorization guarantees that we can absorb this interaction into a Wilson line, $Y(x)$, along the

[7] It is straightforward to see that we do not have additional contributions at LO in λ. Firstly, consider the possibility of operators that do not take the form of a single-field replacement rule. These would depend on the details of the hard process that produced the quark in the first place and could threaten the factorization of the shower. In fact, we will get such terms when we match QCD $\to$ SCET_1, but they are always suppressed, as we discuss in Sec. IV. Returning to single-field replacement, let us consider matching $\mathrm{SCET}_1 \to \mathrm{SCET}_2$, as results in this case will generalize to all SCET_i. Rule (56) sends $\chi_{n_1} \to C\mathcal{B}_{n_3\perp}^\mu \chi_{n_2}$. At LO, we cannot get such a replacement involving multiple gluon fields, $\mathcal{B}_{n_j\perp}$, as this implies that we have integrated out multiple, hard ($\sim Q\lambda^2$) propagators. Such a contribution would not be strongly ordered, and is suppressed. In Sec. IV, we will also see that we do have such contributions at higher orders.

direction of the collinear particle,

$$Y_n(x) = P \exp\Big[ig \int_{-\infty}^{0} \mathrm{d}s\, n\cdot A_s(x+sn)\Big]\,. \tag{67}$$

In SCET, this is accomplished by making field redefinitions [23], so that the new collinear fields no longer couple to soft gluons through their kinetic term, as we review in App. A. The outcome for the composite fields considered here is that

$$\chi_n \to Y_n \chi_n\,, \qquad \mathcal{B}_n^\mu \to Y_n \mathcal{B}_n^\mu Y_n^\dagger\,. \tag{68}$$

Note that here we consider nonabelian soft interactions, which is why the soft Wilson lines do not cancel for the $\mathcal{B}_n^\mu$ field.

In matching SCET_i to SCET_{i+1}, we will only consider external soft modes in SCET_{i+1} with momenta $k \sim Q\lambda^{2(i+1)}$. These are contained as a subset of the softs in SCET_i. We do not consider particles with soft momenta $k \sim Q\lambda^{2i}$ that could not be encoded by onshell modes in SCET_{i+1}. Such modes are forced to have larger momenta than the soft fields in SCET_{i+1}, and they are not responsible for IR divergences. Any contributions from momenta of this type can be encoded in the Wilson coefficients of our SCET_{i+1} operators.

In a given SCET_i, after making the field redefinition, the effect of soft gluons is encoded by Wilson lines Y_n in the operators, with the form

$$\bar\chi^{(0)}_{n_N} Y^\dagger_{n_N} \prod_{k=1}^{N} Y_{n'_k} \mathcal{B}^{(0)\alpha_k}_{n'_k\perp} Y^\dagger_{n'_k}\, \Gamma_\mu Y_{\bar n} \chi_{\bar n}\,. \tag{69}$$

The angular ordering property and the coherent parton branching formalism for soft emissions with multiple hard partons emerge naturally from such operators in SCET_{i+1}. If we take the Fourier transform of $Y_n(x)$ we get

$$Y = 1 + \sum_{m=1}^{\infty} \sum_{\text{perms}} \frac{(-g)^m}{m!} \frac{n\cdot A_s^{a_1} \cdots n\cdot A_s^{a_m}}{n\cdot k_1 n\cdot(k_1+k_2)\cdots n\cdot(\sum_{i=1}^m k_i)} T^{a_m}\cdots T^{a_1} \tag{70}$$

where k_1, k_2, ... k_n are the momenta of the gluon fields. The eikonal structure of (70) leads to angular ordering. If a collinear particle with momentum q_i in the n_i direction emits a soft gluon of momentum k_s, the amplitude acquires a term proportional to

$$F_{\text{soft}} = \frac{n_i\cdot\varepsilon_s}{n\cdot k_s} = \frac{q_i\cdot\varepsilon_s}{q_i\cdot k_s} + O(\lambda)\,, \tag{71}$$

where ε_s is the polarization vector of the soft radiation and $q_i^\mu = \bar q\, n_i^\mu/2$ up to power corrections. If $A_n(q_1, q_2, \cdots, q_n)$ is the amplitude to emit n collinear particles with momenta $q_1, q_2, \cdots, q_n$ and A_{n+1} the amplitude with one more emission, k_s, in the soft region, we get $A_{n+1}(q_1, q_2, \cdots, q_n, k_s) \sim A_n(q_1, q_2, \cdots, q_n) \sum_{i=1}^n C_i\, q_i\cdot\varepsilon_s/q_i\cdot k$, where C_i is a color factor. For the cross section this implies

$$d\sigma_{n+1} = d\sigma_n \frac{dE_s}{E_s} \frac{d\Omega_s}{2\pi} \frac{\alpha_s}{2\pi} \sum_{i,j} C_{i,j} W_{i,j}\,, \tag{72}$$

where $d\Omega_s$ and E_s are the element of solid angle and the energy of the emitted soft gluon, and $C_{i,j}$ is a color factor. Here

$$W_{i,j} = \frac{E_s^2\, q_i\cdot q_j}{q_i\cdot k_s\, q_j\cdot k_s} \tag{73}$$

is known as the radiation function. Without color weights, the integration of $W_{i,j}$ over azimuthal angular variables would imply that soft gluons only contribute when the gluon is confined to the cones centered in the directions of particles i and j, and are hence angular ordered.

To see how coherent branching emerges, we consider effects encoded by operators with exactly the same collinear field content in SCET_i and SCET_{i+1}. Graphs involving soft gluons will agree, and there is no contribution to the matching. If we consider instead the collinear calculations that lead to the LO replacement rule $\bar\chi_{n_0} \to c_{\mathrm{LO}} \bar\chi_{n_1} \mathcal{B}^\perp_{n_1}$, then the soft gluons are encoded by

$$\mathrm{SCET}_i:\ \ \bar\chi_{n_0} Y^\dagger_{n_0}\,, \qquad\qquad \mathrm{SCET}_{i+1}:\ \ c_{\mathrm{LO}} \bar\chi_{n_1} Y^\dagger_{n_1} Y_{n'_1} \mathcal{B}^\perp_{n'_1} Y^\dagger_{n'_1}\,. \tag{74}$$

For soft gluons at wide angles relative to n_0, n_1, and n_1', the effect of attachments to $Y_{n_1}^\dagger Y_{n_1'}$ are power suppressed because soft emission from these two lines cancels up to terms that are power suppressed by $n_1 \cdot n_1' \sim \lambda^{2i}/\eta^4$. The remaining attachment to $Y_{n_1'}^\dagger$ looks the same as those to $Y_{n_0}^\dagger$ at leading power, since $n_0 \cdot n_1' \sim \lambda^{2i}/\eta^4$. Thus, wide angle soft gluons do not resolve the substructure revealed by matching to SCET$_{i+1}$ and effectively only couple to the overall color charge of the parent quark $\bar{\chi}_{n_0}$. Soft radiation that is close in angle to n_1 and n_1' resolves the split into quark $\bar{\chi}_{n_1}$ and gluon $\mathcal{B}_{n_1'}^\perp$, compensating for the $n_1 \cdot n_1'$ suppression by additional collinear singularities in its propagator factors. Thus, the coherent branching formalism for soft gluons emerges naturally for amplitudes in our SCET$_i$ picture.

From the SCET point of view, it would be natural to distinguish soft and collinear radiation in the shower and treat them independently, being careful not to double count. For simplicity, all available shower codes treat them in a simultaneous fashion. Accounting for soft coherent branching in the shower typically leads to modifications of the Sudakov probability factors (see for example Ref. [74]), and affects the choice of evolution variable or adds additional vetoes. In the context of SCET, the implications of this were discussed recently in [75].

C. Summary for LO Parton Shower

In Table I, we summarize results for the mapping between the LL parton shower and our SCET$_i$ picture at LO in λ. In the first column, we put the elements needed for showering, and in the central column the translation to elements in the SCET$_i$ setup. The usual splitting function is related to our replacement rule $\bar{\chi}_{n_0} \to c^{\rm LO} \bar{\chi}_{n_1} \mathcal{B}_{n_1'}^\perp$, that in turn is related to the SCET$_2$ coefficient of the operator $\mathcal{O}_2^{(1)}$. The LL Sudakov comes from LL running factors related to the one-loop cusp anomalous dimension as in [24, 25]. At leading order, soft emission in SCET$_i$ is taken into account by adding soft Wilson lines Y_n into our operators. This leads to angular ordering and coherent branching, which must be accounted for with modifications to the shower to account for the soft singular regions. Finally, showers are constructed with different choices of evolution variables and the choice effects the structure of power corrections. In SCET$_i$, we have seen that we can write all coefficients in terms of the large momenta ($\bar{q}$) and dot product of n vectors ($n_i \cdot n_j$), which are natural variables in the SCET$_i$ picture. One can convert these variables to k_T^2, virtuality, or angles as desired. At LL this translation is straightforward.

Shower Concepts	Quantity in SCET$_i$	Found In:
Splitting function	Replacement rule	Eq.(56)
LL Sudakov factor	One-loop cusp anomalous dimension	Eq. (20)
Soft emission	Soft amplitude	Eq. (69)

TABLE I: Mapping between parton shower and SCET$_i$ at LO/LL.

IV. SCET POWER CORRECTIONS TO THE SHOWER

As we have seen in the previous section, we reproduce the usual parton shower by matching collinear gluon emissions to increasingly lower-scale EFTs, the SCET$_i$. Our goal is to catalog the leading power corrections (in λ) to the differential cross section for the emission of an arbitrary number of collinear gluons to a quark. By this we mean all amplitude terms to LO(λ) and NLO(λ), as well as those at NNLO(λ) that can interfere with LO(λ). As we will argue in Sec. IV D, in most cases of interest, there is no LO(λ)/NLO(λ) interference, and so we focus on the most important power suppressed terms which are NLO(λ)×NLO(λ) and LO(λ)×NNLO(λ). Just as in the strongly-ordered case, it is convenient to integrate down to SCET$_{i+1}$ when describing the emission of i-gluons. We obtain these corrections by doing our matching computations at higher order. We will show that there are two distinct types of subleading matching, and they have a different physical interpretation:

- One type originates in matching QCD → SCET$_1$ at higher orders. This generates a set of subleading terms that remain suppressed as we move down to lower-scale SCET$_i$'s. We call them *hard-scattering* power corrections as they involve the details of the hard-scale process that created our original partons. Also, they are most important for partons radiated closest to the hard vertex.

- The other type comes from the subleading matching $\text{SCET}_i \to \text{SCET}_{i+1}$. They involve processes described by the SCET_i Lagrangian, but ones that get integrated out into higher dimension operators at lower scales. These corrections are ubiquitous. They do not depend on the hard-scattering details, and we can determine them for arbitrary $\text{SCET}_i \to \text{SCET}_{i+1}$ once we have found them in $\text{SCET}_1 \to \text{SCET}_2$. Furthermore, they relate to known $\mathcal{O}(\alpha_s)$ corrections to the $q \to qg$ splitting function, which exponentiate to sum part of NLL. For this reason, we call them *jet-structure* corrections.

Determining the above to NLO(λ) in the cross section will only involve single and double gluon emission. Thus, we will never need to compute in a lower-scale theory than SCET_3. We perform all the necessary QCD$\to$SCET$_1\to$SCET$_2\to$SCET$_3$ matchings for these amplitudes in Appendices C-E. Below, we discuss the final results for the corrections, with Sec. IV A focusing on hard-scattering and Sec. IV B on jet-structure. For these portions of the paper, the matching is only done at tree level, though formulas in the Appendices include one-loop RG kernels. We give the effects of LL running on correction terms in Sec. IV C along with a discussion of how to include NLL resummation for the LO (in λ) Wilson coefficients. In Sec. IV D, we will study the amplitude squared and will see there is a great simplification of the interference structure in SCET_N, and hence for NLO(λ) power corrections in a shower. Lastly, we give in Sec. IV E the NLO counterpart to our LO table in Sec. III C. We describe how our corrections from subleading operators relate to improvement of the parton shower with higher order resummation of logs, corrections at higher order in α_s, as well as corrections to spin correlations and interference. These effects are summarized in a shower reweighting formula, Eq. (104).

A. Hard-Scattering Corrections

Just as in Sec. III A, we begin by examining the matching QCD$\to$SCET$_1$ for single gluon emission collinear to the quark. For this case, all corrections are of the hard-scattering type. Beyond LO, we can have dependence on the process that creates the $\bar{q}q$ pair. For concreteness, we will consider the coupling of QCD quarks to the vector current, $J^\mu_{\text{QCD}} = \bar{q}\gamma^\mu q$. The matching is performed in the center of mass frame with the initial virtual photon having momentum, $p_\gamma = (Q, 0, 0, 0)$. The full details of this matching calculation for QCD to SCET_1 are in Appendix C. To reproduce the full QCD current, J^μ_{QCD}, we need an infinite tower of SCET_1 operators increasingly higher order in λ. However, to get the required amplitude to NNLO(λ), we only need four:

$$\begin{aligned} A^{q\bar{q}g}_{\text{to NNLO}} = {} & C^{(0)}_{1,\,\text{LO}}(n_0) \int dx \langle 0|T\{\mathcal{L}_{\text{SCET}_1}(x)\mathcal{O}^{(0)}_1\}|\, q_{n_0} g_{n_0} \bar{q}_{\bar{n}}\rangle \\ & + C^{(1)}_{1,\,\text{NLO}}(n_0, n_0)\langle 0|\mathcal{O}^{(1)}_1|\, q_{n_0} g_{n_0} \bar{q}_{\bar{n}}\rangle + C^{(1)}_{1,\mathcal{T}}(n_0, n_0)\langle 0|\mathcal{T}^{(1)}_1|\, q_{n_0} g_{n_0} \bar{q}_{\bar{n}}\rangle \\ & + C^{(1)}_1(n_1, n_1')\langle 0|\mathcal{O}^{(1)}_1|\, q_{n_1} g_{n_1'} \bar{q}_{\bar{n}}\rangle, \end{aligned} \tag{75}$$

where

$$\begin{aligned} \mathcal{O}^{(0)}_1(n_0) &= \bar{\chi}_{n_0}\chi_{\bar{n}}\,, \\ \mathcal{O}^{(1)}_1(n_0, n_0) &= \bar{\chi}_{n_0}\, g\mathcal{B}^\alpha_{n_0\perp}\chi_{\bar{n}}\,, \\ \mathcal{T}^{(1)}_1(n_0, n_0) &= \bar{\chi}_{n_0}\left[\mathcal{P}^\beta_{n_0\perp}\, g\mathcal{B}^\alpha_{n_0\perp}\right]\chi_{\bar{n}}\,, \\ \mathcal{O}^{(1)}_1(n_1, n_1') &= \bar{\chi}_{n_1}\, g\mathcal{B}^\alpha_{n_1'\perp}\chi_{\bar{n}}\,. \end{aligned} \tag{76}$$

Here we introduced a short-hand for the notation established in Eq. (14), $\mathcal{T}^{(1)}_1(n_0, n_0) = \mathcal{O}^{(2,1,1)}_1(n_0, n_0^{[1]})$. We give the expression for $C^{(0)}_{1,\,\text{LO}}$ in Eq. (42). The amplitude from the operator $\mathcal{O}^{(0)}_1(n_0)$ is shown in the first diagram in the SCET_1 column of Fig. 9, those from $\mathcal{O}^{(1)}_1(n_0, n_0)$ and $\mathcal{T}^{(1)}_1(n_0, n_0)$ in the second, and that for $\mathcal{O}^{(1)}_1(n_1, n_1')$ in the third.

We call $\mathcal{O}^{(1)}_1(n_0, n_0)$ and $\mathcal{T}^{(1)}_1(n_0, n_0)$ "two-jet" operators as they are labeled with two distinct collinear directions (n_0 and $\bar{n}$) (we do not denote the antiquark direction explicitly, following the convention in Eq. 43). They describe a gluon collinear to the quark. We obtain the coefficients $C^{(1)}_1(n_0, n_0)$ and $C^{(1)}_{1,\mathcal{T}}(n_0, n_0)$ by expanding the QCD amplitude in the limit of small gluon momentum transverse to the quark's direction with the usual SCET proportionality:

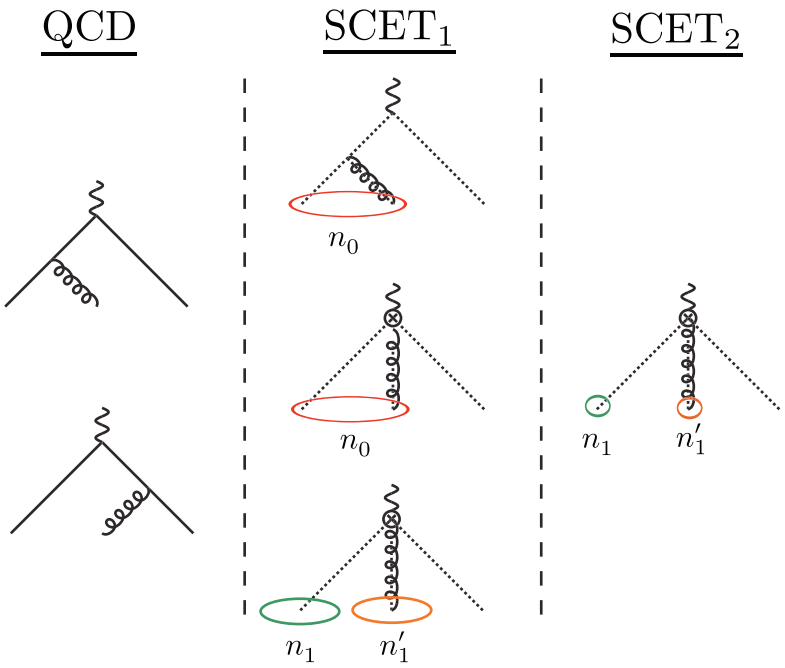

FIG. 9: Matching QCD to SCET$_1$ to SCET$_2$ for one gluon emission which is either collinear to the quark or is in its own direction (SCET graphs for emission collinear to the antiquark are not shown). The figures represent operator structures that describe this process in each of the three theories. The QCD contribution is standard. In SCET$_1$, we either emit a collinear gluon through the time-ordered product of the Lagrangian with an two-parton operator, or from three-parton operators. In SCET$_2$, the emission relevant for us only arises from higher-dimension three-parton operators.

$(n_0 \cdot k_1, \bar{k}_1, k_{1 n_0 \perp}) \sim (\lambda^2, 1, \lambda) Q$. $C_1^{(1)}(n_0, n_0)$ and $C_1^{(1)}(n_1, n_1')$, are derived above Eq. (C13) and given here:

$$
\begin{aligned}
C_{1,\,\mathrm{NLO}}^{(1)}(n_0, n_0) &= \frac{1}{Q}(n_0^\mu - \bar{n}^\mu)\gamma_{n_0\perp}^\alpha \,, \\
C_{1,\mathcal{T}}^{(1)}(n_0, n_0) &= \frac{1}{\bar{q}_1 \bar{k}_1}\gamma_{n_0\perp}^\mu \gamma_{n_0\perp}^\beta \gamma_{n_0\perp}^\alpha - \frac{2}{\bar{q}_1 Q}\, g^{\beta\mu}\gamma_{n_0\perp}^\alpha \,.
\end{aligned}
\tag{77}
$$

We use the same kinematic variables as in Fig. 5. For $C_1^{(1)}(n_0, n_0)$ and $C_{1,\mathcal{T}}^{(1)}(n_0, n_0)$, the initial current is not a spectator, so neither term is simply proportional to the γ^μ with which we started. This dependence on the details of the rest of process is a characteristic feature of hard-scattering corrections. There are an additional set of two-jet configurations corresponding to the gluon collinear to the antiquark. These are trivial to obtain by charge conjugation.

The operator $\mathcal{O}_1^{(1)}(n_1, n_1')$ is a three-jet configuration, as it describes three distinct directions. Whenever we have an operator where each field has its own index label, we can choose the n_i such that they are exactly aligned with the external particle momenta. We give the coefficient $C_1^{(1)}(n_1, n_1')$ in Eq. (C16).

Going to SCET$_2$ for single gluon emission is straightforward. The basis of operators needed to reproduce the amplitude (75) is equal to (76), but with SCET$_2$ fields: $\mathcal{O}_2^{(0)}(n_0)$, $\mathcal{O}_2^{(1)}(n_0, n_0)$, $\mathcal{T}_2^{(1)}(n_0, n_0)$, and $\mathcal{O}_2^{(1)}(n_1, n_1')$. As the computations get more complicated with subsequent emissions, we wish to minimize our effort by only including those terms necessary to give the corrections to a shower Monte Carlo. This means we are only interested in the following:

1. We will need to keep those NNLO(λ) contributions that can interfere with LO(λ). These give terms at the same order as an NLO(λ) operator squared. We do not compute NNLO(λ) amplitude terms which have zero interference with the LO(λ) amplitude. A list of the necessary computations is found in App. D.

2. Our ultimate goal is not a complete SCET$_i$ theory from which one can do computations, but an improved shower algorithm. In Table I, we give a list of those ingredients needed to construct a map between SCET$_i$ and a LL parton shower. We will augment the map with items needed for corrections (Eq. 104, Table II), but will not calculate contributions which only contain redundant information for the shower amplitude.

The latter point has important implications for the sorts of operator structures we need to consider. If we wanted to do computations in SCET$_2$, then we would need all operators and Wilson coefficients to the order we are working.

However, single gluon contributions in SCET_2 where the gluon and the quark are collinear (inside a cone of angle $\sim\lambda^2$, *i.e.* $\mathcal{O}_2^{(1)}(n_0,n_0)$ or $\mathcal{T}_2^{(1)}(n_1,\,n_1)$) correspond to a quark which does not split until after the scale of matching $\mathrm{SCET}_1 \to \mathrm{SCET}_2$. The corresponding no-branching probability, however, is already determined in SCET_1 from the one-loop RG kernel. Thus, the coefficients of these operators in SCET_2 are not required. We only need to calculate those single gluon contributions where each field has its own index label in SCET_2, which means $C_2^{(1)}(n_1,n_1')$ for $\mathcal{O}_2^{(1)}(n_1,n_1')$.

The matching equation for $C_2^{(1)}(n_1,n_1')$ in SCET_2 is:

$$\begin{aligned}
&C_2^{(1)}(n_1,n_1')\langle 0|\mathcal{O}_2^{(1)}|q_{n_1}\,g_{n_1'}\,\bar{q}_{\bar{n}}\rangle \\
&= C_{1,\,\mathrm{LO}}^{(0)}(n_0)\int dx^4\langle 0|T\{\mathcal{L}_{\mathrm{SCET}_1}(x)\mathcal{O}_1^{(0)}\}|q_{n_1}\,g_{n_1'}\,\bar{q}_{\bar{n}}\rangle \\
&\quad + C_{1,\,\mathrm{NLO}}^{(1)}(n_0,n_0)\langle 0|\mathcal{O}_1^{(1)}|q_{n_1}\,g_{n_1'}\,\bar{q}_{\bar{n}}\rangle + C_1^{(1)}(n_1,n_1')\langle 0|\mathcal{O}_1^{(1)}|q_{n_1}\,g_{n_1'}\,\bar{q}_{\bar{n}}\rangle \\
&\quad + C_{1,\mathcal{T}}^{(1)}(n_0,n_0)\langle 0|\mathcal{T}_1^{(1)}|q_{n_1}\,g_{n_1'}\,\bar{q}_{\bar{n}}\rangle\,.
\end{aligned} \tag{78}$$

It is convenient to decompose $C_2^{(1)}(n_1,n_1')$ as

$$C_2^{(1)}(n_1,n_1') = C_{2,\,\mathrm{LO}}^{(1)}(n_1,n_1') + C_{2,\,\mathrm{NLO}}^{(1)H,a}(n_1,n_1') + C_{2,\,\mathrm{NLO}}^{(1)H,b}(n_1,n_1') + C_{2,\,\mathrm{NNLO}}^{(1)H}(n_1,n_1')\,, \tag{79}$$

where the four terms on the RHS of Eq. (79) correspond to each of the contributions on the RHS of Eq. (78). We calculated in $C_{2,\,\mathrm{LO}}^{(1)}$ in Eq. (52) using RPI_1 to rotate objects in the SCET_1 amplitude such that they can come from SCET_2 operators that annihilate the given external state. The second through fourth terms can be calculated in a similar manner. Their values are derived in Eqs. (D17)- (D19):

$$\begin{aligned}
C_{2,\,\mathrm{NLO}}^{(1)H,a}(n_1,n_1') &= \frac{1}{Q}\Big(\frac{\bar{k}_1 n_1'^{\mu}+\bar{q}_1 n_1^{\mu}}{\bar{q}_0} - \Big(1+\frac{\bar{q}_1\bar{k}_1}{2\,\bar{q}_0^2}(n_1\cdot n_1')\Big)\bar{n}^{\mu}\Big)\gamma^{\alpha}_{n_1'\perp}\Theta_{\delta_2}[n_1\cdot n_1']\,, \\
C_{2,\,\mathrm{NLO}}^{(1)H,b}(n_1,n_1') &= -\frac{2}{(n_1\cdot n_1')\bar{q}_1\bar{k}_1}\gamma^{\alpha}\not{p}_{\gamma}\,\gamma_T^{\mu} \\
&\quad + \Big[\frac{1}{(n\cdot p_{\bar{q}})\bar{k}_1}\Big(\gamma_T^{\mu}\not{p}_{\gamma} - \bar{q}_1\,n_{1T}^{\mu}\Big) + \frac{2(n\cdot p_{\bar{q}})}{(n_1\cdot n_1')\bar{q}_1\bar{k}_1}\bar{n}_T^{\mu}\Big]\gamma^{\alpha}\tilde{\Theta}_{\delta_2}[n_1\cdot n_1']\,, \\
C_{2,\,\mathrm{NNLO}}^{(1)H}(n_1,n_1') &= \Big(\frac{1}{2\,Q}\Big(\gamma^{\mu}_{n_1'\perp}\sqrt{n_1\cdot n_1'}\not{v}_1 + \bar{n}^{\mu}\frac{\bar{q}_1}{Q}(n_1\cdot n_1')\Big)\gamma^{\alpha}_{n_1'\perp} \\
&\quad + \frac{\bar{k}_1}{Q^2}\Big(\sqrt{n_1\cdot n_1'}v_1^{\mu} - \bar{n}^{\mu}\,(n_1\cdot n_1')\frac{(\bar{k}_1^2-\bar{q}_1^2)}{2\,Q^2}\Big)\gamma^{\alpha}_{n_1'\perp}\Big)\Theta_{\delta_2}[n_1\cdot n_1']\,.
\end{aligned} \tag{80}$$

Here n_1 and n_1' are aligned with the direction of the quark and the gluon, and v_1 is defined in Eq. (B12). In Eq. (80), we have left off the running factors from evolution of the SCET_1 operators. The terms in Eqs. (76) run differently. In particular, the two-jet and three-jet operators have different LL evolution. Therefore, it is important to decompose $C_2^{(1)}$ as in Eq. (79), so that we can keep track of which SCET_1 evolution factor to include for each. The running of these operators is discussed further in Section IV C.

We also note the different Θ dependence of the terms, where Θ and $\tilde{\Theta}$ we introduced in Eq. (54) and the surrounding discussion. We can read off from $C_{2,\,\mathrm{NLO}}^{(1)H,b}$ its origin as a three-jet term in SCET_1, while the others come from two-jet operators. The Θ functions are necessary because without them SCET_2 operators, (*e.g.* $\mathcal{O}_2^{(2)}(n_1,\,n_1')$) can only tell that the quark and gluon are not collinear according to the SCET_2 definition. By including these phase space cutoffs, we can keep the distinct origins of different contributions manifest. By adopting a smoothed step function, as suggested in Sec. III A and given in Eq. (D21), the amplitude squared for $C_2^{(1)}\mathcal{O}_2^{(1)}$ will be continuous despite having different supports in different parts of phase space. An example of this is shown in Fig. 10. The full expression for the plot is given in Eqs. (D24) and (D25). To illustrate the effects of including hard-scattering corrections, in Fig. 11 we plot the ratios $R_{\mathrm{LO}} = |A^{q\bar{q}g}|^2_{\mathrm{LO}}/|A^{q\bar{q}g}|^2_{\mathrm{QCD}}$ and $R_{\mathrm{NLO}} = (|A^{q\bar{q}g}|^2_{\mathrm{LO}} + |A^{q\bar{q}g}|^2_{\mathrm{NLO},2-\mathrm{jet}})/|A^{q\bar{q}g}|^2_{\mathrm{QCD}}$ versus the gluon perp momentum. Here, $|A^{q\bar{q}g}|^2_{\mathrm{QCD}}$ is the QCD amplitude squared for one-gluon emission, $|A^{q\bar{q}g}|^2_{\mathrm{LO}}$ is the SCET_2 amplitude squared for one-gluon emission from the LO coefficient $C_{2,\,\mathrm{LO}}^{(1)}\mathcal{O}_2^{(1)}$ (from Eq. 52), and $|A^{q\bar{q}g}|^2_{\mathrm{NLO},\,2-\mathrm{jet}}$ is the NLO(λ) amplitude squared for one-gluon emission in the two-jet region that comes from the coefficients $C_{2,\,\mathrm{NLO}}^{(1)H,a}$ and $C_{2,\,\mathrm{NNLO}}^{(1)H}$ (given in Eq. 80). As we expect, including corrections up to NNLO(λ) in the amplitudes squared extends the region

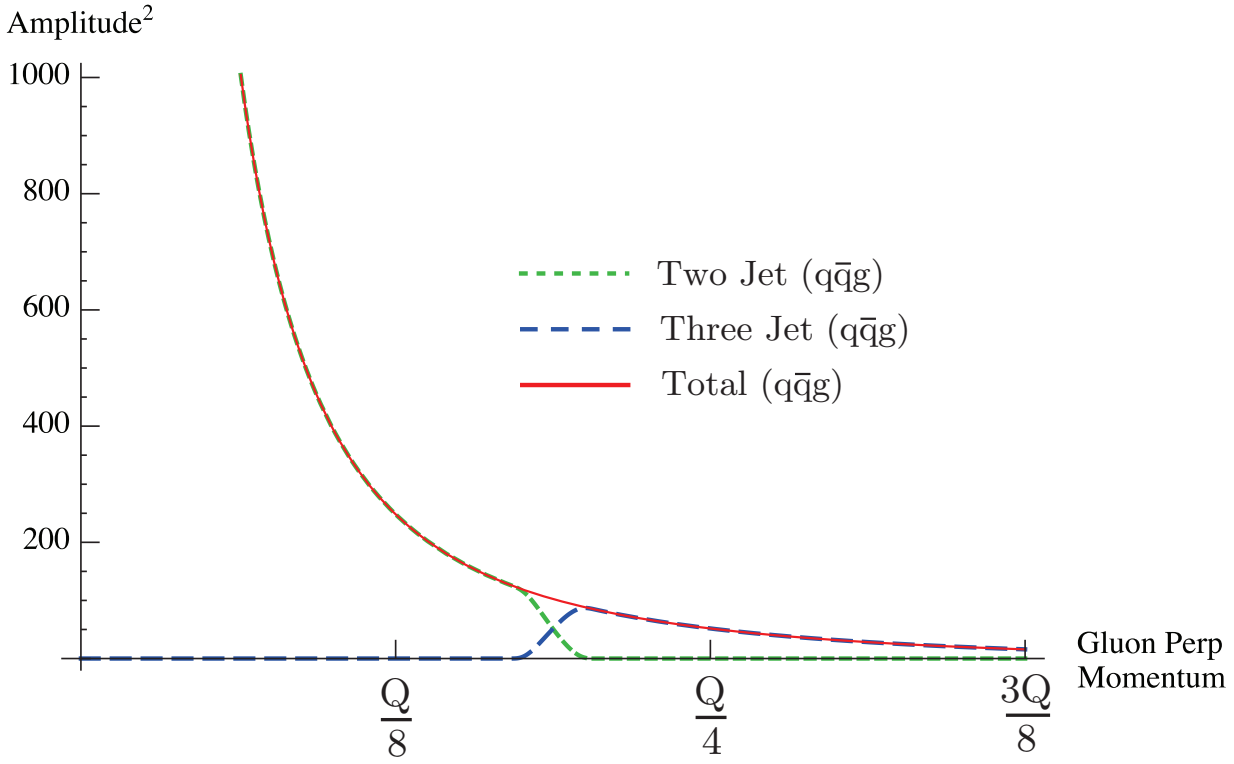

FIG. 10: Merging of the two-jet and and three-jet squared amplitudes using a smooth theta function for the $\gamma^* \to q\bar{q}g$ process. Plots of the amplitude squared components from $C_2^{(1)}\mathcal{O}_2^{(1)}$: $|A^{q\bar{q}g}|^2_{\rm LO} + |A^{q\bar{q}g}|^2_{\rm NLO,\,2-jet}$ (short dashed green), $|A^{q\bar{q}g}|^2_{\rm NLO,\,3-jet}$ (long dashed blue), and sum (solid red) versus $|k_1|_{n_0\perp}$. The amplitudes are evaluated without running coefficients, and taking $\bar{k}_1/\bar{q}_0 = 0.4$. The δ_2 parameter in the Θ-function is 1.2, which for the above $\bar{p}$ fraction corresponds to $\eta = 0.5$, and $\lambda = 0.08$.

where tree-level SCET_2 and QCD agree. The advantage of using the one-gluon SCET_2 amplitude over QCD comes from factorization properties that effect interference as well as renormalization group evolution. For example the one-loop running in SCET_2 performs the LL Sudakov resummation.

With two-gluon emission, the SCET_1 graphs will include jet-structure corrections in addition to hard-scattering ones. It is straightforward to distinguish the types as the former result from taking time-ordered products of the SCET_1 Lagrangian with operators generated by the LO replacement rule, Eq. (56), while the latter will come only from terms involving a power suppressed SCET_1 operator. To fully identify the subleading contributions to two-gluon emission, we must match down to SCET_2 where the LO contribution is first uniquely identified. We already know that it comes from two applications of Eq. (56).

In Fig. 12, we show the contributions to two-gluon emission in QCD, SCET_1, SCET_2, and SCET_3. The first column in the SCET_1 category corresponds to the jet-structure corrections to be considered in the next section. In the second column we have a set of hard-scattering corrections from taking the T-product of the SCET_1 Lagrangian with the suppressed single gluon operators we calculated above in Eqs. (77), $C_1^{(1)}\mathcal{O}_1^{(1)}$ and $C_{1,\mathcal{T}}^{(1)}\mathcal{T}_1^{(1)}$.

In considering the basis of operators in SCET_2 we do not need operators such as $\mathcal{T}_2^{(1)}(n_1,\, n_1')$, since $\mathcal{P}_{n_1'\perp}\mathcal{B}_{n_1'\perp} = 0$, with n_1' lying along the gluon momentum. We can use RPI_2 in SCET_2 to make a coordinate choice where they are not necessary. As mentioned above in the single gluon matching section, our interest is only in calculating those terms needed to improve a shower algorithms, which precludes us from considering operators such as $\mathcal{T}_2^{(1)}(n_0,\, n_0)$ or $\mathcal{O}_2^{(1)}(n_0,\, n_0)$, corresponding to an unbranched quark passing from SCET_1 into SCET_2. Therefore, for double gluon emission we only need to calculate the coefficients of the following operators:

$$\begin{aligned}
\mathcal{O}_2^{(1)}(n_1,\, n_1') &= \bar{\chi}_{n_1} g\mathcal{B}^{\alpha}_{n_1'\perp}\chi_{\bar{n}} \qquad (81)\\
\mathcal{O}_2^{(2)}(n_2, n_2, n_1') &= \bar{\chi}_{n_2} g\mathcal{B}^{\alpha}_{n_2\perp}\, g\mathcal{B}^{\beta}_{n_1'\perp}\chi_{\bar{n}}\,,\\
\mathcal{O}_2^{(2)}(n_2, n_1', n_1') &= \bar{\chi}_{n_2} g\mathcal{B}^{\alpha}_{n_1'\perp}\, g\mathcal{B}^{\beta}_{n_1'\perp}\chi_{\bar{n}}\,,\\
\mathcal{O}_2^{(2)}(n_2, n_1', n_2') &= \bar{\chi}_{n_2} g\mathcal{B}^{\alpha}_{n_1'\perp}\, g\mathcal{B}^{\beta}_{n_2'\perp}\chi_{\bar{n}}\,.
\end{aligned}$$

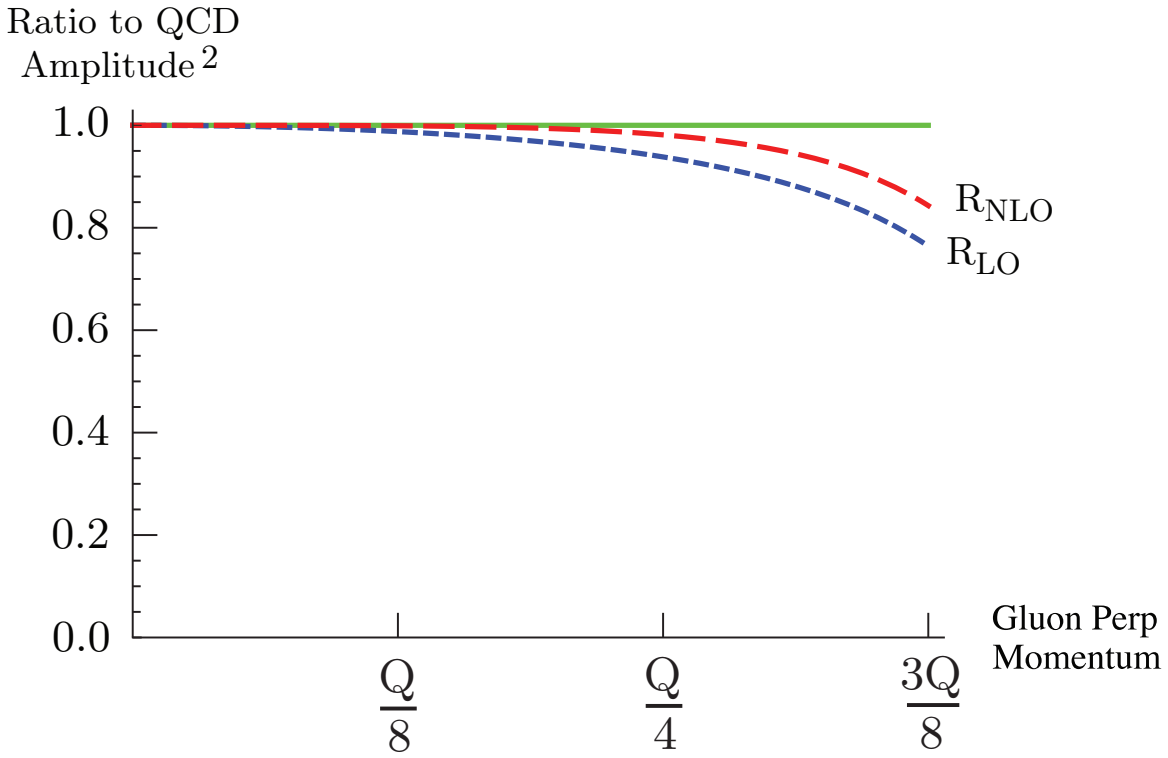

FIG. 11: Plot of the ratios of the amplitudes squared for $\gamma^* \to q\bar{q}g$, namely $R_{\rm LO} = |A^{q\bar{q}g}|^2_{\rm LO}/|A^{q\bar{q}g}|^2_{\rm QCD}$ (blue short dashed) and $R_{\rm NLO} = (|A^{q\bar{q}g}|^2_{\rm LO} + |A^{q\bar{q}g}|^2_{\rm NLO,2-jet})/|A^{q\bar{q}g}|^2_{\rm QCD}$ (red long dashed) versus $|k_1|_{n_0\perp}$, for $\bar{k}_1/\bar{q}_0 = 0.4$. The amplitudes are evaluated without running factors.

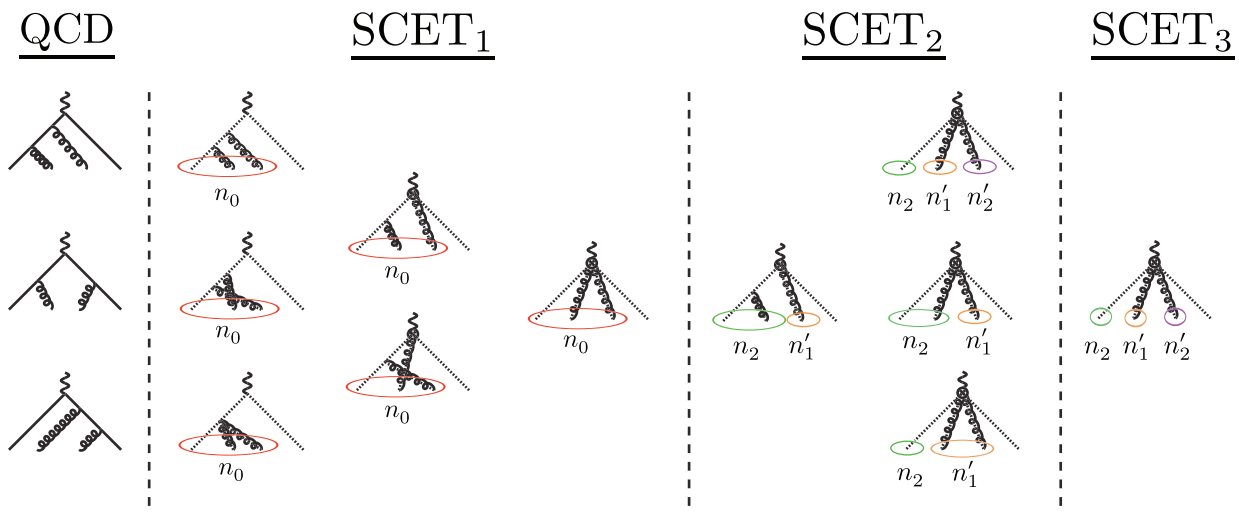

FIG. 12: Matching QCD to SCET_1 to SCET_2 to SCET_3 for two gluons emitted collinear to the quark direction (SCET graphs for other gluon kinematic configurations not shown). Once again, we depict the operator structures that lead to this process in each of the theories. Gluons drawn away from the central vertex are emitted by the leading order Lagrangian in that theory, while those coming from the vertex are due to higher dimension operators.

Thus in SCET_2, we are interested in *two*-gluon operators where two fields can have the same label. When we pass to SCET_3, we can restrict our interest to only $\mathcal{O}_3^{(2)}(n_2, n_1', n_2')$.

We already gave the coefficients of $\mathcal{O}_2^{(1)}(n_1, n_1')$ needed to compute the leading power corrections in Eqs. (80) and (D17)-(D19). We get an NLO(λ) contribution to the two gluon amplitude by computing the matrix element, $C_{2\,\rm NLO}^{(1)}\langle 0|\mathcal{T}\{\mathcal{L}_{\text{SCET}_2}\mathcal{O}_2^{(1)}\}|q\bar{q}gg\rangle$ (first SCET_2 column in Fig. 12). The contribution receives no further suppression as

the gluon from $\mathcal{L}_{\rm SCET_2}$ gives a tree-level vertex×propagator factor of λ^{-2}, just as with LO. There are also coefficients we need from two-gluon matching calculations for the operator $\mathcal{O}_2^{(2)}$ (second $\rm SCET_2$ column in Fig. 12). Putting in the index structures, these include $C^{(2)J}_{2,\,\rm NLO}(n_2,\,n_1',\,n_2')$ for $\mathcal{O}_2^{(2)}(n_2,n_1',n_2')$, $C^{(2)J}_{2,\,\rm NLO}(n_2,\,n_1',\,n_1')$ for $\mathcal{O}_2^{(2)}(n_2,n_1',n_1')$ and $C^{(2)J}_{2,\,\rm NLO}(n_2,\,n_2,\,n_2') + C^{(2)H}_{2,\,\rm NNLO}(n_2,\,n_2,\,n_2')$ for $\mathcal{O}_2^{(2)}(n_2,n_2,n_2')$. We include NNLO($\lambda$) for the last one as only it interferes with LO(λ). In the next subsection, we give the jet-structure corrections. All hard-scattering contributions to these structures just listed are beyond the order we need except for $C^{(2)H}_{2,\,\rm NNLO}(n_2,\,n_2,\,n_1')$, given by the matching equation:

$$\begin{aligned} &C^{(1)}_{1,\,\rm NLO}(n_0,n_0)\int dx\langle 0|T\{\mathcal{L}_{\rm SCET_1}(x)\mathcal{O}_1^{(1)}(n_0,n_0)\}|q_{n_2}g_{n_2}g_{n_1'}\bar{q}_{\bar{n}}\rangle \\ &-C^{(1)H,\,a}_{2,\,\rm NLO}(n_2,n_1')\int dx\langle 0|T\{\mathcal{L}_{\rm SCET_2}(x)\mathcal{O}_2^{(1)}(n_2,n_1')\}|q_{n_2}g_{n_2}g_{n_1'}\bar{q}_{\bar{n}}\rangle \\ &=C^{(2)H}_{2,\,\rm NNLO}(n_2,n_2,n_1')\langle 0|\mathcal{O}_2^{(2)}(n_2,n_2,n_1')|q_{n_2}g_{n_2}g_{n_1'}\bar{q}_{\bar{n}}\rangle\,, \end{aligned} \tag{82}$$

where we subtract the Lagrangian emission graph in $\rm SCET_2$ from that in $\rm SCET_1$ ($C^{(1)}_{1,\,\rm NLO}$ is given in Eq. 77 and $C^{(1)H,\,a}_{2,\,\rm NLO}$ in Eq. 80). The result for $C^{(2)H}_{2,\,\rm NNLO}(n_2,\,n_2,\,n_2')$ is given in Eq. (D61). It is straightforward to see why $\mathcal{O}_2^{(2)}$ only gets hard-scattering at NNLO(λ) and higher. By definition, hard-scattering has to involve a suppressed operator from the QCD $\to$ $\rm SCET_1$ matching, and so we begin at NLO(λ) at the lowest order. Including a second gluon, but demanding that we cannot write it as coming from a $\rm SCET_2$ Lagrangian emission takes us to one order higher, namely NNLO(λ).

All the contributions we have discussed so far have come from the hard-scattering, single-gluon, suppressed operators in $\rm SCET_1$. There are also those with two gluons. That is to say a process where neither gluon comes from the $\rm SCET_1$ Lagrangian, represented by the diagram in the third $\rm SCET_1$ column in Fig. 12. One example is double $\perp$-gluon emission from the antiquark, as shown in the third QCD graph of Fig. 12. We know from applying Eq. (56) twice, that LO for this process is at $\mathcal{O}(\lambda^{-3})$, counting only the tree-level vertex×propagator factors, as these are all we need to compare different $q\bar{q}gg$ processes. We readily see that double antiquark emission is $\sim\lambda^0$ as there are no small virtualities or emission angles for this term. Thus, they are $\rm N^3LO$, and beyond this analysis. Besides antiquark vertices, we also have subleading emissions from the quark in QCD that arise from the suppressed SCET-spinor portion of the QCD quark propagator (*cf.* Appendix A). If both emissions come from the suppressed propagator, once again, this is $\sim\lambda^0$ at lowest order, and so we can neglect it. Mixed antiquark/suppressed spinor contributions are also $\rm N^3LO$.

Thus, we do not need corrections to double emission collinear to the quark if they do not involve at least one $\rm SCET_1$ Lagrangian insertion. We can extend this argument further. If there are no $\rm SCET_1$ Lagrangian insertions, then the contribution goes like $\mathcal{O}(\lambda^0)$, while LO goes like $\mathcal{O}(\lambda^{-\frac{i(i+1)}{2}})$. Thus, to the order we are working, we only need the single gluon hard-scattering corrections given by Eq. (80), plus Lagrangian insertions.

B. Jet-Structure Corrections

The *jet-structure* corrections only involve contributions from the $\rm SCET_1$ Lagrangian. These arise from the graphs in the first $\rm SCET_1$ column in Fig. 12. We specifically designed our leading order replacement rule in Eq. (56), so when used twice it only contains that part of double emission corresponding to the leading strongly-ordered limit. This occurs for the gluons having collinearities $\sim\lambda$, λ^2, respectively. However, $\rm SCET_1$ describes other kinematic situations and in this section we compute the corrections from them.

The prescription for obtaining two-gluon jet-structure corrections is to compute the double gluon emission amplitude in $\rm SCET_1$ coming from two Lagrangian insertions and take different limits on the relative collinearities of n_2, n_2', and n_1', where these labels refer to the null vectors exactly proportional the corresponding particle momenta. We can define:

$$A^{q\bar{q}gg}_{\rm NLO}\;=\;C^{(0)}_{1,\,\rm LO}(n_0)\int dx_1dx_2\langle 0|T\{\mathcal{L}_{\rm SCET_1}(x_1)\mathcal{L}_{\rm SCET_1}(x_2)\mathcal{O}_1^{(0)}\}|q_{n_2}g_{n_1'}g_{n_2'}\bar{q}_{\bar{n}}\rangle, \tag{83}$$

and then calculate,

$$\lim_{n_2\cdot n_2'\sim\lambda^2} A_{\rm NLO}^{q\bar{q}gg} = C_{2,\,\rm NLO}^{(2)J}(n_2,\,n_1',\,n_2')\langle 0|\mathcal{O}_2^{(2)}|q_{n_2}g_{n_1'}g_{n_2'}\bar{q}_{\bar{n}}\rangle\,, \tag{84}$$

$$\lim_{n_1'\cdot n_2'\sim\lambda^4} A_{\rm NLO}^{q\bar{q}gg} = C_{2,\,\rm NLO}^{(2)J}(n_2,\,n_1',\,n_1')\langle 0|\mathcal{O}_2^{(2)}|q_{n_2}g_{n_1'}g_{n_2'}\bar{q}_{\bar{n}}\rangle\,, \tag{85}$$

$$\begin{aligned}\lim_{n_2\cdot n_2'\sim\lambda^4} A_{\rm NLO}^{q\bar{q}gg} &= C_{2,\,\rm LO}^{(1)}(n_2,n_1')\langle 0|T\{\mathcal{L}_{\rm SCET_2}\mathcal{O}_2^{(1)}\}|q_{n_2}g_{n_1'}g_{n_2'}\bar{q}_{\bar{n}}\rangle \\ &\quad + C_{2,\,\rm NLO}^{(2)J}(n_2,\,n_1',\,n_2)\langle 0|\mathcal{O}_2^{(2)}|q_{n_2}g_{n_1'}g_{n_2'}\bar{q}_{\bar{n}}\rangle\,.\end{aligned} \tag{86}$$

We note a few things about the above equations. Firstly, there is a correction to the LO Wilson coefficient obtained from the replacement rule (Eq. 56). We cannot get it purely as a limit of $A_{\rm NLO}^{q\bar{q}gg}$, so we need to subtract off the LO contribution. Secondly, the limit in Eq. (84) does not lead to an expansion of any part of $A_{\rm NLO}^{q\bar{q}gg}$, as the scaling of the n-indices' dot products is exactly that from $\rm SCET_1$. Even though it just gives back the same expression as the $\rm SCET_1$ amplitude, $A_{\rm NLO}^{q\bar{q}gg}$, the $\rm SCET_2$ result for $C_{2,\,\rm NLO}^{(2)J}(n_2,\,n_1',\,n_2')\mathcal{O}_2^{(2)}$ tells us something more. This Wilson coefficient is proportional to $\tilde{\Theta}_{\delta_2}[n_1'\cdot n_2']\tilde{\Theta}_{\delta_2}[n_2\cdot n_2']$, where the $\tilde{\Theta}$'s only have support outside the phase space region of Eq. (85), as well as the strongly-ordered limit, Eq. (86), (see Eqs. (54) and (D21) for the definition of Θ, $\tilde{\Theta}$). The full results for the Wilson coefficients shown in Eq. (86) can be found in Eqs. (D37), (D52), and (D59). At the amplitude level, given a particular phase space configuration for an external state, we will only ever need one of these terms for double gluon emission in $\rm SCET_2$. Squaring the result is straightforward as there will be no interference between them.

We will now examine how to improve the matching of $\rm SCET_i$ to $\rm SCET_{i+1}$, and show that the jet-structure corrections computed here generalize to that case. We first notice that the first two operators above do not interfere with the one giving LO, as they have different index structures. The subleading term in Eq. (86) does inhabit the strongly-ordered region of phase space, but as we will argue in Sec. IV D, LO(λ)/NLO(λ) interference cancels out of most observables of interest. Before proceeding, we note that our description of corrections to two-gluon emission gets even simpler when we match to $\rm SCET_3$. In $\rm SCET_3$, the only operator we need has distinct collinear directions for all fields. Thus, we can write all hard-scattering and jet-structure corrections to two-gluon emission we have found in the coefficient, $C_3^{(2)}$, for the operator $\mathcal{O}_3^{(2)}(n_2,n_1',n_2') = \bar{\chi}_{n_2}g\mathcal{B}^{\alpha}_{n_1'\perp}g\mathcal{B}^{\beta}_{n_2'\perp}\chi_{\bar{n}}$, as we do in Eqs. (E2). The same will hold for i-gluon emission in $\rm SCET_{i+1}$. Our NLO(λ) jet-structure operators therefore have the following form:

$$C_{3,\,\rm NLO}^{(2)J,I}(n_2,\,n_1,\,n_1')\mathcal{O}_3^{(2)} \;=\; h_I^{\alpha\beta}\,\bar{\chi}_{n_2}g\mathcal{B}^{\alpha}_{n_1'\perp}g\mathcal{B}^{\beta}_{n_2'\perp}\Gamma^{\mu}\chi_{\bar{n}}\,, \tag{87}$$

where $h_I^{\alpha\beta}$ is given by Eq. (E11). Here $I=\{1,2,3\}$, and we distinguish the coefficients $C_{3,\,\rm NLO}^{(2)J,I}$ depending on which $\rm SCET_2$ operators they come from in order to properly account for their RG evolution in $\rm SCET_2$.

When doing the LO matching for $\rm SCET_i$ to $\rm SCET_{i+1}$, we found that the replacement rule to go from $\rm SCET_1$ to $\rm SCET_2$ generalized to the case of i-gluon strongly-ordered emission. Similarly, we can take the above operator, Eq. (87), and recast it as a replacement rule for our original current insertion, $C_{1,\,\rm LO}^{(0)}\mathcal{O}_1^{(0)}$. It takes the form of a $1\to 3$ replacement rule:

$$\bar{\chi}_{n_0} \to h_I^{\alpha\beta}\,\bar{\chi}_{n_2}g\mathcal{B}^{\alpha}_{n_1'\perp}g\mathcal{B}^{\beta}_{n_2'\perp}, \tag{88}$$

with contributions from $I=1,2,3$.

If we want to consider the NLO(λ) radiation of $i{+}1$ gluons, we can perform a very similar matching between $\rm SCET_i$ and $\rm SCET_{i+2}$ to the one above for $\rm SCET_1\to SCET_3$ to obtain an operator $C_{i+2,\,\rm NLO}^{(i+1)J}\mathcal{O}_{i+2}^{(i+1)}$. Since the first $(i-1)$ emissions are strongly ordered, they completely factor out. Thus, the amplitude for the emission of the final two gluons will be identical to that for simple two-gluon emission. We can therefore take the $(i-1)$ gluon LO operator, $C_{i,\,\rm LO}^{(i-1)}\mathcal{O}_i^{(i-1)}$, and use the replacement rule in Eq. (88), to obtain $C_{i+2,\,\rm NLO\,I}^{(i+1)J}\mathcal{O}_{i+2}^{(i+1)}$. Our NLO($\lambda$) replacement rule corresponds to violating strong ordering at any location in the shower, either by taking the $j^{\rm th}$ and $(j+1)^{\rm th}$ gluons to have the same parametric collinearity with respect to their parents, $k_{j+1\perp}\sim k_{j\perp}$ (Eqs. 84 and 85); or by including the region of phase space where the propagator between them is hard even in $\rm SCET_1$, and so we get no collinear divergence as the quark and second gluon become collinear (86).[8]

[8] At this point, one may ask why we do not go farther and consider the case $k_{j+1\perp}\gg k_{j\perp}$. In fact, we do not have to. Since the amplitude for i-gluon emission has an underlying Bose symmetry, we are free to partition phase space into $i!$ regions, each of which

It is not difficult to see that this gives an NLO(λ) contribution for any j. If we have i-gluon strongly-ordered emission, the tree-level factors, $c_{\rm LO}^{\alpha_k}(n_{k-1})$, (*cf.* Eq. 63) will go as $\lambda^{-i(i+1)/2}$, where the $j^{\rm th}$ gluon contributes λ^{-j}. If we violate strong ordering as we mention above for any two gluons, the product of their vertices times propagators goes like λ^{-2j} instead of $\lambda^{-(2j+1)}$. Thus, we can insert $\bar\chi_{n_0} \to h_I\, \bar\chi_{n_2} g\mathcal{B}_{n_1'\perp} g\mathcal{B}_{n_2'\perp}$ instead of two successive $\bar\chi_{n_0} \to c_{\rm LO}\bar\chi_{n_1}\mathcal{B}_{n_1'\perp}$'s in operator matching as a "defect" in strong ordering at any stage and obtain an NLO(λ) jet-structure correction. The Θ-functions contained in the Wilson coefficients, $C_{i,\,\rm NLO}^{(i+1)J}$, allow us to read off at which step in the shower we violated strong-ordering.

In App. F, we show that an integrated version of $h_I^{\alpha\beta}$ is related to the splitting function at NLO in α_s, which serves as a cross-check on our computations.

C. Operator Running

Up until now, our discussion of matching has taken place mostly at tree-level. Connecting to the no-branching probabilities and log resummation in the parton shower however, requires that we include the anomalous dimensions needed for running. For this reason, our final expressions for Wilson coefficients in Apps. C-E include the necessary notation for evolution kernels. Identifying the power suppressed amplitudes as corresponding to perturbative corrections to more inclusive observables, it is natural to take only $\rm LL_{exp}$ evolution for power suppressed or α_s suppressed corrections, and include $\rm NLL_{exp}$ evolution only for the leading shower terms. For the former, we assume (without carrying out the proof in SCET$_i$) that we must make the k_T^2 choice for the scales μ_k^2 as in Eq. (64), and that this accounts for the difference between LL and $\rm LL_{exp}$. $\rm NLL_{exp}$ would require full one-loop, two-loop cusp, and NLL α_s running, plus any modifications to the evolution induced by subleading soft effects. If subleading soft effects are neglected then in the terminology of [60, 61], this gives the full *collinear* $\rm NLL_{exp}$ resummation. The subleading logarithms coming from pure soft effects involve the exponentiation of nonabelian matrices. As mentioned earlier, we do not compute the effects of subleading soft SCET$_i$ operators here. (In fact, for more than three hard, colored particles, the problem is quite non-trivial [60].)

In this section, we determine the $\rm LL_{exp}$ running for our subleading operators and discuss what is missing in our setup for a $\rm NLL_{exp}$ evolution kernel for emission anywhere in the shower. To set the stage, we consider SCET$_1$ matched to QCD at the scale Q for the first order power corrections. We then run down to μ in preparation for matching to SCET$_2$. The zero and single gluon operators in SCET$_1$ acquire the following running factors, U, (*cf.* the tree-level version in Eq. (77)):

$$
\begin{aligned}
C_0^{(0)}(n_0) &= U^{(2,0,0)}(n_0;\,Q,\mu)\,\gamma^\mu_{n_0\perp}\\
C_{1,\,\rm NLO}^{(1)}(n_0,n_0) &= U^{(2,1,0)}(n_0,n_0;\,Q,\mu)\otimes\frac{n_0^\mu-\bar n^\mu}{Q}\gamma^\alpha_{n_0\perp}\,,\\
C_{1,\,\mathcal{T}}^{(1)}(n_0,n_0) &= U_{\mathcal{T}}^{(2,1,1)}(n_0,n_0;\,Q,\mu)\otimes\frac{1}{\bar q_1\bar k_1}\Big(\gamma^\mu_{n_0\perp}\gamma^\beta_{n_0\perp}\gamma^\alpha_{n_0\perp}-\frac{2}{\bar q_1 Q}\,g^{\mu\beta}\gamma^\alpha_{n_0\perp}\Big)\,,\\
C_1^{(1)}(n_1,n_1') &= -U^{(2,1,0)}(n_1,n_1';\,Q,\mu)\Big(\frac{2}{(n_1\cdot n_1')\bar q_1\bar k_1}\gamma^\alpha_{n_0\perp}\not{p}_\gamma\,\gamma_T^\mu\\
&\qquad+\Big[\frac{1}{(n\cdot p_{\bar q})\bar k_1}\Big(\gamma_T^\mu\not{p}_\gamma-\bar q_1\,n_{1T}^\mu\Big)+\frac{2(n\cdot p_{\bar q})}{(n_1\cdot n_1')\bar q_1\bar k_1}\bar n_T^\mu\Big]\gamma^\alpha_{n_0\perp}\Big)\,,
\end{aligned}
\tag{89}
$$

where the superscripts follow the convention in Eq. (14). We inserted the symbol $\otimes$ in the second and third line of Eq. (89) since an operator with multiple fields sharing the same collinear direction can convolve the momentum fraction of $\bar p$ between the corresponding RG kernel U and momenta in the tree-level coefficient. This is because collinear fields that are in the same direction in SCET can exchange momentum while running down from Q to μ. The anomalous dimension of an operator is independent of which SCET$_i$ it is defined, but does depend on the field content and in particular how many different collinear directions are in the operator. Thus, the RG-kernel for $\bar\chi_{n_0} g\mathcal{B}^\alpha_{n_0\perp}\chi_{\bar n}$ is different from that of $\bar\chi_{n_1} g\mathcal{B}^\alpha_{n_1'\perp}\chi_{\bar n}$. In Ref. [24, 25], the LL part of $U^{(j,i-j,0)}(Q,\,\mu)$ was related to the Sudakov form factor, Eq. (20) (up to accounting for the soft effects of angular ordering [75]). The cusp term in the

gives an identical contribution to the cross section. Thus, to get the final answer, we only need to integrate over one of them. While we can choose this region such that $k_{j+1\perp}\gg k_{j\perp}$ never occurs, we are forced to include $k_{j+1\perp}\sim k_{j\perp}$. If we do not wish to partition phase space in this manner, then the Bose symmetry implies that the result for $k_{j+1\perp}\gg k_{j\perp}$ can be obtained from the configurations already discussed.

anomalous dimension resums the LL, and comes from soft and collinear one-loop diagrams. The result from the soft diagrams is constrained by that of the collinear diagrams in order to cancel out infrared sensitivity that cannot be absorbed in local counterterms at the hard scale. Here we will use this same argument, but in reverse, in order to determine the $\mathrm{LL}_{\mathrm{exp}}$ anomalous dimension of various subleading operators.

Due to the soft-collinear factorization, the soft structure only depends on the number of collinear directions. After making the field redefinition, operators like $\bar{\chi}_{n_0}\chi_{\bar{n}}$ and $\bar{\chi}_{n_0} g\mathcal{B}^{\alpha}_{n_0\perp}\chi_{\bar{n}}$ both have $Y^{\dagger}_{n_0}Y_{\bar{n}}$, and so both have the same soft divergences. Hence they have the same one-loop cusp term and the same LL anomalous dimension from the sum of collinear and soft loops. Thus, the leading-log resummation only depends on the number of collinear index directions in the operator, and not on the number of active partons. (At leading power these concepts are the same, but it is not so for the power corrections.) We therefore have

$$U_{\mathrm{LL}}^{(2,0,0)}(n_0) = U_{\mathrm{LL}}^{(2,1,1)}(n_0,n_0) = U_{\mathrm{LL},\mathcal{T}}^{(2,1,1)}(n_0,n_0)\,, \tag{90}$$

where we give $U_{\mathrm{LL}}^{(2,0,0)}$ in Eqs. (18) and (19). Thus, at LL order we have the full set of evolution kernels for subleading collinear operators, and we account for these factors in the appendices. Since this is a LL effect, we expect soft radiation and angular ordering to be incorporated in a manner identical to the evolution factor in the LL shower.

An important consequence of this result for the LL evolution is that it justifies treating our hard-scattering corrections as improvements to the fixed-order, matrix-element calculation that goes into a shower algorithm. Correcting the two-jet amplitude with either $C^{(1)}_{1,\,\mathrm{NLO}}$ or $C^{(1)}_{1,\,\mathcal{T}}$, we see that the LL resummation is the same as that in the standard shower except that there is an extra parton already inside the leading jet. We thus get a shower correction just by using a matrix element improved by including our hard-scattering terms. This is unlike simply running a LL shower on higher order matrix elements, as different anomalous dimensions control different operators' evolution. Some, like those just mentioned with only n_0 and $\bar{n}$ collinear directions, run like two-jet configurations, that is with a quark-antiquark Sudakov. Others, (*e.g.* $C_1^{(1)}\mathcal{O}_1^{(1)}(n_1', n_1)$) have three-parton running since they have three distinct collinear directions. This latter set corresponds to the usual implementation of fixed order corrections in parton showers, but the former is a novel type of shower improvement.

On the other hand, the effect of jet-structure corrections is not to modify the initial scattering process, but to go hand in hand with the NLL change to the leading operators' running. Similarly to Eq. (63), we might anticipate the following Wilson coefficient for $\mathcal{O}_N^{(N-1)}$ with evolution:

$$\begin{aligned} C^{(N-1)}_{N,\,\mathrm{NLL},\,1}(m) = \Bigg[\Bigg(\prod_{k=1,\,k\neq m}^{N-1} U_{\mathrm{LL}}^{(k-1)}(\mu_{k-1},\mu_k)\, c_{\mathrm{LO}}^{\alpha_k}(n_{k-1}) \Bigg) \\ \times U_{\mathrm{NLL}}^{(m-1)}(\mu_{m-1},\mu_m)\, c_{\mathrm{LO}}^{\alpha_m}(n_{m-1}) \Bigg] \Gamma^{\mu}, \end{aligned} \tag{91}$$

with a sum over all locations where the NLL evolution can be inserted:

$$C^{(N-1)}_{N,\,\mathrm{NLL},\,1} = \sum_{m=1}^{N-1} C^{(N-1)}_{N,\,\mathrm{NLL},\,1}(m). \tag{92}$$

One would expect to use $C^{(N-1)}_{N,\,\mathrm{NLL},\,1}\mathcal{O}_N^{(N-1)}$ along with our real emission corrections (Eq. E13) to correct a shower to resum at NLL the ratios of all emission scales (*cf.* Eq. 104). The complication we face for the calculation of $U_{\mathrm{NLL}}^{(m-1)}$ is that this correction to the evolution kernel must, in principle, be carried out in the same scheme used to distinguish the phase space regions for the jet-structure corrections, and hence can depend on the choice for the Θ functions. In particular, we could have non-trivial operator mixing on the edge where the cutoff makes a smooth transition between operators with different numbers of jets, and we have not yet performed the analysis that would determine whether this effects the resummation at $\mathrm{NLL}_{\mathrm{exp}}$ order. Furthermore, it is possible that power suppressed soft effects will also have implications for the subleading evolution kernel, and may make the nonabelian generalization of Eq. (92) tricky. Our lack of an appropriate $\mathrm{NLL}_{\mathrm{exp}}$ evolution factor for the shower is due to these two issues.

To setup the distinction between kinematic regions, we used Wilsonian type Θ functions, but from the point of view of evolution $\overline{\mathrm{MS}}$ would be simpler. Although it is only indirectly relevant to our setup, it is nevertheless still interesting to consider how the NLL evolution kernel would arise in $\overline{\mathrm{MS}}$. As we discuss below in App. F, when integrated over phase space in dimensional regularization the jet-structure corrections give the real emission portion of $P_{qq}^{(1)}$, which is the $\mathcal{O}(\alpha_s)$ correction to the Altarelli-Parisi splitting kernel. Combined with known SCET results for single-emission at one-loop, we can recover all of the abelian portion of $P_{qq}^{(1)}$. Obtaining this expression is important conceptually. It validates our formal expansion in λ, showing that corrections to $\mathcal{O}(\lambda^2)$, along with a set of known one-loop diagrams,

capture contributions needed for collinear NLL_{exp} resummation. On the practical side, it provides a cross check on our computations.

With $P_{qq}^{(1)}$ in hand, we can extend the argument of [24, 25] that the Sudakov factor gives the LL part of the the RG kernel $U^{(2,i,0)}(Q,\mu)$ (Eq. 20) to the NLL level, looking at $U^{(2,0,0)}(Q,\mu)$ for running of the operator $C_{1,\,\text{LO}}^{(0)}\mathcal{O}_1^{(0)}$. Using the Sudakov factor of [27] for quarks, we have:

$$\Delta_q(Q,\mu) \,=\, \exp\left\{-\frac{C_F}{2\pi}\int_\mu^Q \frac{d\mu'}{\mu'}\alpha_s(\mu')\int_{\frac{\sqrt{\mu'}}{Q}}^{1-\frac{\sqrt{\mu'}}{Q}} dz\frac{1+z^2}{1-z}\right\}, \tag{93}$$

where we recognize $P_{qq}^{(0)}$, Eq. (3). Performing the z integral and expanding in the limit of large Q gives:

$$\Delta_q(Q,\mu) \,\approx\, \exp\left\{\frac{C_F}{\pi}\int_\mu^Q \frac{d\mu'}{\mu'}\alpha_s(\mu')\left[\log\left(\frac{\mu'^2}{Q^2}\right)+\frac{3}{2}\right]\right\}, \tag{94}$$

which is identical to $U^{(2,0,0)}(Q,\mu)$ at one-loop. The term in the exponent proportional to $\log(\mu'^2/Q^2)$ sums the leading logs in the parton shower. We also see that upon μ' integration, we get the double logarithm characteristic of the soft-collinear divergence of collinear splitting. Interpreting Eq. (94) as an RG kernel, this log piece is coming from the one-loop cusp anomalous dimension, C_F. The factor of $3/2$ is the remaining part of the one-loop anomalous dimension, and it sums part of the collinear NLL.[9] In order to get the full collinear NLL_{exp} summation, one also needs corrections corresponding to the two-loop cusp anomalous dimension. This is a known result in SCET for the operator $\bar{\chi}_n\chi_{\bar{n}}$, which we can relate to $P_{qq}^{(1)}$, by adding the subleading splitting function to the exponent of $\Delta_q(Q,\mu)$. We wish to stress, however, that the ultimate goal of improving parton showers through resummation is to include all next-to-leading-logs.[10] In this paper, as mentioned previously we have not considered the effects of soft NLL, nor those related to the two-loop running of α_s, which will affect collinear NLL. Our formulas in Apps. C-E include LL running for all subleading operators. In App. F we discuss the relation of our $1\to 3$ splitting amplitude with $P_{qq}^{(1)}$ in $\overline{\text{MS}}$. The collinear-NLL-improved Sudakov corresponding to this is

$$\Delta_q^{\text{NLL}}(Q,\mu) \,=\, \exp\left\{-\int_\mu^Q \frac{d\mu'}{\mu'}\int_{\frac{\sqrt{\mu'}}{Q}}^{1-\frac{\sqrt{\mu'}}{Q}} dz\,\left[P_{qq}^{(0)}(z,\alpha_s(\mu'))\,+\,P_{qq}^{(1)}(z,\alpha_s(\mu'))\right]\right\}, \tag{95}$$

where $P_{qq}^{(0)}$ given in Eq. (3) and $P_{qq}^{(1)}$ in [62]. Once again, we integrate in z, expanding in large Q to get:

$$\begin{aligned}\Delta_q^{\text{NLL}}(Q,\mu) = \exp\Bigg\{\int_\mu^Q \frac{d\mu'}{\mu'}\Bigg[&\frac{\alpha_s(\mu')}{\pi}C_F\left(\log\left(\frac{\mu'^2}{Q^2}\right)+\frac{3}{2}\right)\\ &+\,\frac{\alpha_s^2(\mu')}{4\pi^2}C_F\left(C_g\left(\frac{67}{9}-\frac{\pi^2}{3}\right)-\frac{20}{9}C_F T_F\, n_F\right)\log\left(\frac{\mu'^2}{Q^2}\right)\Bigg]\Bigg\},\end{aligned} \tag{96}$$

where the term $\propto \alpha_s^2$ reproduces the known result for the two-loop cusp anomalous dimension. While including this $\overline{\text{MS}}$ NLL effect for "no-branching" was already possible, our result in Eq. (E13) allows one to modify the differential cross section for real emission to include the effects of $P_{qq}^{(1)}$, as well. Without including both, one does not have a systematic improvement beyond LL. In [56], the authors were able to get NLL_{exp} soft resummation by treating the subleading real and virtual effects in semi-inclusive observables for DIS and Drell-Yan. A full implementation in our framework with more exclusive observables must wait for computations that address the missing NLL ingredients mentioned above.

D. Squared Amplitudes and Interference Structures

As discussed previously, our series of matchings terminates with SCET_N, where each field has its own index direction. Further Lagrangian emission from these operators is physically meaningless, as the resolution scale is set

---

[9] Since Eq. (94) resums the NLL contributions expanded in the cross section (*cf.* Eq. 5), Ref. [27] calls it the NLL Sudakov factor.

[10] At a practical level, while we see full collinear NLL_{exp} as coming from a straightforward extension of this work, pure soft NLL may only be possible at the leading orders in $1/N_c$[60, 61].

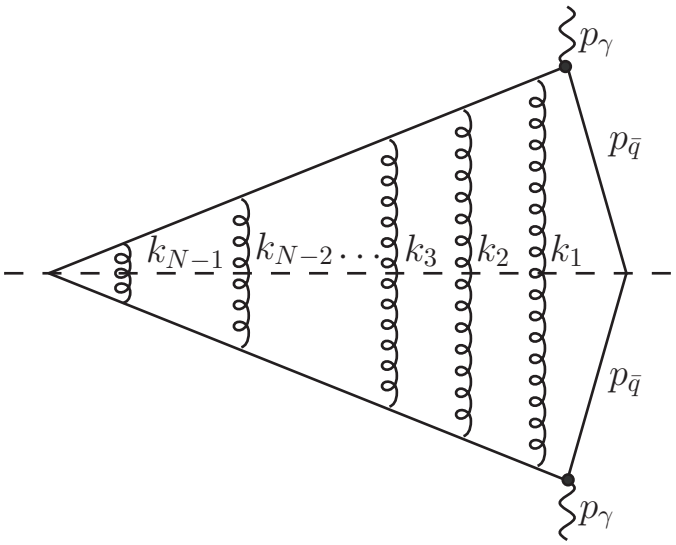

FIG. 13: Amplitude squared for the LO SCET shower operator $C^{(N-1)}_{N,\,\mathrm{LO}}\mathcal{O}^{(N-1)}_N$. Rather than drawing the less intuitive squared amplitude in SCET_N, we illustrate the process here with a cut SCET_1 Feynman diagram in order to emphasize the simple ladder structure.

$\sim \mathcal{O}(\mathrm{GeV})$, below which we stop computing in perturbation theory and pass to a hadronization routine. Thus, we match everything to the single operator $\mathcal{O}^{(N-1)}_N(n_N, n'_1, \ldots, n'_{N-1})$ and all the information about the shower at LO and NLO is encoded in the Wilson coefficients. In this SCET_N, we square amplitudes and compute corrections to observables, as we detail in Sec. IV E. As we saw in Secs. IV A and IV B, for arbitrary N, we only needed one and two-gluon computations to obtain leading corrections in λ to the differential cross section. Using the LO replacement rule (Eq. 56) will account for the rest of the multiplicity. Since the strongly-ordered emissions it describes have trivial interference, we should expect that squaring our results retains the simple picture we have for corrections at the amplitude level.

1. *Interference for* LO^2 *and for Jet-Structure Corrections*

It is a general statement about SCET fields with different n index labels that they have no overlap in Hilbert space. As an example, we can take two different operators, $\mathcal{O}_{n_1}$ and $\mathcal{O}_{n_2}$ where all the fields in $\mathcal{O}_{n_1}$ and $\mathcal{O}_{n_2}$ are identical, except those labeled by n_1 and n_2 (*e.g.* $\bar{\chi}_{n_1}$ versus $\bar{\chi}_{n_2}$). For generality the field labeled by n_2 may or may not be in the same equivalence class as n_1. We thus have:[11]

$$\begin{aligned}&\langle q_1,\, q_2,\, \ldots,\, q_m|\mathcal{O}^\dagger_{n_1}|0\rangle\langle 0|\mathcal{O}_{n_2}|q_1,\, q_2,\, \ldots,\, q_m\rangle \\ &= \delta_{[n_1],[n_2]}\,\langle q_1,\, q_2,\, \ldots,\, q_m|\mathcal{O}^\dagger_{n_1}|0\rangle\langle 0|\mathcal{O}_{n_2}|q_1,\, q_2,\, \ldots,\, q_m\rangle. \end{aligned} \tag{97}$$

This relation between n_1 and n_2 is simple when the difference is encoded in the collinear fields in operators. However, as discussed in Sec. IV A, we also had to deal with situations where this information ended up in Wilson coefficients when matching SCET_i to SCET_{i+1}. It is to guarantee a relation like Eq. (97) that our Wilson coefficients contain Θ-functions (*cf.* Eqs. 54 and D21), which will cutoff the overlap regions in phase space once we begin integrating. The amplitude squared is particularly simple in SCET_N, where we have only the operator $\mathcal{O}^{(N-1)}_N(n_N, n'_1, \ldots, n'_{N-1})$, and where each particle is defined in a different collinear direction.

SCET_N (or SCET_i, in general) easily distinguishes which configurations are strongly-ordered by the structure of their Wilson coefficients. This means that we have no interference between $C^{(N-1)}_{N,\,\mathrm{LO}}\mathcal{O}^{(N-1)}_N$ and $C^{(N-1)J}_{N,\,\mathrm{NLO}}\mathcal{O}^{(N-1)}_N$ where $C^{(N-1)}_{N,\,\mathrm{LO}}$ is the LO SCET_N coefficient given in Eq. (63), and $C^{(N-1)J}_{N,\,\mathrm{NLO}}$ is in Eq. (E12). Even though the $\mathcal{O}$'s are the

[11] By RPI, n_1 and n_2 do not have to be exactly equal, but must concur up to an angle of $\mathcal{O}(\lambda^i)$ in SCET_i.

same, the Θ-functions in the C's enforce different conditions, where the former is strongly ordered, while the latter is not. Thus, in the analog of Eq. (97), the Kronecker delta will give zero.

We get a further simplification when we square the NLO(λ) contributions. Looking at $C^{(N-1)J}_{N,\,\mathrm{NLO}}$ in detail, we have:

$$C^{(N-1)J}_{N,\,\mathrm{NLO}} = \sum_{l=1}^{N-2} C^{(N-1)J}_{N,\,\mathrm{NLO}}(l)\,, \tag{98}$$

where

$$\begin{aligned} C^{(N-1)J}_{N,\,\mathrm{NLO}}(l) =& \sum_{I=1}^{3}\Big[\Big(\prod_{k=1}^{l-1} U^{(k-1)}_{\mathrm{LL}}(\mu_{k-1},\,\mu_k) c^{\alpha_k}_{\mathrm{LO}}(n_{k-1})\Big) U^{(l-1)}_{\mathrm{LL}}(\mu_{k-1},\,\mu_k) \otimes h^{\alpha,\beta}_I(n_{l+1}, n'_l, n'_{l+1}) \\ & \times \Big(\prod_{k=l+1}^{N-1} U^{(k-1)}_{\mathrm{LL}}(\mu_{k-1},\,\mu_k) c^{\alpha_k}_{\mathrm{LO}}(n_{k-1})\Big)\Big]\Gamma^{\mu}\,. \end{aligned} \tag{99}$$

In $C^{(N-1)J}_{N,\,\mathrm{NLO}}(l)$, we have made explicit that the $l, (l+1)^{\mathrm{th}}$ gluons violate strong-ordering and come with the factor $h^{\alpha\beta}$ of the subleading splitting rule, Eq. (88). The sum in the last term over I counts the different types of NLO jet-structure terms given in Eq. (87). The $c^{\alpha_k}_{\mathrm{LO}}$ are defined in Eqs. (63) and (E7), and the U's are running factors given in Eqs. (18)-(20). The complete explanation of the symbols in Eq. (99) can be found in the discussion around Eq. (E13). The convolution factor is explained below Eq. (89). Since different l correspond to a violation of strong-ordering at different points in the shower, each of the $C^{(i+1)J}_{i,\,\mathrm{NLO}}(l, l+1)$ encodes a different Θ structure. Therefore, there is no interference for different values of l, and we have that the amplitude squared to NLO(λ) for jet-structure corrections (we call corrections of $\mathcal{O}(\lambda^2)$ at the amplitude squared level NLO(λ)) is just the sum of squares of the individual operators:

$$|A^{q(N-1)g\bar{q}\,J}|^2_{\text{to NLO}} = |A^{q(N-1)g\bar{q}}|^2_{\mathrm{LO}} + |A^{q(N-1)g\bar{q}J}|^2_{\mathrm{NLO}}\,, \tag{100}$$

where

$$\begin{aligned} |A^{q(N-1)g\bar{q}}|^2_{\mathrm{LO}} =&\ |C^{(N-1)}_{N\,\mathrm{LO}}|^2\,|\langle 0|\mathcal{O}^{(N-1)}_N|q(N-1)g\bar{q}\rangle|^2\,, \\ |A^{q(N-1)g\bar{q}\,J}|^2_{\mathrm{NLO}} =&\ \sum_{l=1}^{N-2} |C^{(N-1)J}_{N,\,\mathrm{NLO}}(l)|^2\,|\langle 0|\mathcal{O}^{(N-1)}_N|q(N-1)g\bar{q}\rangle|^2, \end{aligned} \tag{101}$$

and $|q(N-1)g\bar{q}\rangle$ indicates the state with $N-1$ gluon emission. The simplification even extends inside each of the terms, since the j^{th} gluon only gets contracted with itself. Diagrammatically, this means there are zero nearest-neighbor crossings in the $|\mathrm{LO}|^2$ diagram, as we see in Fig. 13, and a maximum of *one* in the $|\mathrm{NLO}|^2$, Fig. 14. We thus only slightly modify the factorized emission formula, Eq. (2). Even for an arbitrary number of gluon emissions, we at most have to take into account a single defect that involves a full two-particle phase space.

We can see why terms that have non-trivial interference with more than two gluons are suppressed by looking at the propagators in the amplitude. The amplitude for $i+1$ emissions has a factor $1/q_1^2 \times 1/q_2^2 \times \cdots \times 1/q_i^2$. The LO term comes form the strong-ordered region where $q_1^2 \gg q_2^2 \gg \cdots \gg q_i^2$, Eq. (1). The jet-structure NLO(λ) is given when $q_j^2 \sim q_{j+1}^2$, which allows the two gluons k_{j+1} and k_{j+2} to share the same region of the phase space and therefore interfere. To have an overlap of three or more gluons, we would need $q_j^2 \sim q_{j+1}^2 \sim \ldots \sim q_{j+k}^2$, which is clearly suppressed beyond NLO(λ).

2. Interference for Hard-Scattering Corrections

The corrections to the differential cross section to $\mathcal{O}(\lambda^2)$ involve squaring the subleading hard-scattering amplitudes as well. Unlike the jet-structure case, these involve amplitude terms up to NNLO(λ). As we argued above, they only modify the gluons closest to the hard interaction. Thus, we will not need to sum over many terms as we do in Eq. (101). In fact, for hard-scattering corrections, we only need to worry about interfering SCET_i operators that arise from acting with the LO replacement rule Eq. (56) on either $C^{(0)}_{1,\,\mathrm{LO}}$, $C^{(1)}_{1,\,\mathrm{NLO}}$, and $C^{(1)}_{1,\,\mathcal{T}}$, given in Eqs. (42) and (77), or $C^{(2)H}_{2,\,\mathrm{NNLO}}$ given in Eq. (D65). Since the 3^{rd} through i^{th} gluons arise from the LO rule for all three coefficients, they

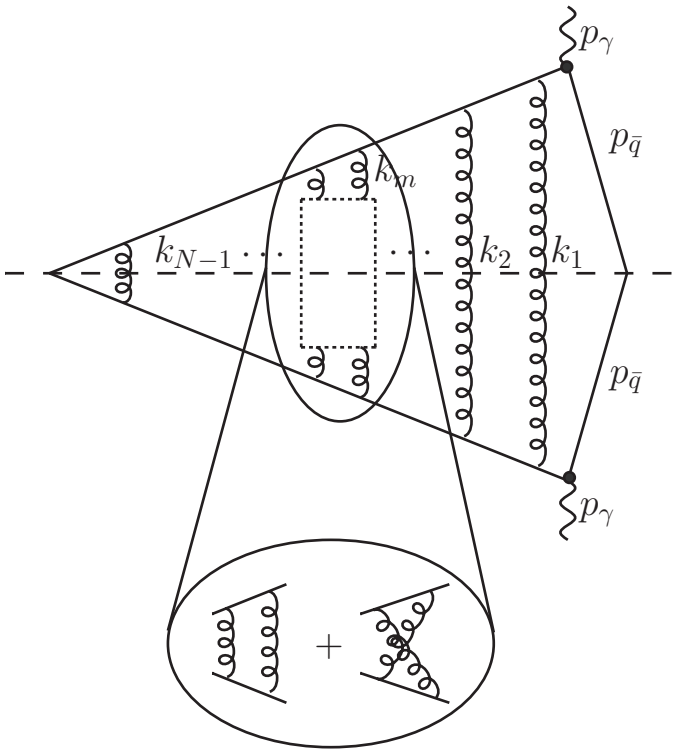

FIG. 14: Contribution to the amplitude squared of the jet-structure piece at NLO. We show a cut SCET_1 Feynman diagram to emphasize that the square of the SCET_N operator, $C^{(N-1)J}_{N,\,\mathrm{NLO}}\mathcal{O}^{(N-1)}_N$, contains only a single deviation from the simple ladder structure appearing at LO in Fig. 13.

proceed as in the $|\mathrm{LO}|^2$ case. The interference to look at in detail is that of the first two gluons. In SCET_N, we have:

$$\begin{aligned}|A^{q(N-1)g\bar{q}\,H}|^2_{\mathrm{to\,NLO}} =& \big(|C^{(N-1)\dagger}_{N,\,\mathrm{LO}}C^{(N-1)H}_{N,\,\mathrm{NLO}} + C^{(N-1)H\dagger}_{N,\,\mathrm{NLO}}C^{(N-1)}_{N,\,\mathrm{LO}}| + |C^{(N-1)H}_{N,\,\mathrm{NLO}}|^2 \\ &+ |C^{(N-1)\dagger}_{N,\,\mathrm{LO}}C^{(N-1)H}_{N,\,\mathrm{NNLO}} + C^{(N-1)H\dagger}_{N,\,\mathrm{NNLO}}C^{(N-1)}_{N,\,\mathrm{LO}}|\big)|\langle 0|\mathcal{O}^{(N-1)}_N|q(N-1)g\bar{q}\rangle|^2\end{aligned} \tag{102}$$

The Wilson coefficients are found in Eqs. (E6), (E8), and (E9), respectively. Nontrivial interference in Eq. (102) occurs between the first two-gluon emissions.

The interference between LO and NLO(λ) simplifies in many cases of interest. For example for one-gluon emission,

$$|A^{qg\bar{q}}_{\mathrm{LO/NLO}}|^2_{\mu\,\nu} \;=\; \frac{4\bar{q}_1\bar{p}_{\bar{q}}}{q_0^2}k_{1\perp\,\nu}(n_\mu - \bar{n}_\mu). \tag{103}$$

If we can cleanly separate the initial and final states (*e.g.* $e^+e^- \to$ jets), then by a classic proof involving the Ward identity (reproduced, for example, in [76]), once we have integrated over final state vector quantities (we can keep scalars such as z_i unintegrated), the resulting differential observable depends on $g^{\mu\nu}|A_{\mathrm{LO/NLO}}|^2_{\mu\,\nu}$, which for Eq. (103) is zero. This is quite straightforward for leptonic initial states, and one may be able to extend it to certain hadronic ones as well.

One can account for these corrections by modifying the hard-scale matrix element and then running a parton shower modified to include the different no-branching probabilities for different phase space configurations of the same particle content. In the next section we discuss using a reweighting to implement these corrections.

E. Correction Summary at Subleading Order

In general, our corrections avoid double counting issues, because all contributions, whether LO, hard-scattering, or jet-structure corrections are kept separately with distinct Θ structures. Given the SCET_N amplitude for $N+1$ final state particles with corrections implemented both for the branching and for the no-branching, one can consider

reweighting a LL shower in order to implement our results. For correcting the abelian emissions off a single quark line, this weight factor would take the following form:

$$w = \frac{[J(N-1,\,0) \,+\, H(N-1,0)]}{A(N-1,\,0)}\,, \tag{104}$$

where $A(N-1,0)$ is the LL amplitude squared for $N-1$ emissions from the quark line, $J(N-1,0)$ includes the LL result along with power corrections and subleading resummation associated with jet-structure corrections, and H contains hard scattering corrections. With our LO(λ) result,

$$A(N-1,0) = |C_{N,\mathrm{LO}}^{(N-1)}|^2 |\langle 0|\mathcal{O}_N^{(N-1)}|q(N-1)g\bar{q}\rangle|^2\,, \tag{105}$$

but in general A could be whatever amplitude squared a particular shower algorithm has for a given configuration. Eq. (104) then reweights that particular shower to our NLO(λ) corrected result. An example of shower Monte Carlo with an analytic expression for $A(N-1,0)$ is GenEvA [54]. For a leading log shower without an explicit formula for $A(N-1,0)$ one can use Eq. (105) with the understanding that it is likely a good approximation to the shower output. For the terms in the numerator of Eq. (104) we have:

$$\begin{aligned}
J(N-1,0) &= |C_{N,\,\mathrm{NLL},\,1}^{(N-1)J}|^2 |\langle 0|\mathcal{O}_N^{(N-1)}|q(N-1)g\bar{q}\rangle|^2 + |C_{N,\,\mathrm{NLO}}^{(N-1)J}|^2 |\langle 0|\mathcal{O}_N^{(N-1)}|q(N-1)g\bar{q}\rangle|^2\,,\\
H(N-1,0) &= |C_{N,\,\mathrm{NLO}}^{(N-1)H}|^2 |\langle 0|\mathcal{O}_N^{(N-1)}|q(N-1)g\bar{q}\rangle|^2\\
&\quad + \Big(C_{N,\mathrm{LO}}^{(N-1)}\, C_{N,\,\mathrm{NNLO}}^{\dagger(N-1)H} \langle 0|\mathcal{O}_N^{(N-1)}|q(N-1)g\bar{q}\rangle\langle q(N-1)g\bar{q}|\mathcal{O}_N^{\dagger(N-1)}|0\rangle + \mathrm{h.c.}\Big),
\end{aligned} \tag{106}$$

where we give formulas for $C_{N,\mathrm{LO}}^{(N-1)}$ and $\mathcal{O}_N^{(N-1)}$ in Eq. (63), $C_{N,\,\mathrm{NLL},\,1}^{(N-1)J}$ is discussed near Eqs. (91) and (92), $C_{N,\,\mathrm{NLO}}^{(N-1)J}$ is given in Eqs. (98) and (99), $C_{N,\,\mathrm{NLO}}^{(N-1)H}$ is given in Eq. (E8), and $C_{N,\,\mathrm{NNLO}}^{(N-1)H}$ is given in Eq. (E9). Our operators, $\mathcal{O}_N^{(N-1)}$, describe a process with $N-1$ emissions off the quark line. The $A(N-1,0)$ amplitude squared in Eq. (105) is contained within the first term in $J(N-1,0)$. As discussed in Sec. IV C, while we have worked out the real emission terms ($C_{N,\,\mathrm{NLO}}^{(N-1)J}$) completely, we have yet to determine the subleading RG kernels needed for $C_{N,\,\mathrm{NLL},\,1}^{(N-1)J}$.

We introduce the A, J, H notation to describe more general abelian processes. $A(j,\,k)$ gives the amplitude squared necessary for the LL shower of j gluons collinear to the quark, and k collinear to the antiquark. The correction, $J(j,\,k)$, contains the virtual and real corrections necessary for $\mathrm{NLL}_{\mathrm{exp}}$ resummation of collinear logs. Since it contains an implicit sum over insertions of a single defect, which can occur anywhere in the shower, it depends on the total number of collinear emissions. Including the hard-scattering contributions to NLO(λ) only requires modification of the first two emissions, after which one simply uses the LO replacement rule, Eq. (56). In the general case we denote it by H', which differs from the above by including corrections to antiquark emissions as well. These are easily obtained by charge conjugation. Thus, an abelian two-jet process with $j+k$ gluons gets the following reweighting factor:

$$w(j,\,k) = \left[J(j,\,k) \,+\, H'(j,\,k)\right]/A(j,\,k). \tag{107}$$

These weight factors are positive definite. All contributing terms are squares of amplitudes, except for LO(λ) $\times$ NNLO(λ) in $H(N-1,0)$. This contributes in the same region of phase space as the LO(λ) amplitude squared, and the sum of these terms is positive. In the full nonabelian case, with the presence of gluon splittings, one must sum over possible shower histories in writing down the analog of Eq. (107). Algorithms for handling this complication can be found in [1, 54].

In Table II we list concepts that are addressed by our shower framework at subleading order, and associate these concepts with corresponding calculations in SCET_i. This table provides a summary of our results which appear in the weights given in Eq. (107), as well as pointers for future calculations. Since it is easier, in the table we use the language of SCET_1 and SCET_2 to discuss the corrections, rather than referring to terms in the final SCET_N. In SCET_N, the features of the SCET_1 operators that avoid double counting and allow the various contributions to be distinguished are encoded by Θ functions in the Wilson coefficients, and the operator language makes the discussion easier. For the total differential cross section, we found at NLO(λ) two kinds of power corrections. This includes a set of matrix-element corrections called hard-scattering corrections (Sec. IV A), and a set of contributions that improve double real emissions that we called jet-structure corrections (Sec. IV B).

In the the hard-scattering category, we have overall three different kinds of corrections. The first is due the the SCET_1 operator $\bar{\chi}_{n_1}\mathcal{B}_{n_1'}\chi_{\bar{n}}$ that gives the SCET_2 coefficient $C_{2,\,\mathrm{NLO}}^{(1)H,b}$ in Eq. (80). This is an improvement of the hard matrix element that takes into account the emission of an extra parton at the hard scale. The second is due to the SCET_1 operators $\bar{\chi}_{n_0}\mathcal{B}_{n_0}\chi_{\bar{n}}$ and $\bar{\chi}_{n_0}[\mathcal{P}_\perp\mathcal{B}_{n_0}]\chi_{\bar{n}}$ that give the SCET_2 coefficients $C_{2,\,\mathrm{NLO}}^{(1)H,a}$ and $C_{2,\,\mathrm{NNLO}}^{(1)H}$ in Eq. (80).

Category	Shower Concepts	Quantity in SCET$_i$	Found In:
Hard Scattering	Hard matrix elements with more partons	Wilson coeff. of $\bar{\chi}_{n_1}\mathcal{B}^{\perp}_{n_1'}\chi_{\bar{n}}$ in SCET$_1$	Eq. (80)
	Power correction to initial branching within the leading jet	Wilson coeff. of $\bar{\chi}_{n_0}\mathcal{B}^{\perp}_{n_0}\chi_{\bar{n}}$ and $\bar{\chi}_{n_0}[\mathcal{P}_{\perp}\mathcal{B}^{\perp}_{n_0}]\chi_{\bar{n}}$	Eq. (80)
	$\mathcal{O}(\alpha_s)$ hard virtual correction	One-loop matching for $\bar{\chi}_{n_1}\chi_{\bar{n}}$	See [24, 25]
Jet Structure	$1 \to 3$ Splitting functions	Double gluon real emission in SCET$_1$	Eq. (87)
	Combining $1 \to 2$ splittings with the various $1 \to 3$ splittings	Compute weights from SCET squared amplitudes	Eq. (107)
	$\mathcal{O}(\alpha_s)$ virtual correction for LO $1 \to 2$ splitting	One-loop correction to $1 \to 2$ replacement rule	Left for future work
No Branching Probabilities	NLL Sudakov factor for leading branching	NLL anomalous dimension for leading operators	See Sec. IV C, Left for future work
	LL Sudakovs for subleading branching	LL anomalous dimensions for subleading operators	Eqs. (20,90)
Soft Emission	Subleading corrections from soft gluons	Include effects of soft emission from subleading SCET soft Lagrangians	Left for future work

TABLE II: Mapping between concepts in a NLO parton shower algorithm and computations in SCET$_i$. For exclusive cross sections these ingredients would together yield results accurate to NLO in the power expansion (λ), and with corresponding NLL resummation.

This correction also accounts for more partons, but it describes a situation where they are initially emitted close to the collinear quark. Therefore, they are corrections which improve the description of the first branching within the leading jet. It is important to note that because these two types of hard corrections occur in different regions of phase space they have different renormalization group evolution, and thus different Sudakov no-branching factors. The required LL Sudakov factors were determined in our analysis. For a full NLO(α_s) treatment we also need a third type of hard scattering correction, the one-loop virtual corrections to the leading shower operator. For the required operator, $\bar{\chi}_{n_0}\chi_n$ these types of corrections were discussed in Refs. [24, 25].

For the jet-structure corrections, there are several ingredients to consider. We derived a replacement rule for two emissions $1 \to 3$, Eq. (88), that involved three different types of terms. This correction takes into account emissions in a region of the phase space that is not strongly-ordered and automatically avoids double counting from multiple $1 \to 2$ emissions.[12] In addition at NLO(α_s)/NLL we require the $\mathcal{O}(\alpha_s)$ virtual correction to the LO splitting rule. This would be derived from a one loop matching computation that should be straightforward, but was not considered here.

We also discussed how no-branching Sudakov factors are associated with the operator RG kernels, and by extension their anomalous dimensions (Section IV C). To NLL, we need the NLL Sudakov factor for leading branching and the LL Sudakovs for subleading branching. These are associated to the full one-loop and two-loop cusp anomalous dimensions for the leading operators, and one-loop cusp for the subleading ones. At LL, we have determined all the Sudakovs for subleading branching (Eqs. 20 and 90). We have not yet calculated the NLL Sudakov for leading branching in the scheme with Θ-functions that is needed for our setup, as described in Sec. IV C.

The last item in the table is the treatment of soft radiation at NLO. This can be achieved by considering time-ordered products for the matching of QCD to SCET$_1$ and SCET$_i$ to SCET$_{i+1}$ that involve soft gluons and subleading

[12] The method by which we avoid double counting for two gluon emission should be obvious, coming directly from our implementation of the Θ functions. Since $\Theta + \tilde{\Theta} = 1$, the double $1 \to 2$ and $1 \to 3$ together cover all of phase space without double counting. For three emissions we have either i) three $1 \to 2$ emissions, ii) a $1 \to 3$ followed by a $1 \to 2$ emission, or iii) a $1 \to 2$ followed by a $1 \to 3$ emission. Here there is an apparent combinatoric issue, as ii) and iii) both provide corrections for the middle gluon in i). However they do so in nonoverlapping regions of phase space. The same is true for more than three emissions. We thank J. Thaler for asking this question.

soft Lagrangians that are known in SCET [64–66] up to $\mathcal{O}(\lambda^2)$. For the terms involving collinear quarks they read

$$\begin{aligned}
\mathcal{L}^{(1)}_{\xi\xi} &= \big(\bar\xi_n W\big)\, i\not{D}^\perp_{us}\frac{1}{\bar{\mathcal{P}}}\big(W^\dagger i\not{D}^\perp_n\frac{\bar{\not n}}{2}\xi_n\big) + \big(\bar\xi_n i\not{D}^\perp_n W\big)\frac{1}{\bar{\mathcal{P}}} i\not{D}^\perp_{us}\big(W^\dagger\frac{\bar{\not n}}{2}\xi_n\big)\,, \\
\mathcal{L}^{(2)}_{\xi\xi} &= \big(\bar\xi_n W\big) i\not{D}^\perp_{us}\frac{1}{\bar{\mathcal{P}}} i\not{D}^\perp_{us}\frac{\bar{\not n}}{2}\big(W^\dagger\xi_n\big) + \big(\bar\xi_n i\not{D}^\perp_n W\big)\frac{1}{\bar{\mathcal{P}}^2} i\bar n\cdot D_{us}\frac{\bar{\not n}}{2}\big(W^\dagger i\not{D}^\perp_n\xi_n\big)\,, \\
\mathcal{L}^{(1)}_{\xi q} &= \bar\xi_n\,\frac{1}{i\bar n\cdot D_n}\, ig\not{B}^n_\perp W q_{us} + \text{h.c.}\,, \qquad \mathcal{L}^{(2b)}_{\xi q} = \bar\xi_n\frac{\bar{\not n}}{2} i\not{D}^c_\perp\frac{1}{(i\bar n\cdot D_n)^2}\, ig\not{B}^n_\perp W\, q_{us} + \text{h.c.}\,, \\
\mathcal{L}^{(2a)}_{\xi q} &= \bar\xi_n\frac{\bar{\not n}}{2}\frac{1}{i\bar n\cdot D_n}\,[i\bar n\cdot D_n, in\cdot D_n + gn\cdot A_{us}]W\, q_{us} + \text{h.c.}\,,
\end{aligned} \tag{108}$$

while the analogous pure glue Lagrangians can be found in Ref. [64]. Here the expressions are prior to the soft field redefinition, and $ig\not{B}^n_\perp = [i\bar n\cdot D_n, i\not{D}^n_\perp]$. One must then work out the effect that these NLO soft amplitudes have on interference. The associated soft calculations and investigations have also been left for future work.

We also briefly comment on how the corrections in Table II relate to those already implemented in parton shower codes in the literature. In most cases, the goal of these codes differed from the power suppressed corrections considered here. This makes a strict association impossible, but there is still a general correspondence that can be made. CKKW [27] is a LO(α_s)/LL procedure whose goal is to merge matrix elements involving multiple partons with a parton shower in a manner that avoids double counting. In our language, this corresponds to the real emission hard-scattering corrections in the first row of Table II. The $\bar\chi_{n_0}\chi_{\bar n}$ and $\bar\chi_{n_1}\mathcal{B}^\perp_{n_1'}\chi_{\bar n}$ operators describe processes with different numbers of initial well-separated jets. In CKKW, a parameter y_{cut} is used to separate the extra emission in the matrix element from emissions in the shower. In our analysis, the contributions from showering $\bar\chi_{n_0}\chi_{\bar n}$ does not interfere with the direct contribution from $\bar\chi_{n_1}\mathcal{B}^\perp_{n_1'}\chi_{\bar n}$, and this is encoded by Θ functions in the Wilson coefficient of SCET$_N$. CKKW carries out this procedure for several matrix element emissions, while we have only considered one.

In MC@NLO [37] and POWHEG [38], virtual and real matrix element corrections at NLO(α_s) are incorporated into the shower, with the goal of ensuring that it reproduces an associated cross section completely at NLO(α_s). The implementation includes careful handling of the cancellation of real and virtual IR divergences. Our goal was to implement corrections at NLO(λ) and we discussed NLL, but for all emissions from the shower rather than just the first jet needed for the NLO(α_s) cross section. At NLL, we would have only terms up to $\mathcal{O}(\alpha_s\log)$ in the total cross section, and hence this does not encode the entire NLO(α_s) result. In our language, the corrections that contribute to the NLO(α_s) cross section correspond to the hard scattering corrections in the first through third rows of Table II. In order to compute the NLO(α_s) cross section it is not necessary to distinguish between the terms in the first and second rows of the table, and these terms are indeed considered simultaneously in MC@NLO and POWHEG. The full NLO(α_s) virtual result are obtained in our language by including the items mentioned in the 3$^{\text{rd}}$ and 9$^{\text{th}}$ rows of Table II.

The work of KRKMC [57–59], on the other side, aims to improve the shower algorithm taking into account an exclusive version of the Altarelli-Parisi splitting function at NLO(α_s), $P^{(1)}_{qq}$. In our language, this corresponds to jet-structure corrections and we show in Appendix F how our replacement rule in Eq. (88) is also related to $P^{(1)}_{qq}$. Hence our $1\to 3$ emission corresponds to an exclusive version of $P^{(1)}_{qq}$, though in a different scheme. Part of the corrections in $P^{(1)}_{qq}$ involve order α_s corrections to the $1\to 2$ splitting function, which are taken into account by $\mathcal{O}(\alpha_s)$ virtual $1\to 2$ matching corrections in our framework (6$^{\text{th}}$ row of Table II). In fact, in Sec. IV D, we saw that SCET$_i$ also leads one to view corrections to the shower as a "defect" insertion just as KRKMC. In addition to these splitting corrections, in our framework the amplitude also involves no-branching probabilities given by evolution kernels that appear in the weight factors, which do not appear in the KRKMC weights. Keeping track of the evolution also determines the appropriate scale for evaluating α_s.

V. CONCLUSION

In this paper we developed a framework based on a tower of independent but related EFTs, the SCET$_i$, to study corrections to the parton shower. The work of [24, 25] showed how to formulate the LL parton shower in terms of SCET, and how virtual corrections are straightforward to incorporate by one-loop matching. Our SCET$_i$ framework extends these ideas in a manner that makes it easy to deal with: double counting, the issue of disentangling coordinate choices from kinematic power corrections, and the construction of a complete set of operators for corrections at a desired order. The interference structures, and hence the leading corrections that give spin and color correlations, also appear in a straightforward manner in the SCET$_i$ setup.

The SCET$_i$ are iteratively used to integrate out the characteristic scale, $Q\lambda^i$ for increasing i. This approach allows us to perform a systematic expansion which can correct both the hard-scale process that produces partons to setup initial conditions for the shower algorithm and the iterative shower itself. We described the parton shower through a set of operators $\mathcal{O}_i^{(j)}$ in SCET$_i$, and used standard matching procedures to make the transition from SCET$_i$ to SCET$_{i+1}$, where more partons become apparent. Performing the matching relied crucially on the RPI symmetry of SCET, and we extended the usual infinitesimal version to carry out the finite rotations that we needed. At LO, a simple operator replacement rule generates the LL shower, $\bar{\chi}_{n_0} \to c_{\rm LO}^{\alpha} \bar{\chi}_{n_1} g\mathcal{B}^{\alpha}_{n_1'\perp}$, where $c_{\rm LO}$ is related to the standard LO splitting-function. Also, angular ordering and coherent branching for LO soft emissions emerge naturally in the SCET$_i$ framework. A summary of ingredients required for the shower with power corrections at NLO(λ) are given in Table II, including both calculations carried out here, as well as those left for future work. The main results of our paper are:

1. At NLO(λ) we found two kinds of branching corrections: hard-scattering and jet-structure. The hard-scattering corrections depend on the hard process and appear near the top of the shower tree. They came from matching QCD to SCET$_1$ at higher order. Since they only occur at the top of the shower, one can treat these as a modified form of matrix-element corrections. A subset of these corrections correspond to the usual implementation of fixed-order matrix elements, while the remaining ones give power corrections to the initial branching in the LL shower. These two types require different Sudakov factors. This effect is apparent for the kinematic power corrections, but is beyond NLO(α_s) for the fixed order counting.

2. The jet-structure corrections are independent from what happens at the hard scale, hence they are universal for any process we want to study. They come from matching SCET$_i$ to SCET$_{i+1}$ at higher order for any i. They can appear anywhere in the shower tree and they take into account emissions in regions of the phase space that are not strongly-ordered. For these corrections we found that the NLO(λ) operators are related to the LO operator via a replacement rule for two emissions: $\bar{\chi}_{n_0} \to h_I^{\alpha\beta} \bar{\chi}_{n_2} g\mathcal{B}^{\alpha}_{n_1'\perp} g\mathcal{B}^{\beta}_{n_2'\perp}$. This NLO($\lambda$) rule automatically avoids double counting with the iteration of two LO operator replacements.

3. The SCET$_i$ picture allowed us to easily take into account interference for the NLO(λ) power corrections. Once we reach the final SCET$_N$ theory, all the fields are labeled in a different collinear directions. Because in SCET we can only contract collinear fields that share the same collinear direction, in SCET$_N$ calculating the amplitude squared becomes very easy. Kinematic information that is encoded by the shower history from passing through earlier SCET$_i$'s is encoded by Θ functions in the final SCET$_N$ Wilson coefficients. We demonstrated that when emitting an arbitrary number of partons, the non-trivial part of the amplitude squared involves at most four fields.

A comparison of how these SCET$_i$ results relate to earlier parton shower literature that goes beyond LL is given in Sec. IV E.

The framework developed here allows for systematic improvement to arbitrary orders in the kinematic expansion. There are still several important steps to take, though, before this picture can lead to a practical implementation, including additional computations that we outlined in Sec. IV E. We list here three topics which are natural next steps, and which we believe should be straightforward to approach:

1. This work has only considered $q \to qg$ splittings and an abelian theory. One should include the full nonabelian results and compute the coefficients required for gluon splitting as well. This is required to properly treat color correlation corrections in a manner determined by the NLO(λ) interference pattern. For collinear particles we expect that one can include the dominant part of these effects by considering nearest-neighbor interference since this arises from the kinematic expansion, and thus leaves the rest of the shower as before.

2. Only a subset of the terms required for a full NLL$_{\rm exp}$ resummation were considered here. We determined the LL$_{\rm exp}$ evolution for subleading operators, but did not carry out the computation of the NLL$_{\rm exp}$ evolution of the leading operator in a scheme that is consistent with our power corrections (we only considered it in $\overline{\rm MS}$). In order for a consistent treatment as a probabilistic process, the real emission probabilities and Sudakov no-branching corrections must go hand in hand. Furthermore, once these evolution factors are determined, the reweighting discussed in Sec. IV E must be tested in an actual shower Monte Carlo.

3. Since soft modes in SCET can communicate between different collinear jets, they carry the ability to spoil their factorization. Fortunately, this does not happen for their LO interactions, which yield angular ordering and coherent branching of soft gluons in SCET$_i$. It is open question as to what extent NLO soft couplings can be factorized in the shower tree and the necessary SCET computations were discussed but not carried out here. The treatment of soft NLO interactions in SCET in other contexts has always led to factorized structures, so we remain optimistic that such effects will be tractable for the shower.

Future investigation of these items is well warranted.

Acknowledgments

This work was supported in part by the NSF grant, nsf-phy/0401513, by the Office of Nuclear Physics of the U.S. Department of Energy under the Contract DE-FG02-94ER40818, and by a Friedrich Wilhelm Bessel award from the Alexander von Humboldt foundation. I.S. thanks the Werner-Heisenberg Max-Planck Institute for Physics for hospitality while this work was completed. The authors would like to thank Christian Bauer, Kirill Melnikov, Frank Tackmann, and Jesse Thaler for useful discussions.

Appendix A: More SCET basics

Soft-Collinear Effective Theory describes the interactions of collinear and soft quarks and gluons [20–23]. As we mentioned in Sec. II A, to define the collinearity of a particle, the momentum is decomposed along two light-cone vectors, n and $\bar{n}$, with $n^2 = 0$, $\bar{n}^2 = 0$ and $n \cdot \bar{n} = 2$

$$p^\mu = n{\cdot}p\frac{\bar{n}^\mu}{2} + \bar{p}\frac{n^\mu}{2} + p_\perp^\mu \,, \tag{A1}$$

where $\bar{p} = \bar{n} \cdot p$. A particle is collinear to the direction n if its momentum scales as:

$$(n \cdot p,\, \bar{p},\, p_\perp) \sim (\lambda^2,\, 1,\, \lambda)\, Q \,, \tag{A2}$$

where Q is the hard scale of the process, and $\lambda \ll 1$. A particle is soft if:

$$(n \cdot p,\, \bar{p},\, p_\perp) \sim (\lambda^2,\, \lambda^2,\, \lambda^2)\, Q \,. \tag{A3}$$

We obtain SCET from QCD by expanding in powers of λ and integrating out modes harder than $\sim Q^2\lambda^2$. Both Eqs. (A2) and (A3) imply that $p^2 = \bar{p}\,(n \cdot p) + p_\perp^2 \lesssim Q^2\lambda^2$.

In addition to the expansion, we also want to divide the quark and gluon fields into separate soft and collinear modes. For the collinear case, the fields are indexed by n, and two collinear sectors are distinct if $n_i \cdot n_j \gg \lambda^2$. In addition, we introduce a momentum-space lattice for the $\mathcal{O}(\lambda^0)$ and $\mathcal{O}(\lambda)$ momenta in order to facilitate carrying out the multipole expansion with respect to the $\mathcal{O}(\lambda^2)$ momenta. To divide the QCD fields in this way, we split the momentum of a collinear particle into a "large" part $\tilde{p}^\mu$ and a residual one $k^\mu \sim \lambda^2$

$$p^\mu = \tilde{p}^\mu + k^\mu \,, \quad \text{where} \quad \tilde{p}^\mu \equiv n{\cdot}p\frac{n^\mu}{2} + p_\perp^\mu \,. \tag{A4}$$

We can pull out the large momenta $\tilde{p}$ from the fermion field by the phase redefinition

$$\psi(x) = \sum_{\tilde{p},\, n} e^{-i\tilde{p}\cdot x}\, \psi_{n,\tilde{p}} \,. \tag{A5}$$

For a collinear particle along n, $\partial^\mu \psi_{n,\tilde{p}}(x) \sim \lambda^2$. The four component field, $\psi_{n,\tilde{p}}$, has two large components, $\xi_{n,\tilde{p}}$, and two small components $\xi_{\bar{n},\tilde{p}}$, that can be separated using the following projectors:

$$\psi_{n,\tilde{p}} = \frac{\not{n}\bar{\not{n}}}{4}\psi_{n,\tilde{p}} + \frac{\bar{\not{n}}\not{n}}{4}\psi_{n,\tilde{p}} \equiv \xi_{n,\tilde{p}} + \xi_{\bar{n},\tilde{p}}. \tag{A6}$$

These satisfy the relations,

$$\begin{aligned} \frac{\not{n}\bar{\not{n}}}{4}\,\xi_{n,\tilde{p}} &= \xi_{n,\tilde{p}} \,, \quad \not{n}\,\xi_{n,\tilde{p}} = 0 \,, \\ \frac{\bar{\not{n}}\not{n}}{4}\,\xi_{\bar{n},\tilde{p}} &= \xi_{\bar{n},\tilde{p}} \,, \quad \bar{\not{n}}\,\xi_{\bar{n},\tilde{p}} = 0 \,. \end{aligned} \tag{A7}$$

Similarly, we can define a collinear gluon field, $A^\mu_{n,\tilde{q}}(x)$. Pictorially, we can think of $\xi_{n,\tilde{p}}(x)$ and $A^\mu_{n,\tilde{q}}(x)$ as fields that create a particle whose three-momentum lies inside a cone with opening angle $\sim \lambda$ about the three-direction $\vec{n}$. $\mathcal{P}_n^\mu$ is the momentum operator that picks up the large components of the momentum, $\mathcal{P}_n^\mu\, \xi_{n,\tilde{p}}(x) = \tilde{p}^\mu\, \xi_{n,\tilde{p}}(x)$. Collinear

fields always appear with a sum over $\tilde{p}$, and both label and residual momenta are separately conserved. Therefore it is often useful to abbreviate the notation as

$$\xi_n = \sum_{\tilde{p}} \xi_{n,\tilde{p}}\,, \quad A_n = \sum_{\tilde{q}} A_{n,\tilde{q}}\,. \tag{A8}$$

The SCET collinear Lagrangian, $\mathcal{L}_n$, describes the interaction between the collinear fields ξ_n and $A_n^\mu(x)$. It is derived from the QCD Lagrangian by integrating out the field, $\xi_{\bar{n}}$. At LO, for the kinetic and purely collinear interaction terms we have [21, 22]:

$$\mathcal{L}_n^{(0)} = \bar{\xi}_n \big(in\cdot\partial + g\, n\cdot A_n + i\not{D}_{n\perp} W_n \frac{1}{\mathcal{P}_n} W_n^\dagger i\not{D}_{n\perp} \big) \frac{\not{\bar{n}}}{2} \xi_n\,, \tag{A9}$$

where we intrinsically sum over the large, label momenta, $\tilde{p}$. The $in\cdot\partial$ derivative picks out the $\mathcal{O}(\lambda^2)$ momenta. The collinear derivative, D_n^μ, and collinear Wilson line, W_n, are defined as [23]:

$$\begin{aligned} iD_n^\mu &= \mathcal{P}_n^\mu + gA_n^\mu\,, \\ W_n(x) &= \Big[\sum_{\text{perms.}} \exp\Big(-\frac{g}{\bar{\mathcal{P}}_n}\, \bar{n}\cdot A_n(x) \Big) \Big]\,. \end{aligned} \tag{A10}$$

The leading order coupling of collinear quarks to soft gluons is eikonal,

$$\mathcal{L}_{sn}^{(0)} = \bar{\xi}_n\, g\, n\cdot A_s\, \frac{\not{\bar{n}}}{2} \xi_n\,, \tag{A11}$$

while the Lagrangian for purely soft quarks and gluons has the same form as full QCD. The LO collinear Lagrangian for gluons has similar properties and is given in Ref. [23]. The interactions between soft and collinear particles, such as the one in Eq. (A11), can be removed from the Lagrangian by the field redefinitions [23]:

$$\xi_n \to Y_n\, \xi_n\,, \qquad\qquad A_n^\mu \to Y_n\, A_n^\mu\, Y_n^\dagger\,, \tag{A12}$$

where the soft Wilson line Y_n is defined in Eq. (67). This causes soft interactions to be represented by Wilson lines in operators, as in Eq. (69).

Now that we have split up gluons according to a momentum-space lattice, the gauge structure of the theory has become more complex and involves global, collinear, and soft gauge transformations. Fortunately, with the collinear Wilson line, it is possible to construct fermion and gluon fields that are manifestly invariant under collinear gauge transformations. The definitions are:

$$\chi_n(x) = W_n^\dagger(x)\xi_n(x)\,, \qquad\qquad \mathcal{B}_n^\mu(x) = \frac{1}{g}\big[W_n^\dagger(x)\, iD_n^\mu(x) W_n(x) \big]\,, \tag{A13}$$

where the derivative in $\mathcal{B}_n^\mu$ does not act outside of the brackets in its definition, and we always have $\bar{n}\cdot\mathcal{B}_n = 0$. In the $\bar{n}\cdot A_n = 0$ light-cone gauge, $W_n = 1$ and $\mathcal{B}_n^\mu = A_n^\mu$. One can construct collinear operators out of just three objects: the fermion field, χ_n, the perpendicular gluon field, $\mathcal{B}_{n\perp}^\mu$, and the perpendicular momentum operator, $\mathcal{P}_{n\perp}^\mu$. All the other operators, like $n\cdot\mathcal{B}_n$, or $n\cdot\partial$ can be written in terms of these three using the equation of motions [67].

Appendix B: Finite RPI

Even though SCET explicitly breaks Lorentz invariance, the symmetry returns at each order in λ by reparametrization invariance (RPI). RPI_i is the version appropriate for SCET_i. As usual, we define p as collinear to the direction n in SCET_i if its components scale as $(n\cdot p,\, \bar{p},\, p_\perp) \sim (\lambda^{2i},\, 1,\, \lambda^i)\, Q$, where Q is the hard scale and $\lambda \ll 1$ (*cf.* Eq. A1). The vector n has physical meaning as its 3-vector subset, $\overrightarrow{n}$, is the direction where most of the momentum is allocated. The direction $\overrightarrow{p}$ is therefore inside a cone of opening angle λ^i around $\overrightarrow{n}$, (*cf.* Fig 15). By contrast, $\bar{n}$ is an auxiliary only needed to decompose the momentum. The parameter λ gives the amount of collinearity to n. The decomposition is not unique since we can shift n by an amount λ and the particle we still be collinear to it. This means that if we move n inside the cone in Fig. 15, p is still collinear to it. This is called a reparametrization invariance (RPI) transformation of type-I. Thus, if a particle is collinear to n, it is also collinear to any direction n' related by a type-I transformation. To be more formal, we can divide the space of light-cone vectors, $\{n_i\}$, into equivalence classes, $\{[n_i]\}$, where $[n_j] = \{n \in [n_j] |\, n\cdot n_j \lesssim \lambda^{2i}\}$. The meaningful objects in SCET_i are the $[n_j]$.

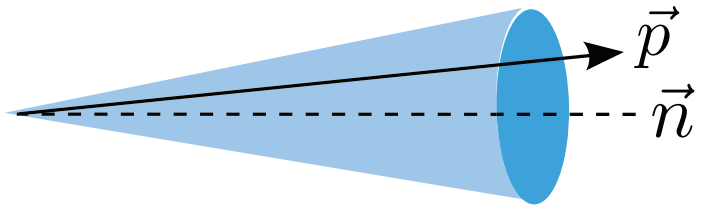

FIG. 15: In SCET, a particle is collinear to the direction n if it is inside a cone centered in $\vec{n}$ and of opening angle λ.

By extension from SCET [63], two collinear sectors in SCET$_i$, n_1 and n_2, are distinct if

$$n_1 \cdot n_2 \gg \lambda^{2i} \,, \tag{B1}$$

Just as in regular SCET, we can write the external state with the n-label to which each particle is collinear. For working in SCET$_i$, we give a subscript to indicate the appropriate definition of collinearity. For example, $|q_{n_1}\rangle_i$ is a state with one quark, collinear to n_1 that can be annihilated by any χ_n such that $n \cdot n_1 \ll \lambda^{2i}$, or $n \in [n_1]$.

For each $\{n, \bar{n}\}$, the type-I RPI infinitesimal transformations are[13]

$$\text{(I)} \begin{cases} n^\mu \to n^\mu + \Delta^\mu_{n\perp} \\ \bar{n}^\mu \to \bar{n}^\mu \end{cases} , \tag{B2}$$

where $\Delta^\mu_{n\perp} \sim \lambda$ and $n \cdot \Delta_{n\perp} = \bar{n} \cdot \Delta_{n\perp} = 0$. These transformations preserve the relations $n^2 = 0$, $\bar{n}^2 = 0$ and $n \cdot \bar{n} = 2$.[14]

The general problem of matching SCET$_i$ $\to$ SCET$_{i+1}$ is our need to rotate the direction n of objects in the amplitude (such as spinors and vectors) to n' that is close enough to the particle momentum such that p is collinear to n' in SCET$_{i+1}$. Thus, RPI$_i$ is crucial for matching as it determines how formerly identical SCET$_i$ configurations wind up in different SCET$_{i+1}$ terms. Any transformation in RPI$_i$/RPI$_{i+1}$ is therefore of consequence. By contrast, the choice within SCET$_{i+1}$ is purely a convention we may use to our convenience (*cf.* Fig. 4). For example, we can pick n' as that direction n_p such that p as zero perpendicular momentum in the $n_p - \bar{n}$ frame:

$$p = \bar{p}\frac{n_p^\mu}{2} + n_p \cdot p \frac{\bar{n}^\mu}{2} \,. \tag{B3}$$

This is satisfied for:

$$n_p^\mu = n^\mu + 2\,\frac{p_\perp^\mu}{\bar{p}} - \bar{n}^\mu \frac{(p_\perp)^2}{\bar{p}^2} \,, \tag{B4}$$

with $p_\perp$ defined in the n-frame. Unlike Eq. (B2), this RPI$_i$ transformation is finite. It is easy to check that $n_p^2 = 0$, $n_p \cdot \bar{n} = 2$ and that $p^\mu_{n_p\perp} = p^\mu - n_p \cdot p\, \bar{n}^\mu/2 - \bar{p}\, n_p^\mu/2 = 0$.

We can derive similar relations for other quantities. To see how the quark field transforms, we use the RPI invariant fermion field [67]:

$$\psi_n = \Big(1 + \frac{\not{D}^\perp_n}{\bar{n}\cdot D_n}\frac{\not{\bar{n}}}{2}\Big)\xi_n \,. \tag{B5}$$

Since (B5) is invariant under RPI, $\psi_n = \psi_{n_p}$ and we can write,

$$\Big(1 + \frac{\not{D}^\perp_n}{\bar{n}\cdot D_n}\frac{\not{\bar{n}}}{2}\Big)\xi_n = \Big(1 + \frac{\not{D}^\perp_{n_p}}{\bar{n}\cdot D_{n_p}}\frac{\not{\bar{n}}}{2}\Big)\xi_{n_p} \,. \tag{B6}$$

---

[13] Infinitesimal does not refer to the expansion in λ.

[14] It is also possible to rotate $\bar{n} \to \bar{n} + \varepsilon_\perp$ where $\varepsilon_\perp \sim \lambda^0$, which is a type-II RPI transformation. Finally, a type-III transformation takes $n \to e^\alpha n$ and $\bar{n} \to e^{-\alpha}\bar{n}$.

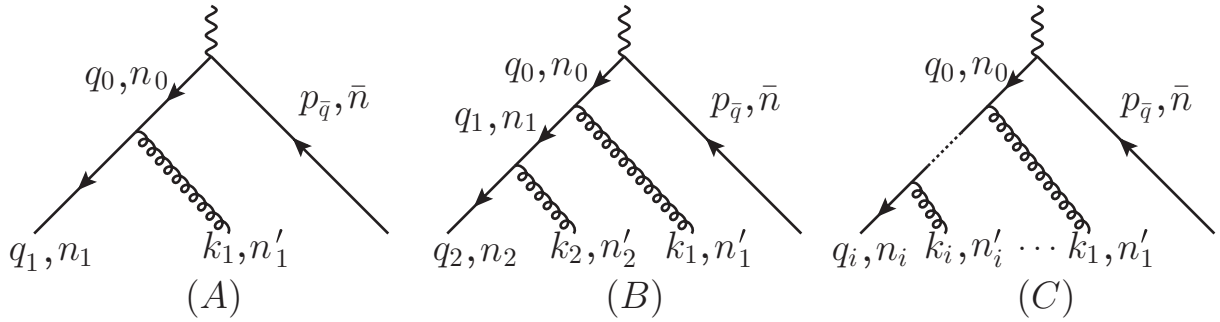

FIG. 16: Kinematic variables for one-gluon emission (A), two-gluon emission (B) and i-gluon emission (C). The n's are defined such that the corresponding particle's momentum has no perpendicular component along the directions $n - \bar{n}$. Note that q_1 is a different vector for single and double emissions.

Multiplying (B6) by the projector $\not{n}\not{\bar{n}}/4$ we get the finite RPI$_i$ relation

$$\xi_n = \frac{\not{n}\not{\bar{n}}}{4}\xi_{n_p}\,. \tag{B7}$$

The relation (B7) is in agreement with the spinor equation (A7) in [24] upon setting $\bar{n}_1 = \bar{n}_2$. Objects with a full Lorentz index, like p^μ or γ^μ, are RPI invariant as there is no reference to the light-cone vectors n and $\bar{n}$. Those in the perpendicular direction though, such as $p_\perp^\mu$ or $\gamma_\perp^\mu$, are not, as $\perp$ is defined with respect to n and $\bar{n}$. Using the relation $\gamma_\perp^\mu = \gamma^\mu - \bar{n}^\mu \not{n}/2 - n^\mu \not{\bar{n}}/2$, we derive the expression

$$\gamma^\mu_{n_p\perp} = \gamma^\mu_\perp - \bar{n}^\mu \frac{\not{p}_\perp}{\bar{p}} - p^\mu_\perp \frac{\not{\bar{n}}}{\bar{p}} + \bar{n}^\mu \frac{(p_\perp)^2}{\bar{p}^2}\not{\bar{n}}\,. \tag{B8}$$

We now focus on those transformations needed for one-gluon emission. As in Sec. III A, we consider the case of a virtual quark with momentum q_0 emitting an external gluon and quark with momentum k_1 and q_1, respectively. In Fig. 16(A), we portray this kinematics for one-gluon emission where the initial quark q_0 comes from a QCD current $\bar{q}\gamma^\mu q$. We call n_0, n_1' and n_1 the directions where q_0, k_1 and q_1 zero have perpendicular component, that is:

$$\begin{aligned} q_0 &= \bar{q}_0 \frac{n_0^\mu}{2} + n_0{\cdot}q_0 \frac{\bar{n}^\mu}{2}\,, \\ k_1 &= \bar{k}_1 \frac{n_1'^\mu}{2}\,, \\ q_1 &= \bar{q}_1 \frac{n_{q_1}^\mu}{2}\,, \end{aligned} \tag{B9}$$

Using Eq. (B4), we can relate n_1' and n_1 to n_0,

$$\begin{aligned} n_1'^\mu &= n_0^\mu - 2\frac{(q_1)^\mu_{n_0\perp}}{\bar{k}_1} - \bar{n}^\mu \frac{(q_1)^2_{n_0\perp}}{\bar{k}_1^2}\,, \\ n_1^\mu &= n_0^\mu + 2\frac{(q_1)^\mu_{n_0\perp}}{\bar{q}_1} - \bar{n}^\mu \frac{(q_1)^2_{n_0\perp}}{\bar{q}_1^2}\,, \end{aligned} \tag{B10}$$

where we have used the equality $(k_1)^\mu_{n_0\perp} = -(q_1)^\mu_{n_0\perp}$. Some useful relations are:

$$\begin{aligned} n_1{\cdot}n_1' &= n_0{\cdot}n_1' \frac{\bar{q}_0^2}{\bar{k}_1^2} = n_0{\cdot}n_1 \frac{\bar{q}_0^2}{\bar{q}_1^2} = -2\frac{(q_1)^2_{n_0\perp}\bar{q}_0^2}{\bar{q}_1^2\,\bar{k}_1^2}\,, \\ n_0^\mu &= \frac{\bar{k}_1 n_1'^\mu + \bar{q}_1 n_1^\mu}{\bar{q}_0} - \bar{n}^\mu\,(n_1{\cdot}n_1')\frac{\bar{q}_1\bar{k}_1}{2\,\bar{q}_0^2}\,, \\ (q_1)^\mu_{n_0\perp} &= \frac{\bar{q}_1\bar{k}_1}{\bar{q}_0}\sqrt{n_1\cdot n_1'}\frac{v_1^\mu}{2} - \bar{n}^\mu\,(n_1{\cdot}n_1')\frac{\bar{q}_1\bar{k}_1(\bar{k}_1^2 - \bar{q}_1^2)}{4\,\bar{q}_0^3}\,, \\ \gamma^\mu_{n_0\perp} &= \gamma^\mu_{n_1'\perp} - \bar{n}^\mu \frac{(\not{q}_1)_{n_0\perp}}{\bar{k}_1} - (q_1)^\mu_{n_0\perp}\frac{\not{\bar{n}}}{\bar{k}_1} + \bar{n}^\mu\,(n_1{\cdot}n_1')\frac{\bar{q}_1^2}{2\,\bar{q}_0^2}\not{\bar{n}}\,, \end{aligned} \tag{B11}$$

where

$$v_1^\mu = \frac{n_1^\mu - n_1'^\mu}{\sqrt{n_1 \cdot n_1'}}\,, \tag{B12}$$

and $|v_1^2| = 2$. Another useful relation is

$$q_0^2 = (q_1 + k_1)^2 = n_1' \cdot n_1 \frac{\bar{q}_1 \bar{k}_1}{2}\,. \tag{B13}$$

We can express all quantities of interest in terms of the vectors n_1', n_1 and the momenta $\bar{q}_1$ and $\bar{k}_1$.

In two-gluon emissions, the kinematic variables are assigned in Fig. 16(B). We define n_0, n_1', n_2' and n_1 as follows (note that q_1 and n_1 are different from above):

$$\begin{aligned}
q_0 &= \bar{q}_0 \frac{n_0^\mu}{2} + n_0 \cdot q_0 \frac{\bar{n}^\mu}{2}\,,\\
k_1 &= \bar{k}_1 \frac{n_1'^\mu}{2}\,,\\
q_1 &= \bar{q}_1 \frac{n_1^\mu}{2} + n_1 \cdot q_1 \frac{\bar{n}^\mu}{2}\,,\\
k_2 &= \bar{k}_2 \frac{n_2'^\mu}{2}\,,\\
q_2 &= \bar{q}_2 \frac{n_2^\mu}{2}\,,
\end{aligned} \tag{B14}$$

Eq. (B10) is still valid, and we can similarly define n_2' and n_2 as:

$$\begin{aligned}
n_2'^\mu &= n_1^\mu - 2\frac{(q_2)_{n_1\perp}^\mu}{\bar{k}_2} - \bar{n}^\mu \frac{(q_2)_{n_1\perp}^2}{\bar{k}_2^2}\,,\\
n_2^\mu &= n_1^\mu + 2\frac{(q_2)_{n_1\perp}^\mu}{\bar{q}_2} - \bar{n}^\mu \frac{(q_2)_{n_1\perp}^2}{\bar{q}_2^2}\,,
\end{aligned} \tag{B15}$$

where $(k_2)_{n_1\perp} = -(q_2)_{n_1\perp}$. Also, Eq. (B11) is still valid, and we get a new set by sending $0 \to 1$ and $1 \to 2$:

$$\begin{aligned}
n_2 \cdot n_2' &= n_1 \cdot n_2' \frac{\bar{q}_1^2}{\bar{k}_2^2} = n_1 \cdot n_2 \frac{\bar{q}_1^2}{\bar{q}_2^2} = -2\frac{(q_2)_{n_1\perp}^2 \bar{q}_1^2}{\bar{q}_2^2\, \bar{k}_2^2}\,,\\
n_1^\mu &= \frac{\bar{k}_2 n_2'^\mu + \bar{q}_2 n_2^\mu}{\bar{q}_1} - \bar{n}^\mu\, (n_2 \cdot n_2') \frac{\bar{q}_2 \bar{k}_2}{2\, \bar{q}_1^2}\,,\\
(q_2)_{n_1\perp}^\mu &= \frac{\bar{q}_2 \bar{k}_2}{\bar{q}_1} \sqrt{n_2 \cdot n_2'} \frac{v_2^\mu}{2} - \bar{n}^\mu\, (n_2 \cdot n_2') \frac{\bar{q}_2 \bar{k}_2 (\bar{k}_2^2 - \bar{q}_2^2)}{4\, \bar{q}_1^3}\,,\\
\gamma_{n_1\perp}^\mu &= \gamma_{n_2'\perp}^\mu - \bar{n}^\mu \frac{(\not{q}_2)_{n_1\perp}}{\bar{k}_2} - (q_2)_{n_1\perp}^\mu \frac{\not{\bar{n}}}{\bar{k}_2} + \bar{n}^\mu\, (n_2 \cdot n_2') \frac{\bar{q}_2^2}{2\, \bar{q}_1^2} \not{\bar{n}}\,,
\end{aligned} \tag{B16}$$

where

$$v_2^\mu = \frac{n_2^\mu - n_2'^\mu}{\sqrt{n_2 \cdot n_2'}}\,, \tag{B17}$$

and $|v_2^2| = 2$. We can write $n_1 \cdot n_1'$ and v_1 in terms of n_2, n_1' and n_2' so that once again we only need to work with external quantities:

$$\begin{aligned}
n_1 \cdot n_1' &= \frac{\bar{k}_2 (n_2' \cdot n_1') + \bar{q}_2 (n_2 \cdot n_1')}{\bar{q}_1} - (n_2 \cdot n_2') \frac{\bar{q}_1 \bar{k}_1}{\bar{q}_0^2}\,,\\
v_1^\mu &= \frac{2\, \bar{k}_2 \bar{q}_1\, n_2'^\mu + 2\, \bar{q}_1 \bar{q}_2 n_1^\mu - \bar{k}_2 \bar{q}_2\, (n_2 \cdot n_2')\, \bar{n}^\mu - 2\, (\bar{q}_1)^2 n_1'^\mu}{2 (\bar{q}_1)^2 \sqrt{n_1 \cdot n_1'}}\,.
\end{aligned} \tag{B18}$$

Eq. (B13) for two emissions is modified to:

$$q_0^2 = (q_2 + k_1 + k_2)^2 = n_1' \cdot n_2 \frac{\bar{q}_2 \bar{k}_1}{2} + n_2' \cdot n_2 \frac{\bar{q}_2 \bar{k}_2}{2} + n_1' \cdot n_2' \frac{\bar{k}_1 \bar{k}_2}{2} \,. \tag{B19}$$

Other useful relations are

$$\begin{aligned}
\gamma^\mu_{n_0\perp} = \gamma^\mu_{n_2'\perp} - \bar{n}^\mu \Big(\frac{(\not{q}_1)_{n_0\perp}}{\bar{k}_1} + \frac{(\not{q}_2)_{n_1\perp}}{\bar{k}_2} \Big) - \Big(\frac{(q_1)^\mu_{n_0\perp}}{\bar{k}_1} + \frac{(q_2)^\mu_{n_1\perp}}{\bar{k}_2} \Big) \not{\bar{n}} \\
- \bar{n}^\mu \not{\bar{n}} \Big(\frac{(q_1)^2_{n_0\perp}}{\bar{k}_1^2} + \frac{(q_2)^2_{n_1\perp}}{\bar{k}_2^2} \Big), \\
q_1^2 = (k_2 + q_2)^2 = n_2' \cdot n_2 \frac{\bar{k}_2 \bar{q}_2}{2} \,, \\
(k_1 + q_2)^2 = n_1' \cdot n_2 \frac{\bar{k}_1 \bar{q}_2}{2} \,.
\end{aligned} \tag{B20}$$

For i gluon emissions, Fig. 16(C), n_k' is parallel to the k-gluon, n_i parallel to the external quark, and n_k is the light cone vector such that the k^{th} virtual quark has zero perpendicular momentum with respect to $(n_k, \bar{n})$. To calculate n_i, n_i' we can iterate the formulas above up to i emissions. That is we can calculate n_i, n_i' from n_{i-1} using Eq. (B10) with $0 \to (i-1)$, $1 \to i$.

Appendix C: Matching QCD to SCET_1

To study the process of $q \to qg$ emission, we match the QCD current,

$$J^\mu_{\text{QCD}} = \bar{q} \gamma^\mu q \,, \tag{C1}$$

to SCET_1 operators for a final state with a quark, antiquark, and gluon. The particle momenta are q_1 for the quark, $p_{\bar{q}}$ for the antiquark, and k_1 for the gluon, (*cf.* Fig. 17). We do the matching in the center of mass frame with

$$p_\gamma = q_1 + p_{\bar{q}} + k_1 = (Q, 0, 0, 0) \,. \tag{C2}$$

SCET_1, being equivalent to the usual SCET, is formulated as an expansion in the parameter λ. The current in Eq. (C1) matches onto an infinite series of SCET_1 operators. We will perform the matching up to NNLO(λ) for one gluon emission, and focus only on the cases when the gluon is either collinear to the quark or has its own direction. Obtaining the result for gluon-antiquark collinearity from our work is a simple exercise in charge conjugation. We can construct the SCET_1 operators out of a few building blocks: the quark field χ_n, the gluon field $\mathcal{B}^\alpha_{n\perp}$ and the perpendicular momentum operator $\mathcal{P}^\alpha_{n\perp}$, plus Dirac structures. χ_n, $\mathcal{B}^\alpha_{n\perp}$ and $\mathcal{P}^\alpha_{n\perp}$ all scale $\sim \lambda$. The basis of SCET_1 operators for one emission up to NNLO(λ) is [67]: [15]

$$\begin{aligned}
\mathcal{O}_1^{(0)}(n_0) &= \bar{\chi}_{n_0} \chi_{\bar{n}} \,, \\
\mathcal{O}_1^{(1)}(n_0, n_0) &= \bar{\chi}_{n_0} \, g \mathcal{B}^\alpha_{n_0\perp} \chi_{\bar{n}} \,, \\
\mathcal{T}_1^{(1)}(n_0, n_0) &= \bar{\chi}_{n_0} \Big[\mathcal{P}^\beta_{n_0\perp} \, g \mathcal{B}^\alpha_{n_0\perp} \Big] \chi_{\bar{n}} \,, \\
\mathcal{O}_1^{(1)}(n_1, n_1') &= \bar{\chi}_{n_1} g \mathcal{B}^\alpha_{n_1'\perp} \chi_{\bar{n}} \,,
\end{aligned} \tag{C3}$$

Following the convention of Eq. (14), we do not write the antiquark direction as it is always $\bar{n}$. $\mathcal{O}_1^{(0)}$ is the LO operator and scales as λ^2, $\mathcal{O}_1^{(1)}(n_0, n_0)$ and $\mathcal{O}_1^{(1)}(n_1, n_1')$ are NLO(λ) operators, scaling like λ^3, and $\mathcal{T}_1^{(1)} \sim \lambda^4$.

In SCET_1, two particles are collinear if they are inside a cone with opening angle $\sim \lambda$, equivalently $p_1 \cdot p_2 \lesssim (Q\lambda)^2/\eta^4$. Usually, we formulate this condition with dimensionless quantities, $n_{p_1} \cdot n_{p_2} \lesssim \lambda^2/\eta^4$, where n_{p_i} is exactly proportional to the particle momentum. To distinguish a "two-jet" from a "three-jet" state, we label the external states with the

[15] $\mathcal{T}_1^{(1)}(n_1, n_1')$ encodes redundant information that can be obtained with RPI. For example we can choose the directions n_1 and n_1' to align perfectly with particle momenta such that *e.g.*. $\mathcal{P}_{n_1\perp} \mathcal{B}_{n_1\perp} = 0$. This is not possible for $\mathcal{T}_1^{(1)}(n_0, n_0)$.

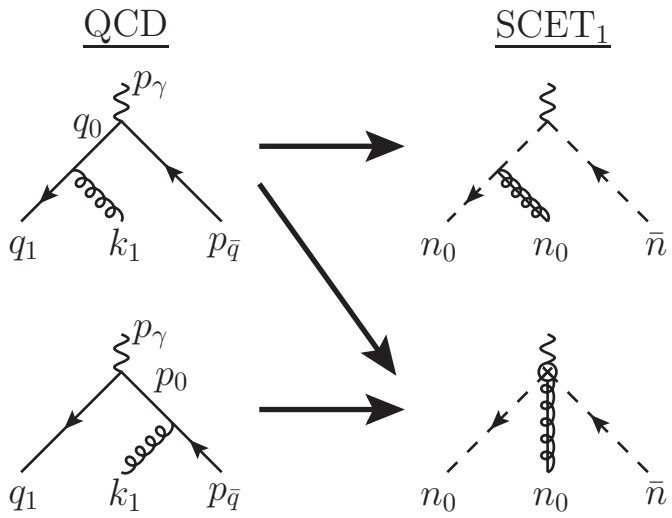

FIG. 17: Matching QCD to SCET$_1$ for the two-jet configuration: In the first column there are the two Feynman graphs for one-gluon emission in QCD, labeled by the 4-momenta. In the second column there are the two Feynman graphs in SCET$_1$ that reproduce the same amplitude in the case the quark and gluon are collinear along the direction n_0. The first graph comes from the operator $\mathcal{O}_1^{(0)}(n_0)$ with the insertion of the SCET$_1$ Lagrangian, the second graph comes from the operators $\mathcal{O}_1^{(1)}(n_0,\, n_0)$ and $\mathcal{T}_1^{(1)}(n_0,\, n_0)$.

direction to which the particles are collinear. A state $|q_{n_0}\rangle_1$ indicates a state where a quark with momentum q_1 is collinear to the direction n_0, that is $(\bar q_1, n_0\cdot q_1, (q_1)_{n_0\perp}) \sim (1,\lambda^2,\lambda)Q$, and the subscript, 1, tells us the state can be annihilated by any operator, χ_n, where n and n_0 are in the same SCET$_1$ equivalence class, $\{[n]\}$. As we will see, when we match to lower-scale SCET$_i$, we will change this number appropriately. A two-jet state with a collinear quark and gluon, and an antiquark is given by $|q_{n_0}\, g_{n_0}\, \bar q_{\bar n}\rangle_1$. The fact that the quark and gluon share an index label implies that $q_1\cdot k_1 \lesssim (Q\lambda)^2/\eta^4$. A three-jet state is indicated by $|q_{n_1}\, g_{n_1'}\, \bar q_{\bar n}\rangle_1$, where each particle is collinear to a different direction. The operators $\mathcal{O}_1^{(0)}(n_0)$, $\mathcal{O}_1^{(1)}(n_0,n_0)$ and $\mathcal{T}_1^{(1)}(n_0,n_0)$ can only create a two-jet state, whereas $\mathcal{O}_1^{(1)}(n_1,n_1')$ is for three-jets. Multiplying the terms in (C3) by the Wilson coefficients, we have:

$$\begin{aligned} J^\mu_{\rm QCD} =& C^{(0)}_{1,\rm LO}(n_0)\mathcal{O}_1^{(0)} + C^{(1)}_{1,\rm NLO}(n_0,n_0)\mathcal{O}_1^{(1)} + C^{(1)}_{1,\mathcal{T}}(n_1,n_1')\mathcal{T}_1^{(1)} \\ &+ C_1^{(1)}(n_1,n_1')\mathcal{O}_1^{(1)} + \dots\,, \end{aligned} \tag{C4}$$

where the ellipses indicate higher order terms in λ. When it is unambiguous, we will only write the n-labels in the Wilson coefficients, as above. We begin by looking at two-jet operators in detail. Here, because we are in the center of mass frame, the two jets are back to back. We define the kinematics as follows, the antiquark is exactly parallel to $\bar n = (1,0,0,-1)$, while the quark and the gluon are collinear to $n_0 = (1,0,0,1)$, such that $q_0 = q_1 + k_1$ has no component perpendicular to n_0 and $\bar n$, and:

$$\begin{aligned} p_{\bar q}^\mu &= n_0\cdot p_{\bar q}\frac{\bar n^\mu}{2}\,, \\ q_1^\mu &= \bar q_1\frac{n_0^\mu}{2} + n_0\cdot q_1\frac{\bar n^\mu}{2} + (q_1)^\mu_{n_0\perp}\,, \\ k_1^\mu &= \bar q_1\frac{n_0^\mu}{2} + n_0\cdot k_1\frac{\bar n^\mu}{2} + (k_1)^\mu_{n_0\perp}\,, \end{aligned} \tag{C5}$$

where $(n_0\cdot q_1, \bar q_1, q_{1\perp})$ and $(n_0\cdot k_1, \bar k_1, k_{1\perp})$ scale as $(\lambda^2,1,\lambda)$, and $(q_1)^\mu_{n_0\perp} = -(k_1)^\mu_{n_0\perp}$ by momentum conservation. The Wilson coefficients are defined through the equation

$$\begin{aligned} \langle 0|J^\mu_{\rm QCD}|q_{n_0}\, g_{n_0}\, \bar q_{\bar n}\rangle_1 =& C^{(0)}_{1,\rm LO}(n_0,n_0)\int dx^4\langle 0|T\{\mathcal{L}_{\rm SCET_1}(x)\mathcal{O}_1^{(0)}\}|q_{n_0}\, g_{n_0}\, \bar q_{\bar n}\rangle_1 \\ &+ C_1^{(1)}(n_0,n_0)\langle 0|\mathcal{O}_1^{(1)}|q_{n_0}\, g_{n_0}\, \bar q_{\bar n}\rangle_1 + C^{(1)}_{1,\mathcal{T}}(n_0,n_0)\langle 0|\mathcal{T}_1^{(1)}|q_{n_0}\, g_{n_0}\, \bar q_{\bar n}\rangle_1\,. \end{aligned} \tag{C6}$$

Calculating the C's for this two-jet process goes as follows. We decompose the QCD amplitude along n_0 and $\bar n$, using Eq. (C5), and we write the QCD spinor in terms of the SCET$_1$ spinor, Eq. (C8). Expanding in λ up to NNLO, on

the RHS we compute the amplitudes for the three SCET_1 terms. The coefficient $C_{1,\mathrm{LO}}^{(0)}$ was already determined from matching QCD to SCET_1 for zero gluon emission, it is:

$$C_{1,\mathrm{LO}}^{(0)} = \gamma^\mu \,. \tag{C7}$$

The coefficients $C_1^{(1)}$ and $C_{1,\mathcal{T}}^{(1)}$ come from solving Eq. (C6) at NLO(λ) and NNLO(λ), respectively. Since $\mathcal{O}_1^{(1)}$ and $\mathcal{T}_1^{(1)}$ are at different orders in λ, there are no ambiguities.

In order to do the matching, we need the relation between the QCD and SCET spinors. Using Eq. (B5), we can write:

$$u(p) = \Big(1 + \frac{\not{p}_\perp \bar{\not{n}}}{2\,\bar{p}}\Big) u_n(p) \,, \tag{C8}$$

where $u(p)$ is the QCD spinor and $u_n(p)$ is the SCET_1 one. It easy to see that the SCET spinor satisfies:

$$\begin{aligned} \frac{\bar{\not{n}}\not{n}}{4} u_n &= 0 \,, \\ \frac{\not{n}\bar{\not{n}}}{4} u_n &= u_n \,, \\ \sum_s \bar{u}_n^s u_n^s &= \bar{p}\frac{\bar{\not{n}}}{2} \,. \end{aligned} \tag{C9}$$

The QCD amplitude for $\gamma^* \to q\bar{q}g$ (shown in Fig. 17) is:

$$A_{\mathrm{QCD}}^{q\bar{q}g} = \bar{u}(q_1) i g \gamma^\alpha \frac{i\not{q}_0}{q_0^2} \gamma^\mu v(p_{\bar{q}}) - \bar{u}(q_1) i g \gamma^\mu \frac{i\not{p}_0}{p_0^2} \gamma^\alpha v(p_{\bar{q}}) \,. \tag{C10}$$

Using Eqs. (C5) & (C8) in (C10) and expanding to NNLO in λ we get:

$$A_{\mathrm{QCD}}^{q\bar{q}g} = A_{\mathrm{LO}}^{q\bar{q}g} + A_{\mathrm{NLO}}^{q\bar{q}g} + A_{\mathrm{NNLO}}^{q\bar{q}g} \,, \tag{C11}$$

where,

$$\begin{aligned} A_{\mathrm{LO}}^{q\bar{q}g} &= -g\bar{u}_{n_0}\Big[\Big(n_0^\alpha + \frac{(\not{q}_1)_{n_0\perp}}{\bar{q}_1}\gamma_{n_0\perp}^\alpha\Big)\frac{\bar{q}_0}{q_0^2} + \frac{\bar{n}^\alpha}{\bar{k}_1}\Big]\gamma_{n_0\perp}^\mu v_{\bar{n}} \,, \\ A_{\mathrm{NLO}}^{q\bar{q}g} &= g\frac{n_0^\mu - \bar{n}^\mu}{Q}\bar{u}_{n_0}\Big(\gamma_{n_0\perp}^\alpha - \frac{(\not{k}_1)_{n_0\perp}}{\bar{k}_1}\bar{n}^\alpha\Big)v_{\bar{n}} \,, \\ A_{\mathrm{NNLO}}^{q\bar{q}g} &= g\Big(\frac{1}{\bar{q}_1} + \frac{1}{\bar{k}_1}\Big)\frac{1}{Q}\bar{u}_{n_0}\gamma_{n_0\perp}^\mu(\not{k}_1)_{n_0\perp}\Big(\gamma_{n_0\perp}^\alpha - \frac{(\not{k}_1)_{n_0\perp}}{\bar{k}_1}\bar{n}^\alpha\Big)v_{\bar{n}} \\ &\quad - g\frac{2}{\bar{q}_1 Q}\bar{u}_{n_0}(k_1)_{n_0\perp}^\mu\Big(\gamma_{n_0\perp}^\alpha - \frac{(\not{k}_1)_{n_0\perp}}{\bar{k}_1}\bar{n}^\alpha\Big)v_{\bar{n}} \,. \end{aligned} \tag{C12}$$

We already know $C_{1,\mathrm{LO}}^{(0)}$, and it is easy to determine the other two Wilson coefficients to reproduce $A_{\mathrm{QCD}}^{q\bar{q}g}$, they are:

$$\begin{aligned} C_{1,\,\mathrm{NLO}}^{(1)}(n_0, n_0) &= \frac{1}{Q}(n_0^\mu - \bar{n}^\mu)\gamma_{n_0\perp}^\alpha \,, \\ C_{1,\mathcal{T}}^{(1)}(n_0, n_0) &= \frac{1}{\bar{q}_1\bar{k}_1}\gamma_{n_0\perp}^\mu\gamma_{n_0\perp}^\beta\gamma_{n_0\perp}^\alpha - \frac{2}{\bar{q}_1 Q}\, g^{\beta\mu}\gamma_{n_0\perp}^\alpha \,, \end{aligned} \tag{C13}$$

where we have used the relation $\bar{q}_1 + \bar{k}_1 = Q$.

For the three-jet operator $O_1^{(1)}(n_1, n_1')$, the matching was already done in [67], but we will translate it to the notation used here. In this case, we need three distinct directions in SCET_1 to describe the three external particles, and there is no small parameter to expand in. This means that the amplitude for this operator is exactly equal to the tree-level QCD amplitude for a $q\bar{q}g$ process. One may wonder then, why we simply do not apply this everywhere instead of just the three-jet region. The answer has to do with factorization and running effects. The RG kernels of our two-jet operators, $\mathcal{O}_1^{(0)}$, $\mathcal{O}_1^{(1)}$, and $\mathcal{T}_1^{(1)}$, will resum the large collinear logarithms of those configurations (*cf.* Sec. IV C). It is for this reason that we gain by keeping track of them as separate contributions.

Even though they are all in independent directions, we need only four independent vectors to decompose the particles. In the center of mass frame, $q_0 = q_1 + k_1$ is back to back with the antiquark, $p_{\bar q} \propto \bar n$. We decompose q_0 along $(n_0,\, \bar n)$ such that it has no component perpendicular to them: $q_0 = \bar n \cdot q_0\, n_0/2 + n_0 \cdot q_0\, \bar n/2$. Using Eq. (B10) we can define n_1 and n_1' such that they are parallel to q_1 and k_1, respectively and such that the quark is decomposed along $(n_1,\, \bar n)$ and the gluon along $(n_1',\, \bar n)$, both without $\perp$ components. Unlike the two-jet case, where $(q_1)_{n_0\perp} \lesssim \lambda$, since the quark was collinear to n_0, here $(q_1)_{n_0\perp} > \lambda$ in Eq. (B10). We have:

$$\begin{aligned} q_1^\mu &= \bar n\cdot q_1 \frac{n_1^\mu}{2}\,, \\ p_{\bar q}^\mu &= n_0\cdot p_{\bar q} \frac{\bar n^\mu}{2}\,, \\ k_1^\mu &= \bar n\cdot k_1 \frac{n_1'^\mu}{2}\,, \end{aligned} \tag{C14}$$

where $\bar n \cdot q_1$, $n_0 \cdot p_{\bar q}$ and $\bar n \cdot k_1$ are $\mathcal{O}(Q)$, and $n_1 \cdot n_1' > \lambda^2/\eta^4$. With this setup $\mathcal{T}_1^{(1)}(n_1, n_1') = \bar\chi_{n_1} \mathcal{P}_{n_1'}^\perp \mathcal{B}^\alpha_{n_1'\perp} \chi_{\bar n} = 0$.

The matching is therefore given by:

$$\langle 0|J^\mu_{\rm QCD}|q_{n_1}\, g_{n_1'}\, \bar q_{\bar n}\rangle_1 = C_1^{(1)}(n_1, n_1')\langle 0|O_1^{(1)}|q_{n_1}\, g_{n_1'}\, \bar q_{\bar n}\rangle_1\,, \tag{C15}$$

and the Wilson coefficient is:

$$\begin{aligned} C_1^{(1)}(n_1, n_1') = &-\frac{2}{(n_1\cdot n_1')\bar q_1 \bar k_1}\gamma^\alpha \not p_\gamma\, \gamma_T^\mu \\ &+ \Big[\frac{1}{(n\cdot p_{\bar q})\bar k_1}\Big(\gamma_T^\mu \not p_\gamma - \bar q_1\, n_{1T}^\mu\Big) + \frac{2(n\cdot p_{\bar q})}{(n_1\cdot n_1')\bar q_1 \bar k_1}\bar n_T^\mu\Big]\gamma^\alpha_{n_1'\,\perp}\,, \end{aligned} \tag{C16}$$

where the subscript T applied to a generic four vector f^μ means: $f_T^\mu \equiv f^\mu - p_\gamma^\mu\,(f\cdot p_\gamma)/p_\gamma^2$, and p_γ is defined in Eq. (C2).

Before moving on to lower scale SCET$_i$, we note that all the Wilson coefficients in SCET$_1$ are of order λ^0. This will change with SCET$_2$ as these factors will determine the relative importance of different contributions. As we discussed at the very end of Sec. IV A, we do not need to compute any suppressed two-gluon operators in SCET$_1$ to the order at which we are working. Their Wilson coefficient will be $\mathcal{O}(\lambda^0)$. Matching this contribution to a two-gluon SCET$_2$ operator will leave this factor unchanged as there are no further emissions from it. The field content in SCET$_2$ will scale $\sim \lambda^8$. As shown in Eq. (D7) though, LO in SCET$_2$ is at λ^5.

Lastly, we described the effects of adding running effects in Sec. IV C. In the next Appendix we will match SCET$_1$ to SCET$_2$. Before doing it we have to run the SCET$_1$ operators from Q down to μ_1, where we have the first emission:

$$\begin{aligned} C_0^{(0)}(n_0) &= U^{(2,0,0)}(n_0;\, Q,\mu)\,\gamma^\mu_{n_0\perp} \\ C^{(1)}_{1,\,\rm NLO}(n_0, n_0) &= U^{(2,1,0)}(n_0, n_0;\, Q,\mu) \otimes \frac{n_0^\mu - \bar n^\mu}{Q}\gamma^\alpha_{n_0\perp}\,, \\ C^{(1)}_{1,\mathcal{T}}(n_0, n_0) &= U^{(2,1,1)}_{\mathcal{T}}(n_0, n_0;\, Q,\mu) \otimes \frac{1}{\bar q_1 \bar k_1}\Big(\gamma^\mu_{n_0\perp}\gamma^\beta_{n_0\perp}\gamma^\alpha_{n_0\perp} - \frac{2}{\bar q_1 Q}\, g^{\mu\beta}\gamma^\alpha_{n_0\perp}\Big)\,, \\ C_1^{(1)}(n_1, n_1') &= U^{(2,1,0)}(n_1, n_1';\, Q,\mu)\,\Big(-\frac{2}{(n_1\cdot n_1')\bar q_1 \bar k_1}\gamma^\alpha_{n_0\perp}\not p_\gamma\,\gamma_T^\mu \\ &\quad - \Big[\frac{1}{(n\cdot p_{\bar q})\bar k_1}\Big(\gamma_T^\mu \not p_\gamma - \bar q_1\, n_{1T}^\mu\Big) + \frac{2(n\cdot p_{\bar q})}{(n_1\cdot n_1')\bar q_1 \bar k_1}\bar n_T^\mu\Big]\gamma^\alpha_{n_0\perp}\Big)\,. \end{aligned} \tag{C17}$$

For the definition of the running factors $U^{(i,j,k)}(Q,\mu)$ see Eqs. (18)-(20), and (90). The convolution symbol, $\otimes$, is only relevant beyond LL, that is beyond the level required here.

Appendix D: Matching SCET$_1$ to SCET$_2$

1. One-Gluon Emission

We now match SCET$_1$ to SCET$_2$ for one and two-gluon emissions, starting with the former. The basis of SCET$_2$ operators necessary for the matching up to NNLO(λ) is equal to Eq. (C3), but defined in SCET$_2$: $\mathcal{O}_2^{(0)}(n_0)$, $\mathcal{O}_2^{(1)}(n_0, n_0)$,

$\mathcal{T}_2^{(1)}(n_0,n_0)$,$\mathcal{O}_2^{(1)}(n_1,n_1')$.[16] In the previous section, we matched QCD to SCET$_1$ for one emission and found either a two-jet ($|q_{n_0}\, g_{n_0}\, \bar{q}_{\bar{n}}\rangle_1$) or three-jet configuration ($|q_{n_1}\, g_{n_1'}\, \bar{q}_{\bar{n}}\rangle_1$), depending on the collinearity of the external particles. When we go to SCET$_2$, our definition of collinearity becomes stricter. Particles with momenta p_1 and p_2 are collinear only if $p_1\cdot p_2 \lesssim Q^2\lambda^4/\eta^4$, where $\eta\sim\frac{1}{2}$ is the average energy loss factor between mother and daughters discussed in Sec. II C. As a result of this change, a two-jet configuration in SCET$_1$ can be matched both onto $|q_{n_0}\, g_{n_0}\, \bar{q}_{\bar{n}}\rangle_2$ and $|q_{n_1}\, g_{n_1'}\, \bar{q}_{\bar{n}}\rangle_2$ in SCET$_2$. The three-jet configuration in SCET$_1$ can, of course, only go to the three-jet state $|q_{n_1}\, g_{n_1'}\, \bar{q}_{\bar{n}}\rangle_2$ in SCET$_2$. The matching is given by

$$\begin{aligned} J^\mu_{\rm QCD} &= C^{(0)}_{1,\,\rm LO}(n_0)\mathcal{O}_1^{(0)} + C^{(1)}_{1,\,\rm NLO}(n_0,n_0)\mathcal{O}_1^{(1)} + C_1^{(1)}(n_1,n_1')\mathcal{O}_1^{(1)} \qquad \text{(D1)}\\ &\quad + C^{(1)}_{1,\mathcal{T}}(n_0,n_0)\mathcal{T}_1^{(1)} + \cdots \\ &= C_2^{(0)}(n_0)\mathcal{O}_2^{(0)} + C_2^{(1)}(n_0,n_0)\mathcal{O}_2^{(1)} + C_2^{(1)}(n_1,n_1')\mathcal{O}_2^{(1)} \qquad \text{(D2)}\\ &\quad + C^{(1)}_{2,\mathcal{T}}(n_0,n_0)\mathcal{T}_2^{(1)} + \cdots\,, \end{aligned}$$

where we give the decomposition into both SCET$_1$ and SCET$_2$ operators. The ellipses indicate higher order terms. If we close Eq. (D2) with the state $|q_{n_0}\, g_{n_0}\, \bar{q}_{\bar{n}}\rangle_2$, we get

$$\begin{aligned} &C^{(0)}_{1,\,\rm LO}(n_0)\int dx^4\langle 0|T\{\mathcal{L}_{\rm SCET_1}(x)\mathcal{O}_1^{(0)}\}|q_{n_0}\, g_{n_0}\, \bar{q}_{\bar{n}}\rangle_2 \\ &+ C^{(1)}_{1,\,rmNLO}(n_0,n_0)\langle 0|\mathcal{O}_1^{(1)}|q_{n_0}\, g_{n_0}\, \bar{q}_{\bar{n}}\rangle_2 + C^{(1)}_{1,\mathcal{T}}(n_0,\,n_0)\langle 0|\mathcal{T}_1^{(1)}|q_{n_0}\, g_{n_0}\, \bar{q}_{\bar{n}}\rangle_2 \\ &= C_2^{(0)}(n_0)\int dx^4\langle 0|T\{\mathcal{L}_{\rm SCET_2}(x)\mathcal{O}_2^{(0)}\}|q_{n_0}\, g_{n_0}\, \bar{q}_{\bar{n}}\rangle_2 \\ &+ C_2^{(1)}(n_0,n_0)\langle 0|\mathcal{O}_2^{(1)}|q_{n_0}\, g_{n_0}\, \bar{q}_{\bar{n}}\rangle_2 + C^{(1)}_{2,\mathcal{T}}(n_0,n_0)\langle 0|\mathcal{T}_2^{(1)}|q_{n_0}\, g_{n_0}\, \bar{q}_{\bar{n}}\rangle_2\,. \end{aligned} \qquad \text{(D3)}$$

Since the structure of the operators in Eq. (D3) is the same on the LHS and RHS, we simply get:

$$\begin{aligned} C_2^{(0)}(n_0) &= C^{(0)}_{1,\,\rm LO}(n_0)\,, \\ C_2^{(1)}(n_0,n_0) &= C^{(1)}_{1,\,\rm NLO}(n_0,n_0)\,, \\ C^{(1)}_{2,\mathcal{T}}(n_0,n_0) &= C^{(1)}_{1,\mathcal{T}}(n_0,n_0)\,. \end{aligned} \qquad \text{(D4)}$$

Acting on Eq. (D2) with the state $|q_{n_1}\, g_{n_1'}\, \bar{q}_{\bar{n}}\rangle_2$, we have:

$$\begin{aligned} &C^{(0)}_{1,\,\rm LO}(n_0)\int dx^4\langle 0|T\{\mathcal{L}_{\rm SCET_1}(x)\mathcal{O}_1^{(0)}\}|q_{n_1}\, g_{n_1'}\, \bar{q}_{\bar{n}}\rangle_2 + C^{(1)}_{1,\,\rm NLO}(n_0,n_0)\langle 0|\mathcal{O}_1^{(1)}|q_{n_1}\, g_{n_1'}\, \bar{q}_{\bar{n}}\rangle_2 \\ &+ C_1^{(1)}(n_1,n_1')\langle 0|\mathcal{O}_1^{(1)}|q_{n_1}\, g_{n_1'}\, \bar{q}_{\bar{n}}\rangle_2 + C^{(1)}_{1,\mathcal{T}}(n_0,n_0)\langle 0|\mathcal{T}_1^{(1)}|q_{n_1}\, g_{n_1'}\, \bar{q}_{\bar{n}}\rangle_2 \\ &= C_2^{(1)}(n_1,n_1')\langle 0|\mathcal{O}_2^{(1)}|q_{n_1}\, g_{n_1'}\, \bar{q}_{\bar{n}}\rangle_2\,. \end{aligned} \qquad \text{(D5)}$$

We decompose $C_2^{(1)}(n_1,n_1')$ as

$$C_2^{(1)}(n_1,n_1') = C^{(1)}_{2,\,\rm LO}(n_1,n_1') + C^{(1)H,a}_{2,\,\rm NLO}(n_1,n_1') + C^{(1)H,b}_{2,\,\rm NLO}(n_1,n_1') + C^{(1)H}_{2,\,\rm NNLO}(n_1,n_1')\,, \qquad \text{(D6)}$$

where $C^{(1)}_{2,\,\rm LO}$ is the coefficient that reproduces the first term on the LHS of Eq. (D5), *etc.* All the SCET$_2$ coefficients in Eq. (D4) scale as λ^0, like in SCET$_1$, but we will see that those in Eq. (D6) scale differently, giving the hierarchy indicated in the subscript. We will show that:

$$\begin{aligned} C_2^{(0)}(n_0)\mathcal{O}_2^{(0)} &\sim \lambda^4\,, & C^{(1)}_{2,\,\rm LO}(n_1,n_1')\mathcal{O}_2^{(1)} &\sim \lambda^5\,, \\ C_2^{(1)}(n_0,n_0)\mathcal{O}_2^{(1)} &\sim \lambda^6\,, & C^{(1)H,\,a}_{2,\,\rm NLO}(n_1,n_1')\mathcal{O}_2^{(1)} &\sim \lambda^6\,, \\ C^{(1)}_{2,\mathcal{T}}(n_0,n_0)\mathcal{T}_2^{(1)} &\sim \lambda^8\,, & C^{(1)H,\,b}_{2,\,\rm NLO}(n_1,n_1')\mathcal{O}_2^{(1)} &\sim \lambda^6\,, \\ & & C^{(1)H}_{2,\,\rm NNLO}(n_1,n_1')\mathcal{O}_2^{(1)} &\sim \lambda^7\,. \end{aligned} \qquad \text{(D7)}$$

[16] As before, we do not consider operators like $\mathcal{O}_2^{(1)}(n_0,\bar{n})$ that describe a gluon collinear to the antiquark.

In the second column we have only one operator $\mathcal{O}_2^{(1)}(n_1, n_1')$ and we have decomposed its coefficient according to Eq. (D6). The matching does not conserve the power counting, as collinear SCET_1 fields scale as λ, but in SCET_2 they go as λ^2. For example, we have that the LO operator in SCET_1 is $C_1^{(0)}\mathcal{O}_1^{(0)} \sim \lambda^2$, but for the LO operator in SCET_2 we have $C_2^{(0)}\,\mathcal{O}_2^{(0)} \sim \lambda^4$.

If we want to calculate a cross section for a fixed number of external particles, then we need all the SCET_2 operators in Eq. (D2). Our interest, though, is in improving shower Monte Carlo, and so we only calculate operators needed for that (*cf.* discussion in Sec. III A). To reproduce the LL emission of two gluons, the only higher dimension operator we need is $C^{(1)}_{2,\,\mathrm{LO}}(n_1, n_1')\mathcal{O}_2^{(1)}$. The operators $\mathcal{O}_2^{(0)}(n_0)$ and $\mathcal{O}_2^{(1)}(n_0, n_0)$ only tell us about the no-branching probabilities already determined by the one-loop cusp anomalous dimension. For example, $\mathcal{O}_2^{(0)}(n_0)$ describes a quark which does not emit until after the scale of matching $k_{1\perp}$. For this reason, we call $C^{(1)}_{2,\,\mathrm{LO}}(n_1, n_1')\mathcal{O}_2^{(1)}$ our LO operator. Naively, two-gluon contributions from $\mathcal{O}_2^{(0)}(n_0)$ and $\mathcal{O}_2^{(1)}(n_0,\, n_0)$ are lower order at tree-level, but this does not take into account the exponential suppression from running. The dominant contribution to showers comes from strong-ordering, not "every emission as collinear as possible." Thus, we build our shower around $C^{(1)}_{2,\,\mathrm{LO}}(n_1, n_1')\mathcal{O}_2^{(1)}$. The coefficients $C^{(1),H}_{2,\,\mathrm{NLO}}(n_1, n_1')$ and $C^{(1),H}_{2,\,\mathrm{NNLO}}(n_1, n_1')$ give corrections for one emission. We therefore obtain a correction if we run a LL shower based on a matrix element computed with one of these suppressed terms.

We now turn to calculate the terms in Eq. (D6). in three steps: first we calculate the amplitudes in SCET_1 on the LHS of (D5); second we rotate it using the finite RPI_1 transformations defined in App. B, so that the necessary operators overlap with SCET_2 states; and third we calculate the Wilson coefficients necessary to match the two sides. We do it order by order and we start calculating the coefficient $C^{(1)}_{2,\,\mathrm{LO}}$. The first term of the LHS of (D5) is

$$A^{q\bar{q}g}_{\mathrm{LO}} = U^{(2,0,0)}(n_0;\, Q, \mu_1)\, g\, \bar{\xi}_{n_0} \left(n_0^\alpha + \frac{(\not{q}_1)_{n_0\perp}\gamma^\alpha_{n_0\perp}}{\bar{q}_1} \right) \gamma^\mu_{n_0\perp} \xi_{\bar{n}}\,, \tag{D8}$$

where $U^{(2,0,0)}(n_0)$ is the running factor (*cf.* Eqs. 18, 19, and 90), and $\mu_1 \sim \lambda Q$ is at the scale of the emission. In (D8), we have omitted the terms proportional to $\bar{n}^\alpha$ as they are unnecessary for matching. Gauge invariance constrains all appearances of $\bar{n}\cdot A_n$ to come from the Wilson lines in χ and $\mathcal{B}$. The amplitude is written in terms of objects projected in the n_0 and $\bar{n}$ directions. As discussed in Appendix B, these directions are not suitable for a SCET_2 states, but we can use the formulas (B7) and write (D8) in terms of the directions n_1 and n_1' where the quark and gluon have zero perpendicular component, this gives

$$A^{q\bar{q}g}_{\mathrm{LO}} = U^{(2,0,0)}(n_0;\, Q, \mu_1)\, g\, \bar{\xi}_{n_1} \left(n_1'^\alpha + 2\frac{(q_1)^\alpha_{n_0\perp}}{\bar{k}_1} + \frac{(\not{q}_1)_{n_0\perp}\gamma^\alpha_{n_1'\perp}}{\bar{q}_1} \right) \frac{\bar{q}_0}{q_0^2} \gamma^\mu_{n_0\perp} \xi_{\bar{n}}\,. \tag{D9}$$

In (D9) we have rotated the spinor in the n_1 direction, $\gamma_{n_0\perp}$ in the n_1' direction and we have written n_0 in terms of n_1, n_1' and $(q_1)_{n_0\perp}$. We have dropped all the terms proportional to $\bar{n}^\alpha$ and we made use of relations $\not{n}\not{\bar{n}} = 0$ and $\bar{\xi}_{n_1}\not{n}_1 = 0$. Since the gluon momentum is parallel to $n_1'^\mu$, only the polarizations in the perpendicular direction with respect to $n_1'^\mu$ are physical, thus we can neglect the term proportional to n_1' in Eq. (D9). The SCET_2 amplitude $\langle 0|\bar{\chi}_{n_1} g\mathcal{B}^\alpha_{n_1'\perp}\chi_{\bar{n}}|q_{n_1} g_{n_1'}\bar{q}_{\bar{n}}\rangle_2$ is

$$\langle 0|\bar{\chi}_{n_1} g\mathcal{B}^\alpha_{n_1'\perp}\chi_{\bar{n}}|q_{n_1} g_{n_1'}\bar{q}_{\bar{n}}\rangle_2 = g\,\bar{u}_{n_1}\epsilon^\alpha_{n_1'\perp} v_{\bar{n}}\,, \tag{D10}$$

where in Eq. (D10) we have explicitly written the polarization vector for the gluon. From Eq. (D9) and Eq. (D10), we can see that the LO Wilson coefficient is

$$C^{(1)}_{2,\,\mathrm{LO}} = U^{(2,0,0)}(n_0;\, Q, \mu_1) c^\alpha_{\mathrm{LO}}(n_0) \frac{\bar{q}_0}{q_0^2}\gamma^\mu_{n_0\perp}\,, \tag{D11}$$

where

$$c^\alpha_{\mathrm{LO}}(n_0) = \left(2\frac{(q_1)^\alpha_{n_0\perp}}{\bar{k}_1} + \frac{(\not{q}_1)_{n_0\perp}\gamma^\alpha_{n_1'\perp}}{\bar{q}_1} \right) \frac{\not{\bar{n}}\not{n}_0}{4}\, \Theta_{\delta_2}[n_1\cdot n_1']\,. \tag{D12}$$

The difference with Eq. (57) is that we replaced n_0 in terms of external vectors. $\Theta_{\delta_2}[n_1\cdot n_1']$ is the phase space cutoff that guarantees $(n_1\cdot n_1') \lesssim \lambda^2/\eta^4$,[17] we will say more about it below. Since this comes from matching to a SCET_1

[17] The factor of $\eta \simeq \frac{1}{2}$ tracks the average energy loss between mother and daughter. In choosing appropriate values for the parameters δ_k in the numerical implementation of Θ it is important to track these η factors in the scaling of $n_1\cdot n_1'$.

operator, $(q_1)_{n_0\perp} \sim \lambda$ and $q_0^2 \sim \lambda^2$, thus $C_{2,\,\rm LO}^{(1)}$ scales as λ^{-1}. Using formulas (B11), we can write (D11) only in terms of n_1 and n_1', this gives

$$C_{2,\,\rm LO}^{(1)} = U^{(2,0,0)}(n_0;\,Q,\,\mu_1)\left(\frac{\bar q_1}{Q}\sqrt{n_1\cdot n_1'}v_1^\alpha + \frac{\bar k_1}{2Q}\sqrt{n_1\cdot n_1'}\not{v}_1\,\gamma^\alpha_{n_1'\perp}\right)\frac{2\bar q_0}{(n_1\cdot n_1')\,\bar q_1\bar k_1}$$
$$\times\left(\gamma^\mu_{n_1'} - \bar n^\mu\frac{1}{2}\frac{\bar q_1}{\bar q_0}\sqrt{n_1\cdot n_1'}\not{v}_1\right), \tag{D13}$$

where v_1^μ is defined in Eq. (B12), $\bar q_1 + \bar k_1 = Q$. For μ_1, as explained in Sec. III A, we take it at the scale of $(k_1)_{n_0\perp}$ as in Eq. (64) for $k = 1$. Since $|v_1^2| = 2$, the power counting of (D13) is given by the scalar product $n_1\cdot n_1'$, that is $\mathcal{O}(\lambda^2)$. In a similar way, we can calculate $C_{2,\,\rm NLO}^{(1)H,a}$ and $C_{2,\,\rm NNLO}^{(1)H}$.

We have done the matching starting from the vector current $J^\mu_{\rm QCD} = \bar q\,\gamma^\mu q$. If we had started from a general structure, $\bar q\,\Gamma^\mu q$, the results (D11) for $C_{2,\,\rm LO}^{(1)}$ would have been the same upon the substitution

$$\gamma^\mu_{n_0\perp} \to \Gamma^\mu\,. \tag{D14}$$

We can obtain $C_{2,\,\rm LO}^{(1)}(n_1,n_1')\mathcal{O}_2^{(2)}$ from the SCET$_1$ operator $\bar\chi_{n_0}\Gamma^\mu\chi_{\bar n}$ by running down from Q to μ_1, multiplying by the factor $U^{(2,0,0)}(n_0;\,Q,\,\mu_1)$, and subsequently using the replacement rule

$$(\bar\chi_{n_0})_i \to\ (c^\alpha_{\rm LO}(n_0))_{ji}(\bar\chi_{n_1})_j\,g\mathcal{B}^{n_1'\perp}_\alpha\,. \tag{D15}$$

The coefficients $C_{2,\,\rm NLO}^{(1)H,\,a}$, $C_{2,\,\rm NLO}^{(1)H,\,b}$, $C_{2,\,\rm NNLO}^{(1)H}$, however, are sensitive to the particular QCD current. This is why we refer to them as hard-scattering corrections, denoted by the superscript, H.

For the NLO(λ) and NNLO(λ) amplitudes in the second and third line of the LHS of Eq. (D5) we have

$$A^{q\bar qg}_{\rm NLO} = U^{(2,1,0)}(n_0,n_0;\,Q,\,\mu_1)\frac{n_0^\mu-\bar n^\mu}{Q}g\bar u_{n_0}\gamma^\alpha_{n_0\perp}v_{\bar n} = \frac{n_0^\mu-\bar n^\mu}{Q}g\bar u_{n_1}\gamma^\alpha_{n_1'\perp}v_{\bar n}\,,$$
$$A^{q\bar qg}_{\rm NNLO} = U^{(2,1,1)}(n_0,n_0;\,Q,\,\mu_1)$$
$$\times\Big(\frac{1}{\bar q_1}+\frac{1}{\bar k_1}\Big)\frac{1}{Q}g\bar u_{n_0}\gamma^\mu_{n_0\perp}(\not k_1)_{n_0\perp}\gamma^\alpha_{n_0\perp}v_{\bar n} - \frac{2}{\bar q_1 Q}g\bar u_{n_0}(k_1)^\mu_{n_0\perp}\gamma^\alpha_{n_0\perp}v_{\bar n}$$
$$= U^{(2,1,1)}(n_0,n_0;\,Q,\,\mu_1)$$
$$\times\Big(\frac{1}{\bar q_1}+\frac{1}{\bar k_1}\Big)\frac{1}{Q}g\bar u_{n_1}\gamma^\mu_{n_0\perp}(\not k_1)_{n_0\perp}\gamma^\alpha_{n_1'\perp}v_{\bar n} - \frac{2}{\bar q_1 Q}g\bar u_{n_1}(k_1)^\mu_{n_0\perp}\gamma^\alpha_{n_1'\perp}v_{\bar n}\,. \tag{D16}$$

The SCET$_2$ coefficients needed to reproduce the amplitudes in Eq. (D16) are:

$$C_{2,\,\rm NLO}^{(1)H,a} = U^{(2,1,0)}(n_0,n_0;\,Q,\,\mu_1)\otimes c^{H,a}_{2,\,\rm NLO}(n_0,n_0),$$
$$C_{2,\,\rm NNLO}^{(1)H} = U^{(2,1,1)}_{\mathcal{I}}(n_0,n_0;\,Q,\,\mu_1)\otimes c^{H}_{2,\,\rm NNLO}(n_0,n_0), \tag{D17}$$

where

$$c^{H,a}_{2,\,\rm NLO}(n_0,n_0) = U^{(2,1,0)}(n_0,n_0;\,Q,\,\mu_1)\frac{n_0^\mu-\bar n^\mu}{Q}\gamma^\alpha_{n_0\perp}\Theta_{\delta_2}[n_1\cdot n_1'] \tag{D18}$$
$$= U^{(2,1,0)}(n_0,n_0;\,Q,\,\mu_1)\frac{1}{Q}\left[\frac{\bar k_1 n_1'^\mu + \bar q_1 n_1^\mu}{\bar q_0} - \Big(1+\frac{\bar q_1\bar k_1}{2\,\bar q_0^2}(n_1\cdot n_1')\Big)\bar n^\mu\right]$$
$$\times\gamma^\alpha_{n_1'\perp}\Theta_{\delta_2}[n_1\cdot n_1']\,,$$
$$c^{H}_{2,\,\rm NNLO}(n_0,n_0) = U^{(2,1,1)}_{\mathcal{I}}(n_0,n_0;\,Q,\,\mu_1)\Big[\Big(\frac{1}{\bar q_1}+\frac{1}{\bar k_1}\Big)\frac{1}{Q}\gamma^\mu_{n_0\perp}(\not k_1)_{n_0\perp}\gamma^\alpha_{n_1'\perp} - \frac{2}{\bar q_1 Q}(k_1)^\mu_{n_0\perp}\gamma^\alpha_{n_1'\perp}\Big]$$
$$\times\Theta_{\delta_2}[n_1\cdot n_1']$$
$$= -U^{(2,1,1)}_{\mathcal{I}}(n_0,n_0;\,Q,\,\mu_1)\Big(\frac{1}{2\,Q}\Big(\gamma^\mu_{n_1'\perp}\sqrt{n_1\cdot n_1'}\not v_1 + \bar n^\mu\frac{\bar q_1}{Q}(n_1\cdot n_1')\Big)\gamma^\alpha_{n_1'\perp}$$
$$+\frac{\bar k_1}{Q^2}\Big(\sqrt{n_1\cdot n_1'}v_1^\mu - \bar n^\mu\,(n_1\cdot n_1')\frac{(\bar k_1^2-\bar q_1^2)}{2\,Q^2}\Big)\gamma^\alpha_{n_1'\perp}\Big)\Theta_{\delta_2}[n_1\cdot n_1']\,.$$

The coefficients scale $C_{2,\,\mathrm{NLO}}^{(1)H,a} \sim \lambda^0$ and $C_{2,\,\mathrm{NNLO}}^{(1)H} \sim \lambda$. As discussed below Eq. (89), we have a convolution because SCET fields collinear to the same direction can exchange longitudinal momentum during the running. However, this convolution is only needed beyond the LL level considered here.

For the coefficient $C_{2,\,\mathrm{NLO}}^{(1)H,b}$, the matching comes from the SCET_1 three-jet operator where $n_1 \cdot n_1' \sim \lambda^0/\eta^4$.[18] Since the n-labels in $C_1^{(1)}(n_1, n_1')$ are already parallel to the external particles, we can simply write:

$$C_{2,\,\mathrm{NLO}}^{(1)H,b}(n_1, n_1') = C_1^{(1)}(n_1, n_1')\tilde{\Theta}_{\delta_2}[n_1 \cdot n_1']\,, \tag{D19}$$

where $\tilde{\Theta}_{\delta_2}[n_1 \cdot n_1']$ only has support for $(n_1 \cdot n_1') > \lambda/\eta^4$, where it is equal to 1. Knowing that for this term, $n_1 \cdot n_1' \sim \lambda^0/\eta^4$, $C_{2,\,\mathrm{NLO}}^{(1)H,b}(n_1, n_1')$ scales $\sim \lambda^0$, and

$$C_{2,\,\mathrm{NLO}}^{(1)H,b}(n_1, n_1')\mathcal{O}_2^{(1)} \sim \lambda^6\,. \tag{D20}$$

In keeping with our conventions, we keep track of dependence on $\eta \sim \frac{1}{2}$ for our Θ functions and their dot product arguments, where the various 2^n factors affect where the step function turns over. We do not include them in the power counting for operators, where λ parametrizes strong-ordering and the deviations from it. Accounting for η here is certainly possible, but in the end we always will compare amplitudes with the same number of external particles, so η factors from operators will not play any role.

The operator $\mathcal{O}_2^{(1)}(n_1, n_1')$ only knows that $n_1 \cdot n_1' > \lambda^4/\eta^4$, it is not able to distinguish its two-jet contributions, Eq. (D13) and Eq. (D17), from its three-jet one, Eq. (D19). This information must then be in the Wilson coefficients, and we have put it in the functions Θ and $\tilde{\Theta}$, first described in Sec. III A. We can think of $\Theta_{\delta_2}[x]$ as usual theta function: $\Theta_{\delta_2}[x] = \theta[\delta_2 - x]$ and $\tilde{\Theta}_{\delta_2}[x] = 1 - \Theta_{\delta_2}[x]$, but for integrating phase space, this can lead to numerical problems. Instead, we can use a smoother theta function, such as the following, plotted in Fig. 7

$$\Theta_{\Lambda,a}(x) = \begin{cases} 0 & \text{if } x < \Lambda - a \\ -\frac{\mathrm{Sign}(x-\Lambda)}{2} e^{2+\frac{2a\,\mathrm{Sign}(x-\Lambda)}{(x-\Lambda)-a\,\mathrm{Sign}(x-\Lambda)}} + \frac{\mathrm{Sign}(x-\Lambda)+1}{2} & \text{if } \Lambda - a < x < \Lambda + a \\ 1 & \text{if } x > \Lambda + a \end{cases}, \tag{D21}$$

The parameter Λ determines where the function switches from 0 to 1, and a governs how fast it does it. For the SCET_2 coefficients, we have $\Lambda \simeq \delta_2$. In order to have $n_1 \cdot n_1' \lesssim \lambda^2/\eta^4$, we need $\lambda^2/\eta^4 \ll \delta_2 < 1/\eta^4$, so we choose $\delta_2 = \lambda/\eta^4$. When we go down to lower SCET_i, in general the Wilson coefficient has to encode the that either $n_i \cdot n_j \leq \lambda^{2(i-1)}/\eta^4$ or $n_i \cdot n_j > \lambda^{2(i-1)}/\eta^4$, in order to do so, we will use Θ_{δ_i} where $\delta_i = \lambda^{2i-3}/\eta^4$. To see how this Θ works, we look at the amplitude squared up to NLO(λ).[19] The LO amplitude squared is

$$|A^{q\bar{q}g}|^2_{\mathrm{LO}} = |C_{2,\mathrm{LO}}^{(1)}(n_1, n_1')|^2 G(q_1, k_1, k_2, p_{\bar{q}})\,, \tag{D22}$$

where

$$G(q_1, k_1, k_2, p_{\bar{q}}) = {}_2\langle q_{n_1}\, g_{n_1'}\, \bar{q}_{\bar{n}} | \mathcal{O}_1^{(1)\dagger}(n_1, n_1') | 0\rangle\langle 0 | \mathcal{O}_1^{(1)}(n_1, n_1') | q_{n_1}\, g_{n_1'}\, \bar{q}_{\bar{n}}\rangle_2\,. \tag{D23}$$

The NLO(λ) amplitude squared is

$$|A^{q\bar{q}g}|^2_{\mathrm{NLO}} = |A^{q\bar{q}g}|^2_{\mathrm{NLO},\,2-\mathrm{jet}} + |A^{q\bar{q}g}|^2_{\mathrm{NLO},\,3-\mathrm{jet}}\,, \tag{D24}$$

where

$$\begin{aligned} |A^{q\bar{q}g}|^2_{\mathrm{to\,NLO},\,2-\mathrm{jet}} &= (C_{2,\mathrm{LO}}^{(1)\dagger}(n_1, n_1')C_{2,\mathrm{NNLO}}^{(1),H}(n_1, n_1') \\ &\quad + C_{2,\mathrm{NNLO}}^{(1),H\dagger}(n_1, n_1')C_{2,\mathrm{LO}}^{(1)}(n_1, n_1') \\ &\quad + |C_{2,\mathrm{NLO}}^{(1),Ha}(n_1, n_1')|^2)G(q_1, k_1, k_2, p_{\bar{q}})\,, \\ |A^{q\bar{q}g}|^2_{\mathrm{NLO},\,3-\mathrm{jet}} &= |C_{2,\mathrm{NLO}}^{(1),Hb}(n_1, n_1')|^2 G(q_1, k_1, k_2, p_{\bar{q}})\,. \end{aligned} \tag{D25}$$

---

[18] With our conventions where $n_i \cdot \bar{n} = 2$, two well seperated directions n_1 and n_2 really do give $n_1 \cdot n_2 \sim 16$.

[19] We perform some trivial azimuthal integrals in order to eliminate some terms that will drop out of typical observables. Also, by NLO(λ) corrections for amplitudes squared, we mean suppressed by two powers of λ. Since there are no odd powers of λ in the expansion, this means NLO(λ) for the cross section.

In Fig. 11 we plot the ratios $|A^{q\bar{q}g}|^2_{\rm LO}/|A^{q\bar{q}g}|^2_{\rm QCD}$ and $(|A^{q\bar{q}g}|^2_{\rm LO}+|A^{q\bar{q}g}|^2_{\rm NLO,\,2-jet})/|A^{q\bar{q}g}|^2_{\rm QCD}$ versus $(k_1)_{n_0\perp}$, We note that including NLO(λ) corrections extends the region where tree-level SCET$_2$ and QCD agree. In Fig. 10, we plot the the merging of the two-jet and and three-jet amplitude squared using the theta function. Although we have not undertaken any systematic study of how our phase space cutoff enters observables, we take Fig. 10 as visual evidence of minimal sensitivity. Lastly, in Fig. 18 we plot $|A^{q\bar{q}g}|^2_{\rm LO}+|A^{q\bar{q}g}|^2_{\rm NLO}$ with and without running factors. As expected,

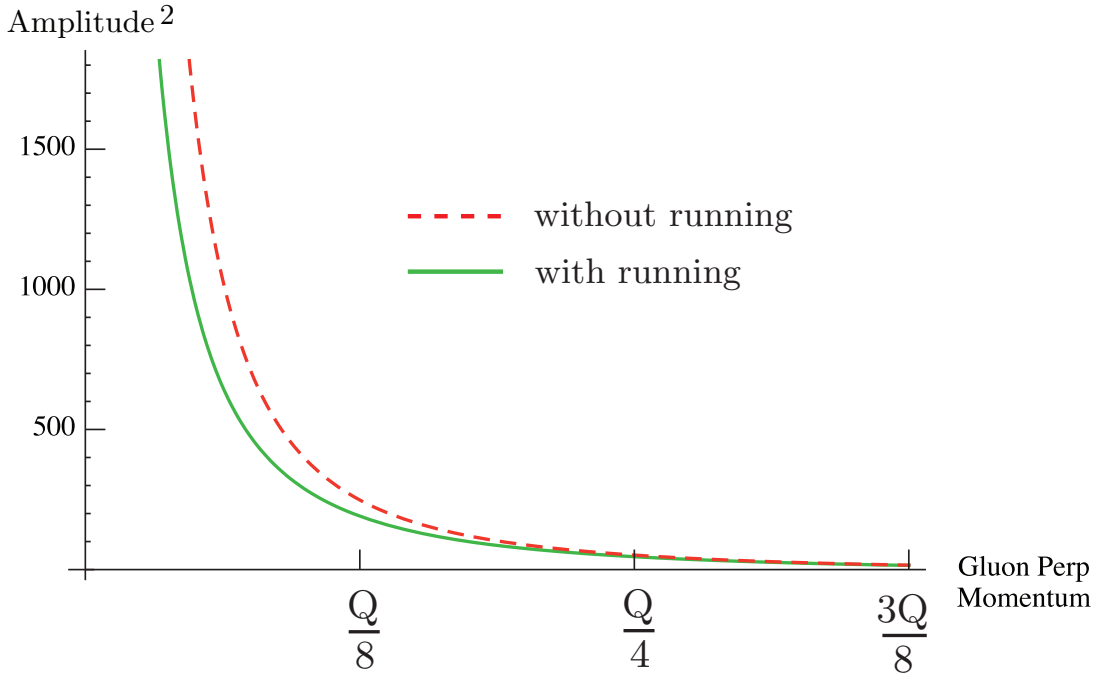

FIG. 18: Plot of the SCET$_2$ amplitude square up to NLO, $|A^{q\bar{q}g}|^2_{\rm LO}+|A^{q\bar{q}g}|^2_{\rm NLO}$, with (green) and without (red) running factors versus $(k_1)_{n_0\perp}$ for $\bar{k}_1/\bar{q}_0 = 0.4$.

the latter is suppressed relative to the former.

2. Two-Gluon Emission

As discussed at the very end of of Sec. IV A and in App. C, we do not need the two-gluon, SCET$_1$ operator, $\mathcal{O}_1^{(2)}(n_0,n_0,n_0)$ at this order. Thus, the ones in (C3) are sufficient.

The SCET$_2$ basis has the following two gluon operators:

$$\begin{aligned}
\mathcal{O}_2^{(2)}(n_2,n_1',n_2) &= \bar{\chi}_{n_2} g\mathcal{B}^{\alpha}_{n_1'\perp} g\mathcal{B}^{\beta}_{n_2\perp}\chi_{\bar{n}}\,,\\
\mathcal{O}_2^{(2)}(n_2,n_1',n_1') &= \bar{\chi}_{n_2} g\mathcal{B}^{\alpha}_{n_1'\perp} g\mathcal{B}^{\beta}_{n_1'\perp}\chi_{\bar{n}}\,,\\
\mathcal{O}_2^{(2)}(n_2,n_1',n_2') &= \bar{\chi}_{n_2} g\mathcal{B}^{\alpha}_{n_1'\perp} g\mathcal{B}^{\beta}_{n_2'\perp}\chi_{\bar{n}}\,,\\
\mathcal{O}_2^{(2)}(n_0,n_0,n_0) &= \bar{\chi}_{n_0} g\mathcal{B}^{\alpha}_{n_0\perp} g\mathcal{B}^{\beta}_{n_0\perp}\chi_{\bar{n}}\,.
\end{aligned} \tag{D26}$$

The last operator in (D26) is not necessary for the matching at NNLO(λ). It can only be closed with states $|q_{n_0}g_{n_0}g_{n_0}\bar{q}_{\bar{n}}\rangle_2$ having both gluons collinear in SCET$_2$. Its coefficient can only come from the SCET$_1$ operator $\mathcal{O}_1^{(2)}(n_0,n_0,n_0)$. Any contribution involving SCET$_1$ Lagrangian emission that matches to a higher-dimension operator in SCET$_2$ will necessarily have some partons in different SCET$_2$ directions, *e.g.* (n_0,n_0,n_1'). Since $C_1^{(2)}(n_0,n_0,n_0)\sim\lambda^0$, and the matching does not change this, $\mathcal{O}_2^{(2)}(n_0,n_0,n_0)$ contributes at N^{3}LO. The Wilson coefficients of the

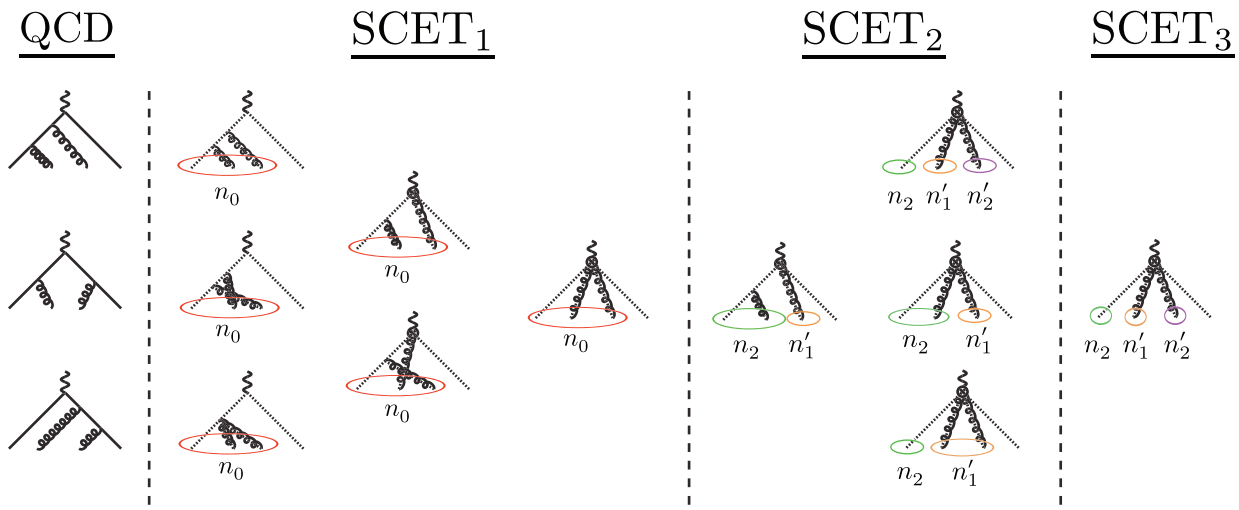

FIG. 19: Matching SCET$_1$ to SCET$_2$ to SCET$_3$ for two emissions to the two-jet configuration in SCET$_1$. We organize here by column number: (1) QCD Feynman diagrams; (2) SCET$_1$ diagrams from the operator $\mathcal{O}_1^{(0)}(n_0)$; (3) SCET$_1$ diagrams from the operators $\mathcal{O}_1^{(1)}(n_0,n_0)$ and $\mathcal{T}_1^{(1)}(n_0,n_0)$; (4) SCET$_1$ diagram from the operator $\mathcal{O}_1^{(2)}(n_0,n_0,n_0)$, this operator contributes only at N^{3}LO to the SCET$_2$ matching; (5) SCET$_2$ diagram from the operator $\mathcal{O}_1^{(1)}(n_2,n_1')$; (6) SCET$_2$ diagrams from the operators $\mathcal{O}_2^{(2)}(n_2,n_1',n_2')$, $\mathcal{O}_2^{(2)}(n_2,n_1',n_2)$ and $\mathcal{O}_2^{(2)}(n_2,n_1',n_1')$; (7) SCET$_3$ diagram from the operator $\mathcal{O}_3^{(2)}(n_1,n_1',n_2')$.

operators (D26) are defined such that

$$\begin{aligned} J^\mu_{\rm QCD} =& C^{(0)}_{1,\,\rm LO}(n_0)\mathcal{O}_1^{(0)} + C_1^{(1)}(n_0,n_0)\mathcal{O}_1^{(1)} + C^{(1)}_{1,\mathcal{T}}\mathcal{T}_1^{(1)} \\ &+ C_1^{(1)}(n_1,n_1')\mathcal{O}_1^{(1)} + \cdots \\ =& C_2^{(0)}(n_0)\mathcal{O}_2^{(0)} + C_1^{(1)}(n_0,n_0)\mathcal{O}_2^{(2)} + C^{(2)}_{2,\mathcal{T}}(n_0,n_0)\mathcal{T}_2^{(2)} \\ &+ C_2^{(1)}(n_1,n_1')\mathcal{O}_2^{(1)} + C_2^{(2)}(n_2,n_1',n_2)\mathcal{O}_2^{(2)} \\ &+ C_2^{(2)}(n_2,n_1',n_1')\mathcal{O}_2^{(2)} + C_2^{(2)}(n_2,n_1',n_2')\mathcal{O}_2^{(2)} + \cdots \end{aligned} \tag{D27}$$

where we have written the QCD current in terms of SCET$_1$ and SCET$_2$ operators. The ellipses indicate higher order terms.

We divide the subleading Wilson coefficients in two categories: jet-structure and hard-scattering, labeling their contributions with the superscripts J and H. As mentioned previously, the latter come from suppressed operators in the QCD $\to$ SCET$_1$ matching and depend on the details of the hard partons' creation. The former are subleading terms from the SCET$_1$ Lagrangian that correct Eq. (56) as we match to lower-scale theories. They are completely independent of the initial hard process.

We have seen in the previous section that the LO single gluon coefficient$\times$operator is $C_2^{(1)}(n_1,n_1')\mathcal{O}_2^{(1)} \sim \lambda^5$, Eq. (D7). We are interested in calculating the amplitude squared to NLO(λ). We therefore only need to calculate those NNLO(λ) contributions that can interfere with the LO amplitude. These operators are of the form $\mathcal{O}_2^{(2)}(n_2,n_2,n_1')$, as the others in Eq. (D26) are not strongly-ordered.[20]

We now calculate the coefficients in (D26), starting with $C_2^{(2)}(n_2,n_1',n_2')$, which we decompose as:

$$C_2^{(2)}(n_2,n_1',n_2') = C^{(2)J}_{2,\,\rm NLO}(n_2,n_1',n_2') + C_2^{(2)H}(n_2,n_1',n_2')\,, \tag{D28}$$

where

$$\begin{aligned} &C^{(2)J}_{2,\,\rm NLO}(n_2,n_1',n_2')\langle 0|\mathcal{O}_2^{(2)}|q_{n_2}g_{n_1'}g_{n_2'}\bar{q}_{\bar{n}}\rangle_2, = \\ &C^{(0)}_{1,\,\rm LO}(n_0)\int dx_1dx_2\langle 0|T\{\mathcal{L}_{\rm SCET_1}(x_1)\mathcal{L}_{\rm SCET_1}(x_2)\mathcal{O}_1^{(0)}(n_0,n_0)\}|q_{n_2}g_{n_1'}g_{n_2'}\bar{q}_{\bar{n}}\rangle_2 \end{aligned} \tag{D29}$$

[20] In principle, we also have $\mathcal{T}_2^{(2)}(n_2,n_2,n_1')$. However, the field content alone makes this λ^{10}, but all our correction operators have Wilson coefficients at $\mathcal{O}(\lambda^{-2})$, so its contribution is beyond NNLO(λ).

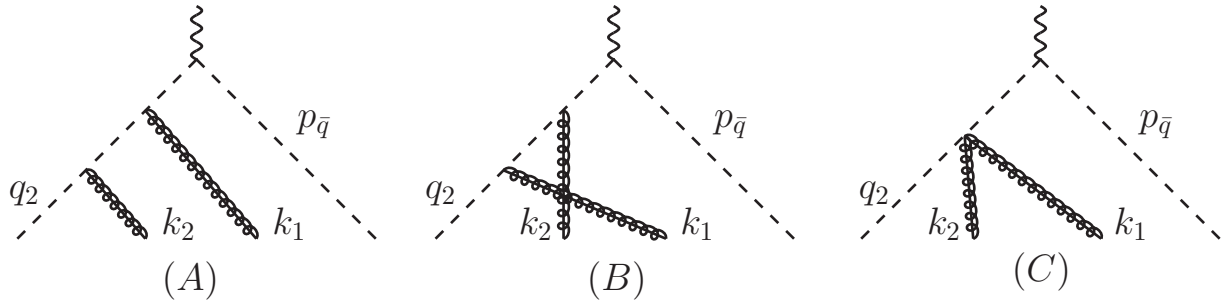

FIG. 20: Amplitudes for two emissions in SCET_1 from the operator $\mathcal{O}_1^{(0)}$.

and

$$\begin{aligned} &C_2^{(2)H}(n_2,n_1',n_2')\langle 0|\mathcal{O}_2^{(2)}|q_{n_2}g_{n_1'}g_{n_2'}\bar{q}_{\bar{n}}\rangle_2 = \\ &+C_1^{(1)}(n_0,n_0)\int dx\langle 0|T\{\mathcal{L}_{\mathrm{SCET}_1}(x)\mathcal{O}_1^{(1)}\}|q_{n_2}g_{n_1'}g_{n_2'}\bar{q}_{\bar{n}}\rangle_2 \\ &+C_{1,\mathcal{T}}^{(1)}(n_0,n_0)\int dx\langle 0|T\{\mathcal{L}_{\mathrm{SCET}_1}(x)\mathcal{T}_1^{(1)}\}|q_{n_2}g_{n_1'}g_{n_2'}\bar{q}_{\bar{n}}\rangle_2 \\ &+C_1^{(1)}(n_1,n_1')\int dx\langle 0|T\{\mathcal{L}_{\mathrm{SCET}_1}(x)\mathcal{O}_1^{(1)}\}|q_{n_2}g_{n_1'}g_{n_2'}\bar{q}_{\bar{n}}\rangle_2\,. \end{aligned} \tag{D30}$$

We decompose $C_2^{(2)H}(n_2,n_1',n_2')$ as

$$C_2^{(2)H}(n_2,n_1',n_2') = C_{2,\,\mathrm{NNLO}}^{(2)H,\,a}(n_2,n_1',n_2') + C_{2,\,\mathrm{N^3LO}}^{(2)H}(n_2,n_1',n_2') + C_{2,\,\mathrm{NNLO}}^{(2)H,\,b}(n_2,n_1',n_2')\,, \tag{D31}$$

where $C_{2,\,\mathrm{NNLO}}^{(2)H,\,a}(n_2,n_1',n_2')$ is the coefficient that reproduces the the second line in Eq. (D30), *etc.*

Since $\mathcal{O}_2^{(2)}(n_2,n_1',n_2')$ does not interfere with the LO operator, we only need the coefficient, $C_{2,\,\mathrm{NLO}}^{(2)J}(n_2,n_1',n_2')$. We also calculate $C_{2,\,\mathrm{NNLO}}^{(2)H,\,a}(n_2,n_1',n_2')$ though, because it will be useful later. We prove below that these coefficients and their corresponding operators are of order λ^6 and λ^7, respectively (in Eq. D7, we show that LO is at λ^5). $C_{2,\,\mathrm{NLO}}^{(2)J}(n_2,n_1',n_2')$ and $C_{2,\,\mathrm{NNLO}}^{(2)H,\,a}(n_2,n_1',n_2')$ come from two-jet operators in SCET_1. Thus, they both contain factors of $\Theta_{\delta_2}[n_2\cdot n_1']\Theta_{\delta_2}[n_2\cdot n_2']\Theta_{\delta_2}[n_2'\cdot n_1']$. We first described these phase space cutoffs in Sec. III A, and made use of them in previous section on single-gluon matching. The subscript, δ_2, constrains the argument to be $\lesssim \lambda/\eta^4$.

To calculate the coefficients, we proceed as with one-gluon emission: on the LHS of Eqs. (D29) and (D30) we calculate the SCET_1 amplitude and rotate it along the directions n_2, n_1', n_2' where the quark and the two gluons are aligned using the finite RPI_1 described in App.(B); on the RHS we write the SCET_2 amplitude and calculate the Wilson coefficient necessary for the matching. We decompose the SCET_1 amplitude:

$$A_{\mathrm{NLO}}^{q\bar{q}gg} = C_1^{(0)}(n_0)\int dx_1dx_2\langle 0|T\{\mathcal{L}_{\mathrm{SCET}_1}(x_1)\mathcal{L}_{\mathrm{SCET}_1}(x_2)\mathcal{O}_1^{(0)}\}|q_{n_2}g_{n_1'}g_{n_2'}\bar{q}_{\bar{n}}\rangle_2\,, \tag{D32}$$

in

$$A_{\mathrm{NLO}}^{q\bar{q}gg} = A_{\mathrm{NLO},\,A}^{q\bar{q}gg} + A_{\mathrm{NLO},\,B}^{q\bar{q}gg} + A_{\mathrm{NLO},\,C}^{q\bar{q}gg}\,, \tag{D33}$$

where A, B, C correspond to the three graphs in Fig. 20. Using the SCET_1 Feynman rules, we have:

$$
\begin{aligned}
A^{q\bar{q}gg}_{\mathrm{NLO},\,A} &= U^{(2,0,0)}(n_0;\,Q,\mu_1)\,g^2\,\bar{u}_{n_0}\Big[n_0^\beta+\gamma^\beta_{n_0\perp}\frac{(\not{q}_1)_{n_0\perp}}{\bar{q}_1}+\frac{(\not{q}_2)_{n_0\perp}}{\bar{q}_2}\gamma^\beta_{n_0\perp}\Big] \\
&\quad\times\Big[n_0^\alpha+\frac{(\not{q}_1)_{n_0\perp}}{\bar{q}_1}\gamma^\alpha_{n_0\perp}\Big]\frac{\bar{q}_1}{q_1^2}\frac{\bar{q}_0}{q_0^2}\gamma^\mu_{n_0\perp}v_{\bar{n}}\,, \\
A^{q\bar{q}gg}_{\mathrm{NLO},\,B} &= U^{(2,0,0)}(n_0;\,Q,\mu_1)\,g^2\,\bar{u}_{n_0}\Big[n_0^\alpha+\gamma^\alpha_{n_0\perp}\frac{(\not{q}_2+\not{k}_1)_{n_0\perp}}{\bar{q}_2+\bar{k}_1}+\frac{(\not{q}_2)_{n_0\perp}}{\bar{q}_2}\gamma^\alpha_{n_0\perp}\Big] \\
&\quad\times\Big[n_0^\beta+\frac{(\not{q}_2+\not{k}_1)_{n_0\perp}}{\bar{q}_2+\bar{k}_1}\gamma^\beta_{n_0\perp}\Big]\frac{\bar{q}_2+\bar{k}_1}{(q_2+k_1)^2}\frac{\bar{q}_0}{q_0^2}\gamma^\mu_{n_0\perp}v_{\bar{n}}\,, \\
A^{q\bar{q}gg}_{\mathrm{NLO},\,C} &= U^{(2,0,0)}(n_0;\,Q,\mu_1)\,g^2\,\bar{u}_{n_0}\Big[\frac{1}{\bar{q}_2+\bar{k}_1}\gamma^\alpha_{n_0\perp}\gamma^\beta_{n_0\perp}+\frac{1}{\bar{q}_2+\bar{k}_2}\gamma^\beta_{n_0\perp}\gamma^\alpha_{n_0\perp}\Big]\frac{\bar{q}_0}{q_0^2}\gamma^\mu_{n_0\perp}v_{\bar{n}}\,,
\end{aligned}
\tag{D34}
$$

where $q_1 = q_2 + k_2$ and $q_0 = q_2 + k_1 + k_2$. As before, we do not write terms with $\bar{n}^\alpha$ and $\bar{n}^\beta$, as they are not necessary for the matching because the operator $\bar{n}\cdot A_n$ is constrained by gauge invariance to be only in Wilson lines. Now we rotate the amplitude (D34) to the directions n_2 and n_1' and n_2' parallel to the quark and the two gluons, as described in Eq. (B14)

$$
\begin{aligned}
A^{q\bar{q}gg}_{\mathrm{NLO},\,A} &= U^{(2,0,0)}(n_0;\,Q,\mu_1)\,g^2\,\bar{u}_{n_2}\Big[\frac{\bar{q}_2}{\bar{q}_1}\sqrt{n_2\cdot n_2'}\,v_2^\beta+\frac{\bar{k}_2}{\bar{q}_1}\sqrt{n_2\cdot n_2'}\,\frac{\not{v}_2}{2}\gamma^\beta_{n_2'\perp}\Big] \\
&\quad\times\Big[\frac{\bar{q}_1}{\bar{q}_0}\sqrt{n_1\cdot n_1'}\,v_1^\alpha+\frac{\bar{k}_1}{\bar{q}_0}\sqrt{n_1\cdot n_1'}\,\frac{\not{v}_1}{2}\gamma^\alpha_{n_1'\perp}\Big]\frac{\bar{q}_1}{q_1^2}\frac{\bar{q}_0}{q_0^2}\,\gamma^\mu_{n_0\perp}v_{\bar{n}}\,, \\
A^{q\bar{q}gg}_{\mathrm{NLO},\,B} &= U^{(2,0,0)}(n_0;\,Q,\mu_1)\,g^2\,\bar{u}_{n_2}\Big[\frac{\bar{q}_1}{\bar{q}_0}\sqrt{n_1\cdot n_1'}\,v_1^\alpha+\frac{\bar{k}_2}{\bar{q}_1}\sqrt{n_2\cdot n_2'}\,\frac{\not{v}_2}{2}\gamma^\alpha_{n_1'\perp} \\
&\quad+\frac{\bar{k}_1}{\bar{q}_0}\sqrt{n_1\cdot n_1'}\frac{\not{v}_1}{2}\gamma^\alpha_{n_1'\perp}+\frac{\bar{q}_2\,\bar{k}_2}{\bar{q}_1(\bar{q}_2+\bar{k}_1)}\sqrt{n_2\cdot n_2'}\,\gamma^\alpha_{n_1'\perp}\frac{\not{v}_2}{2} \\
&\quad-\frac{\bar{k}_1\bar{k}_2}{\bar{q}_0(\bar{q}_2+\bar{k}_1)}\sqrt{n_1\cdot n_1'}\,\gamma^\alpha_{n_1'\perp}\frac{\not{v}_1}{2}\Big]\Big[\frac{\bar{q}_2}{\bar{q}_1}\sqrt{n_2\cdot n_2'}\,v_2^\beta-\frac{\bar{k}_1}{\bar{q}_0}\sqrt{n_1\cdot n_1'}\,v_1^\beta \\
&\quad+\frac{\bar{q}_2\,\bar{k}_2}{(\bar{q}_2+\bar{k}_1)\bar{q}_1}\sqrt{n_2\cdot n_2'}\frac{\not{v}_2}{2}\gamma^\beta_{n_2'\perp}-\frac{\bar{k}_2\,\bar{k}_1}{(\bar{q}_2+\bar{k}_1)\bar{q}_0}\sqrt{n_1\cdot n_1'}\,\frac{\not{v}_1}{2}\gamma^\beta_{n_2'\perp}\Big]\frac{\bar{q}_2+\bar{k}_1}{(q_2+k_1)^2}\frac{\bar{q}_0}{q_0^2}\gamma^\mu_{n_0\perp}v_{\bar{n}}\,, \\
A^{q\bar{q}gg}_{\mathrm{NLO},\,C} &= U^{(2,0,0)}(n_0;\,Q,\mu_1)\,g^2\,\bar{u}_{n_2}\Big[\frac{1}{\bar{q}_2+\bar{k}_1}\gamma^\alpha_{n_1'\perp}\gamma^\beta_{n_2'\perp}+\frac{1}{\bar{q}_2+\bar{k}_2}\gamma^\beta_{n_2'\perp}\gamma^\alpha_{n_1'\perp}\Big]\frac{\bar{q}_0}{q_0^2}\,\gamma^\mu_{n_0\perp}v_{\bar{n}}\,,
\end{aligned}
\tag{D35}
$$

and $n_1\cdot n_1'$ is defined in terms of n_2, n_1' and n_2' in Eqs. (B18),

The vectors v_1 and v_2 are defined in Eqs. (B12), (B17) and (B18). The values of q_0^2, q_1^2 and $(q_1+k_2)^2$ are given in Eqs. (B19) and (B20). As with the one-gluon emission, we can neglect the terms with $n_1'^\alpha$ and $n_2'^\beta$ as they are orthogonal to the $\mathcal{B}^\alpha_{n_1'\perp}$ and $\mathcal{B}^\beta_{n_2'\perp}$ fields. The SCET_2 amplitude for $\langle 0|\mathcal{O}_2^{(2)}(n_2,n_1',n_2')|q_{n_2}g_{n_1'}g_{n_2'}\bar{q}_{\bar{n}}\rangle$ is:

$$
\langle 0|\bar{\chi}_{n_2}g\mathcal{B}^\alpha_{n_2'\perp}g\mathcal{B}^\beta_{n_1'\perp}\chi_{\bar{n}}|q_{n_2}g_{n_1'}g_{n_2'}\bar{q}_{\bar{n}}\rangle = g^2\bar{u}_{n_2}\epsilon^\alpha_{n_1'\perp}\epsilon^\beta_{n_2'\perp}v_{\bar{n}}\,. \tag{D36}
$$

In Eq. (D36) we have explicitly written the polarization vectors of the external gluons. For the jet-structure corrections, we get:

$$
C^{(2)J}_{2,\,\mathrm{NLO}}(n_2,n_1',n_2') = U^{(2,0,0)}(n_0;\,Q,\mu_1)\,d_1^{J\,\alpha\beta}(n_2,n_1',n_2')\Theta_{\delta_2}[n_2\cdot n_1']\Theta_{\delta_2}[n_2\cdot n_2']\Theta_{\delta_2}[n_2'\cdot n_1']\,, \tag{D37}
$$

where

$$
d_1^{J\,\alpha\beta}(n_2,n_1',n_2') = d_{1,A}^{J\,\alpha\beta}(n_2,n_1',n_2')+d_{1,B}^{J\,\alpha\beta}(n_2,n_1',n_2')+d_{1,C}^{J\,\alpha\beta}(n_2,n_1',n_2')\,, \tag{D38}
$$

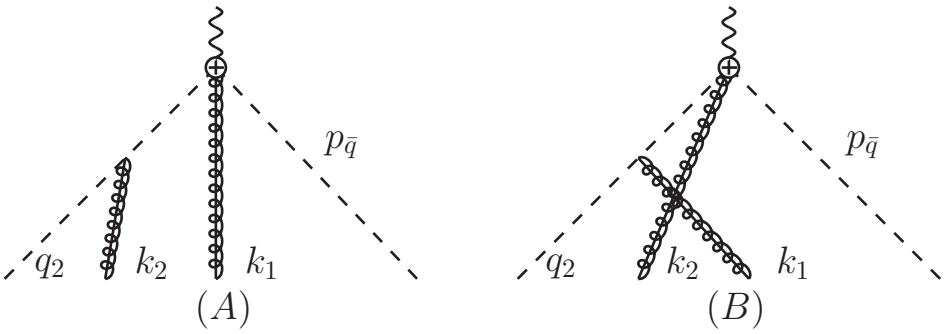

FIG. 21: Amplitudes for two emissions in SCET_1 from the operator $\mathcal{O}_1^{(1)}$.

with

$$
\begin{aligned}
d_{1,A}^{J\,\alpha\beta}(n_2,n_1',n_2') &= \Big[\frac{\bar{q}_2}{\bar{q}_1}\sqrt{n_2\cdot n_2'}\,v_2^\beta + \frac{\bar{k}_2}{\bar{q}_1}\sqrt{n_2\cdot n_2'}\,\frac{\not{n}_2}{2}\gamma^\beta_{n_2'\perp}\Big] \\
&\quad\times\Big[\frac{\bar{q}_1}{\bar{q}_0}\sqrt{n_1\cdot n_1'}\,v_1^\alpha + \frac{\bar{k}_1}{\bar{q}_0}\sqrt{n_1\cdot n_1'}\,\frac{\not{n}_1}{2}\gamma^\alpha_{n_1'\perp}\Big]\frac{\bar{q}_1}{q_1^2}\frac{\bar{q}_0}{q_0^2}\,\gamma^\mu_{n_0\perp}\,, \\
d_{1,B}^{J\,\alpha\beta}(n_2,n_1',n_2') &= \Big[\frac{\bar{q}_1}{\bar{q}_0}\sqrt{n_1\cdot n_1'}\,v_1^\alpha + \frac{\bar{k}_2}{\bar{q}_1}\sqrt{n_2\cdot n_2'}\,\frac{\not{n}_2}{2}\gamma^\alpha_{n_1'\perp} \\
&\quad+\frac{\bar{k}_1}{\bar{q}_0}\sqrt{n_1\cdot n_1'}\frac{\not{n}_1}{2}\gamma^\alpha_{n_1'\perp} + \frac{\bar{q}_2\,\bar{k}_2}{\bar{q}_1(\bar{q}_2+\bar{k}_1)}\sqrt{n_2\cdot n_2'}\,\gamma^\alpha_{n_1'\perp}\frac{\not{n}_2}{2} \\
&\quad-\frac{\bar{k}_1\bar{k}_2}{\bar{q}_0(\bar{q}_2+\bar{k}_1)}\sqrt{n_1\cdot n_1'}\,\gamma^\alpha_{n_1'\perp}\frac{\not{n}_1}{2}\Big] \\
&\quad\times\Big[\frac{\bar{q}_2}{\bar{q}_1}\sqrt{n_2\cdot n_2'}\,v_2^\beta - \frac{\bar{k}_1}{\bar{q}_0}\sqrt{n_1\cdot n_1'}\,v_1^\beta \\
&\quad+\frac{\bar{q}_2\,\bar{k}_2}{(\bar{q}_2+\bar{k}_1)\bar{q}_1}\sqrt{n_2\cdot n_2'}\frac{\not{n}_2}{2}\gamma^\beta_{n_2'\perp} - \frac{\bar{k}_2\,\bar{k}_1}{(\bar{q}_2+\bar{k}_1)\bar{q}_0}\sqrt{n_1\cdot n_1'}\,\frac{\not{n}_1}{2}\gamma^\beta_{n_2'\perp}\Big] \\
&\quad\times\frac{\bar{q}_2+\bar{k}_1}{(q_2+k_1)^2}\frac{\bar{q}_0}{q_0^2}\gamma^\mu_{n_0\perp}\,, \\
d_{1,C}^{J\,\alpha\beta}(n_2,n_1',n_2') &= \Big[\frac{1}{\bar{q}_2+\bar{k}_1}\gamma^\alpha_{n_1'\perp}\gamma^\beta_{n_2'\perp} + \frac{1}{\bar{q}_2+\bar{k}_2}\gamma^\beta_{n_2'\perp}\gamma^\alpha_{n_1'\perp}\Big]\frac{\bar{q}_0}{q_0^2}\,\gamma^\mu_{n_0\perp}\,.
\end{aligned}
\tag{D39}
$$

$$
\tag{D40}
$$

The Θ functions in Eq. (D37) show that $C^{(2)J}_{2,\,\mathrm{NLO}}(n_2,n_1',n_2')$ comes from the two-jet SCET_1 operators. To examine the power counting of $C^{(2)J}_{2,\,\mathrm{NLO}}(n_2,n_1',n_2')$, we have to consider that this coefficient comes from matching SCET_1 to SCET_2 in the region where $n_2\cdot n_1'\sim n_2\cdot n_2'\sim n_1'\cdot n_2'\sim\lambda^2/\eta^4$, thus we have

$$
C^{(2)J}_{2,\,\mathrm{NLO}}(n_2,n_1',n_2')\sim\lambda^{-2}\,, \tag{D41}
$$

and since this multiplies $\mathcal{O}_2^{(2)}\sim\lambda^8$, by comparison with Eq. (D7) we see that we get an NLO(λ) contribution.

We proceed similarly to calculate the coefficient $C^{(2),H,\,a}_{2,\,\mathrm{NNLO}}(n_2,n_1',n_2')$ and show that it is $\mathcal{O}(\lambda^{-1})$. We decompose the SCET_1 amplitude:

$$
A^{q\bar{q}gg}_{\mathrm{NNLO}} = C^{(1)}_{1,\,\mathrm{NLO}}(n_0,n_0)\int dx\langle 0|T\{\mathcal{L}_{\mathrm{SCET}_1}(x)\mathcal{O}_1^{(1)}\}|q_{n_2}g_{n_1'}g_{n_2'}\bar{q}_{\bar{n}}\rangle_2\,,
$$

in

$$
A^{q\bar{q}gg}_{\mathrm{NNLO}} = A^{q\bar{q}gg}_{\mathrm{NNLO},\,A} + A^{q\bar{q}gg}_{\mathrm{NNLO},\,B}\,, \tag{D42}
$$

where A, B correspond to the two graphs in Fig. 21. We have:

$$
\begin{aligned}
A^{q\bar{q}gg}_{\mathrm{NNLO},\,A} &= -U^{(2,1,0)}(n_0,n_0;\,Q,\mu_1)\,g^2\,\bar{u}_{n_2}\Big[\frac{\bar{q}_2}{\bar{q}_1}\sqrt{n_2\cdot n_2'}\,v_2^\beta \\
&\quad+\frac{\bar{k}_2}{\bar{q}_1}\sqrt{n_2\cdot n_2'}\,\frac{\not{v}_2}{2}\gamma^\beta_{n_2'\perp}\Big]\gamma^\alpha_{n_1'\perp}\frac{\bar{q}_1}{q_1^2}\,\frac{n_0^\mu-\bar{n}^\mu}{Q}v_{\bar{n}}\,, \\
A^{q\bar{q}gg}_{\mathrm{NNLO},\,B} &= -U^{(2,1,0)}(n_0,n_0;\,Q,\mu_1)\,g^2\,\bar{u}_{n_2}\Big[\frac{\bar{q}_1}{\bar{q}_0}\sqrt{n_1\cdot n_1'}\,v_1^\alpha+\frac{\bar{k}_2}{\bar{q}_1}\sqrt{n_2\cdot n_2'}\,\frac{\not{v}_2}{2}\gamma^\alpha_{n_1'\perp} \\
&\quad+\frac{\bar{k}_1}{\bar{q}_0}\sqrt{n_1\cdot n_1'}\frac{\not{v}_1}{2}\gamma^\alpha_{n_1'\perp}+\frac{\bar{q}_2\,\bar{k}_2}{\bar{q}_1(\bar{q}_2+\bar{k}_1)}\sqrt{n_2\cdot n_2'}\,\gamma^\alpha_{n_1'\perp}\frac{\not{v}_2}{2} \\
&\quad-\frac{\bar{k}_1\bar{k}_2}{\bar{q}_0(\bar{q}_2+\bar{k}_1)}\sqrt{n_1\cdot n_1'}\,\gamma^\alpha_{n_1'\perp}\frac{\not{v}_1}{2}\Big]\gamma^\beta_{n_1'\perp}\frac{\bar{q}_1}{q_1^2}\,\frac{n_0^\mu-\bar{n}^\mu}{Q}v_{\bar{n}}\,,
\end{aligned}
\tag{D43}
$$

where in Eq. (D43) we have already rotated the amplitude to the directions n_2, n_1' and n_2'. From Eqs. (D36) and (D43) we can see that the Wilson coefficient $C^{(2)H,\,a}_{2,\,\mathrm{NNLO}}(n_2,n_1',n_2')$ is

$$
\begin{aligned}
C^{(2)H,\,a}_{2,\,\mathrm{NNLO}}(n_2,n_1',n_2') =& U^{(2,1,0)}(n_0,n_0;\,Q,\mu_1)d_1^{H\,\alpha\beta}(n_2,n_1',n_2') \\
&\times\Theta_{\delta_2}[n_2\cdot n_1']\Theta_{\delta_2}[n_2\cdot n_2']\Theta_{\delta_2}[n_2'\cdot n_1']\,,
\end{aligned}
\tag{D44}
$$

where

$$
d_1^{H\,\alpha\beta}(n_2,n_1',n_2') = d_{1,A}^{H\,\alpha\beta}(n_2,n_1',n_2')+d_{1,B}^{H\,\alpha\beta}(n_2,n_1',n_2')
\tag{D45}
$$

with

$$
\begin{aligned}
d_{1,A}^{H\,\alpha\beta}(n_2,n_1',n_2') &= \Big[\frac{\bar{q}_2}{\bar{q}_2+\bar{k}_2}\sqrt{n_2\cdot n_2'}\,v_2^\beta \\
&\quad+\frac{\bar{k}_2}{\bar{q}_2+\bar{k}_2}\sqrt{n_2\cdot n_2'}\,\frac{\not{v}_2}{2}\gamma^\beta_{n_2'\perp}\Big]\gamma^\alpha_{n_1'\perp}\frac{\bar{q}_1}{q_1^2}\,\frac{n_0^\mu-\bar{n}^\mu}{Q}\,, \\
d_{1,B}^{H\,\alpha\beta}(n_2,n_1',n_2') &= \Big[\frac{\bar{q}_1}{\bar{q}_0}\sqrt{n_1\cdot n_1'}\,v_1^\alpha+\frac{\bar{k}_2}{\bar{q}_1}\sqrt{n_2\cdot n_2'}\,\frac{\not{v}_2}{2}\gamma^\alpha_{n_1'\perp} \\
&\quad+\frac{\bar{k}_1}{\bar{q}_0}\sqrt{n_1\cdot n_1'}\frac{\not{v}_1}{2}\gamma^\alpha_{n_1'\perp}+\frac{\bar{q}_2\,\bar{k}_2}{\bar{q}_1(\bar{q}_2+\bar{k}_1)}\sqrt{n_2\cdot n_2'}\,\gamma^\alpha_{n_1'\perp}\frac{\not{v}_2}{2} \\
&\quad-\frac{\bar{k}_1\bar{k}_2}{\bar{q}_0(\bar{q}_2+\bar{k}_1)}\sqrt{n_1\cdot n_1'}\,\gamma^\alpha_{n_1'\perp}\frac{\not{v}_1}{2}\Big]\gamma^\beta_{n_1'\perp}\frac{\bar{q}_1}{q_1^2}\,\frac{n_0^\mu-\bar{n}^\mu}{Q}\,.
\end{aligned}
\tag{D46}
$$

To get the power counting of $C^{(2)H,\,a}_{2,\,\mathrm{NNLO}}(n_2,n_1',n_2')$, as in the previous case, we have to consider that the matching is done in a region where $n_2\cdot n_1'\sim n_2\cdot n_2'\sim n_1'\cdot n_2'\sim\lambda^2/\eta^4$. This implies:

$$
C^{(2)H,\,a}_{2,\,\mathrm{NNLO}}(n_2,n_1',n_2')\sim\lambda^{-1}\,,
\tag{D47}
$$

which justifies its labeling as NNLO(λ).

We now turn to calculate the coefficient $C_2^{(2)}(n_1,n_1',n_1')$. We will proceed as above. We decompose $C_2^{(2)}(n_1,n_1',n_1')$ as:

$$
C_2^{(2)}(n_2,n_1',n_1') = C^{(2)J}_{2,\,\mathrm{NLO}}(n_2,n_1',n_1')+C_2^{(2)H}(n_2,n_1',n_1')\,,
\tag{D48}
$$

where

$$
\begin{aligned}
&C^{(2)J}_{2,\,\mathrm{NLO}}(n_2,n_1',n_1')\langle 0|\mathcal{O}_2^{(2)}(n_2,n_1',n_1')|q_{n_2}g_{n_1'}g_{n_1'}\bar{q}_{\bar{n}}\rangle_2 \\
&=C^{(0)}_{1,\,\mathrm{LO}}(n_0)\int dx_1dx_2\langle 0|T\{\mathcal{L}_{\mathrm{SCET}_1}(x_1)\mathcal{L}_{\mathrm{SCET}_1}(x_2)\mathcal{O}_1^{(0)}(n_0)\}|q_{n_2}g_{n_1'}g_{n_1'}\bar{q}_{\bar{n}}\rangle_2\,,
\end{aligned}
\tag{D49}
$$

and

$$
\begin{aligned}
&C_2^{(2)H}(n_2,n_1',n_1')\langle 0|\mathcal{O}_2^{(2)}|q_{n_2}g_{n_1'}g_{n_1'}\bar{q}_{\bar{n}}\rangle_2 \\
&=C^{(1)}_{1,\,\mathrm{NLO}}(n_0,n_0)\int dx\langle 0|T\{\mathcal{L}_{\mathrm{SCET}_1}(x)\mathcal{O}_1^{(1)}\}|q_{n_2}g_{n_1'}g_{n_1'}\bar{q}_{\bar{n}}\rangle_2 \\
&+C^{(1)}_{1,\mathcal{T}}(n_0,n_0)\int dx\langle 0|T\{\mathcal{L}_{\mathrm{SCET}_1}(x)\mathcal{T}_1^{(1)}\}|q_{n_2}g_{n_1'}g_{n_1'}\bar{q}_{\bar{n}}\rangle_2\,.
\end{aligned}
\tag{D50}
$$

We further set:

$$C_2^{(2)H}(n_2,n_1',n_1') = C_{2,\,\mathrm{NNLO}}^{(2)H}(n_2,n_1',n_1') + C_{2,\,\mathrm{N^3LO}}^{(2)H}(n_2,n_1',n_1')\,, \tag{D51}$$

where $C_{2,\,\mathrm{NLO}}^{(2)H}(n_2,n_1',n_1')$ is the coefficient of the contribution that reproduces the second line in Eq. (D50), *etc.* We will only calculate $C_{2,\,\mathrm{NLO}}^{(2)J}(n_2,n_1',n_1')$ and show that it scales as λ^{-2}. This is the only operator of this form that we need to calculate the amplitude squared at NLO(λ).

To calculate the amplitude on the RHS of Eq. (D49), we can use Eqs. (D35), which are written in terms of n_2, n_1' and n_2' that are parallel to the external particles, and take the limit $n_2'\cdot n_1' \to \lambda^4/\eta^4$. In this case the two gluons are collinear in SCET$_2$. Thus, we can define $C_{2,\,\mathrm{NLO}}^{(2)J}(n_2,n_1',n_1')$ as

$$C_{2,\,\mathrm{NLO}}^{(2)J}(n_2,n_1',n_1') = U^{(2,0,0)}(n_0;\,Q,\mu_1)\, d_2^{J\,\alpha\beta}(n_2,n_1',n_1')\,\Theta_{\delta_2}[n_2\cdot n_1']\,, \tag{D52}$$

where

$$\begin{aligned}
d_2^{J\,\alpha\beta}(n_2,n_1',n_1') &= \lim_{n_2'\cdot n_1'\to\lambda^4/\eta^4} d_1^{\alpha\beta}(n_2,n_1',n_2') \qquad\qquad (\mathrm{D53})\\
&= \Bigg(\Big[\frac{\bar q_2}{\bar q_1}\sqrt{n_2\cdot n_2'}\,v_2^\beta + \frac{\bar k_2}{\bar q_1}\sqrt{n_2\cdot n_2'}\,\frac{\bar{\not n}_2}{2}\gamma_{n_2'\perp}^\beta\Big] \\
&\times \Big[\frac{\bar q_1}{\bar q_0}\sqrt{n_1\cdot n_1'}\,v_1^\alpha + \frac{\bar k_1}{\bar q_0}\sqrt{n_1\cdot n_1'}\,\frac{\bar{\not n}_1}{2}\gamma_{n_1'\perp}^\alpha\Big]\frac{\bar q_1}{q_1^2}\frac{2\bar q_0}{\bar q_2\,\bar k_1(n_2\cdot n_1') + \bar q_2\,\bar k_2(n_2\cdot n_2')} \\
&+ \Big[\frac{\bar q_1}{\bar q_0}\sqrt{n_1\cdot n_1'}\,v_1^\alpha + \frac{\bar k_2}{\bar q_1}\sqrt{n_2\cdot n_2'}\,\frac{\bar{\not n}_2}{2}\gamma_{n_1'\perp}^\alpha \\
&+ \frac{\bar k_1}{\bar q_0}\sqrt{n_1\cdot n_1'}\frac{\bar{\not n}_1}{2}\gamma_{n_1'\perp}^\alpha + \frac{\bar q_2\,\bar k_2}{\bar q_1(\bar q_2+\bar k_1)}\sqrt{n_2\cdot n_2'}\,\gamma_{n_1'\perp}^\alpha\frac{\bar{\not n}_2}{2} \\
&- \frac{\bar k_1\bar k_2}{\bar q_0(\bar q_2+\bar k_1)}\sqrt{n_1\cdot n_1'}\,\gamma_{n_1'\perp}^\alpha\frac{\bar{\not n}_1}{2}\Big]\times\Big[\frac{\bar q_2}{\bar q_1}\sqrt{n_2\cdot n_2'}\,v_2^\beta - \frac{\bar k_1}{\bar q_0}\sqrt{n_1\cdot n_1'}\,v_1^\beta \\
&+ \frac{\bar q_2\,\bar k_2}{(\bar q_2+\bar k_1)\bar q_1}\sqrt{n_2\cdot n_2'}\frac{\bar{\not n}_2}{2}\gamma_{n_2'\perp}^\beta - \frac{\bar k_2\,\bar k_1}{(\bar q_2+\bar k_1)\bar q_0}\sqrt{n_1\cdot n_1'}\,\frac{\bar{\not n}_1}{2}\gamma_{n_2'\perp}^\beta\Big] \\
&\times \frac{\bar q_2+\bar k_1}{(q_2+k_1)^2}\frac{2\bar q_0}{\bar q_2\,\bar k_1(n_2\cdot n_1') + \bar q_2\,\bar k_2(n_2\cdot n_2')} \\
&+ \Big[\frac{1}{\bar q_2+\bar k_1}\gamma_{n_1'\perp}^\alpha\gamma_{n_2'\perp}^\beta + \frac{1}{\bar q_2+\bar k_2}\gamma_{n_2'\perp}^\beta\gamma_{n_1'\perp}^\alpha\Big]\frac{\bar q_0}{\bar q_2\,\bar k_1(n_2\cdot n_1') + \bar q_2\,\bar k_2(n_2\cdot n_2')}\Bigg) \\
&\times \gamma_{n_0\perp}^\mu\Big|_{n_1'=n_2'}\,.
\end{aligned}$$

In Eqs. (D53) there is a difference in the notation between the LHS and RHS. On the LHS, we have labeled the quark with n_2 and the two gluons with n_1' because the coefficient (D52) is for the operator $\mathcal{O}_2^{(2)}(n_2,n_1',n_1')$, where the gluons are collinear. On the RHS, n_2, n_1' and n_2' are the directions parallel to the quarks and the two gluons as defined in Eqs. (B10) and (B15). We encode that the two gluons are collinear using the Θ function on the RHS of Eq. (D53) with $\delta_3 = \lambda^3/\eta^4$. It restricts that $n_1'\cdot n_2' \lesssim \lambda^4/\eta^4$. On the RHS of Eq. (D53) we could decompose n_2' in terms of n_1' and avoid inserting the Θ, but it is convenient to leave n_2' explicit because it will make the matching easier to SCET$_3$. We notice that the RHS of Eq. (D53) is just equal to the coefficient $C_{2,\,\mathrm{NLO}}^{(2)J}(n_2,n_1',n_2')$ defined in Eq. (D37) with the substitution $q_0^2 \to \bar q_2\bar k_1(n_2\cdot n_1')/4 + \bar q_2\bar k_2(n_2\cdot n_2')/4$. Knowing that $n_1'\cdot n_2' \sim \lambda^4/\eta^4$, $n_1\cdot n_2' \sim \lambda^2/\eta^4$ and $n_1\cdot n_1' \sim \lambda^2/\eta^4$, it is easy to check that Eq. (D53) scales as λ^{-2}. The information that $C_{2,\,\mathrm{LO}}^{(2)J}(n_2,n_1',n_1')$ comes from a two-jet SCET$_1$ operator, is encoded in the Θ-functions of Eq. (D52).

For the coefficient $C_2^{(2)}(n_2,n_1',n_2)$, we decompose it as:

$$C_2^{(2)}(n_2,n_1',n_2) = C_{2,\,\mathrm{NLO}}^{(2)J}(n_2,n_1',n_2) + C_2^{(2)H}(n_2,n_1',n_2)\,, \tag{D54}$$

where

$$
\begin{aligned}
&C_{2,\,\mathrm{NLO}}^{(2)J}(n_2,n_1',n_2)\langle 0|\mathcal{O}_2^{(2)}|q_{n_2}g_{n_1'}g_{n_2}\bar{q}_{\bar{n}}\rangle_2 \\
&= C_{1,\,\mathrm{LO}}^{(0)}(n_0)\int dx_1dx_2\langle 0|T\{\mathcal{L}_{\mathrm{SCET}_1}(x_1)\mathcal{L}_{\mathrm{SCET}_1}(x_2)\mathcal{O}_1^{(0)}\}|q_{n_2}g_{n_1'}g_{n_2}\bar{q}_{\bar{n}}\rangle_2 \\
&- C_{2,\mathrm{LO}}^{(1)}(n_1,n_1')\int dx\langle 0|T\{\mathcal{L}_{\mathrm{SCET}_2}(x)\mathcal{O}_2^{(1)}\}|q_{n_2}g_{n_1'}g_{n_2}\bar{q}_{\bar{n}}\rangle_2\,,
\end{aligned}
\tag{D55}
$$

and

$$
\begin{aligned}
&C_2^{(2)H}(n_2,n_1',n_2)\langle 0|\mathcal{O}_2^{(2)}|q_{n_2}g_{n_1'}g_{n_2}\bar{q}_{\bar{n}}\rangle_2 \\
&= C_{1,\,\mathrm{NLO}}^{(1)}(n_0,n_0)\int dx\langle 0|T\{\mathcal{L}_{\mathrm{SCET}_1}(x)\mathcal{O}_1^{(1)}\}|q_{n_2}g_{n_1'}g_{n_2}\bar{q}_{\bar{n}}\rangle_2 \\
&- C_{2,\mathrm{NLO}}^{(1)}(n_2,n_1')\int dx\langle 0|T\{\mathcal{L}_{\mathrm{SCET}_2}(x)\mathcal{O}_2^{(1)}\}|q_{n_2}g_{n_1'}g_{n_2}\bar{q}_{\bar{n}}\rangle_2 \\
&+ C_{1,\mathcal{T}}^{(1)}(n_0,n_0)\int dx\langle 0|T\{\mathcal{L}_{\mathrm{SCET}_1}(x)\mathcal{T}_1^{(1)}\}|q_{n_2}g_{n_1'}g_{n_2}\bar{q}_{\bar{n}}\rangle_2 \\
&- C_{2,\mathrm{NNLO}}^{(1)}(n_2,n_1')\int dx\langle 0|T\{\mathcal{L}_{\mathrm{SCET}_2}(x)\mathcal{O}_2^{(1)}\}|q_{n_2}g_{n_1'}g_{n_2}\bar{q}_{\bar{n}}\rangle_2\,,
\end{aligned}
\tag{D56}
$$

We write $C_2^{(2)H}(n_2,n_2,n_1')$ as

$$
C_2^{(2)}(n_2,n_1',n_2) = C_{2,\,\mathrm{NNLO}}^{(2)H}(n_2,n_1',n_2) + C_{2,\,\mathrm{N^3LO}}^{(2)H}(n_2,n_1',n_2)\,,
\tag{D57}
$$

where $C_{2,\,\mathrm{NNLO}}^{(2)H}(n_2,n_1',n_2')$ is the coefficient of the contribution that reproduces the the second and third line in the Eq. (D56), and $C_{2,\,\mathrm{N^3LO}}^{(2)H}$ the fourth and fifth line. As for the previous cases, the coefficient $C_{2,\,\mathrm{NLO}}^{(2)J}(n_2,n_1',n_2)$ scales as λ^{-2}, $C_{2,\,\mathrm{NNLO}}^{(2)H}(n_2,n_1',n_2)$ as λ^{-1} and $C_{2,\,\mathrm{N^3LO}}^{(2)H}(n_2,n_1',n_2)$ as λ^0. Since $\mathcal{O}_2^{(2)}(n_2,n_1',n_2)$ interferes with the LO operator, $\mathcal{O}_2^{(1)}(n_1,n_1')$, to have the amplitude squared up to NLO(λ) we need both $C_{2,\,\mathrm{NLO}}^{(2)J}$ and $C_{2,\,\mathrm{NNLO}}^{(2)H}$. We start with $C_{2,\,\mathrm{NLO}}^{(2)J}$. To calculate the amplitude in the second line in Eq. (D55), we use Eq. (D35) and take the limit $n_2\cdot n_2'\to\lambda^4/\eta^4$ with $n_2\cdot n_1'\sim n_1'\cdot n_2'\sim\lambda^2/\eta^4$. (We could alternatively take the limit $n_2\cdot n_1'\to\lambda^4/\eta^4$ with $n_2\cdot n_2'\sim n_2'\cdot n_1'\sim\lambda^2/\eta^4$.) It is easy to check that

$$
\begin{aligned}
&\lim_{n_2\cdot n_2'\to\lambda^4/\eta^4} d_{1,A}^{J\,\alpha\beta}(n_2,n_1',n_2')\langle 0|\mathcal{O}_2^{(2)}|q_{n_2}g_{n_1'}g_{n_2}\bar{q}_{\bar{n}}\rangle_2 \\
&\quad = C_{2,\mathrm{LO}}^{(1)}(n_2,n_1')\int dx\langle 0|T\{\mathcal{L}_{\mathrm{SCET}_2}(x)\mathcal{O}_2^{(1)}\}|q_{n_2}g_{n_1'}g_{n_2}\bar{q}_{\bar{n}}\rangle_2\,.
\end{aligned}
\tag{D58}
$$

With Eq. (D58), we can write $C_{2,\mathrm{NLO}}^{(2)J}(n_2,n_1',n_2)$ as

$$
C_{2,\,\mathrm{NLO}}^{(2)J}(n_2,n_1',n_2) = U^{(2,0,0)}(n_0;\,Q,\mu_1)\,d_3^{J\,\alpha\beta}(n_2,n_1',n_2)\Theta_{\delta_2}[n_2\cdot n_1']
\tag{D59}
$$

where

$$
\begin{aligned}
d_3^{J\,\alpha\beta}(n_2,n_1',n_2) &= \lim_{n_2\cdot n_2'\to\lambda^4/\eta^4}(d_{1B}^{J\,\alpha\beta}(n_2,n_1',n_2') + d_{1C}^{J\,\alpha\beta}(n_2,n_1',n_2')) \\
&= \Big(\Big[\frac{\bar{q}_1}{\bar{q}_0}\sqrt{n_1\cdot n_1'}\,v_1^\alpha + \frac{\bar{k}_1}{\bar{q}_0}\sqrt{n_1\cdot n_1'}\frac{\not{v}_1}{2}\gamma_{n_1'\perp}^\alpha \\
&\quad - \frac{\bar{k}_1\bar{k}_2}{\bar{q}_0(\bar{q}_2+\bar{k}_1)}\sqrt{n_1\cdot n_1'}\,\gamma_{n_1'\perp}^\alpha\frac{\not{v}_1}{2}\Big] \\
&\quad \times\Big[-\frac{\bar{k}_1}{\bar{q}_0}\sqrt{n_1\cdot n_1'}\,v_1^\beta - \frac{\bar{k}_2\,\bar{k}_1}{(\bar{q}_2+\bar{k}_1)\bar{q}_0}\sqrt{n_1\cdot n_1'}\,\frac{\not{v}_1}{2}\gamma_{n_2'\perp}^\beta\Big] \\
&\quad + \Big[\frac{1}{\bar{q}_2+\bar{k}_1}\gamma_{n_1'\perp}^\alpha\gamma_{n_2'\perp}^\beta + \frac{1}{\bar{q}_2+\bar{k}_2}\gamma_{n_2'\perp}^\beta\gamma_{n_1'\perp}^\alpha\Big]\gamma_{n_0\perp}^\mu\Big) \\
&\quad \times\frac{2\bar{q}_0}{\bar{k}_1(\bar{k}_2(n_2'\cdot n_1') + \bar{q}_2(n_2\cdot n_1'))}\Big|_{n_2=n_2'}\,.
\end{aligned}
\tag{D60}
$$

The scaling of the dot products of n's in this configuration make the coefficient $C^{(2)J}_{2,\,\rm NLO}(n_2,n_2,n_1')\sim\lambda^{-2}$. As previously for $C^{(2)J}_{2,\,\rm NLO}(n_1,n_1',n_1')$, we prefer leaving (D59) in terms of n_2, n_1' and n_2'. To calculate $C^{(2)H}_{2\,,\rm NNLO}(n_2,n_2,n_1')$ we proceed in the same way. We have

$$C^{(2)H}_{2\,,\rm NNLO}(n_2,n_1',n_2)=U^{(2,1,0)}(n_0,n_0;\,Q,\mu_1)d_3^{H\,\alpha\beta}(n_2,n_1',n_2)\Theta_{\delta_2}[n_2\cdot n_1']\,, \tag{D61}$$

where

$$\begin{aligned} d_3^{H\,\alpha\beta}(n_2,n_1',n_2)&=\lim_{n_2\cdot n_2'\to\lambda^4/\eta^4} d_{1B}^{H\,\alpha\beta}(n_2,n_1',n_2')\\ &=\Big[\frac{\bar q_1}{\bar q_0}\sqrt{n_1\cdot n_1'}\,v_1^\alpha+\frac{\bar k_1}{\bar q_0}\sqrt{n_1\cdot n_1'}\frac{\bar{\not n}_1}{2}\gamma^\alpha_{n_1'\perp}\\ &-\frac{\bar k_1\bar k_2}{\bar q_0(\bar q_2+\bar k_1)}\sqrt{n_1\cdot n_1'}\,\gamma^\alpha_{n_1'\perp}\frac{\bar{\not n}_1}{2}\Big]\gamma^\beta_{n_1'\perp}\frac{\bar q_1}{q_1^2}\,\frac{n_0^\mu-\bar n^\mu}{Q}\Big|_{n_2=n_2'}. \end{aligned} \tag{D62}$$

In Eq. (D61) we use the fact that,

$$\begin{aligned} &\lim_{n_2\cdot n_2'\to\lambda^4/\eta^4} d_{1,\,A}^{H\,\alpha\beta}(n_2,n_1',n_2')\langle 0|\mathcal{O}_2^{(2)}|q_{n_2}g_{n_1'}g_{n_2}\bar q_{\bar n}\rangle_2\\ &\quad=C^{(1)}_{2\,,\rm NLO}\int dx\langle 0|T\{\mathcal{L}_{\rm SCET_2}(x)\mathcal{O}_2^{(1)}\}|q_{n_2}g_{n_1'}g_{n_2}\bar q_{\bar n}\rangle_2\,. \end{aligned} \tag{D63}$$

In Eqs. (D60, D62) there is again a difference in the notation between the LHS and RHS similar to Eq. (D53). Since $C^{(2)J}_{2,\,\rm LO}(n_2,n_1',n_2)$ and $C^{(2)H}_{2\,,\rm NNLO}(n_2,n_1',n_2)$ come from $\rm SCET_1$ two-jet operators, we include the appropriate Θ-functions in Eqs. (D59, D61).

We have that all the NLO(λ) terms for two gluon matching come from the $\rm SCET_1$ operator, $\mathcal{O}_1^{(0)}(n_0)$, and are jet-structure corrections. At NNLO(λ) we have only hard corrections. Before matching $\rm SCET_2$ to $\rm SCET_3$, we have to insert in the coefficients the $\rm SCET_2$ running factors. Below we list all the needed $\rm SCET_2$ coefficients to NNLO(λ) that we have calculated with the appropriate RG kernels. From the matching of one-gluon emission, we have:

$$\begin{aligned} C^{(1)}_{2,\,\rm LO}(n_1,n_1')&=U^{(2,1,0)}(n_1,n_1';\,\mu_1,\mu)U^{(2,0,0)}(n_0;\,Q,\mu_1)c_{\rm LO}(n_0)\frac{\bar q_0}{q_0^2}\gamma^\mu_{n_0\perp}\,,\\ C^{(1)H,a}_{2,\,\rm NLO}(n_1,n_1')&=U^{(2,1,0)}(n_1,n_1';\,\mu_1,\mu)U^{(2,1,0)}(n_0,n_0;\,Q,\,\mu_1)\otimes c^{H,a}_{2,\,\rm NLO}(n_0,n_0)\,,\\ C^{(1)H}_{2,\,\rm NNLO}(n_1,n_1')&=U^{(2,1,0)}(n_1,n_1';\,\mu_1,\mu)U^{(2,1,0)}(n_0,n_0;\,Q,\,\mu_1)\otimes c^{H}_{2,\,\rm NNLO}(n_0,n_0)\,,\\ C^{(1)H,b}_{2,\,\rm NLO}(n_1,n_1')&=U^{(2,1,0)}(n_1,n_1';\,\mu_1,\mu)C_1^{(1)}(n_1,n_1')\tilde\Theta_{\delta_2}[n_1\cdot n_1']\,, \end{aligned} \tag{D64}$$

where the coefficient in (D64) without the $\rm SCET_2$ RG-kernel is defined in Eq. (D11), the second and third in Eqs. (D17), and the last in (D19). From the matching of two-gluon emission we have the coefficients:

$$\begin{aligned} C^{(2)J}_{2\,,\rm NLO}(n_2,n_1',n_2')&=\,U^{(2,1,0)}(n_2,n_1',n_2';\,\mu_1,\mu)\,U^{(2,0,0)}(n_0;\,Q,\mu_1)\\ &\quad\times d_1^J(n_2,n_1',n_2')\Theta_{\delta_2}[n_2\cdot n_1']\Theta_{\delta_2}[n_2\cdot n_2']\Theta_{\delta_2}[n_2'\cdot n_1']\,,\\ C^{(2)J}_{2,\,\rm NLO}(n_2,n_1',n_1')&=\,U^{(2,1,0)}(n_2,n_1',n_1';\,\mu_1,\mu)\otimes U^{(2,0,0)}(n_0;\,Q,\mu_1)\\ &\quad\times d_2^J(n_2,n_1',n_1')\Theta_{\delta_2}[n_2\cdot n_1']\Theta_{\delta_2}[n_2\cdot n_2']\,,\\ C^{(2)J}_{2,\,\rm NLO}(n_2,n_1',n_2)&=\,U^{(2,1,0)}(n_2,n_1',n_2;\,\mu_1,\mu)\otimes U^{(2,0,0)}(n_0;\,Q,\mu_1)\\ &\quad\times d_3^J(n_2,n_1',n_2)\Theta_{\delta_2}[n_2\cdot n_2']\Theta_{\delta_2}[n_1'\cdot n_2']\,,\\ C^{(2)H}_{2\,,\rm NNLO}(n_2,n_1',n_2)&=\,U^{(2,1,0)}(n_2,n_1',n_2;\,\mu_1,\mu)\otimes U^{(2,1,0)}(n_0,n_0;\,Q,\mu_1)\\ &\quad\otimes d_3^H(n_2,n_1',n_2)\Theta_{\delta_2}[n_2\cdot n_2']\Theta_{\delta_2}[n_1'\cdot n_2']\,, \end{aligned} \tag{D65}$$

where the coefficients without $\rm SCET_2$ running are defined in Eqs. (D37, D52, D59, D61). The RG kernels are given in Eqs. (18, 19, and 90). As discussed below Eq. (89), we have a convolution because SCET fields collinear to the same direction can exchange longitudinal momentum during the running.

Appendix E: Matching SCET_2 to SCET_3, SCET_N

We match SCET_2 to SCET_3 before proceeding to the general case and listing a set of master operators for SCET_N The SCET_3 operators necessary for matching up to two-gluon emission are: $\mathcal{O}_3^{(0)}(n_0)$, $\mathcal{O}_3^{(1)}(n_0,n_0)$, $\mathcal{O}_3^{(1)}(n_1,n_1')$, $\mathcal{O}_3^{(2)}(n_2,n_1',n_2')$, $\mathcal{O}_3^{(2)}(n_2,n_2,n_1')$, $\mathcal{O}_3^{(2)}(n_2,n_1',n_1')$. We have seen that to describe the parton shower for one emission, we only need the coefficient of the SCET_2 operator, $\mathcal{O}_2^{(1)}(n_1,n_1')$. Similarly, in SCET_3 we need the coefficient of the operator $\mathcal{O}_3^{(2)}(n_2,n_1',n_2')$. We can follow the same steps from App. D to calculate the Wilson coefficients $C_3^{(2)}(n_2,n_1',n_2')$. In this way, it is not difficult to show that

$$\begin{aligned} C_3^{(2)}(n_2,n_1',n_2') = {}& C_{3,\,\mathrm{LO}}^{(2)} \\ &+ C_{3,\,\mathrm{NLO}}^{(2)H,a} + C_{3,\,\mathrm{NLO}}^{(2)H,b} + C_{3,\,\mathrm{NLO}}^{(2)J\,a} + C_{3,\,\mathrm{NLO}}^{(2)J\,b} + C_{3,\,\mathrm{NLO}}^{(2)J\,c} \\ &+ C_{3,\,\mathrm{NNLO}}^{(2)H,a} + C_{3,\,\mathrm{NNLO}}^{(2)H,b}\,, \end{aligned} \tag{E1}$$

where

$$\begin{aligned} C_{3,\,\mathrm{LO}}^{(2)}(n_2,n_1',n_2') &= C_{3,\,\mathrm{LO}}^{(1)}(n_2,n_2')C_{2,\,\mathrm{LO}}^{(1)}(n_1,n_1')\,, \\ C_{3,\,\mathrm{NLO}}^{(2)H,\,a}(n_2,n_1',n_2') &= C_{3,\,\mathrm{LO}}^{(1)}(n_2,n_2')C_{2,\,\mathrm{NLO}}^{(1)H,a}(n_1,n_1')\,, \\ C_{3,\,\mathrm{NLO}}^{(2)H,\,b}(n_2,n_1',n_2') &= C_{3,\,\mathrm{LO}}^{(1)}(n_2,n_2')C_{2,\,\mathrm{NLO}}^{(1)H,b}(n_1,n_1')\,, \\ C_{3,\,\mathrm{NLO}}^{(2)J,\,1}(n_2,n_1',n_2') &= C_{2,\,\mathrm{NLO}}^{(2)J}(n_2,n_1',n_2')\tilde{\Theta}_{\delta_3}[n_2\cdot n_2']\tilde{\Theta}_{\delta_3}[n_2\cdot n_1']\tilde{\Theta}_{\delta_3}[n_2'\cdot n_1']\,, \\ C_{3,\,\mathrm{NLO}}^{(2)J,\,2}(n_2,n_1',n_2') &= C_{2,\,\mathrm{NLO}}^{(2)J}(n_2,n_1',n_1')\tilde{\Theta}_{\delta_3}[n_2\cdot n_2']\tilde{\Theta}_{\delta_3}[n_2\cdot n_1']\Theta_{\delta_3}[n_2'\cdot n_1']\,, \\ C_{3,\,\mathrm{NLO}}^{(2)J,\,3}(n_2,n_1',n_2') &= C_{2,\,\mathrm{NLO}}^{(2)J}(n_2,n_1',n_2)\Theta_{\delta_3}[n_2\cdot n_2']\tilde{\Theta}_{\delta_3}[n_2\cdot n_1']\tilde{\Theta}_{\delta_3}[n_2'\cdot n_1']\,, \\ C_{3,\,\mathrm{NNLO}}^{(2)H,\,a}(n_2,n_1',n_2') &= C_{3,\,\mathrm{LO}}^{(1)}(n_2,n_2')C_{2,\,\mathrm{NNLO}}^{(1)}(n_1,n_1')\,, \\ C_{3,\,\mathrm{NNLO}}^{(2)H,\,b}(n_2,n_1',n_2') &= C_{2,\,\mathrm{NNLO}}^{(2)H}(n_2,n_1',n_2)\Theta_{\delta_3}[n_2\cdot n_2']\tilde{\Theta}_{\delta_3}[n_2\cdot n_1']\tilde{\Theta}_{\delta_3}[n_2'\cdot n_1']\,, \end{aligned} \tag{E2}$$

and

$$C_{3,\,\mathrm{LO}}^{(1)}(n_2,n_2') = \left(2\frac{(q_2)_{n_1\perp}^{\beta}}{\bar{k}_2} + \frac{(\not{q}_2)_{n_0\perp}\gamma_{n_2'\perp}^{\beta}}{\bar{q}_2}\right)\frac{\bar{q}_1}{q_1^2}\frac{\not{n}\not{n}_1}{4}\,\Theta_{\delta_3}[n_2\cdot n_2']\,. \tag{E3}$$

On the LHS of the equations in the first, second and third line of (E2) we can write n_1 in terms of n_2, n_2' and n_1' using the formulas in (B16). The SCET_2 coefficients $C_{2,\,\mathrm{NLO}}^{(2)J}$ and $C_{2,\,\mathrm{NNLO}}^{(2)H}$ are defined in Eqs. (D65). $C_{2,\,\mathrm{NLO}}^{(1)H,a}(n_1,n_1')$, $C_{2,\,\mathrm{NLO}}^{(1)H,b}(n_1,n_1')$, and $C_{2,\,\mathrm{NNLO}}^{(1)}(n_1,n_1')$ are given in Eq. (D64), and $C_{2,\,\mathrm{LO}}^{(1)}(n_1,n_1')$ in Eq. (52). As with any $\mathrm{SCET}_i \to \mathrm{SCET}_{i+1}$ matching, we encode the definition of collinearity from the higher scale theory in the lower one by Θ functions (*cf.* discussion in Sec. III A). Some of the SCET_2 coefficients above already contained such factors as a result of matching to SCET_1. In Eq. (E2), we write out the new ones that appear with Θ_{δ_3}, with $\delta_3 = \lambda^3/\eta^4$ according to our usual convention. Since all the coefficients above multiply $\mathcal{O}_3^{(2)}$, the scaling of contributions comes from them alone, with $C_{3,\,\mathrm{LO}}^{(2)} \sim \lambda^{-3}$, the NLO terms $\sim \lambda^{-2}$, and NNLO going as λ^{-1}.

At LO, the contribution in SCET_3 is given by the replacement procedure on the LO contribution in SCET_2, $C_{2,\,\mathrm{LO}}^{(1)}(n_1,n_1')\mathcal{O}_2^{(1)}$. We multiply it by the running function $U^{(1)}(n_1,n_1';\,\mu_1,\,\mu)$ and apply the replacement:

$$(\bar{\chi}_{n_2})_i \to (c_{\mathrm{LO}}^{\alpha}(n_1))_{ji}(\bar{\chi}_{n_1})_j g\mathcal{B}_{\alpha}^{n_1'\perp}\,, \tag{E4}$$

where $c_{\mathrm{LO}}^{\alpha}(n_1)$ is

$$c_{\mathrm{LO}}^{\alpha}(n_1) = \left(2\frac{(q_2)_{n_1\perp}^{\alpha}}{\bar{k}_2} + \frac{(\not{q}_2)_{n_1\perp}\gamma_{n_2'\perp}^{\alpha}}{\bar{q}_2}\right)\frac{\not{n}\not{n}_1}{4}\,\Theta_{\delta_3}[n_2\cdot n_2']\,. \tag{E5}$$

Eq. (E4) has the same structure as Eq. (D15). If we go on with the matching down to SCET_N, we find that the LO result would be given applying the above replacement $N-1$ times. At SCET_N we could match everything to the operator $\mathcal{O}_N^{(N-1)}(n_{N-1},n_1',\ldots,n_{N-1}')$, and the LO coefficient is

$$C_{N,\,\mathrm{LO}}^{(N-1)} = \prod_{k=1}^{N-1} U^{(2,k-1,0)}(n_{k-1},n_1',\ldots,n_{k-1}';\mu_{k-1},\,\mu_k)c_{\mathrm{LO}}^{\alpha_k}(n_{k-1})\Gamma^{\mu}\,, \tag{E6}$$

with $\mu_k \sim (k_k)_{n_{k-1}\perp}$ given in Eq. (64) and

$$c_{\rm LO}^{\alpha}(n_k) = \left(2\frac{(q_{k+1})^{\alpha}_{n_0\perp}}{\bar{k}_{k+1}} + \frac{(\not{q}_{k+1})_{n_k\perp}\gamma^{\alpha}_{n'_{k+1}\perp}}{\bar{q}_{k+1}} \right) \frac{\not{\bar{n}}\not{n}_k}{4}\, \Theta_{\delta_k}[n_{k+1}\cdot n'_{k+1}]\,, \tag{E7}$$

where $\delta_k = \lambda^{2k-3}/\eta^4$.

At NLO(λ), we have two kinds of corrections: hard-scattering and jet-structure. We notice that the NLO(λ) hard-scattering terms in SCET$_3$ are just given by those in SCET$_2$ with the application of the replacement rule (E4). If we go on with the matching down to SCET$_N$, we find that we get NLO(λ) hard-scattering by applying the above replacement rule $N-2$ times to the SCET$_2$ hard-scattering operators. Thus, we can consider this as a correction to the matrix elements that we pass to a LL shower:

$$\begin{aligned} C_{N,\rm NLO}^{(N-1)H} &= \big(C_{2,\rm NLO}^{(1)H,a}(n_1,n'_1) + C_{2,\rm NLO}^{(1)H,b}(n_1,n'_1)\big) \\ &\quad\times \Big(\prod_{k=2}^{N-1} U^{(2,k-1,0)}(n_{k-1},n'_1,\dots,n'_{k-1};\mu_{k-1}\,,\mu_k) c_{\rm LO}^{\alpha_k}(n_{k-1})\Big)\,. \end{aligned} \tag{E8}$$

This approach also works for hard-scattering at NNLO(λ). Since we did not get $C_{3,\rm NNLO}^{(2)H,\,b}$ from a replacement rule, it contains one less factor of $c_{\rm LO}^{\alpha_k}$.

$$\begin{aligned} C_{N,\rm NNLO}^{(N-1)H} =\; & C_{2,\rm NNLO}^{(1)H,a}(n_1,n'_1)\left(\prod_{k=2}^{N-2} U^{(2,k-1,0)}(\mu_{k-1},\,\mu_k) c_{\rm LO}^{\alpha_k}(n_{k-1})\right) \\ & + C_{2,\rm NNLO}^{(1)H,b}(n_2,n'_1,n'_2)\left(\prod_{k=3}^{N-3} U^{(2,k-1,0)}(\mu_{k-1},\,\mu_k) c_{\rm LO}^{\alpha_k}(n_{k-1})\right)\,, \end{aligned} \tag{E9}$$

where the coefficients $C_{2,\rm NNLO}^{(1)H,a}(n_1,n'_1)$ and $C_{2,\rm NNLO}^{(1)H,b}(n_2,n'_1,n'_2)$ are defined in Eqs. (D65).

The NLO(λ) jet-structure corrections in SCET$_3$ are given by $C_{3,\rm NLO}^{(2)J,\,I}(n_2,n'_1,n'_2)\mathcal{O}_3^{(2)}$, where $I=\{1,2,3\}$, are given by the LO SCET$_1$ operator $\bar{\chi}_{n_0}\gamma^{\mu}\chi_{\bar{n}}$ in three steps: First, we multiply it by the running factor $U^{(1)}(n_0;\,Q,\,\mu_1)$, second, we apply the replacements

$$(\bar{\chi}_{n_2})_i \to (h_I^{\alpha\beta})_{ji}(n_2,n'_1,n'_2)(\bar{\chi}_{n_1})_j\, g\mathcal{B}_{\alpha}^{n'_1\perp} g\mathcal{B}_{\beta}^{n'_2\perp}\,, \tag{E10}$$

where

$$\begin{aligned} h_1^{\alpha\beta}(n_2,n'_1,n'_2) &= d_1^{\alpha\beta}(n_2,n'_1,n'_2)\tilde{\Theta}_{\delta_3}[n_2\cdot n'_2]\tilde{\Theta}_{\delta_3}[n_2\cdot n'_1]\tilde{\Theta}_{\delta_3}[n'_2\cdot n'_1]\,, \\ h_2^{\alpha\beta}(n_2,n'_1,n'_2) &= d_2^{\alpha\beta}(n_2,n'_1,n'_1)\tilde{\Theta}_{\delta_3}[n_2\cdot n'_2]\tilde{\Theta}_{\delta_3}[n_2\cdot n'_1]\Theta_{\delta_3}[n'_2\cdot n'_1]\,, \\ h_3^{\alpha\beta}(n_2,n'_1,n'_2) &= d_3^{\alpha\beta}(n_2,n'_1,n_2)\Theta_{\delta_2}[n_2\cdot n'_2]\tilde{\Theta}_{\delta_3}[n_2\cdot n'_1]\tilde{\Theta}_{\delta_3}[n'_2\cdot n'_1]\,. \end{aligned} \tag{E11}$$

The $d_I^{\alpha\beta}$ coefficients are defined in Eqs.(D38, D53, D60). Third, we multiply the operators that come from applying Eqs. (E11) by the second running factor. This depends on the SCET$_2$ operator so each replacement rule (E10) is followed by a different factor: $h_1^{\alpha\beta}$ by $U^{(2,2,0)}(n_2,n'_1,n'_2;\,\mu_1,\mu_2)$, $h_2^{\alpha\beta}$ by $U^{(2,2,0)}(n_2,n'_1,n'_1;\,\mu_1,\mu_2)$ and $h_3^{\alpha\beta}$by $U^{(2,2,0)}(n_2,n'_1,n_2;\,\mu_1,\,\mu_2)$. Since these corrections are independent of the initial hard process, we would encounter the same calculations we have done just now for SCET$_1$ to SCET$_3$, at any matching SCET$_i$ to SCET$_{i+2}$. Thus, the NLO(λ) jet-structure coefficients for the SCET$_N$ operator are:

$$C_{N,\rm NLO}^{(N-1)J} = \sum_{l=1}^{N-2} C_{N,\rm NLO}^{(N)J}(l)\,, \tag{E12}$$

where

$$\begin{aligned} C_{N,\rm NLO}^{(N-1)J}(l) = \sum_{I=1}^{3}\Big[\Big(\prod_{k=1}^{l-1} & U^{(2,k-1,0)}(n_{k-1},n'_1,\dots,n'_{k-1};\mu_{k-1},\,\mu_k) c_{\rm LO}^{\alpha_k}(n_{k-1})\Big) \\ & \times U_I^{(l+1)}(\mu_l,\,\mu_{l+1})\otimes h_I^{\alpha\beta}(n_{l+1},n'_l,n'_{l+1}) \\ & \times\Big(\prod_{k=l+1}^{N-1} U^{(2,k-1,0)}(n_{k-1},n'_1,\dots,n'_{k-1};\mu_{k-1},\,\mu_k) c_{\rm LO}^{\alpha_k}(n_{k-1})\Big)\Big]\Gamma^{\mu}\,, \end{aligned} \tag{E13}$$

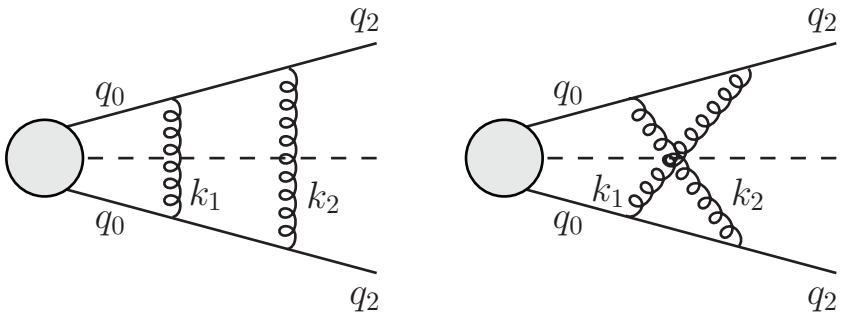

FIG. 22: Two distinct real emission contributions to $P_{qq}^{(1)}$ drawn as amplitudes squared. They are referred to as the box (**L**) and crossed (**R**) contributions.

with

$$U_1^{(l+1)}(\mu_l,\,\mu_{l+1}) = U^{(2,l+1,0)}(n_{l+1}, n_1', \ldots, n_l', n_{l+1}'; \mu_l,\,\mu_{l+1})\,, \tag{E14}$$
$$U_2^{(l+1)}(\mu_l,\,\mu_{l+1}) = U^{(2,l+1,0)}(n_{l+1}, n_1', \ldots, n_l', n_l'; \mu_l,\,\mu_{l+1})\,, \tag{E15}$$
$$U_3^{(l+1)}(\mu_l,\,\mu_{l+1}) = U^{(2,l+1,0)}(n_{l+1}, n_1', \ldots, n_l', n_{l+1}; \mu_l,\,\mu_{l+1})\,,$$

and

$$\begin{aligned}
h_1^{\alpha\beta}(n_{l+1}, n_l', n_{l+1}') &= d_1^{\alpha\beta}(n_{l+1}, n_l', n_{l+1}')\tilde{\Theta}_{\delta_{l+1}}[n_{l+1}\cdot n_{l+1}']\tilde{\Theta}_{\delta_{l+1}}[n_{l+1}\cdot n_l']\tilde{\Theta}_{\delta_{l+1}}[n_{l+1}'\cdot n_1']\,,\\
h_1^{\alpha\beta}(n_{l+1}, n_l', n_l') &= d_2^{\alpha\beta}(n_{l+1}, n_l', n_{l+1}')\tilde{\Theta}_{\delta_{l+1}}[n_{l+1}\cdot n_{l+1}']\tilde{\Theta}_{\delta_{l+1}}[n_{l+1}\cdot n_l']\Theta_{\delta_{l+1}}[n_{l+1}'\cdot n_l']\,,\\
h_3^{\alpha\beta}(n_{l+1}, n_l', n_{l+1}) &= d_3^{\alpha\beta}(n_{l+1}, n_l', n_{l+1}')\Theta_{\delta_{l+1}}[n_{l+1}\cdot n_{l+1}']\tilde{\Theta}_{\delta_{l+1}}[n_{l+1}\cdot n_l']\tilde{\Theta}_{\delta_{l+1}}[n_{l+1}'\cdot n_l']\,.
\end{aligned} \tag{E16}$$

The coefficients $d_I^{\alpha\beta}$ here are equal to the coefficients $d_I^{\alpha\beta}$ defined in Eqs.(D38, D53, D60) upon the substitution $(n_2, n_1', n_2') \to (n_{l+1}, n_l', n_{l+1}')$ and $\delta_3 \to \delta_{l+1}$.

Appendix F: $\mathcal{O}(\alpha_s^2)$ Correction to Splitting Function

One of the cross-checks on our results is the rederivation of (the abelian part of) the $\mathcal{O}(\alpha_s^2)$ correction to the $q \to qg$ splitting function, $P_{qq}^{(1)}$. This follows from obtaining the NLO(λ) correction to two-gluon emission. For comparison, we have chosen the classic result of Curci *et al.* [62]. The full expression for $P_{qq}^{(1)}$ involves many real and virtual contributions. Here we will only explicitly calculate the $\sim C_F^2$ component of $P_{qq}^{(1)}$ and show it agrees. (Obtaining the full result requires additional non-abelian diagrams.) Ref. [62] splits the abelian, two-gluon, real emission contributions to $P_{qq}^{(1)}$ into two topologically inequivalent diagrams, the box and crossed graphs, Fig. 22. We calculated each of these individually.

The SCET_1 amplitude contains three graphs for two-gluon emission. These are shown in Fig. 20, and we give the corresponding amplitudes in Eqs. (D34). In order to obtain $P_{qq}^{(1)}$, we will need to square the amplitudes and partially integrate over phase space. Thus, we need to choose an explicit kinematics. We redraw, in Fig. (23), our vector labels for two-gluon emission. We choose a somewhat nonstandard assignment for our variables. This is to aid in the comparison with [62]. The final state parton shower occurs for timelike virtual particles, and momentum fractions decrease the farther we are from the initial hard scattering. By contrast, [62] considered a DIS-type process where the shower is spacelike. Since the radiation in that case comes from initial states, the momentum fractions decrease toward the hard interaction. Only at LO in α_s are the spacelike and timelike splitting functions equal, by the Gribov-Lipatov relation [77]. At higher orders, this gets violated, but there is a straightforward conversion procedure, detailed in [62, 78]. We, however, choose our kinematics such that our variable relations are equivalent to those for a spacelike process. For example, $P_{qq}^{(1)}$ is a function of $x \equiv \bar{q}_0/\bar{q}_2$. In a spacelike process, $x \in [0,1]$. Rather than convert our answer, we will also define x as above, even though this means for us $x \in [1,\infty)$. Other integration variables will have their ranges shifted so that they have the same relation with x as in DIS, and thus they enter into our expression in the same way. Lastly, we do not do the phase space integration for q_2. While this *is* necessary for the timelike splitting function, the analogous particle for a spacelike process is a fixed initial state. Thus, for comparison purposes,

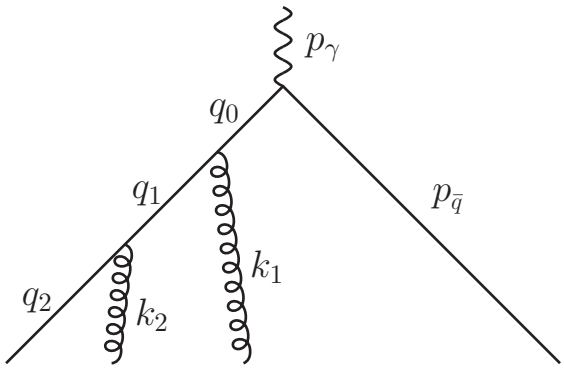

FIG. 23: Kinematics for double gluon emission. This particular diagram corresponds to the "A" graph of Fig. (20).

we can leave it undone. Our vectors are as follows (note that this is a different frame from the one used previously for matching):

$$\begin{aligned}
q_2 &= \{p, 0, 0, p\} \\
k_1 &= \left\{-z_1 p - \frac{k_{1\perp}^2}{4pz_1},\, k_{1\perp}\cos(\phi_1),\, k_{1\perp}\sin(\phi_1), -z_1 p + \frac{k_{1\perp}^2}{4pz_1}\right\} \\
k_2 &= \left\{-z_2 p - \frac{k_{2\perp}^2}{4pz_2},\, k_{2\perp},\, 0, -z_2 p + \frac{k_{2\perp}^2}{4pz_2}\right\} \\
q_0 &= \left\{x\, p + \frac{q_0^2 + |\overrightarrow{\mathbf{k_1}}_\perp + \overrightarrow{\mathbf{k_2}}_\perp|^2}{4px}, \overrightarrow{\mathbf{k_1}}_\perp + \overrightarrow{\mathbf{k_2}}_\perp, x\, p - \frac{q_0^2 + |\overrightarrow{\mathbf{k_1}}_\perp + \overrightarrow{\mathbf{k_2}}_\perp|^2}{4px}\right\}.
\end{aligned} \tag{F1}$$

Before proceeding, we wish to note some things about our assignment. First of all, while it is redundant to include $q_0 = k_1 + k_2 + q_2$, we will integrate over $d^4 q_0$ and wanted to present our parametrization. We see that $x = 1 - z_1 - z_2$. This is consistent with the spacelike case, but here, $z_1, z_2 \in (-\infty, 0]$, hence the minus signs in k_1 and k_2. Additionally, only the relative azimuthal angle between k_1 and k_2 is physical. Thus, to simplify our formulas, we fix k_2 in the $x - z$ plane.

As a last step before squaring and integrating, we will introduce our measure and integral parametrization. While one could integrate the full final state phase space including the antiquark, we instead exploit the factorization of the the cross section into a hard interaction $\mathcal{H}$, a radiation-function $\mathcal{K}$, and fragmentation functions $q_{B,\,F}(x)$ which determine how the partons arrange themselves into hadrons. Schematically, $\sigma = \mathcal{H} \otimes (\mathcal{K}_{\rm LO}(x, q^2) + \mathcal{K}_{J,\,\rm NLO}(x, q^2) + \ldots) \otimes \Pi\, q_{B,\,F}(x) = \mathcal{H} \otimes (\mathcal{R}_{\rm LO} + \mathcal{R}_{\rm NLO} + \ldots)$. For our computations we need only integrate the phase space for $\mathcal{R}$, and it will remain independent of the details of $\mathcal{H}$. Taking $d \equiv 4 + \epsilon$:

$$\begin{aligned}
\mathcal{R}_{\rm LO} &= \sum_i \frac{2}{\bar{q}_i} \int \prod_{j=1}^{i} \frac{\not{d}^{d-1} k_j}{z_j}\, \not{d}^d q_0\, dq^2\, \mathrm{PP}\left[|C_{i,\,\rm LO}^{(i-1)} \langle 0|\mathcal{O}_i^{(i-1)}|q(i-1)g\bar{q}\rangle|^2\right] \\
&\quad \times \delta(x - \bar{q}_0/\bar{q}_i)\delta(q^2 - (q_i + \sum_{j=1}^{i} k_j)^2)\,(2\pi)^d \delta^{(d)}(q_0 - \sum_{j=1}^{i} k_j)), \\
\mathcal{R}_{J,\,\rm NLO} &= \sum_i \frac{2}{\bar{q}_i} \int \prod_{j=1}^{i} \frac{\not{d}^{d-1} k_j}{z_j}\, \not{d}^d q_0\, dq^2\, \mathrm{PP}\left[|C_{i,\,\rm NLO}^{(i-1)J} \langle 0|\mathcal{O}_i^{(i-1)}|q(i-1)g\bar{q}\rangle|^2\right] \\
&\quad \times \delta(x - \bar{q}_0/\bar{q}_i)\delta(q^2 - (q_i + \sum_{j=1}^{i} k_j)^2)\,(2\pi)^d \delta^{(d)}(q_0 - \sum_{j=1}^{i} k_j)),
\end{aligned} \tag{F2}$$

and the q_i phase space and spin-sum are moved into $\mathcal{H}$. We define z_j analogously to Eqs. (F1). The setup we describe in the body of the paper uses Wilsonian cutoffs in phase space, both to keep the contributions of different operators distinct via Θ's and to cutoff soft and collinear divergences via some shower resolution parameter which keeps configurations outside of nonperturbative regimes. In the shower language the $\Pi\, q_{B,F}(x)$ term in $\mathcal{R}$ signifies the hadronization model and may depend on more than just x variables, and the $\mathcal{K}$ term signifies the infrared finite fully differential shower computations. In Eq. (F2) we are integrating over $\perp$-momenta to carry out the perturbative

comparison with Curci *et al.* Here we are implicitly in the $\overline{\rm MS}$ scheme, and it is the perturbative IR divergences in $\mathcal{R}$ that get absorbed by $q_{B,\,F}(x)$. The $\mathcal{R}$ terms that we need consist of only the $1/\epsilon^2$ and $1/\epsilon$ portions of the corresponding operator expectation values. The non-pole contributions from $C_{i,\,\rm LO}^{(i-1)}$ and $C_{i,\,\rm NLO}^{(i-1)J}$ (Eqs. E6 and E13), along with higher-order corrections are in higher order terms in the $\mathcal{R}$ functions. The hard-scattering corrections are in $\mathcal{H}$. The reason we extract only the pole terms is that these are precisely what give the expression for $P_{qq}^{(0)}$ and $P_{qq}^{(1)}$. We also define PP to remove those portions of the matrix element which enter into $\mathcal{H}$ such as the final quark spin-sum, current Γ, and antiquark quantities.

In this $\overline{\rm MS}$ factorization scheme, we need to define our correction operator differently than in Apps. D and E. Since $P_{qq}^{(1)}$ requires the calculation of two-gluon emission, we find it simplest here to calculate in SCET$_3$ where only $C_{3,\,\rm NLO}^{(2)J,\,1}$ in Eq. (E2) contributes. This corresponds to taking limits such that only its Θ-function equals one, while the other jet-structure coefficients are zero. Since we integrate it over all of phase space, which includes the strongly-ordered limit, we need to subtract the LO contribution. This just comes from $C_{3,\,\rm LO}^{(2)}(n_2,n_1',n_2')\mathcal{O}_3^{(2)}$, but we take care to only remove the pole parts consistent with $\overline{\rm MS}$. We can thus write the subtraction as:

$$\mathcal{R}_{J,\,\rm NLO}^{q\to qgg} \;=\; \int d\Pi_{k_1,\,k_2,\,q_0}\,\mathrm{PP}\Big[|C_{3,\,\rm NLO}^{(2)J,\,1}(n_2,n_1',n_2')\langle 0|\mathcal{O}_3^{(2)}|qgg\bar{q}\rangle|^2 - \Big(|C_{3,\,\rm LO}^{(2)}(n_2,n_1',n_2')\langle 0|\mathcal{O}_3^{(2)}\Gamma^\mu|qgg\bar{q}\rangle|^2\Big)_{\overline{\rm MS}}\Big], \tag{F3}$$

where $C_{3,\,\rm NLO}^{(2)J,\,1}$ is evaluated such that $\Theta=1$ over all of phase space. We will describe the subtraction portion in detail below, but first we concentrate on the correction term.

By fixing the virtuality of $q_0^2\equiv q^2$, we can obtain an expression without having to know its exact limits, which will depend on the details of the hard scattering. For $P_{qq}^{(1)}$, one only needs to calculate one-loop corrections to single emission and tree-level double emission, and we now specialize to the latter case. We perform the d-dimensional integration over d^dq_0 and rewrite the integral in terms of $k_{1\perp}$ and $k_{2\perp}$ dependent functions with $z_{1,2}$-dependent coefficients. Using the same parametrization as Ref. [79], we can write:

$$\mathcal{R}_{J,\,\rm NLO}^{q\to qgg} = \frac{1}{(16\pi^2)^2}\int dq^2\,\frac{dz_1}{z_1}\,\frac{dz_2}{z_2}\,\frac{d^{d-2}\mathbf{k_1}_\perp}{\pi}\,\frac{d^{d-2}\mathbf{k_2}_\perp}{\pi}\,\delta(1-x-z_1-z_2) \tag{F4}$$

$$\times\delta\left(q^2-(a_1\,\mathbf{k_1}_\perp^2+a_2\,\mathbf{k_2}_\perp^2-\mathbf{k_1}_\perp\cdot\mathbf{k_2}_\perp)\right)$$

$$\times\frac{1}{q^4}\left(A(z_1,z_2)+B(z_1,z_2)\frac{\mathbf{k_1}_\perp\cdot\mathbf{k_2}_\perp}{\mathbf{k_1}_\perp^2}+C(z_1,z_2)\frac{\mathbf{k_1}_\perp\cdot\mathbf{k_2}_\perp}{\mathbf{k_2}_\perp^2}\right.$$

$$\left.+\,D(z_1,z_2)\frac{(\mathbf{k_1}_\perp\cdot\mathbf{k_2}_\perp)^2}{\mathbf{k_1}_\perp^2\mathbf{k_2}_\perp^2}+\;E(z_1,z_2)\,\frac{\mathbf{k_1}_\perp^2}{\mathbf{k_2}_\perp^2}\;+\;F(z_1,z_2)\,\frac{\mathbf{k_2}_\perp^2}{\mathbf{k_1}_\perp^2}\right)-[\mathrm{LO}]\,, \tag{F5}$$

where $a_1=-(1-z_2)/z_1$ and $a_2=-(1-z_1)/z_2$. The functions A, B, C, D are defined in [79], and their corresponding $\mathbf{k_i}_\perp$ integrals are finite. We can check the intermediate step of their integration with [79]. The terms in our q^2 δ-function have a relative sign compared to theirs, as our $q^2>0$. As a computational aside, we found it easiest to pass to a change of variables: ($u\equiv k_{1\perp}k_{2\perp}$, $w\equiv k_{1\perp}/k_{2\perp}$). Then the δ-function just enforces:

$$u\;=\;u_0\;\equiv\;\frac{q^2\,w}{a_1w^2+a_2-2\,w\cos(\phi_1)}. \tag{F6}$$

Performing all but the dz_i integrals in $\mathcal{R}$, we get Table III, which corresponds to [79]'s Table 5.

We thus reproduce the earlier result.

The E, F functions multiply integrals that lead to single ϵ poles after the $dk_{i\perp}$ integrals (and double poles after integrating q^2), and so we must be more careful in treating them. These double poles correspond to the LO contribution, which we are explicitly subtracting as it does not contribute to $P_{qq}^{(1)}$. We discuss the subtraction in detail below Eq. (F12). For now we concentrate on the divergent integrals multiplying E and F. When we did our computations for Table (III), we were helped by the finiteness of the expressions under the $dk_{i\perp}$ integration. We could thus take $\epsilon\to 0$ for these terms, which greatly simplifies their integrals. By contrast, we will need to keep the ϵ-dependence of the E, F terms, which results in an intractable computation. To get around this, one can introduce subtraction functions, which simply reproduce the ϵ poles (these are merely a computational aid and are not related to the subtraction of

Function of $\mathbf{k_i}_\perp$ in integrand of equation (F4)	Contribution to $\mathcal{R}$ multiplying $\frac{q^2}{(16\pi^2)^2 x}\int dz_1\, dz_2\, \delta(1-z_1-z_2-x)$
1	$A(z_1,z_2)$
$\frac{\mathbf{k_1}_\perp\cdot\mathbf{k_2}_\perp}{{\mathbf{k_1}_\perp}^2}$	$-\frac{z_2}{1-z1}B(z_1,z_2)$
$\frac{\mathbf{k_1}_\perp\cdot\mathbf{k_2}_\perp}{{\mathbf{k_2}_\perp}^2}$	$-\frac{z_1}{1-z2}C(z_1,z_2)$
$\frac{(\mathbf{k_1}_\perp\cdot\mathbf{k_2}_\perp)^2}{{\mathbf{k_1}_\perp}^2{\mathbf{k_2}_\perp}^2}$	$\left(1+\frac{x}{2z_1z_2}\ln\left[\frac{x}{(1-z_1)(1-z_2)}\right]\right)D(z_1,z_2)$

TABLE III: Purely finite contributions to $\mathcal{R}$

LO). We will need to take care that they do not remove any finite pieces. Secondly, since their full contribution to $\mathcal{R}$ is $\propto 1/\epsilon^2$, we will need to include for E and F any terms $\propto \epsilon$ that multiply $\frac{{\mathbf{k_1}_\perp}^2}{{\mathbf{k_2}_\perp}^2}$ or $\frac{{\mathbf{k_1}_\perp}^2}{{\mathbf{k_2}_\perp}^2}$. These arise from doing Dirac algebra in d-dimensions.

To do the integrals in $\mathcal{R}$ which multiply E and F, we will change variables to u, w, and perform the u integration as well as the trivial ϕ_2 azimuthal one. We get for this contribution to $\mathcal{R}$:

$$\begin{aligned}\mathcal{R}|_{E,\,F} = \frac{1}{(16\pi^2)^2}\frac{2}{\pi}\int dq^2\,\frac{dz_1}{z_1}\frac{dz_2}{z_2}\,d\phi_1\,dw\,\delta(1-x-z_1-z_2)\\ \times\left(\frac{w\,u_0^{2+\epsilon}}{2\,q^2}E(z_1,z_2)\,+\,\frac{u_0^{2+\epsilon}}{2\,w\,q^2}F(z_1,z_2)\right)\frac{1}{q^4},\end{aligned} \tag{F7}$$

where u_0 is defined by equation (F6). We only need the leading poles in ϵ, and so rather than performing the w and ϕ_1 integrals for the functions multiplying E, F, we will define subtraction functions to reproduce the poles of $\frac{w\,u_0^{2+\epsilon}}{2\,q^2}$, $\frac{u_0^{2+\epsilon}}{2\,w\,q^2}$, respectively:

$$\begin{aligned}\mathcal{S}_E &= \frac{q^2}{2\,a_1^2}\frac{w^{-\epsilon}}{(w+1)}\,,\\ \mathcal{S}_F &= \frac{q^2}{2\,a_2^2}\frac{w^{\epsilon}}{(w+w^2)}.\end{aligned} \tag{F8}$$

Integrating these in w gives us a pure $1/\epsilon$ term. Subtracting them from the functions in equation (F7):

$$\begin{aligned}\mathcal{A}_E \;\equiv\; \tfrac{w\,u_0^{2+\epsilon}}{2\,q^2} \;&=\; \frac{q^2\,w^3}{2(a_2+a_1w^2-2w\cos(\phi_1))^2}\left(\frac{w\,q^2}{a_2+a_1w^2-2w\cos(\phi_1)}\right)^{\epsilon},\\ \mathcal{A}_F \;\equiv\; \tfrac{u_0^{2+\epsilon}}{2\,w\,q^2} \;&=\; \frac{q^2}{2\,w(a_2+a_1w^2-2w\cos(\phi_1))^2}\left(\frac{w\,q^2}{a_2+a_1w^2-2w\cos(\phi_1)}\right)^{\epsilon}\end{aligned} \tag{F9}$$

leads to finite integrals, allowing us to pass to the $\epsilon\to 0$ limit prior to integration, making the calculation tractable. After integrating w and ϕ_1, we want the $\epsilon^{-1,\,0}$ pieces as these turn into the single and double poles upon doing the q^2 integral and contribute to $\mathcal{R}_{J,\,\mathrm{NLO}}$. The ϵ^0 piece has one contribution besides that from $(\mathcal{A}_{E,F}-\mathcal{S}_{E,F})|_{\epsilon=0}$ ($\mathcal{S}_{E,F}$ contributes a pure $1/\epsilon$ pole). Our w integration goes from 0 to ∞, and we obtained $\mathcal{S}_{E,F}$ by expanding $\mathcal{A}_{E,F}$ in the appropriate $w\to 0,\infty$ limit to pick up the pole, while carefully regulating the other integration limit so as not to contribute its own spurious divergence or any subleading terms. However, we see that in equation (F9), taking these limits actually results in factors $(a_1w)^{-\epsilon}$ and $(w/a_2)^{\epsilon}$. Expanding the $a_i^{\pm\epsilon}$ to LO in ϵ does not affect $\mathcal{S}_{E,F}$. Nonetheless, since the subtraction functions have $1/\epsilon$ poles, including the NLO part of the ϵ-expansion will yield an ϵ^0 contribution. This $\mathcal{O}(\epsilon^0)$ term is not in $\mathcal{A}_{E,F}|_{\epsilon=0}$ since they send $u_0^\epsilon\to 1$. Thus, we have the following addition to the contributions from the integration of $\mathcal{R}|_{E,\,F}$:

$$\begin{aligned}\mathcal{B}_E &= -\epsilon\ln(a_1)\frac{q^2}{2\,a_1^2}\frac{w^{-\epsilon}}{(w+1)}\,,\\ \mathcal{B}_F &= -\epsilon\ln(a_2)\frac{q^2}{2\,a_2^2}\frac{w^{\epsilon}}{(w+w^2)}.\end{aligned} \tag{F10}$$

In the end, our $\epsilon^{-1,\,0}$ contributions after w and ϕ_1 integration come from: $\mathcal{S}_{E,F}+\mathcal{B}_{E,F}+(\mathcal{A}_{E,F}-\mathcal{S}_{E,F})|_{\epsilon=0}$. For

Function of $\mathbf{k_i}_\perp$ in integrand of equation (F4)	Contribution to $\mathcal{R}$ multiplying $\frac{q^2}{(16\pi^2)^2 x}\int dz_1\, dz_2\, \delta(1-z_1-z_2-x)$
$\frac{\mathbf{k_1}_\perp^2}{\mathbf{k_2}_\perp^2}$	$\left[\frac{2\,x\,z_1}{(1-z_2)^2 z_2\,\epsilon}\left(1-\epsilon\ln\left[-\frac{1-z_2}{z_1}\right]\right)\right.$ $\left.+\,\frac{z_1}{z_2(1-z_2)^2}\left(z_1 z_2 + x\,\left(\ln\left[\frac{z_2(1-z_2)}{z_1 x}\right]-1\right)\right)\right] E(z_1,z_2)$
$\frac{\mathbf{k_2}_\perp^2}{\mathbf{k_1}_\perp^2}$	$\left[\frac{2\,x\,z_2}{(1-z_1)^2 z_1\,\epsilon}\left(1-\epsilon\ln\left[-\frac{1-z_1}{z_2}\right]\right)\right.$ $\left.+\,\frac{z_2}{z_1(1-z_1)^2}\left(z_1 z_2 + x\,\left(\ln\left[\frac{z_1(1-z_1)}{z_2 x}\right]-1\right)\right)\right] F(z_1,z_2)$

TABLE IV: Contributions to $\mathcal{R}|_{E,\,F}$

integrating the first two terms, we leave the full ϵ dependence as this was tractable. Collecting everything, we can obtain the counterpart to Table III for E, F, (Table IV).

Having set up this much of the integration, we can take the amplitude squared from the process of interest and decompose it in terms of the $A(z_1,z_2)$, $B(z_1,z_2)$, *etc.* basis. We then simply have to read off the results from Tables III and IV, and perform the $z_{1,2}$ integrals. One of these is made trivial by the remaining x-dependent δ-function. As mentioned at the beginning of this Appendix, [62] recognizes two topologically distinct contributions, which we shall refer to as box and crossed (*cf.* Fig. 22), because of their appearance as cut two-loop diagrams. We can identify them in our calculation by their color structures (C_F^2 and $C_F^2-\frac{1}{2}C_F\,C_A$, respectively). In fact, we can already calculate the entire crossed contribution as it only involves terms from Table III, having no double pole contribution to $\mathcal{R}$ and thus requiring no subtraction of LO. Determining the box graph, however, involves treating the LO subtraction properly.

As this subtraction is one of the more subtle points of the computation, we will present it in some detail. Its handling is tied up with what one means precisely by a "subleading splitting function." At LO in α_s, the definition is clear. The same splitting function that gives us the probability for a $1\to 2$ radiation also determines the running of parton densities:

$$Q^2\frac{\partial}{\partial Q^2}f(x,Q^2) \;=\; \int_x^1 \frac{dz}{z}\,P_{qq}\left(\frac{x}{z},\alpha_s(Q^2)\right)\,f(z,\,Q^2), \tag{F11}$$

where the $\mathcal{O}(\alpha_s)$ part of P_{qq}, $P_{qq}^{(0)}$ is given by Eq. (3). To determine $P_{qq}^{(1)}$, we have had to calculate a $1\to 3$ splitting, thus the probabilistic interpretation in terms of radiation is nontrivial as it involves a mix of $1\to 2$ and $1\to 3$ processes. At the level of Eq. (F11) though, we see that we are just correcting PDF evolution. In addition to the real-emission calculation that we are pursuing, one can alternatively determine P_{qq} from the anomalous dimension of certain twist-2 operators [80, 81]. Ref. [62] made a comparison to this approach and found agreement to $\mathcal{O}(\alpha_s^2)$. Since $P_{qq}^{(1)}$ is thus a two-loop object, it has the scheme dependence one would expect at this order, and so we need to make sure that we compute in the same one, which is why we do our LO subtraction in $\overline{\rm MS}$. In SCET, one could attempt the same cross-check from a straightforward two-loop calculation after fixing to one's renormalization scheme of choice.

We will now show how to subtract the LO portion in the calculation of $\mathcal{R}_{J,\,\rm NLO}^{q\to qgg}$. We get a double collinear pole associated with the strongly-ordered emission of two gluons. We want to write this as removing the emission coming from our LO operator, $C_{3,\,\rm LO}^{(2)}\mathcal{O}_3^{(2)}$. As with any subtraction scheme, while the pole is unambiguous, we need to make sure to remove the appropriate finite pieces. We note that $c_{\rm LO}^{\alpha}$ defined by Eq. (57) contains NLO(λ) pieces (in SCET$_3$ power counting) which come from the offshellness of the intermediate quark. It is true that the LO replacement rule, Eq. (56), gives only the splitting function times the logarithmic, collinear divergence. Nonetheless, the Wilson coefficients given by Eq. (63) for offshell quarks have additional terms. From the point of view of amplitude matching, this poses no problem. However, if we want to copy [62]'s scheme, then we can only subtract poles associated with the pure LO result after integration. As an operator subtraction in SCET$_3$, this means we need to change $C_{3,\,\rm LO}^{(2)}$. In order to recover the correct splitting function with no NLO contribution, we will need to project the offshell quark momentum to an onshell one with the same $\bar p$-fraction. This alone, though, does not specify the spatial orientation of the vector and will not necessarily kill the subleading terms. To do that, we write the replacement rule, but in the limit that the offshell quark's daughters are exactly collinear with it. Equivalently, if we are in the frame determined by $\bar n=\{1,0,0,-1\}$, we can project the quark momentum along $n=\{1,0,0,1\}$, *i.e.* $q_i\to\frac{\bar q_i}{2}n=q_i'$. Since the replacement rule also makes reference to the quark's parent's momentum, we also need to project it to what it would be if it had emitted an onshell quark with q_i'. Thus, $q_{i-1}\to k_i+q_i'=q_{i-1}'$. In the end, this changes our replacement

rule coefficient for the j^{th} quark to:

$$c'_{\text{LO}}{}^{\alpha_{j+1}} = \frac{\bar{q}_j}{q_j'^2}\left(n_{j'}^{\alpha} + \frac{(\not{q}'_{j+1})_{n_{j'}\perp}\,\gamma^{\alpha}_{n'_{j+1}\perp}}{\bar{q}_{j+1}}\right)\frac{\not{n}\not{\bar{n}}_j}{4}\,, \tag{F12}$$

where $q_j'^{\mu} = \bar{q}_j\, n_{j'}^{\mu}/2$. Thus c'_{LO} has the same form as c_{LO} but with a different orientation for its momenta. This changes the expression for $C^{(2)}_{3,\,\text{LO}}\mathcal{O}^{(2)}_3$ to involve c'_{LO} instead of c_{LO} (*cf.* Eq. 63)

After the dq^2 integration, the $1/\epsilon$ term in $\mathcal{R}^{q\to qgg}_{J,\,\text{NLO}}$ will allow us to read off $P^{(1)}_{qq}$. As a reminder, we need this subtraction operator because our NLO(λ) term, $C^{(2)J,\,1}_{3,\,\text{NLO}}(n_2, n'_1, n'_2)\mathcal{O}^{(2)}_3$ is supported over all of phase space, and thus contains LO portions. We therefore have

$$\begin{aligned}\mathcal{R}^{q\to qgg}_{J,\,\text{NLO}} \;=\; \int d\Pi_{k_1,\,k_2,\,q_0}\text{PP}\Big[&|C^{(2)J,\,1}_{3,\,\text{NLO}}(n_2, n'_1, n'_2)\langle 0|\mathcal{O}^{(2)}_3|qgg\bar{q}\rangle|^2 \\ &-\Big(|c'_{\text{LO}}{}^{\alpha_1}\, c'_{\text{LO}}{}^{\alpha_2}\langle 0|\mathcal{O}^{(2)}_3\Gamma^{\mu}|qgg\bar{q}\rangle|^2\Big)_{\overline{\text{MS}}}\Big]\,.\end{aligned} \tag{F13}$$

The $\overline{\text{MS}}$ indicates that we are only subtracting pole parts of the LO contribution with no finite pieces. However, there is still an ambiguity over *which* pole parts we subtract, since the LO contribution has a double pole from its two collinear divergences, but we are at some liberty to decide which single pole parts we remove as well. As we expect, this subtraction operator squared takes the form of a convolution of two splitting functions:

$$\begin{aligned}\int d\Pi\,\Big(|c'_{\text{LO}}{}^{\alpha_1}\, c'_{\text{LO}}{}^{\alpha_2}\langle 0|\mathcal{O}^{(2)}_3\Gamma^{\mu}|q\bar{q}gg\rangle|^2\Big)_{\overline{\text{MS}}} &= 2\int \not{d}^4 q_2\,\delta(q_2^2)\,dq^2\,dy\,x\,p\;(1-y)^{\frac{\epsilon}{2}}\,(q^2)^{-1+\epsilon/2}\frac{\alpha^2}{2\pi^2} \\ &\times\frac{1}{y}P^{(0)}_{d,qq}(y)\frac{P^{(0)}_{4,qq}(x/y)}{\epsilon}\text{Tr}\left[\bar{q}_2\frac{\not{n}_2}{2}\Omega\Omega^{\dagger}\right],\end{aligned} \tag{F14}$$

where the trace contains those terms that get passed to the hard function, $\mathcal{H}$, along with the q_2 phase space by the projector PP. This includes the final quark spin-sum and phase space, the current Γ which is a spectator for both LO and jet-structure corrections, and quantities related to the antiquark (*cf.* Eq. 27). What may seem surprising is that the two splitting functions live in different dimensions. The reason for this particular scheme for regulating phase space has to do with the alternate, two-loop method for calculating $P^{(1)}_{qq}$, which was the original approach. For that result, in $\overline{\text{MS}}$ we would subtract a pure pole counterterm, regulate the loop integral in d-dimensions, and leave external particles in 4d. Since the phase space integrals are related to loops by cuts, we see above that our y-integral is, in fact, in d-dimensions, but the splitting involving two external particles is left simply in four.

Looking at the SCET$_1$ diagrams for the process (Fig. 20), the amplitude $c'_{\text{LO}}{}^{\alpha_1}\, c'_{\text{LO}}{}^{\alpha_2}\langle 0|\mathcal{O}^{(2)}_{\text{S}_3}\Gamma^{\mu}|qgg\bar{q}\rangle$ comes from a subset of diagrams A^2 and B^2. The expression for subtraction is thus:

$$\begin{aligned}\text{PP}\Big[\int d\Pi\,\Big(|c'_{\text{LO}}{}^{\alpha_1}\, c'_{\text{LO}}{}^{\alpha_2}\langle 0|\mathcal{O}^{(2)}_{\text{S}_3}\Gamma^{\mu}|q\bar{q}gg\rangle|^2\Big)_{\overline{\text{MS}}}\Big] &= \int dq^2\,dz_1 x\,p\,\left(\frac{z_1}{x+z_1}\right)^{\frac{\epsilon}{2}} \\ &\times\frac{(q^2)^{-1+\epsilon/2}}{\epsilon}\frac{\alpha^2}{2\pi^2}\,\frac{1}{x+z_1}\left[\frac{1+\left(\frac{x}{x+z_1}\right)^2}{\frac{x}{x+z_1}-1}+\frac{\epsilon}{2}\left(1-\frac{x}{x+z_1}\right)\right]\left(\frac{1+(x+z_1)^2}{x+z_1-1}\right)\Big] \\ &+ z_1\leftrightarrow z_2,\end{aligned} \tag{F15}$$

where we now act with PP, dropping the trace from Eq. (F14) and keeping only those terms needed for the computation of $\mathcal{R}$ and $P^{(1)}_{qq}$. We can note several things about this expression. For concreteness, we discuss the z_1-dependent term corresponding to graph A^2, Fig. 20. The $\bar{p}$ fraction of q_0 relative to q_1 is $x/(x+z_1)$, and that of q_1 to q_2 is $x+z_1$, in terms of the variables in Eq. (F14), $y' = x/(x+z_1)$. Performing the integrals leads to double and single poles. For later use, we write down the result of doing the dq^2, dz_i integrals, where one of latter is trivial since we have

$\delta(1-x-z_1-z_2)$ sitting inside Π (*cf.* Eq. F4).

$$\begin{aligned}
&\int d\Pi \mathrm{PP}\left[\left(|c'_{\mathrm{LO}}{}^{\alpha_1}\, c'_{\mathrm{LO}}{}^{\alpha_2}\langle 0|\mathcal{O}_3^{(2)}\Gamma^\mu|q\bar{q}gg\rangle|^2\right)_{\overline{\mathrm{MS}}}\right] = \\
&2\,x\,p\,\frac{\alpha^2}{2\pi^2}\left(\frac{1}{\epsilon^2}\frac{2}{x-1}\left[\left(-2\left(2\left(x^2+1\right)\log(\lambda)+(x-1)^2\right)\right.\right.\right. \\
&\qquad\qquad\left.\left.\left.+4\left(x^2+1\right)\log(x-1)-\left(x^2-1\right)\log(x)\right)\right] \\
&+\frac{2}{\epsilon}\frac{1}{(x-1)^2 x}\left[2x(x-1)\left(2\left(x^2+1\right)\left(\mathrm{Li}_2(1-x)-\mathrm{Li}_2\left(\frac{1}{x}\right)\right)+\left(x^2-1\right)\mathrm{Li}_2\left(\frac{x-1}{x}\right)\right)\right. \\
&+x\left(-2\left(x^2+1\right)(x-1)\log^2(\lambda)+4\left(\left(x^2+1\right)\left(\log\left(\frac{x-1}{x}\right)+x\log\left(\frac{x}{x-1}\right)\right)\right)\right. \\
&-\left.(x-1)^3\right)\log(\lambda)-\left(3x^2+5\right)(x-1)\log^2(x)+2(x-1)^2\log(x)\Big) \\
&\qquad +6x\left(x^2+1\right)(x-1)\log^2(x-1)-2x(x-1)^3 \\
&\qquad -2x(x+1)(x-1)^2\log(x-1)\log(x)((x-1)^2x)\Big]\Big)
\end{aligned} \tag{F16}$$

where we have done the dz_i integrals between $1-x+\lambda$ and $-\lambda$ to regulate soft divergences. All λ-dependence cancels out of the final answer, which gives us a consistency check on the scheme.

Before comparing $P_{qq}^{(1)}$, we can check our setup with $P_{qq}^{(0)}$, by looking at the $\mathcal{O}(\alpha_s)$ contribution to $\mathcal{R}_{\mathrm{LO}}$ We see that [62] gets the following contribution:

$$P_{qq}^{(0)} \;=\; \left(\frac{\alpha_s}{2\pi}\right)\frac{2}{\epsilon}\frac{1+x^2}{1-x}. \tag{F17}$$

Calculating in SCET_1, we get the following amplitude squared:

$$A_{q\to qg} \;=\; \frac{\bar{q}_0}{q_0^2}\left(\frac{2n\cdot k_1}{\bar{k}_1}+\frac{2k_{1\perp}\cdot q_{1\perp}}{\bar{q}_1\bar{k}_1}-\frac{q_{1\perp}^2}{\bar{q}_1^2}\right)\mathrm{Tr}[\bar{q}_0\frac{\bar{n}\!\!\!/_0}{2}\Omega\Omega^\dagger] \tag{F18}$$

With our definition of $\mathcal{R}_{\mathrm{LO}}$ in Eq. (F4), we get:

$$P_{qq}^{(0)} \;=\; \left(\frac{\alpha_s}{2\pi}\right)\frac{2}{\epsilon}\frac{1+x^2}{x-1}. \tag{F19}$$

The overall minus sign between Eqs. (F17) and (F19) is due to the difference between the spacelike and timelike processes. It arises in the dz_i integral. Even though the z_i dependence is the same in the two calculations, and the integration limits are the same, 0 and $1-x$. For us, $1-x<0$, but in [62], it is positive.

We will compare the different contributions to double emission separately. In SCET_1, the C graph in Fig. 20 will give box and crossed terms when interfered with itself and the A and B ones. We identify the crossed contribution by inserting the color structure and taking those terms proportional to $C_F^2-\frac{1}{2}C_F\,C_A$. As mentioned above, it only contains the integrals in Table III. In terms of its notation, we have:

Function defined in Eq. (F4)	Value in crossed diagram
$A(z_1,z_2)$	$-\frac{16x\left(x^2+xz_1+(z_1-1)z_1+1\right)}{z_1(x+z_1-1)}$
$B(z_1,z_2)$	$\frac{8\left(x^2(z_1-2)-xz_1+z_1-1\right)}{x+z_1-1}$
$C(z_1,z_2)$	$\frac{8\left(x\left(x^2+(x-1)z_1+2\right)+z_1\right)}{z_1}$
$D(z_1,z_2)$	$16\left(x^2+1\right)$

TABLE V: Contributions to crossed amplitude squared diagram

The box contribution additionally contains the functions in Table IV, though we are only interested in the finite parts. Their z_i dependence is:

Function defined in Eq. (F4)	Value in box diagram
$A(z_1, z_2)$	$12x^2 + 8xz_1 + 8(z_1 - 1)z_1 + 12$
$B(z_1, z_2)$	$\frac{8(z_1-1)\left(x^2+(z_1-2)z_1+2\right)}{x+z_1-1}$
$C(z_1, z_2)$	$\frac{8(x+z_1)\left(2x^2+2xz_1+z_1^2+1\right)}{z_1}$
$D(z_1, z_2)$	0
$E(z_1, z_2)$	$4\left[\frac{\left(2x^4+6x^3z_1+x^2\left(7z_1^2+2\right)+2x\left(2z_1^3+z_1\right)+z_1^4+z_1^2\right)}{z_1^2}\right]$ $+4\epsilon\left[\frac{\left(x^2(x+z_1-1)^2+z_1^2\left((x+z_1-1)^2+x+z_1\right)+xz_1(x+z_1-1)^2\right)}{z_1^2}\right]$
$F(z_1, z_2)$	$4\left[\frac{\left(z_1^2-2z_1+2\right)\left(x^2+(z_1-1)^2\right)}{(x+z_1-1)^2}\right]$ $+4\epsilon\left[\frac{\left(x^2((z_1-1)z_1+1)+x(z_1-1)((z_1-2)z_1+2)+(z_1-1)^2((z_1-1)z_1+1)\right)}{(x+z_1-1)^2}\right]$

TABLE VI: Contributions to box amplitude squared diagram

For the crossed contribution, we perform the multiplication in Table III with the functions defined in Table V and integrate dz_1, having already done the trivial dz_2 integral. We again use a cutoff to avoid soft divergences, thus its range is between $1 - x + \lambda$ and $-\lambda$. In the end, we obtain:

$$P^{(1)}_{qq\,\text{crossed}} = \left(\frac{\alpha_s}{2\pi}\right)^2 \left[\left(\frac{1+x^2}{x-1}\right)\left(4\ln(x-1) - \ln^2(x) - \ln(\lambda)\right) - 2(x+1)\ln(x)\right]. \tag{F20}$$

The λ-dependent pieces will cancel against those from the box contribution. The other terms agree with [62] up to the previously discussed minus sign, and wherever $\ln(1-x)$ appears in the spacelike calculation, we get $\ln(x-1)$. Since our integrand and integration region are real, the imaginary pieces generated by $\ln(1-x)$ when making $x > 1$ all must cancel.

The box calculation proceeds similarly except that we also include the terms proportional to $E(z_1, z_2)$ and $F(z_1, z_2)$ and we have subtracted the appropriate contribution, Eq. (F16) from that given by $C^{(2)J,1}_{3,\,\text{NLO}}$. Doing all this, we get:

$$P^{(1)}_{qq\,\text{box}} = \left(\frac{\alpha_s}{2\pi}\right)^2 \left[\left(\frac{1+x^2}{x-1}\right)\left(\ln(\lambda) - \ln(x-1)\right) + 2(2x-1)\ln(x)\right]. \tag{F21}$$

The soft divergent pieces cancel against the crossed contribution, and once again we agree with [62] up to an overall sign, and the continuation $\ln(1-x) \to \ln(x-1)$.

In addition to these real emission contributions to the C_F^2 portion of $P^{(1)}_{qq}$, there are also single-emission, one-loop diagrams, shown in Fig. 24. We can account for their contributions in SCET easily. We have already derived the tree-

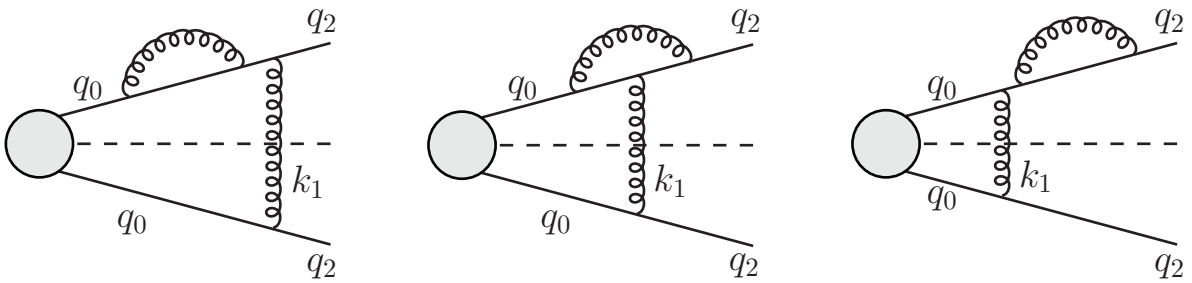

FIG. 24: Single emission, one-loop contributions to $P^{(1)}_{qq}$.

level expression for single emission (Eqs. F17 and F19). Furthermore, both the quark wavefunction renormalization and the vertex renormalization are the same in SCET as in QCD [21]. Thus, we recover the entire, gauge-invariant,

$\propto \alpha_s^2 C_F^2$ contribution to the splitting function, in agreement with Ref. [62],

$$P^{(1)}_{qq\,\mathrm{abelian}} = C_F^2 \frac{\alpha_s^2}{2\pi}\left[(1-x)\ln(x) - \frac{3}{2}\frac{1+x^2}{1-x}\ln(x) - 2\frac{1+x^2}{1-x}\ln(x)\,\ln(1-x) - \frac{1}{2}(1+x)\ln^2(x) - 5(1-x) - \frac{5}{2}(1+x)\ln(x)\right]. \tag{F22}$$

Here we have written $P^{(1)}_{qq}$ with its usual sign conventions for spacelike evolution.

[1] M. L. Mangano, M. Moretti, F. Piccinini, R. Pittau, and A. D. Polosa, JHEP **07**, 001 (2003), [hep-ph/0206293].
[2] T. Gleisberg and S. Hoche, JHEP **12**, 039 (2008), [0808.3674].
[3] C. G. Papadopoulos and M. Worek, hep-ph/0606320.
[4] W. Kilian, T. Ohl, and J. Reuter, 0708.4233.
[5] R. Keith Ellis, K. Melnikov, and G. Zanderighi, Phys. Rev. **D80**, 094002 (2009), [0906.1445].
[6] C. F. Berger *et al.*, Phys. Rev. **D80**, 074036 (2009), [0907.1984].
[7] A. Bredenstein, A. Denner, S. Dittmaier, and S. Pozzorini, 1001.4006.
[8] C. Anastasiou, L. J. Dixon, K. Melnikov, and F. Petriello, Phys. Rev. D **69**, 094008 (2004), [hep-ph/0312266].
[9] S. Catani, G. Ferrera, and M. Grazzini, 1002.3115.
[10] C. Anastasiou, K. Melnikov, and F. Petriello, Nucl. Phys. **B724**, 197 (2005), [hep-ph/0501130].
[11] S. Catani and M. Grazzini, Phys. Rev. Lett. **98**, 222002 (2007), [hep-ph/0703012].
[12] A. Gehrmann-De Ridder, T. Gehrmann, E. W. N. Glover, and G. Heinrich, Phys. Rev. Lett. **99**, 132002 (2007), [0707.1285].
[13] A. Gehrmann-De Ridder, T. Gehrmann, E. W. N. Glover, and G. Heinrich, JHEP **12**, 094 (2007), [0711.4711].
[14] S. Weinzierl, Phys. Rev. Lett. **101**, 162001 (2008), [0807.3241].
[15] S. Weinzierl, JHEP **06**, 041 (2009), [0904.1077].
[16] T. Sjöstrand, S. Mrenna, and P. Skands, JHEP **05**, 026 (2006), [hep-ph/0603175].
[17] T. Sjöstrand, S. Mrenna, and P. Skands, Comput. Phys. Commun. **178**, 852 (2008), [arXiv:0710.3820].
[18] G. Corcella *et al.*, JHEP **01**, 010 (2001), [hep-ph/0011363].
[19] M. Bahr *et al.*, Eur. Phys. J. C **58**, 639 (2008), [arXiv:0803.0883].
[20] C. W. Bauer, S. Fleming, and M. E. Luke, Phys. Rev. D **63**, 014006 (2001), [hep-ph/0005275].
[21] C. W. Bauer, S. Fleming, D. Pirjol, and I. W. Stewart, Phys. Rev. D **63**, 114020 (2001), [hep-ph/0011336].
[22] C. W. Bauer and I. W. Stewart, Phys. Lett. B **516**, 134 (2001), [hep-ph/0107001].
[23] C. W. Bauer, D. Pirjol, and I. W. Stewart, Phys. Rev. D **65**, 054022 (2002), [hep-ph/0109045].
[24] C. W. Bauer and M. D. Schwartz, Phys. Rev. **D76**, 074004 (2007), [hep-ph/0607296].
[25] C. W. Bauer and M. D. Schwartz, Phys. Rev. Lett. **97**, 142001 (2006), [hep-ph/0604065].
[26] L. Lonnblad, JHEP **05**, 046 (2002), [hep-ph/0112284].
[27] S. Catani, F. Krauss, R. Kuhn, and B. R. Webber, JHEP **11**, 063 (2001), [hep-ph/0109231].
[28] F. Caravaglios, M. L. Mangano, M. Moretti, and R. Pittau, Nucl. Phys. **B539**, 215 (1999), [hep-ph/9807570].
[29] S. Catani, Y. L. Dokshitzer, M. Olsson, G. Turnock, and B. R. Webber, Phys. Lett. **B269**, 432 (1991).
[30] T. Gleisberg *et al.*, JHEP **02**, 056 (2004), [hep-ph/0311263].
[31] G. Marchesini *et al.*, Comput. Phys. Commun. **67**, 465 (1992).
[32] A. H. Mueller, Phys. Lett. **B104**, 161 (1981).
[33] B. I. Ermolaev and V. S. Fadin, JETP Lett. **33**, 269 (1981).
[34] A. Bassetto, M. Ciafaloni, G. Marchesini, and A. H. Mueller, Nucl. Phys. **B207**, 189 (1982).
[35] Y. L. Dokshitzer, V. S. Fadin, and V. A. Khoze, Zeit. Phys. **C15**, 325 (1982).
[36] Y. L. Dokshitzer, V. S. Fadin, and V. A. Khoze, Z. Phys. **C18**, 37 (1983).
[37] S. Frixione and B. R. Webber, JHEP **06**, 029 (2002), [hep-ph/0204244].
[38] P. Nason, JHEP **11**, 040 (2004), [hep-ph/0409146].
[39] S. Catani and M. H. Seymour, Nucl. Phys. **B485**, 291 (1997), [hep-ph/9605323].
[40] S. Catani, S. Dittmaier, M. H. Seymour, and Z. Trocsanyi, Nucl. Phys. **B627**, 189 (2002), [hep-ph/0201036].
[41] S. Schumann and F. Krauss, JHEP **03**, 038 (2008), [0709.1027].
[42] M. Dinsdale, M. Ternick, and S. Weinzierl, Phys. Rev. **D76**, 094003 (2007), [0709.1026].
[43] Z. Nagy and D. E. Soper, JHEP **09**, 114 (2007), [0706.0017].
[44] Z. Nagy and D. E. Soper, JHEP **03**, 030 (2008), [0801.1917].
[45] Z. Nagy and D. E. Soper, JHEP **07**, 025 (2008), [0805.0216].
[46] D. E. Soper and Z. Nagy, 0805.4371.
[47] T. Robens and C. H. Chung, 1001.2704.
[48] G. Gustafson and U. Pettersson, Nucl. Phys. **B306**, 746 (1988).
[49] B. Andersson, G. Gustafson, and L. Lonnblad, Nucl. Phys. **B339**, 393 (1990).
[50] U. Pettersson, LU-TP-88-5.
[51] L. Lonnblad, Comput. Phys. Commun. **71**, 15 (1992).

[52] W. T. Giele, D. A. Kosower, and P. Z. Skands, Phys. Rev. **D78**, 014026 (2008), [0707.3652].
[53] A. J. Larkoski and M. E. Peskin, Phys. Rev. **D81**, 054010 (2010), [0908.2450].
[54] C. W. Bauer, F. J. Tackmann, and J. Thaler, JHEP **12**, 010 (2008), [0801.4026].
[55] C. W. Bauer, F. J. Tackmann, and J. Thaler, JHEP **12**, 011 (2008), [0801.4028].
[56] S. Catani, B. R. Webber, and G. Marchesini, Nucl. Phys. **B349**, 635 (1991).
[57] S. Jadach and M. Skrzypek, Acta Phys. Polon. **B40**, 2071 (2009), [0905.1399].
[58] M. Skrzypek and S. Jadach, 0909.5588.
[59] S. Jadach, M. Skrzypek, A. Kusina, and M. Slawinska, 1002.0010.
[60] R. Bonciani, S. Catani, M. L. Mangano, and P. Nason, Phys. Lett. B **575**, 268 (2003), [hep-ph/0307035].
[61] S. Frixione, P. Nason, and C. Oleari, JHEP **11**, 070 (2007), [0709.2092].
[62] G. Curci, W. Furmanski, and R. Petronzio, Nucl. Phys. **B175**, 27 (1980).
[63] C. W. Bauer, S. Fleming, D. Pirjol, I. Z. Rothstein, and I. W. Stewart, Phys. Rev. D **66**, 014017 (2002), [hep-ph/0202088].
[64] C. W. Bauer, D. Pirjol, and I. W. Stewart, Phys. Rev. **D68**, 034021 (2003), [hep-ph/0303156].
[65] M. Beneke, A. P. Chapovsky, M. Diehl, and T. Feldmann, Nucl. Phys. **B643**, 431 (2002), [hep-ph/0206152].
[66] M. Beneke and T. Feldmann, Phys. Lett. **B553**, 267 (2003), [hep-ph/0211358].
[67] C. Marcantonini and I. W. Stewart, arXiv:0809.1093.
[68] D. Amati, A. Bassetto, M. Ciafaloni, G. Marchesini, and G. Veneziano, Nucl. Phys. **B173**, 429 (1980).
[69] A. Bassetto, M. Ciafaloni, and G. Marchesini, Phys. Rept. **100**, 201 (1983).
[70] N. Brown and W. J. Stirling, Phys. Lett. **B252**, 657 (1990).
[71] Y. L. Dokshitzer, G. Marchesini, and G. Oriani, Nucl. Phys. **B387**, 675 (1992).
[72] A. V. Manohar and I. W. Stewart, Phys. Rev. D **76**, 074002 (2007), [hep-ph/0605001].
[73] S. Frixione, Z. Kunszt, and A. Signer, Nucl. Phys. **B467**, 399 (1996), [hep-ph/9512328].
[74] R. K. Ellis, W. J. Stirling, and B. R. Webber, Camb. Monogr. Part. Phys. Nucl. Phys. Cosmol. **8**, 1 (1996).
[75] C. W. Bauer, F. J. Tackmann, and J. Thaler, talk by C.W. Bauer at SCET 2010, http://wwwth.mppmu.mpg.de/members/scet2010/.
[76] M. E. Peskin and D. V. Schroeder, Reading, USA: Addison-Wesley (1995) 842 p.
[77] V. N. Gribov and L. N. Lipatov, Sov. J. Nucl. Phys. **15**, 675 (1972).
[78] M. Stratmann and W. Vogelsang, Nucl. Phys. **B496**, 41 (1997), [hep-ph/9612250].
[79] R. K. Ellis and W. Vogelsang, hep-ph/9602356.
[80] E. G. Floratos, D. A. Ross, and C. T. Sachrajda, Nucl. Phys. **B129**, 66 (1977).
[81] E. G. Floratos, D. A. Ross, and C. T. Sachrajda, Nucl. Phys. **B152**, 493 (1979).